# AN INVESTIGATION OF PARTICLE COLLECTION EFFICIENCY IN DIFFERENT PARTICLE-BUBBLE CONTACTING ENVIRONMENTS IN FLOTATION

A Thesis Submitted to the
UNIVERSITY OF CAPE TOWN
in Fulfilment of the Requirements for the Degree of
MASTER OF SCIENCE IN ENGINEERING

by
Jacobus Nicolaas Breytenbach
B Eng (Chemical Engineering) (Pretoria)

Department of Chemical Engineering
University of Cape Town
Rondebosch
7700
South Africa

December 1995

# SYNOPSIS

The collection efficiency of quartz particles in four different particle-bubble contacting environments was investigated during this thesis. Flotation experiments were carried out in a hybrid flotation column that could be modified into three different cell configurations (a quiescent column cell, an agitated column cell and a Jameson-type cell), while the fourth cell environment comprised a laboratory batch subaeration flotation cell.

High purity quartz was used as a probe ore in conjunction with a cationic collector and a commercial frother blend. The quartz was initially contaminated with organic material and needed to be cleaned by calcination. The cleaned quartz was divided into four narrow particle size fractions to determine the effect of particle size on particle collection efficiency.

The quartz was floated over a wide range of collector dosages and frother dosage was kept constant during experiments. The flotation was conducted using tap water at neutral pH. Froth depth was kept shallow during all experiments in the hybrid column cell configurations to enable the investigation to focus specifically on the collection zone.

The effect of contacting environment (cell type) on particle collection efficiency was investigated by considering the effect of particle hydrophobicity, particle size and agitation speed (turbulence) on flotation recovery in the different cell types. The unique particle-bubble contacting environments resulted in different particle collection efficiencies and it was found that increased contacting intensity generally led to increased efficiency of collection.

Increased particle hydrophobicity generally resulted in increased particle collection efficiency, although the overdosing of collector led to decreased flotation recovery which was probably caused by combined collector double layer and flocculation effects.

The effect of particle size on flotation recovery exhibited classical n-curve behaviour at intermediate collector dosages and the optimum particle size range as reported in the literature was confirmed. Intense contacting between particles and bubbles followed by relatively quiescent disengagement (such as the mechanism employed in the Jameson cell configuration) proved to be beneficial to collection of both fine and coarse particles.

# ACKNOWLEDGEMENTS

I would like to acknowledge the following people and organizations for their help and assistance throughout this study:

Gencor and Impala Platinum Limited for the funding of this project

Professor J P Franzidis for his invaluable guidance as supervisor

Mr Martin Harris for his constructive input and assistance as co-supervisor

Professor Cyril O'Connor for his ideas and contribution as co-supervisor

Mrs Dee Bradshaw for her support and encouragement

Dr Jan Cilliers for his constructive ideas and encouragement

Ms Lauren Basson for her ever patient ear as well as her help during write-up

Mr Granville de la Crux for his help with printing and binding of the thesis

Members of the Minerals Processing group for their help and assistance

Mr Joachim Mackie for his assistance in the design and the manufacture of the hybrid column flotation cell

Telemechanique for the donation of a frequency speed controller system

The personnel at the Department of Chemical and Metallurgical Engineering at the University of Stellenbosch for use of their laboratory facilities

Mr Christo Cilliers for the use of his computer

My parents and family for their love and support.

# TABLE OF CONTENTS

## CHAPTER 3
## DESIGN AND OPERATION OF EXPERIMENTAL EQUIPMENT

## CHAPTER 4
## EXPERIMENTAL DETAILS

## CHAPTER 5
## RESULTS AND DISCUSSION

## CHAPTER 6
## CONCLUSIONS AND RECOMMENDATIONS

# LIST OF TABLES

# LIST OF FIGURES

# NOMENCLATURE

| | |
|---|---|
| a | Bubble Radius |
| a | Parameter in the Axial Dispersion Model |
| a, b | Constants in the Probability of Detachment Equation (Equation (49) on page 23) |
| a, b, c, d | Constants in the Surface Vorticity Correlation (Equation (41) on page 21) |
| A | Bubble Surface Area per Volume of Pulp |
| A | Constant in Bubble Drift Velocity Correlation (Equation (68) on page 35 and Equation (71) on page 36) |
| $B_c$ | Coefficient (Equation (72) on page 36) |
| $B_d$ | Coefficient (Equation (75) on page 36) |
| $c(x_{av})$ | Concentration of Particles of an Average Size $x_{av}$ in the Flotation Cell |
| C | Frother Concentration |
| $C_c$ | Contamination Factor |
| $C_i$ | Tracer Concentration in the Tailings Stream at time $t_i$ |
| $d_b$ | Bubble Diameter |
| $d_p$ | Particle Diameter |
| D | Axial Dispersion Coefficient |
| $D_c$ | Column Diameter |
| $D_I$ | Impeller diameter |
| E | Normalized Residence Time Distribution |
| $E_A$ | Particle Attachment Efficiency |
| $E_C$ | Particle-Bubble Collision Efficiency |
| $E_{Cg}$ | Gravitational Collision Efficiency |
| $E_{Ci}$ | Interceptional Collision Efficiency |
| $E_K$ | Particle Collection Efficiency |
| $E_S$ | Fraction of Particles that remain attached throughout the Flotation Process |
| $E_\theta$ | Normalized Residence Time Distribution (In terms of Dimensionless Time) |
| F | Froth Stability Factor |
| g | Gravitational Acceleration |
| G | Air Flow Rate |
| $H_c$ | Column Collection Zone Height |
| $J_g$ | Superficial Gas Velocity |
| $J_l$ | Superficial Liquid Velocity |

| | |
|---|---|
| $k$ | First Order Rate constant in Batch or Continuous Flotation Model |
| $k_c$ | First Order rate Constant in the Collection Zone of Flotation Columns |
| $k_g$ | Gas Holdup Coefficient |
| $K$ | Curve Fitting Parameter in Klimpel Model |
| $K_2$ | Mass Transfer Rate Constant |
| $L$ | Length of the Collection Zone |
| $M$ | Amount of Mineral floated at time t in Batch Cell |
| $M_0$ | Initial amount of Mineral in the Batch Cell |
| $n_\theta$ | Fraction of Colliding Particles that Collide between the Front Stagnation Point on the Bubble and some angle $\theta$ |
| $N_b$ | Number of Bubbles per Unit Volume of Pulp |
| $N_d$ | Vessel Dispersion Number |
| $N_p$ | Number of Particles per Unit Volume of Pulp |
| $P$ | Probability of a Particle being Collected by an Air Bubble in the Pulp |
| $P_a$ | Probability of Adhesion of a Particle to a Bubble or Aggregate after Collision |
| $P_c$ | Probability of Particle-Bubble or Particle-Bubble Aggregate Collision |
| $P_d$ | Probability of Detachment of a Particle from a Bubble |
| $P_s$ | Probability of the Particle Remaining Attached to the Bubble throughout the Flotation Process |
| $r$ | Cumulative Recovery of Mineral or of Gangue in Klimpel Model |
| $R$ | Curve Fitting Parameter in the Klimpel Model, Equilibrium Recovery |
| $R_c$ | Collection Zone Recovery in Flotation Columns |
| $R_f$ | Froth Zone Recovery in Flotation Columns |
| $R_{fc}$ | Overall Recovery in Flotation Columns |
| $R_v$ | Bubble Radius |
| $Re_b$ | Bubble Reynolds Number |
| $Re_m$ | Mixing Reynolds Number |
| $S$ | Fraction of the Bubble Surface not covered by Adhering Particles |
| $Sk$ | Stokes Number |
| $t$ | Flotation time |
| $t_i$ | Induction Time |
| $t_i$ | Discrete Time at which Tracer Concentration is Measured |
| $\Delta t_i$ | Discrete Time Interval during Tracer Measurements |
| $t^*$ | Dimensionless Time |
| $u$ | Interstitial Liquid Velocity |

| | |
|---|---|
| $u_b$ | Mean Relative Velocity of Bubbles in the Pulp |
| $u_{br}$ | Bubble Rise Velocity |
| $u_p$ | Mean Relative Velocity of Particles in the Pulp |
| $u_{x,y}$ | Liquid Dimensionless Velocity in the x and y directions |
| $U_b$ | Terminal Rise Velocity of a Single Bubble |
| $U_{ba}$ | Average Bubble Upward Velocity |
| $U_{bd}$ | Bubble Drift Velocity |
| v | Velocity of the Particle Relative to the Bubble |
| $v_{x,y}$ | Particle Dimensionless Velocity in the x and y directions |
| $v_\theta$ | Particle Sliding Velocity over the Bubble Surface |
| $v_{\theta,av}$ | Average Particle Sliding Velocity over the Bubble Surface |
| V | Volume of Pulp in the Cell |
| w | Concentration of Mineral in the Froth |
| $W_A$ | Work of Adhesion of Liquid to Solid |
| $W_A^d$ | Work of Adhesion from Dispersion Forces |
| $W_A^h$ | Work of Adhesion from Hydrogen Bonding of Water to Solid Surface Groups |
| $W_A^i$ | Work of Adhesion from Electrical Charge at the Interface |
| $W_C$ | Work of Cohesion of Liquid |
| x | Particle Radius |
| $Z_{pb}$ | Number of Particle-Bubble Collisions per Unit Volume and Time |
| $\gamma_{LV}$ | Surface Tension between Liquid and Vapour Phases |
| $\gamma_{SL}$ | Surface Tension between Solid and Liquid Phases |
| $\gamma_{SV}$ | Surface Tension between Solid and Vapour Phases |
| $\gamma^d$ | Surface Tension due to Dispersion Forces |
| $\epsilon$ | Specific Energy Dissipation |
| $\epsilon_g$ | Gas Holdup |
| $\theta$ | Static Contact Angle at the Liquid/Solid Interface or the Angle between the Centre of a Bubble and the Point of Collision on the Bubble Surface |
| $\theta$ | Dimensionless Time in Residence Time Distributions |
| $\theta'$ | Angle $\theta$ in Equation (44) on page 21 when $t_s = t_i$ |
| $\theta_c$ | Fraction of Particles Retained in the Froth after Fruitful Collision or the Angle where the Fluid Streamlines come Closest to the Bubble |
| $\theta_m$ | Maximum Angle of Contact of a Particle onto a Bubble |
| $\mu$ | Bulk Liquid viscosity |
| $\mu_l$ | Liquid viscosity |

| | |
|---|---|
| $\nu$ | Kinematic Viscosity |
| $\xi_s$ | Surface Vorticity |
| $\rho$ | Density of the Medium (Pulp) |
| $\rho_b$ | Bubble Density |
| $\rho_g$ | Density of the Gas |
| $\rho_l$ | Liquid Density |
| $\rho_p$ | Particle Density |
| $\rho_{sl}$ | Slurry Density |
| $\Delta\rho$ | Density Difference between Bubble or Particle ($i$) and the Medium |
| $\sigma$ | Bubble Surface Area per Unit Volume of Air |
| $\sigma^2$ | Variance of a Residence Time Distribution Curve |
| $\tau$ | Bubble Average Residence Time in the Slurry |
| $\tau$ | Mean Residence Time of Pulp in a Vessel |
| $\phi$(D) | Particle Size Correction Factor |
| $\omega$ | Rotational Speed of the Impeller (rpm). |

# CHAPTER 1
# INTRODUCTION

## 1.1 BACKGROUND

Froth flotation is a physico-chemical process widely used in mineral beneficiation for the separation of finely divided solids from a mixture of solids initially present in a water-based suspension. The technique involves the contacting of air bubbles with the solids. The solids are treated with chemical reagents (collectors) to create conditions favourable for the attachment of certain solids to the air bubbles. The selected particles are subsequently removed in a froth stabilized by chemical agents (frothers), from which they are recovered.

The flotation process is governed by the principles of surface chemistry and fluid mechanics. Much research effort has gone into the investigation of the chemical and electrochemical aspects involved in the flotation process (especially collector adsorption), while the theory behind the collection process is still poorly understood [Jameson *et al.*, 1977]. However, recent activity in the field of flotation cell design has catalyzed an interest shift from the chemical and electrochemical aspects of flotation to the physical processes involved in particle collection.

The first application of the modern flotation process occurred as early as 1905 [1] in which the characteristics of the modern mechanical flotation machine could already be recognized. Probably the most significant area of change in mechanical flotation machines during the following years has been the very dramatic increase in machine size, with the basic design staying virtually the same. The volume of the Wemco flotation machine, for example, increased from $2m^3$ in 1935 to 45 $m^3$ in 1980 [Klimpel, 1987].

A completely different design came to life in the early 1960's with the invention of the column flotation cell by two Canadians, Boutin and Tremblay [1964]. Column-type flotation cells differ from conventional mechanical flotation units both in design and operating philosophy. The column separated the bubble generation system from the particle suspension function of the impeller; the impeller was eliminated. No fewer than 80 patents on column-type devices were taken out worldwide from 1964 until 1991 [Brzezina and Sablik, 1991]. Columns have obtained widespread acceptance only since 1981 [Finch and Dobby, 1990],

---

1. A process in which air was introduced into a pulp through a submerged pipe and by direct introduction of air by a beater or impeller was patented by Sulman and Pickard in 1905, and Sulman, Pickard and Ballot in 1906. A similar device was patented by Hoover in 1910 [Gaudin, 1931].

although the mechanical flotation machine is still the work-horse of the minerals flotation industry.

The arrival of the column cell redefined the problem of recovery by particle size; in conventional cells the ultrafine gangue is recovered indiscriminately by entrainment, whereas in columns the ultrafines are cleaned by the addition of wash water. On the other hand, while the action of the impeller in mechanical flotation cells helps to suspend coarse particles, they are lost very rapidly in column cells. The hybrid cell of Harris *et al.* [1992], being a combination of a mechanical cell and a flotation column, addressed this dilemma, and resulted in improved recovery of coarse material, while still maintaining selectivity in the ultrafine particle size region.

One of the main differences between different flotation devices is that they employ different particle-bubble contacting environments. In a mechanical flotation cell ore particles and bubbles are contacted in a highly turbulent environment whereas in a column flotation cell the contacting environment is essentially quiescent. In other column-type flotation cells such as the Jameson and pneumatic cells the air and particles are pre-mixed under high intensity conditions; the flotation column is simply used to allow disengagement of the mineralised bubbles from the tailings. The most important differences between these cell environments may be found in the degree of turbulence created in the pulp, the characteristics of mixing in the vessel, the rate of shear due to agitation and the size of bubbles employed.

A valid question would be: how do different particle-bubble contacting environments affect the collection of particles of different sizes and hydrophobicities? The aim of this thesis can be stated as an investigation of the effect of different particle-bubble contacting environments on particle collection efficiency in flotation.

## 1.2 SCOPE OF THE THESIS

A hybrid flotation column cell was designed and constructed for the purposes of this investigation. It could be modified to act as a conventional column flotation cell, a mechanically agitated column cell or a Jameson cell. The three different bubble-particle contacting environments were consequently housed inside the same vessel, which was beneficial for comparative purposes.

These three cell configurations were used to carry out an array of tests covering a wide spectrum of operating conditions such as size and hydrophobicity of the particles to be floated, and turbulence created in the cell, using an ore which was pre-treated and sized into different particle size fractions. Comparative test work was conducted in a laboratory batch

subaeration flotation cell. The results obtained were analyzed with respect to factors such as mixing characteristics in the different cell configurations, particle and bubble size effects and hydrophobicity of the floated particles. Flotation recovery in the different cells were compared and conclusions were drawn from the way in which particle collection efficiency is affected by flotation in these particle-bubble contacting environments.

The thesis begins with a review (Chapter 2) of available literature on the theory of particle floatability. A particle collection model is introduced to illustrate the basic principles, after which some important operating parameter effects in flotation are discussed. Mixing characteristics in flotation columns are reviewed and the literature review concludes with an overview of cell technologies available to industry. The equipment used during this investigation is discussed in Chapter 3, in which a detailed description of the design of the hybrid column cell and the rig is given. The ore chosen for this investigation is described in Chapter 4 and details are given on the way in which it was pre-treated and sized. The chemicals used during this investigation and the chemical conditions employed are discussed. Chapter 4 also discusses the experimental program and the way in which the work was approached. The experimental techniques and procedures which were used are described and reproducibility is discussed. The results obtained are presented and discussed in Chapter 5 with respect to their significance on the effect of particle-bubble contacting environment on particle collection efficiency. The thesis concludes with a final Chapter (Chapter 6) in which the conclusions drawn from the results and some recommendations for future work are given.

# CHAPTER 2
# LITERATURE REVIEW

## 2.1 INTRODUCTION

This Chapter gives an overview of the available literature relevant to this thesis. The principles of particle floatability are discussed, the influence of some typical operating parameters on flotation are reviewed, and some methods of determining the mixing characteristics in flotation vessels are discussed. The Chapter concludes with an overview of the state-of-the-art developments in flotation machine design.

## 2.2 PARTICLE FLOATABILITY

As a bubble rises through a flotation pulp it will encounter particles of ore or gangue. Provided that a particle is hydrophobic [2], it may pass sufficiently close to a bubble for coalescence to occur between them. Coalescence will almost certainly occur over the front of the bubble [Jameson *et al.*, 1977], and particles adhering to the surface will be swept to the rear by the relative motion between bubble and liquid, as has been proved by photographic evidence [Brown, 1965]. Sutherland and Wark [1955] have shown a striking photograph of galena particles (single and in aggregate) suspended from the rear of a bubble. Provided the force of adhesion is strong enough, the particles will remain at the rear of the bubble until it reaches the pulp-froth interface. The bubble-particle aggregate will then enter the froth layer along with entrained liquid and particles. The particle may be recovered in the froth concentrate if bubble breakage or aggregate disruption with consequent particle dropback in the froth does not occur.

A mineral particle is thus classified as floatable if it can successfully attach to an air bubble and be removed with it from the flotation slurry. The principles of floatability are discussed in section 2.4.2 on page 11 with the aid of a flotation model. An overview of particle hydrophobicity, which is a prerequisite for floatability, is given in the following section.

## 2.3 PARTICLE HYDROPHOBICITY

Hydrophobicity is the ability of a solid surface to repel water; the term wettability instead of hydrophobicity is often used in flotation literature. A mineral particle has to be

---

2. An overview of hydrophobicity is given below in section 2.3.

hydrophobic in order for it to be floatable under normal flotation conditions. Hydrophobicity is frequently characterized by the contact angle ($\theta$) between the solid and liquid phases at the interface. The relationship between hydrophobicity and contact angle has been comprehensively described in flotation literature [Taggart, 1945; Kelly and Spottiswood, 1982; King, 1982] and the following brief theoretical treatment was summarized from a paper by Laskowski [1986].

### 2.3.1 Hydrophobicity and Contact Angle

The classical boundary condition for the hydrophilic -hydrophobic transition is the equality of $W_A$, the work of adhesion of liquid to solid, and $W_C$, the work of cohesion of the liquid

$$W_A = \gamma_{SV} + \gamma_{LV} - \gamma_{SL} \quad (1)$$

$$W_C = 2\gamma_{LV} \quad (2)$$

where $\gamma$ denotes surface tension, and the subscripts indicate solid/vapour, liquid/vapour and solid/liquid interfaces, respectively. A descriptive illustration is given in Figure 1.

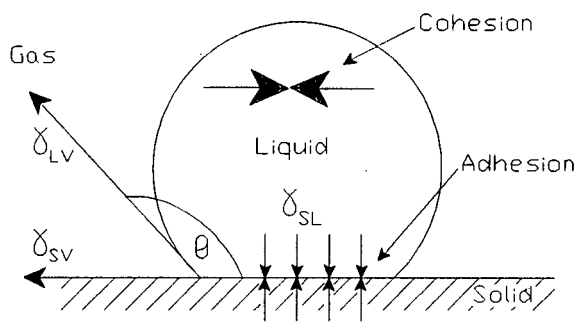


Figure 1 : The Effect of the Work of Cohesion of Liquid and the Work of Adhesion of Liquid to Solid on the Solid Wettability.

By introducing Young's equation [King, 1982],

$$\gamma_{SV} = \gamma_{SL} + \gamma_{LV} \cos \theta \quad (3)$$

which is obtained by resolving the three interfacial tensions horizontally, and in which $\theta$ is the static contact angle, Equation (1) can be converted to

$$W_A = \gamma_{LV} (1 + \cos \theta) \quad (4)$$

Then

$$\frac{W_A}{W_C} = \frac{\gamma_{LV} (1 + \cos \theta)}{2\gamma_{LV}} \quad (5)$$

which gives

$$\cos\theta = 2\frac{W_A}{W_C} - 1 \tag{6}$$

The condition of hydrophobicity follows directly from Equation (6), i.e. only for $W_A < W_C$ is $\theta > 0°$. According to Fowkes [1967] there are three main contributions to the work of adhesion of water to solid

$$W_A = W_A^d + W_A^h + W_A^i \tag{7}$$

where $W_A^d$ is the contribution from dispersion forces, $W_A^h$ is the contribution from the hydrogen bonding of water to solid surface groups (hydroxyl), and $W_A^i$ is the contribution from the electrical charge at the interface. $W_A^d$ can be calculated from

$$W_A^d = 2[\gamma_{H_2O}^d \cdot \gamma_s^d]^{1/2} \tag{8}$$

where $\gamma^d$ denotes surface tension due to dispersion forces, the subscripts s and $H_2O$ denote solid phase and water phase, respectively, and $\gamma_{H2O}^d \approx 22$ erg/cm$^2$. It has been pointed out [Laskowski and Kitchener, 1969] that for no substance (except fluorocarbons) is $W_A^d$ as large as the exceptionally high work of cohesion of water (for water $W_C \approx 145$ erg/cm$^2$). Therefore because

$$\cos\theta = 2\frac{[W_A^d + W_A^h + W_A^i]}{W_C} - 1 \tag{9}$$

and since $W_A^h \approx 0$ and $W_A^i \approx 0$,

$$\cos\theta \approx 2\frac{W_A^d}{W_C} - 1 \tag{10}$$

it follows from Equation (10) that the solid is always hydrophobic (that is, $\theta > 0°$) whenever $W_A \approx W_A^d$. The main conclusion is therefore that all solids would be hydrophobic if they did not carry polar or ionic groups.

### 2.3.2 Hydrophobicity and Collectors

Mineral particles are normally hydrophilic in the natural form and collectors are added to the pulp to render the particles hydrophobic. Equation (3) (Young's equation) indicates that for a finite value of the contact angle (*i.e.* $\theta > 0°$), the following condition must be fulfilled [Laskowski, 1974]

$$\gamma_{SV} - \gamma_{SL} < \gamma_{LV} \tag{11}$$

The contact angle is zero (mineral hydrophilic) when

$$\gamma_{SV} - \gamma_{SL} > \gamma_{LV} \quad (12)$$

The function of collectors in flotation slurries is to decrease the value of $(\gamma_{SV} - \gamma_{SL})$, thereby increasing the value of the contact angle. The study of the adsorption of surfactants (and specifically collectors) is a complex field and it is not the purpose of this thesis to cover this aspect of flotation theory. Collector theory has been comprehensively covered by many authors in the flotation literature [King, 1982; Klimpel, 1984; Pope and Sutton, 1971].

### 2.3.3 Quantifying Hydrophobicity

Equations (1) - (10) only define solid hydrophobicity in terms of the contact angle and its relationship to the work of cohesion of water. In spite of all simplifying approaches, it is still difficult to relate hydrophobicity defined in such a way to floatability. When film rupture (which is a very important process in bubble-particle aggregate formation) occurs, it is highly unlikely that the contact angle of the liquid on the solid is the static equilibrium angle, so stresses will be induced, molecular in origin, which will cause the contact line [3] to move and adopt an equilibrium configuration [Jameson *et al.*, 1977].

Sheludko [1963] concluded that flotation could be characterized by contact angle only if there were no kinetic resistance to the attachment of particles to bubbles or if the resistances depended on the same parameters as the angle of contact. The circumstances under which static contact angles are measured consequently do not approach the real situation in any way and are in fact very unrealistic. Mineral particles are far from smooth and are typically much smaller than the bubbles. However, it has been widely accepted in the literature that Equation (3) (Young's equation) provides an adequate basis for the thermodynamic analysis of three-phase systems [Kelly and Spottiswood, 1982] and static contact angle measurements still provide very valuable information about the hydrophobicity of solids.

Crawford and Ralston [1988] reported good agreement between contact angle measurements on packed beds of quartz particles and smooth quartz plates for angles up to 70°. They used the rate-of-wetting technique [Crawford *et al.*, 1987] which measures advancing water contact angles. Gaudin and Morrow [1954] measured contact angles between 0° and 10° on smooth quartz surfaces for the solution

3. See Figure 1 on page 6 for an illustration of the contact line.

concentration range $3x10^{-6}$ to $1.3x10^{-5}$ moles per litre of dodecyl-ammoniumacetate. Dynamic contact angles and hysteresis effects have been the subject of many reviews and papers [Elliot and Riddiford, 1964; Johnson and Dettre, 1969; Blake and Haynes, 1973].

The measurement of induction time [4] may be a more convenient way of measuring hydrophobicity than contact angle measurement [Yordan and Yoon, 1986], since induction time is a strong function of particle hydrophobicity.

In the present investigation, the degree of hydrophobicity was assumed to be a function of the dosage of collector added to the pulp. The degree of hydrophobicity is therefore quantified as grams of collector (salt) per ton of ore throughout the thesis.

### 2.3.4 The Quartz-Amine System

The quartz-amine flotation system has been widely used by researchers, with the most common amine previously used being dodecylamine [Smith and Scott, 1990]. The popularity of the quartz-amine system in fundamental flotation studies can probably be attributed to the following factors:

1) Quartz is available in very high purity and is naturally totally hydrophilic,
2) The relative simplicity of the physisorption mechanism of adsorption as opposed to chemisorption makes it a very desirable choice, and
3) It is a relatively inexpensive system to work with.

Apart from amines, other cationic collectors which may also be used for flotation of non-metallic minerals (such as quartz) are organic ammonium and pyridinium salts, as well as organic sulphonium, phosphonium and arsonium compounds in which S, P and As have replaced the N in the ammonium salts. The amines, which exist in the cationic form below certain pH values, are the most widely used cationic collectors in industry [King, 1982]. This pH-dependence is the basis of their collecting action. A review of proposed mechanisms of amine adsorption onto quartz has been given in a recent paper by Smith and Scott [1990].

Another method of rendering quartz hydrophobic is by means of methylation. This widely used technique consists of the treatment of quartz particles with solutions of trimethyl-chlorosilane in Analar grade benzene [Laskowski and Kitchener, 1969; Laskowski and Iskra, 1970; Blake and Ralston, 1985; Crawford and Ralston, 1988;

4. See section 2.4.2.2 on page 18 for a discussion of induction time.

Smith and Rajala, 1989]. Different degrees of hydrophobicity are achievable by varying the time of contact between the quartz particles and the solution of trimethyl-chlorosilane. The quartz particles are washed or boiled in hydrochloric acid to remove Fe and Cl ions prior to methylation. NaOH is typically used as the neutralizing agent after the acid wash step.

## 2.4 MODELLING OF FLOTATION KINETICS

The term flotation rate means the rate of transfer of a mineral from the cell to the froth product. In conditions of free flotation, where the bubbles are only sparsely coated with mineral particles (bubble surface available at all times), the rate of flotation is first order [Tomlinson and Fleming, 1965], although it is possible to have higher order relationships under certain conditions, as was shown by Arbiter [1951].

### 2.4.1 Modelling of Batch Flotation Operations

The first instance of batch flotation modelling can be tracked back as far as 1935 when Zuniga found his experimental data could be fitted by an equation of the form

$$M = M_0 \, (1-e^{-kt}) \tag{13}$$

where M is the amount of mineral floated, $M_0$ the initial amount of mineral in the cell, t the flotation time and k a constant [Fichera and Chudacek, 1992]. This equation was derived by integration of the expression showing flotation rate to be proportional to the amount of mineral in the cell

$$\frac{dM}{dt} = k \, (M_0-M) \tag{14}$$

Equations (13) and (14) are analogous to those describing a first order chemical reaction.

A modification of the classical first order model was done by Klimpel [1984; Klimpel, *et al.*, 1982] and is given as

$$r = R \, [1-\frac{1}{Kt}(1-e^{-Kt})] \tag{15}$$

where r is cumulative recovery of mineral or gangue, t is flotation time, and R and K are curve fitting parameters. It is evident from Equation (15) that when t is large, r will approach R, the equilibrium recovery. Although the Klimpel model is a regression model and is unable to predict flotation rate or recovery in any system, it has been

used extensively as a tool for evaluation of relative performances of different flotation reagent types and other flotation conditions [Klimpel, 1984; Klimpel, 1987; Klimpel and Isherwood, 1987]. It can be applied to discrete particle size fractions or to a whole range of particle size fractions in a specific flotation ore.

### 2.4.2 Modelling of Continuous Flotation Operations

Determination of the rate constant in column-type flotation machines with continuous operation can be done by continuously recycling the tailings stream back to the column feed point, an approach followed by Mular and Musara [1991]. This configuration results in a closed or semi-batch system in which only the froth is removed out of the system. The data are then treated in a similar way as batch cell data.

Determination of kinetic data from continuous systems has been done by modelling the particle collection process using physical parameters of the flotation operation. Determination of flotation rate from the analysis of the actual mechanism of the process was first done by Schuhmann [1942]. He linked the flotation rate to physical parameters with the following relationship

$$\frac{dw}{dt} = P_c\ P_a\ c(x_{av})\ V\ F \qquad (16)$$

where $P_c$ and $P_a$ represent the probability of collision between a particle and an air bubble and the probability of adhesion of the particle to the bubble after collision, respectively. The concentration of particles of an average size $x_{av}$ is denoted by $c(x_{av})$, V is the volume of pulp in the cell, and w represents the concentration of mineral in the froth. The factor F characterizes the froth stability. Sutherland [1948], attempting to include the effects of physical parameters in the rate of flotation, transformed the (by then famous) Schuhmann equation to the much more complex relationship

$$\frac{dw}{dt} = [3\pi axv\ N_b][sech^2\ (\frac{3vt_i}{4a})]\theta_c V\ (w_o - w) \qquad (17)$$

where a is the bubble radius, x is the particle radius, v is the velocity of the particle relative to the bubble, $N_b$ denotes the number of bubbles per unit volume of pulp, $t_i$ is the induction time, and $\theta_c$ denotes the proportion of particles retained in the froth after fruitful collision. $\theta_c$ can be compared to the term F in the Schuhmann equation. The term ($w_o$ - w) is the concentration of solids in the pulp at time t. Thus, the first term in brackets defines $P_c$ and the second, $P_a$ of the Schuhmann equation. More recently, it was presented in the following general form [Schultze, 1984; Laskowski, 1986; Jordan and Spears, 1990]

$$P = P_c P_a P_s \tag{18}$$

This agrees with the observation by Jameson *et al.* [1977] that the collision process has some of the similarities of a chemical reaction [5], so that the rate of collection of particles can been described in terms of the probability of occurrence of a series of events. $P_c$ and $P_a$ have the same meaning as in equation (16), while $P_s$ is the probability of formation of a stable particle-bubble aggregate and P denotes the probability of flotation of a mineral particle.

Column-type flotation cells can be divided into two sections *viz.* a section which is occupied by aerated pulp (the collection zone) and one which is occupied by froth (the cleaning zone). A recycle process exists between the collection and cleaning zones whereby hydrophobic material enters the froth, drops back into the pulp and is then subject to recollection. Overall recovery (froth overflowing the cell lip) will thus be different from collection zone recovery and can be predicted using the following relationship [Finch and Dobby, 1990]

$$R_{fc} = \frac{R_c R_f}{R_c R_f + 1 - R_c} \tag{19}$$

where $R_c$ is the recovery in the collection zone, and $R_f$ is the froth zone recovery. The effect of particle drop-back becomes smaller as the froth depth decreases: it is evident from Equation (19) that $R_{fc}$ approaches $R_c$ as $R_f$ approaches unity. Froth beds in industrial columns are typically 0.5 to 2.0 m deep [Yianatos *et al.*, 1987], representing approximately 10% of the column length. The column-type hybrid cell [6] used in this investigation was operated at a froth depth of 1% of the column length. It was therefore assumed that $R_{fc} = R_c$, which made it possible to focus on the collection zone throughout the thesis, while overlooking complex froth phenomena.

An expression for the rate constant in flotation columns in terms of physical parameters of the process can be derived from a mass balance over a cubic volume of pulp in the collection zone [Finch and Dobby, 1990]

$$k = \frac{1.5 J_g E_K}{d_b} \tag{20}$$

where k is the first order rate constant in the collection zone, $J_g$ is the superficial gas velocity, $d_b$ is the mean bubble diameter and $E_K$ is the particle collection efficiency.

5. Also compare with section 2.4.1 on page 10.
6. A description of the hybrid cell is given in section 3.2 on page 55.

Equation (20) should apply to all column-type flotation machines in which the pulp is fed near the top and the air is introduced at the bottom of the column, irrespective of the degree of turbulence in the column [7]. $E_K$ can be expressed as a function of three components as follows [Finch and Dobby, 1990]

$$E_K = E_C E_A E_S \tag{21}$$

where $E_C$ is the collision efficiency between a particle and a bubble, $E_A$ is the efficiency of attachment of a particle to a bubble and $E_S$ is the fraction of particles that remain attached to a bubble throughout the flotation process. Equation (21) is essentially identical to Equation (18). The following sections describe how each of the efficiency terms in Equation (21) can be determined from fundamental relationships.

#### 2.4.2.1 Probability of Collision ($P_c$) or Collision Efficiency ($E_C$)

The probability of collision between particle and bubble, $P_c$, has been studied by many researchers [Gaudin *et al.*, 1931, Sutherland, 1948; Laskowski, 1974] and is found to be independent of particle hydrophobicity, while being dependent on particle size and bubble size, as well as the general hydrodynamic conditions prevailing in the pulp [Laskowski, 1986]. Many attempts have been made to find an accurate relationship between $P_c$ and physical flotation parameters. Sutherland [1948] and Gaudin [1957] were among the first to derive very simple expressions for $P_c$ from stream functions, only incorporating the particle diameter, $d_p$, and the bubble diameter, $d_b$. These relationships proved to be practically useless because of the assumption of potential flow and Stokes flow, respectively. Sutherland's equation applies to bubbles much larger than those used in the flotation industry, while Gaudin's is valid for very small bubbles only. Recognizing the limited applicability of the expressions of Sutherland and Gaudin, Flint and Howarth [1971] numerically solved the Navier-Stokes equations to determine $P_c$. This approach was modified by Reay and Ratcliff [1973] to show that

$$P_c \propto \left(\frac{d_p}{d_b}\right)^2 \tag{22}$$

More recently, Weber and Paddock [1983] derived an analytical expression for $P_c$ for bubbles of low Reynolds numbers by numerically solving the Navier-Stokes equations. This relationship takes the dependence of $P_c$ on the hydrodynamics of the system into account by incorporating Reynolds number. The essence of predicting $P_c$ accurately is to derive stream functions for different

7. An identical expression has been cited by Yoon [1993] and Jameson *et al.* [1977] for turbulent systems.

ranges of bubble sizes. Although the stream functions for the Stokes and potential flow conditions have been known for a long time, those for the intermediate Reynolds numbers have not. It happens that most of the flotation-size bubbles have their Reynolds numbers in the intermediate range. For this reason, Yoon and Luttrell [1989] derived a stream function applicable for flotation-size bubbles. Using this relationship, they derived yet another expression for the probability of collision, $P_c$ [Yoon, 1993]

$$P_c = [\frac{3}{2} + \frac{4\ Re_b^{0.72}}{15}](\frac{d_p}{d_b})^2 \tag{23}$$

which shows that $P_c$ varies as $d_b^{-2}$ for small bubbles with $Re_b = 0$. With larger bubbles, $P_c$ becomes less dependent on $d_b$. It can be readily shown that for very large bubbles, $P_c$ varies with $d_b^{-0.46}$. Thus, the power relationship between $P_c$ and the $d_b/d_p$-ratio changes with bubble size and may be represented in a generalized form [Yoon, 1993]

$$P_c = A\ (\frac{d_p}{d_b})^n \tag{24}$$

Values for A and n for different flow scenarios are given in Table 1.

Table 1 : Values of A and n of Equation (24) on page 14.

| Flow Conditions | A | n |
|---|---|---|
| Stokes | $\frac{2}{3}$ | 2 |
| Intermediate | $\frac{2}{3} + \frac{4\ Re^{0.72}}{15}$ | 2 |
| Intermediate | $\frac{2}{3}[1 + \frac{(3/16)\ Re}{1 + 0.249\ Re^{0.56}}]$ | 2 |
| Potential | 3 | 1 |

It is important to note that all the $P_c$ expressions given in this table are based on the interceptional collision model, which may be useful for flotation under relatively quiescent conditions such as in column flotation only. A turbulence model may be more appropriate in the case of flotation cells with a higher degree of turbulence (*e.g.* mechanically agitated cells and Jameson cells). Based on the collision model derived by Abrahamson [1975], Schubert and Bischofberger [1979] derived the following expression for predicting the number of bubble-

particle collisions, $Z_{pb}$, per unit volume and time [Jordan and Spears, 1990]

$$Z_{pb} = 5\ N_p\ N_b\ [\frac{d_p+d_b}{2}]^2\sqrt{u_p^2+u_b^2} \tag{25}$$

In this equation, $N_p$ is the number of particles per unit volume of pulp, $N_b$ denotes the number of bubbles per unit volume of pulp and $u_p$ and $u_b$ are the mean relative velocities of the particles and bubbles to the liquid, respectively. These relative velocities can be estimated by [Schubert, 1986]

$$\sqrt{u_i^2} = 0.33\ \frac{\epsilon^{4/9} d_i^{7/9}}{\nu^{1/3}} (\frac{\Delta\rho}{\rho})^{2/3} \tag{26}$$

in which the subscript $i$ refers to bubble or particle, $\epsilon$ is the specific energy dissipation, $\rho$ the density of the medium, $\Delta\rho$ is the density difference between $i$ and the medium, and $\nu$ is the kinematic viscosity.

#### 2.4.2.1.1 Calculation of Collision Efficiency ($E_C$) using a Collision Model [Finch and Dobby, 1990]

The following approach to the calculation of $E_C$ was taken from Finch and Dobby [1990], which only applies to conditions of quiescent contacting (*e.g.* column flotation), and can not be used to describe flotation in more turbulent systems. The theories developed by many researchers over the years have been condensed into one model. These authors based their analysis of the collision process on the equation of motion of a spherical particle relative to a spherical bubble (which is large compared to the particle) rising in an infinite pool of liquid. Hydrodynamic drag will tend to sweep the particle around the bubble, following the fluid streamlines. Particle inertia and gravity act in a combined manner to move the particle out of the fluid streamline and toward the top surface of the bubble. An illustration of this process is given in Figure 2 below.

The equations of motion of the particle in the horizontal (x) and vertical (y) direction are

$$Sk = \frac{dv_x^*}{dt^*}\ u_x^* - v_x^* \tag{27}$$

$$Sk = \frac{dv_y^*}{dt^*}\ (u_p^* + u_y^*) - v_y^* \tag{28}$$

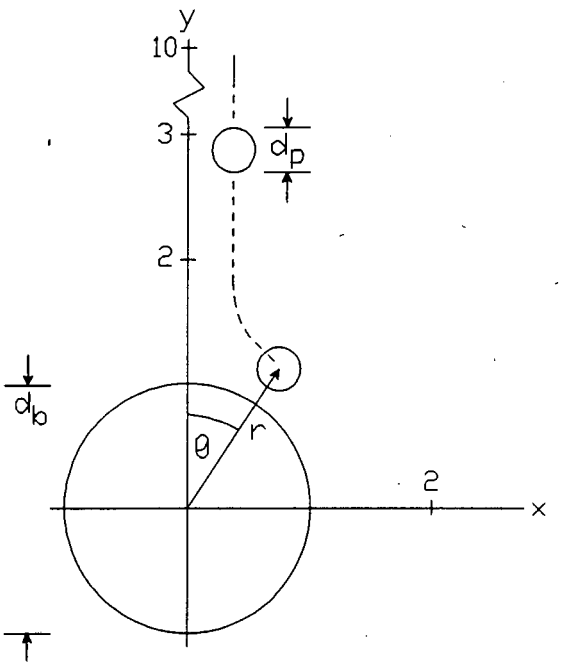


Figure 2 : Illustration of a an Ore Particle Approaching a Gas Bubble.

The first term on the right hand side of Equations (27) and (28) is the inertial term, $v_{x,y}^*$ and $u_{x,y}^*$ are particle and liquid velocities, respectively and $u_p^*$ is the particle terminal velocity. All velocities are made dimensionless by dividing by the bubble rise velocity, $u_b$, while $t^*$ is made dimensionless by multiplying by $(u_b/d_b)$. Sk is the Stokes number, given by

$$Sk = \frac{1}{9} \left(\frac{\rho_p}{\rho_l}\right) \left(\frac{d_p}{d_b}\right) Re_b \tag{29}$$

where $\rho_p$ and $\rho_l$ refer to the particle and liquid densities respectively, $d_p$ and $d_b$ denote particle and bubble diameters. $Re_b$ is the bubble Reynolds number, given by

$$Re_b = \frac{d_b \, U_b \, \rho_{sl}}{\mu_{sl}} \tag{30}$$

where $U_b$ is the terminal rise velocity of a single bubble in a slurry, $\rho_{sl}$ is the density of the slurry and $\mu_{sl}$ is the slurry viscosity. $U_b$ can be calculated by an adaptation of the multi-species settling equation of Masliyah [Mills, 1992]

$$U_b = \frac{g \, d_b^2 \, (\rho_{sl} - \rho_b)}{18 \, \mu_{sl} \, (1 + 0.15 \, Re_b^{0.687})} \tag{31}$$

Equations (30) and (31) are solved iteratively to determine both $U_b$ and $Re_b$. Particle terminal velocity is calculated using Stokes' equation

$$u_p = \frac{g\ (\rho_p - \rho_l)\ d_p^2}{18\ \mu_l} \tag{32}$$

In flotation the most important parameter determining the Stokes number is particle diameter. Sk is less than 0.1 for very fine particles (*e.g.* -30 $\mu$m) and can be assumed to be equal to zero (the physical significance of this is that the particle adjusts instantaneously to changes in the fluid flow). This situation is described first, after which the analysis is extended to intermediate sized particles. The most comprehensive collision model to date is the one of Weber and Paddock [1983] [8] in which the collision efficiency is the sum of gravitational and interceptional collision

$$E_C = E_{Cg} + E_{Ci} \tag{33}$$

Interceptional collision alone ($E_{Cg} = 0$) corresponds to neutrally buoyant particles which follow the streamlines exactly. Gravitational collision accounts for particle mass. Gravitational collision alone ($E_{Ci} = 0$) is hypothetical; it corresponds to particles having a finite settling velocity but zero dimension. $E_{Ci}$ is given as

$$E_{Ci} = \frac{1.5}{1 + u_p^*} \left(\frac{d_p}{d_b}\right)^2 \left[1 + \frac{(3/16)\ Re_b}{1 + 0.249\ Re_b^{0.56}}\right] \tag{34}$$

for $0 < Re_b \leq 300$. $E_{Cg}$ is given by

$$E_{Cg} = \frac{u_p^*}{(1 + u_p^*)} \left(1 + \frac{d_p}{d_b}\right)^2 \sin^2 \theta_c \tag{35}$$

where $\theta_c$ is the angle (measured from the front stagnation point of the bubble) where the fluid streamlines come closest to the bubble. The following correlation applies for $20 < Re_b < 400$

$$\theta_c = 78.1 - 7.37 \log Re_b \tag{36}$$

For $Sk > 0.1$ (intermediate particle inertia), an analytical solution is no longer possible and collision efficiencies have been calculated by determining particle trajectories using a numerical solution to the equations of motion (Equations (27) and (28) on page 15), and finding the trajectory by trial and error. From this, collision efficiency have been correlated as

8. See the previous discussion of this model in section 2.4.2.1 on page 13.

$$E_C = E_{Co} (1.63\ Re_b^{0.06} Sk^{0.54}\ u_p^{*\,-0.16}) \quad (37)$$

where $E_{Co}$ is $E_C$ obtained from Equation (33) on page 17 for conditions when Sk = 0.

### 2.4.2.2 Probability of Attachment ($P_a$) or Attachment Efficiency ($E_A$)

Sliding time is that period of time in which the particle stays in contact with the bubble during collision. Attachment time is the time required for the particle to attach to the bubble. Attachment time includes induction (rupture) time and film displacement time. Sliding time and attachment time must be clearly distinguished. Sliding time is determined by bubble-particle motion and controlled by the hydrodynamics of the system. Attachment time is dominated by surface chemistry features of the bubble and the particle and can be altered by flotation reagents [Ye and Miller, 1989]. It is still unknown exactly how the probability of adhesion, $P_a$ is related to particle hydrophobicity, but it has been shown that induction time is a strong function of particle hydrophobicity [Laskowski, 1986]. Induction time is measurable with powdered samples, using a relatively simple device, and is seen as a more convenient way of measuring (quantifying) hydrophobicity [9] than contact angle measurements [Yordan and Yoon, 1986]. Sutherland [1948] clearly stated that the probability of adhesion, $P_a$, is connected with the induction time, $t_i$. This means that not necessarily every collision will result in particle-bubble attachment, but only when the contact time between bubble and particle is longer than the attachment time. During this short interval, the liquid film must thin, then rupture and recede. The induction time, $t_i$, is therefore defined as the time required for the disjoining film to thin to such a thickness that rupture can take place; thus the rupture of the disjoining film determines $P_a$ [Laskowski, 1974]. Schultze [1984] reported typical contact times of approximately 10 ms or less.

An expression for $P_a$ was developed by Yoon and Luttrell [1989] using the stream function they derived previously [10]

$$P_a = \sin^2 [2 \arctan \exp(\frac{-45 + 8\ Re^{0.72}\ u_{br}\ t_i}{15\ d_b(d_b/d_p + 1)})] \quad (38)$$

9. See the previous discussion of hydrophobicity in section 2.3.3 on page 8.
10. See section 2.4.2.1 on page 13 for a discussion of the stream function.

in which $t_i$ is the induction time and $u_{br}$ is the bubble rise velocity. This expression is applicable for the intermediate Reynolds number range. Apart from the induction time, $P_a$ also depends on the particle size, and decreases with decreasing particle size [Jordan and Spears, 1990]. This equation also shows that $P_a$ is dependent on bubble size.

Contact time was calculated by Ye and Miller [1989] by taking into account the effect of bubble and particle motion, buoyant force, bubble size, particle size and specific densities for different cases of collision. They found that a significant reduction in induction time occurred with increased particle hydrophobicity, resulting in increased ease of film rupture by the particles. Crawford and Ralston [1988] studied the influence of particle size and contact angle on the flotation behaviour of methylated quartz particles. They also calculated induction time, using the expression of Sutherland [1948], and showed that induction time decreases with increasing particle surface coverage of collector, *i.e.* with increasing contact angle (thus, more hydrophobic particles). Induction time was also shown to be influenced by particle size: $t_i$ decreases with decreased particle size [Jordan and Spears, 1990].

Modelling of sliding time has been done by many authors. One such model was presented by Dobby and Finch [1986b]. The model is based on determinations of the liquid velocity distribution over the surface of rigid spheres for Reynolds numbers of less than 400 (which is in the typical flotation range). The model predictions fitted the available data on sliding time well, and shows that sliding time is strongly particle size dependent. A later version of this model is described in the next section.

#### 2.4.2.2.1 Calculation of Attachment Efficiency ($E_A$) using an Attachment Model [Finch and Dobby, 1990]

The principles behind the determination of $E_A$ are described using the model by Finch and Dobby [1990] as was the case with $E_C$ in section 2.4.2.1.1 on page 15. The model determines sliding time by applying the fluid mechanical arguments already introduced in the collision model [11], while no attempt has been made to include surface forces, as they are not readily quantified. The induction time is user-selected in the model and no

11. The collision model of Finch and Dobby has been discussed in section 2.4.2.1.1 on page 15 and applies to quiescent contacting (*e.g.* column flotation cells) only.

attempt is made to predict it from first principles. This model acknowledges the fact that induction time is related to particle hydrophobicity; the less hydrophobic the particle, the larger is $t_i$, although it does not take the particle size dependence of $t_i$ into account and assumes a constant $t_i$ for the whole particle size range.

An illustration of the collision process between a particle and a bubble with the streamlines has been given in Figure 2 on page 16. The calculation of sliding time, $t_s$ requires a knowledge of

1) The distribution of particle collision angles on the bubble surface,
2) The angle at which the fluid streamlines start to carry the particle radially away from the bubble, *i.e.* the maximum angle of contact, $\theta_m$, and
3) The particle sliding velocity.

The distribution of collision angles is quantified by $n_\theta$, the fraction of all colliding particles that collide between the front stagnation point of the bubble and some angle $\theta$. This is calculated using the trajectory model; a good approximation is

$$n_\theta = \frac{\sin^2 \theta}{\sin^2 \theta_c} \qquad (39)$$

where $\theta_c$ is given by Equation (36) on page 17.

The maximum angle of contact, $\theta_m$ is calculated by determining the angle at which the radial component of the particle settling velocity (directed toward the bubble surface) is equal to the radial component of the liquid velocity (directed away from the bubble surface). At $\theta > \theta_m$ the particle no longer contacts the bubble, unless attachment has already occurred. A correlation between $\theta_m$, $\rho_p$ and $\theta_c$ is

$$\theta_m = 9 + 8.1\ \rho_p + \theta_c\ (0.9 - 0.09\ \rho_p) \qquad (40)$$

where $\theta_c$ is calculated using Equation (36) on page 17.

Particle sliding velocity, $v_\theta$, over the bubble surface is the sum of the tangential component of particle settling velocity, $u_p \sin\theta$, and the local tangential liquid velocity. Assumptions of Stokes and potential flow to determine the local tangential velocity have been found to be invalid. The

flow regime has, however, been modelled using two linear functions. The model makes use of the parameter surface vorticity, $\xi_s$ which is the tangential velocity gradient at the surface of the sphere. The following correlation holds for $0° < \theta \leq 90°$ [Dobby and Finch, 1987]

$$\xi_s = a + b\,\theta + c\,\theta^2 + d\,\theta^3 \tag{41}$$

The coefficients a, b, c and d are a function of $Re_b$ and the correlations used to determine these coefficients are described in Appendix A on page 161.

For $d_p/d_b < 0.03$ particle tangential sliding velocity $v_\theta$ is

$$v_\theta = 0.7\,\xi_s\,u_b\,\frac{d_p}{d_b} + u_p \sin\theta \tag{42}$$

For $d_p/d_b > 0.03$ the particle velocity is calculated by dividing the particle into two zones: the lower part that sees a velocity gradient and the upper part that sees a constant velocity. Then $v_\theta$ is given by

$$v_\theta = 0.07\,\xi_s\,u_b\,[\frac{(d_p - 0.03\,d_b)}{d_p}\,0.06 + (\frac{0.03\,d_b}{d_p})\,0.03] + u_p \sin\theta \tag{43}$$

The particle sliding time $t_s$ can now be calculated by

$$t_s = (\frac{\theta_m - \theta}{360})\,\pi\,(\frac{d_p + d_b}{v_{\theta,av}}) \tag{44}$$

where $\theta$ is in degrees and $v_{\theta,av}$ is the average particle sliding velocity, determined from Equation (42) or (43) using average values of $\xi_s$ and $\sin\theta$.

Attachment efficiency, $E_A$ can now be calculated using the theory which has been described above. A particle attaches to a bubble when the sliding time, $t_s$ exceeds the induction time, $t_i$. Let $\theta'$ be the angle $\theta$ in Equation (44) when $t_s = t_i$. After rearrangement this gives

$$\theta' = \theta_m - \frac{360\,v_\theta\,t_i}{\pi\,(d_b + d_p)} \tag{45}$$

Consequently, attachment efficiency is given by

$$E_A = \frac{\sin^2\theta'}{\sin^2\theta_c} \tag{46}$$

### 2.4.2.3 Probability of Formation of a Stable Particle-Bubble Aggregate ($P_s$) or Fraction of Particles that stay Attached to a Bubble ($E_S$)

The probability of formation of a stable particle-bubble aggregate, $P_s$ can be expressed in terms of the probability of detachment of a particle from a bubble, $P_d$, as follows

$$P_s = 1 - P_d \tag{47}$$

$P_s$ can be taken as a function of contact angle, particle radius, bubble radius and particle density in quiescent flotation operations [Laskowski, 1974]. Woodburn *et al.* [1971] showed that

$$P_s = 1 - \left(\frac{d_p}{d_{\max p}}\right)^{3/2} \tag{48}$$

where $d_{\max p}$ is the maximum particle size that will remain attached under the prevailing turbulent conditions. The strong effect of turbulence on $P_s$ may thus be explained by the term $d_{\max p}$ in Equation (48) [Jordan and Spears, 1990]. This equation may also serve to explain why coarse particles normally have a lower probability of forming strong bubble-particle aggregates than fine particles. The work of Ahmed and Jameson [1985] illustrates the particle size and turbulence dependence of flotation rate very clearly. They used quartz to investigate the effect of bubble size on the rate of flotation. From their results it is clear that coarse particles benefitted from increased agitation, but only up to a certain point, after which flotation rate decreased. This may be directly attributed to a decrease in $P_s$. Fine particle flotation increased throughout the entire agitation range and was not influenced by bubble-particle disruption, as was the case with coarse particles. It is commonly recognized that $P_s$ can be assumed to be equal to unity for fine particles [Jordan and Spears, 1990; Finch and Dobby, 1990; Yoon, 1993]. Jordan and Spears [1990] also found that $P_s$ is lowest for coarse particles and approaches unity for fine particles.

Laskowski [1986] reported that there is a direct relationship between the strength of the particle-bubble aggregate and the contact angle (thus, hydrophobicity): the larger the value of the contact angle, the stronger is the particle-bubble aggregate, i.e. the larger is the value of $P_s$. The influence of hydrophobicity on $P_s$ may also explain by the $d_{\max p}$-term in Equation (48). The greater the hydrophobicity, the stronger the force between bubble and particle, and the larger the particle size that can be held by the bubble for a certain degree of turbulence. This is supported by the findings of Crawford and Ralston [1988].

The probability of detachment of quartz particles from bubbles during bubble oscillation was investigated by means of a vibration method by Holtham and Cheng [1991]. They found that for any given particle size and bubble size the probability of detachment of a particle from an air bubble is related to vibration time, collector concentration and vibrational acceleration. In a flotation pulp the duration of bubble oscillations is determined by the magnitude of collision energy and the frequency of collisions, both of which are dependent on agitation rate or impeller speed. They also found that a relationship between $P_d$ and the ratio of particle size to bubble size exists at any given acceleration and is given by

$$P_d = a + b \frac{d_p}{d_b} \tag{49}$$

where a and b are constants that decrease with particle size.

### 2.4.3 The Entrainment of Particles

The efficiency of recovery in flotation cells is determined by the amount of material that is recovered by true flotation, *i.e.* those particles which are physically attached to bubble surfaces by virtue of their hydrophobicity. Particles can be entrained in the froth by mechanical entrapment. If the froth were removed before it had a chance to drain, thereby permitting the entrapped particles to return to the liquid phase, there could be a significant carry-over of particles, whose recovery would be wrongly attributed to true flotation by hydrophobic attachment to bubbles. Selectivity therefore depends on the extent to which unwanted or gangue particles are entrained with the water into the froth, and hence, contaminate the froth. The mechanical entrapment of hydrophilic particles into the froth is affected by many parameters, such as pulp density, particle size, and the shape of particles. However, it is also influenced by the characteristics of the froth. For example, entrainment of gangue particles could be high in small-bubbled, closely knit froths, which are normally stable and wet, but lower in well-drained, loosely structured froths. The stability and structure of the froth are largely determined by the characteristics and concentration of collector and frother added to the pulp, as well as by the hydrophobicity of particles, the presence of very fine particles (slimes), *etc.* and are therefore unique to every type of ore. In addition to this, entrainment is affected by the rate of froth removal, and consequently by the residence time of particles in the froth [Engelbrecht and Woodburn, 1975].

The froth phase was kept shallow during this investigation and it was assumed that the residence time of particles in the froth was zero. Selectivity was not an important factor, since a pure ore (quartz) was used without the presence of gangue minerals.

## 2.5 MIXING CHARACTERISTICS OF THE COLLECTION ZONE IN FLOTATION COLUMNS

Flotation is considered to be a first order process [12]. The calculation of the recovery of a component from a first order rate process is dependent upon three variables [Finch and Dobby, 1990]:

1) The first order rate constant,
2) The mean residence time, and
3) A mixing parameter.

One extreme of mixing is plug flow transport, where the residence time of all elements of the fluid (and all mineral particles) is the same. Plug flow in a column-type vessel will mean there is a concentration gradient of floatable material along the length of the column. The recovery in this case is given by [Levenspiel, 1972]

$$R_c = 1 - \exp(-k_c t) \tag{50}$$

where $R_c$ is the recovery in the collection zone, $k_c$ is the first order collection zone rate constant and t is flotation time. The other extreme is a perfectly mixed reactor, where there is a distribution of residence time and the concentration is the same throughout the vessel. The recovery in this case is given by [Levenspiel, 1972]

$$R_c = 1 - (1 + k_c\tau)^{-1} \tag{51}$$

where $\tau$ is the mean residence time of pulp in the vessel. Different flotation machine types will exhibit different mixing characteristics owing to different hydrodynamics present in each system. Tall columns with small diameters (*e.g.* a 5 to 10 m long pilot scale column with an inside diameter of 5 cm) approach plug flow transport, while the liquid and solids in industrial scale plant columns have mixing characteristics between that of plug flow and perfectly mixed vessels [Finch and Dobby, 1990]. Transport conditions that do not approach either of the two extremes are usually described by mixing models. Mixing models and their applicability to column-type flotation cells are discussed in the next section.

### 2.5.1 Mixing Models and the Mixing Characteristics in Column-Type Flotation Machines

Two models have been used to describe the characteristics of mixing in the collection zone of column-type flotation machines *viz.* the dispersion model and the tanks-in-series model [Mills, 1992]. The recovery in the collection zone can be predicted by the *axial*

12. See the discussion in section 2.4 on page 10.

*dispersion model* with the following relationship [Levenspiel, 1972]

$$R_c = 1 - \frac{4a \exp\left(\frac{1}{2N_d}\right)}{(1+a)^2 \exp\left(\frac{a}{2N_d}\right) - (1-a)^2 \exp\left(\frac{-a}{2N_d}\right)} \quad (52)$$

where $N_d$ is the vessel dispersion number and a is a parameter given as

$$a = (1 + 4 k_c \tau N_d)^{0.5} \quad (53)$$

in which $\tau$ and $k_c$ have the same meaning as before.

The *tanks-in-series model* predicts the collection zone recovery from the following relationship [Levenspiel, 1972]

$$R_c = 1 - (1 + k_c (\tau/N))^{-N} \quad (54)$$

where N is the number of tanks in series and $\tau$ is the mean residence time.

### 2.5.2 Residence Time Distribution Studies (RTD Studies)

A suitable method for the determination of mixing parameters in column-type vessels is residence time distribution measurement, which has been used extensively by many researchers [Nesset, 1988; Finch and Dobby, 1990; Manqiu and Finch, 1991; Mills, 1992]. A tracer is injected at the top of the collection zone (normally at the feed point) and the concentration of tracer in the tailings outlet is measured. The mean residence time of pulp in the vessel, $\tau$, and variance of the distribution $\sigma^2$ can be determined from the RTD data. If the tracer concentration at the tailings outlet is sampled at discrete time intervals, $t_i$, then

$$\tau = \frac{\Sigma\, t_i\, C_i\, \Delta t_i}{\Sigma\, C_i\, \Delta t_i} \quad (55)$$

and

$$\sigma^2 = \frac{\Sigma\, t_i^2\, C_i\, \Delta t_i}{\Sigma\, C_i\, \Delta t_i} - \tau^2 \quad (56)$$

where $C_i$ is the tracer concentration in the tailings outlet at time $t_i$. It is convenient to represent the RTD data in a normalized form, in which case

$$\int_0^\infty E\, dt = \int_0^\theta E_\theta\, d\theta = 1 \quad (57)$$

where E is the normalized RTD curve. It is also customary to measure time in units

of mean residence time, which gives a dimensionless measure; the following relationships are then applicable

$$\theta = \frac{t}{\tau} \tag{58}$$

and

$$\theta E_\theta = t E \tag{59}$$

where $\theta$ is dimensionless time and $E_\theta$ denotes the residence time distribution in terms of dimensionless time.

The residence time distribution of solids in a flotation pulp is different from the liquid phase because of the density difference between the two phases; settling of solids occurs. It has been postulated that the dispersion coefficient of the liquid phase is the same as for fine particles [Dobby and Finch, 1985], although the validity of this assumption has been questioned by Mills and O'Connor [1990]. They observed that the solids were more mixed than the liquid phase, and an increase in the feed percent solids, while not changing the liquid vessel dispersion number, reduced the solids dispersion number. The determination of solids residence time requires the use of special tracers which do not interfere with the flotation process (*e.g.* radio-active tracers) and can be difficult to carry out in practice.

Determination of the vessel dispersion number, $N_d$, or the number of tanks in series, N [13], can be made from RTD data. The application of RTD data in determining the mixing parameters in the axial dispersion and tanks-in-series model is discussed in the next two sections.

#### 2.5.2.1 RTD Data and the Axial Dispersion Model

The dispersion model is represented by the following differential equation [Levenspiel, 1972]

$$\frac{\delta C}{\delta \theta} = \left(\frac{D}{uL}\right) \frac{\delta^2 C}{\delta z^2} - \frac{\delta C}{\delta z} \tag{60}$$

where D is known as the axial dispersion coefficient, u denotes the interstitial liquid velocity in the z direction and L is the length of the collection zone. The dimensionless group (D/uL), represents the vessel dispersion number, $N_d$. $N_d$ is the parameter which measures the extent of axial dispersion. Thus

13. See Equations (52) and (54) on page 25.

$$\frac{D}{uL} \rightarrow 0 \tag{61}$$

means negligible dispersion, hence plug flow, while

$$\frac{D}{uL} \rightarrow \infty \tag{62}$$

means large dispersion, hence mixed flow.

Manqiu and Finch [1991] developed a general correlation for the liquid dispersion number, $N_d$, which was shown to fit most data in the literature

$$N_d = 1.85 \left(\frac{D_c}{H_c} \frac{J_g}{J_l}\right)^{0.63} \tag{63}$$

where $D_c$ is the diameter of the column, $H_c$ is the column height, and $J_g$ and $J_l$ are the gas and liquid superficial velocities.

Application of the dispersion model requires a solution for Equation (60). A choice of three boundary conditions exists *viz.* open-open, closed-open and closed-closed. These boundary conditions are determined by the way in which the tracer is injected into the column and the way in which tracer concentration is measured. Closed-closed means the tracer is injected into the feed stream at the feed point, while the concentration measurement takes place at the tailings exit point. Open-open conditions refers to the tracer being injected at a point in the collection zone itself, with the measurement also taking place at a point in the collection zone. Closed-open would therefore be a combination of the above mentioned two situations.

A solution to Equation (60) for small extents of dispersion (*e.g.* $N_d < 0.1$), is given by Levenspiel [1972] as

$$C_\theta = \frac{1}{2\sqrt{\pi\ (D/uL)}} \exp\left[-\frac{(1-\theta)^2}{4\ (D/uL)}\right] \tag{64}$$

For large extents of dispersion, an analytical solution of Equation (60) is no longer possible, except for open-open boundary conditions. A numerical solution for closed-closed conditions using the finite difference method has been developed by Manqiu *et al.* [1991]. Numerical solution of the axial dispersion model, together with a least squares fitting routine has been recommended by Manqiu and Finch [1991] and was shown to give the best fit to existing

experimental data on column flotation cells. They also found that the analytical solution (Equation (64)) adequately described mixing with small extents of dispersion ($N_d < 0.25$).

#### 2.5.2.2 RTD Data and the Tanks-in-Series Model

The tanks-in series model is simpler to use than the axial dispersion model, but can only interpret RTD data from tracer tests where closed-closed boundary conditions were used. The RTD curve is described analytically and does not need a numerical solution as is the case with the axial dispersion model. The RTD curve is given as [Levenspiel, 1972]

$$E(\theta) = \frac{N\,(N\theta)^{N-1}}{(N-1)!}\,e^{-N\theta} \qquad (65)$$

where N and $\theta$ are as defined before.

## 2.6 OPERATING PARAMETER EFFECTS IN FLOTATION

Flotation recovery, flotation rate and collection efficiency are influenced by certain operating parameters. Operating parameters can be defined as those variables in the flotation process which can be manipulated by plant operators. Examples of these parameters are particle size, bubble size, particle hydrophobicity, air flow rate, contacting intensity and turbulence in the flotation cell. The way in which the flotation process, and more specifically particle collection efficiency, is influenced by these parameters, is discussed in subsequent sections.

### 2.6.1 Particle Size

Particle size is a critical parameter in flotation operations. A significant part of the present study was devoted to the investigation of particle size phenomena.

Gaudin *et al.* [1931] were the first to note the important influence of particle size on flotation. Since then, the effect of particle size on flotation has been investigated by many researchers [Trahar and Warren, 1976; Sivamohan, 1990; Harris *et al.*, 1992]. It is commonly recognized that there are conflicting factors affecting the rate of flotation in terms of particle size. Given that the surfaces of small and large particles are equally hydrophobic, large particles are more likely than small ones to collide with a bubble and make contact because of a higher probability of collision [14]. On the

14. The probability of collision or collision efficiency has been discussed in section 2.4.2.1 on page 13.

other hand, the probability of a given bubble-mineral attachment being strong enough to withstand the buffeting in an agitated cell is less for a large particle than for a small one [15] [Ewers, 1955]. Particle size-recovery curves have a characteristic shape, as illustrated by Figure 3.

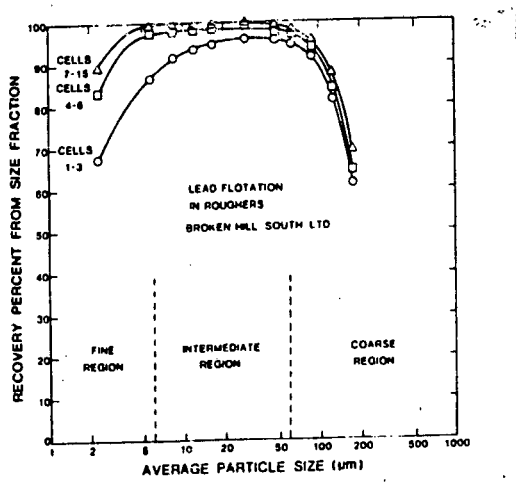


Figure 3 : Typical Particle Size - Recovery Curve.

This Figure may be divided into three regions [Trahar, 1981]:

1) The region below 5 $\mu$m - 10 $\mu$m comprises the fines which are difficult to float and more difficult to separate owing to a very low collision efficiency, $E_C$. The fraction of particles which stay attached to a bubble, $E_S$, will be close to unity for very fine particles [16]; thus the poorer recovery may be attributed to the $P_c$-effect. In addition to this, fines have smaller momentum than large particles and will consequently have a smaller chance of deviating from the fluid streamlines around a bubble [17] to rupture the film between the liquid and air phases than large particles; $E_A$ will consequently be lower for fines.
2) The region from $\pm$10 $\mu$m to 70 $\mu$m comprises the intermediate particles which are usually the most floatable because of a balance between the effects mentioned in point 1.
3) The particle sizes above 70 $\mu$m and below some more or less undefined upper limit is the coarse particle region where $E_C$ and $E_A$ become much higher, while $E_S$ decreases significantly. The drop in recovery with coarse particles has been attributed to the decrease in $E_S$ by many authors [18].

15. Attachment efficiency has been discussed in section 2.4.2.2 on page 18.
16. See the discussion in section 2.4.2.3 on page 22.
17. Attachment efficiency and streamlines have been discussed in section 2.4.2.2 on page 18.
18. This aspect has been discussed in section 2.4.2.3 on page 22.

The above explanation of particle size behaviour may be an oversimplification if industrial flotation operations are considered, since froth phase phenomena have not been taken into account. The entrainment of fine particles into the froth phase and their stabilizing effect on the froth, are but two factors that might influence total recoveries in flotation cells. Mular and Musara [1991] investigated the flotation rate constant as a function of the froth depth in a batch column system and found a linear relationship to exist between the two. Thus a focus on the collection zone is only strictly correct if the froth phase effects are ignored, as was done by de Bruyn and Modi [1956], by keeping the froth phase as shallow as possible [19]. They investigated the influence of particle size on the flotation rate of quartz, using dodecylammonium acetate as collector. This work was done on a continuous basis in a laboratory scale agitated flotation cell. Some of their findings were that the flotation rate was proportional to the pulp density for particle sizes of 65 $\mu$m and finer, provided that the pulp density was kept below 5.2%. With the specific collector, the size range of optimum flotation was between 10 $\mu$m and 37 $\mu$m, possibly indicating that for the quartz-amine system, the probability of disruption of a bubble-particle aggregate ($1-E_S$) is more strongly influenced by particle size than is the collision efficiency, $E_C$. They also found a similar relationship between particle size and flotation rate to that shown in Figure 3 on the previous page.

The flotation of coarse particles has been investigated by Soto and Barbery [1991]. Quartz with a size range between 75 $\mu$m and 200 $\mu$m was floated. They made use of a low-turbulence column-type cell and found that much higher recoveries were obtained compared to conventional mechanical laboratory cells. This may again be explained by a decrease in detachment of particle-bubble aggregates because of lower turbulence present in the cell.

Evans *et al.* [1962] investigated the influence of collector dosage on flotation recovery. They found that the first particles collected (at starvation amounts of collector) were fine and became increasingly coarser with further collector addition. Assuming that particles of all sizes were conditioned to the same extent, they concluded that a smaller contact angle was necessary for small particles to allow stable bubble attachment. Subsequently others [Trahar, 1981; Crawford and Ralston, 1988] have confirmed that the minimum degree of hydrophobicity necessary for the flotation of a particle depends upon its size. Blake and Ralston [1985] found a critical bubble surface coverage for each particle size, using methylated quartz. It has been suggested that the separate conditioning of particles of different size would be beneficial for flotation recovery

19. This approach was also followed during the experimental work of this thesis.

[Trahar, 1981]. This has in fact been implemented in many industrial flotation plants with great success.

#### 2.6.1.1 Fine Particle Flotation

The presence of a large fines or slime fraction in a flotation feed is in general detrimental to the flotation of the coarser particles, because of the excess reagent take-up by the fines with their high surface-area-to-mass ratio and the possible adsorption of these fines on larger particles [20]. From the hydrodynamic viewpoint, fine particles are a problem mainly because they have a small mass and high surface area. Small particle mass leads to low momentum, low probability of collision with a bubble and difficulty in overcoming the energy barrier between particle and bubble. High surface area leads to a high pulp viscosity and undesirable coating of the valuable particles by ultra fine gangue particles [Sivamohan, 1990].

One of many practical solutions to the problems associated with fines flotation is the use of novel technology like column flotation, packed bed flotation or the Jameson cell, amongst many others.

### 2.6.2 Bubble Size

Bubble size is another critical parameter in flotation. The size of bubbles produced is a function of the air flow rate, the chemical conditioning of the pulp and the method of air introduction into the cell (mechanical design . Frothers are used to lower the surface tension of water so that the probability of coalescence of bubbles is reduced and the life of the particle-laden air bubbles is prolonged when they reach the surface of the pulp. Frother addition thus causes a decrease in bubble size. Higher air flow rates lead to bigger bubbles and consequently higher bubble rise velocities. The equilibrium shape of a bubble is determined by stress balances at the interface. Thus, a finite volume of gas injected into a liquid will rise at such a velocity, and assume such a shape, that every point on the interface is a balance between the normal and tangential stresses in each phase. The hydrostatic pressure acts on all bubbles in such a way as to cause a pressure gradient that make them rise. The velocity of bubbles rising freely in a large body of water has been the subject of many investigations [Jameson, 1984]. A graphical representation of a composite of the available data on bubble rise velocity which was compiled by Clift *et al.* [1978] is shown below in Figure 4.

20. This principle has been used to recover fine particles and is termed carrier flotation.

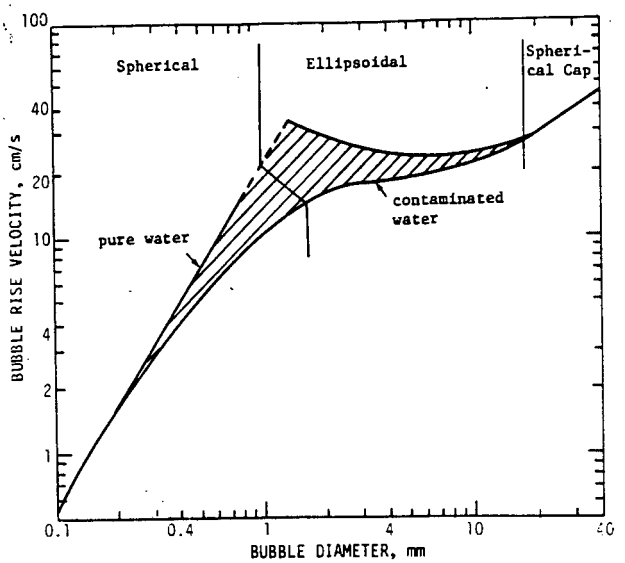


Figure 4 : The Terminal Velocity of Air Bubbles in Water at 20 °C.

The well known trend of higher rise velocities for bigger bubbles is evident. Bubble rise velocity in turn influences the gas holdup, which is an important parameter in bubble residence time. The first order rate constant can be seen from Equation (20) on page 12 to be a function of both the air flow rate and bubble size in a flotation column.

Figure 4 also shows the dependence of the shape of bubbles on the bubble size; the specific bubble size range is divided into three regions of different shape. Very small bubbles, less than 1 mm in diameter, are spherical in appearance, and rise with a steady rectilineal motion. For bubbles greater than 1 mm in diameter, the vertical motion appears to become unstable and the bubbles resemble flattened spheroids or ellipsoids. Small bubbles are held in the spherical form by surface tension, the effect of which diminishes inversely as the radius. Very large bubbles (> 10 mm) of spherical cap shape are generally not encountered, except with cell flooding.

In addition to having an effect on the first order rate constant, as discussed above, bubble size has an influence on the collection efficiency, $E_K$ through the collision and attachment efficiencies, $E_C$ and $E_A$, as well as through the $E_S$-term [21]. All three these terms are affected by bubble size in some or other way [22].

The effect of bubble size in flotation has received considerable research interest in the past. Many attempts have been made to determine the most effective bubble size for

21. See Equation (20) on page 12 and Equation (21) on page 13.
22. See the discussion of the individual contribution of each of these terms in section 2.4.2 from page 11 onwards.

a given set of flotation conditions. Assuming, for the time being, that bubbles of any size can be produced, arguments have been advanced to show the desirability of having large or small bubbles. Gaudin [1931] realized at a very early stage that:

1) A given volume of air will have more surface if finely dispersed, therefore the amount of solid particles that can be accommodated at its surface as a layer one particle deep (monolayer coverage) is greater,
2) It costs energy to disperse the gas, and the finer the dispersion, the greater the cost per unit volume of gas. It is likely that past a certain dispersion of gas in water, the cost of dispersion increases faster than the gas-liquid surface that is produced by it,
3) Of fully loaded bubbles (monolayer coverage), those having smaller diameters have a greater apparent specific gravity, as may be deduced from the fact that the buoyancy-consuming load of mineral varies as the square of the diameter. Bubbles may conceivably be small enough to have the same specific gravity as the surrounding pulp and therefore no tendency to rise with their mineral load. Such a situation is particularly likely to arise in mechanically agitated machines and may be the source of losses, and
4) Smaller bubbles have a better opportunity to become attached to mineral particles and therefore are likely to result in a slightly higher recovery. This would appear to hold for mechanically agitated pulps as well as for pneumatically aerated pulps.

Bubble break-up and coalescence is caused by (amongst other factors) mechanical agitation and differences in bubble rise velocity. Prince and Blanch [1990] proposed a phenomenological model for the rates of coalescence and break-up in turbulent systems. They found favourable agreement between their model and the behaviour of distilled water and salt water systems (two phase systems). Jordan and Spears [1990] measured the improvement provided by fine bubbles in the flotation of fine-sized particles. A turbulent flow model [23] was fitted to the results and good agreement between model and practice was found.

The effect of bubble size on the rate of flotation of very fine particles (less than 50 $\mu$m) was investigated by Ahmed and Jameson [1985], using quartz, latex and zircon. They used a batch flotation cell in which bubbles of known size could be generated, independently of turbulence levels. Flotation rate was found to be strongly affected by bubble size, there being an increase of up to one hundred-fold when the bubble size was reduced from 655 $\mu$m to 75 $\mu$m. Effects of impeller speed (level of agitation) and

23. This model has been discussed in section 2.4.2.1 on page 13.

particle density were also investigated. The benefit of using smaller bubbles was comparatively reduced with increased agitation. The most likely explanation is that although the frequency of particle-bubble collision increases with agitation, the detachment forces become dominant at fairly high agitation levels due to the effect of turbulence. For light particles of density close to water, high agitation increased the rate of flotation.

Dobby and Finch [1986c] analyzed the interrelationship between gas flow rate, bubble size and bubble collection efficiency in flotation columns. They found that very small bubbles will not always yield higher rate constants in conventional flotation column operation. Their results applied to bubble sizes smaller than 80 $\mu$m.

#### 2.6.2.1 Bubble Size Measurement

Different methods of bubble diameter measurement have been used by researchers. Photographic techniques have been used to obtain valuable information on bubble size, as well as on the mechanism of bubble-particle contacting [Brown, 1965]. The biggest drawback of this method is the restriction of visibility, so that practical three phase systems are virtually out of reach.

A method of direct measurement of bubble size in two and three phase systems has been developed in the Department of Chemical Engineering at the University of Cape Town [O'Connor *et al.*, 1990]. The method is a development of the method of Dunne *et al.* [1976]. Liquid from the flotation cell in which the bubble size is measured is sucked through a capillary. The bubbles present in the liquid are consequently forced into tall cylinders. The length of the cylinders are measured by two electronic eyes on the capillary to give an indication of the bubbles size, and the number of bubbles per unit time is counted. The recorded bubble size data are processed statistically by computer software.

Using this method, Tucker *et al.* [1993a] measured bubble sizes in pyrite-quartz mixtures containing up to 97% quartz. They found the effect of frother type on bubble size becomes less significant with increase in frother dosage in a batch flotation cell. Subsequently Tucker *et al.* [1993b] measured bubble sizes in different flotation cell types. All bubble sizes measured were smaller than 2 mm, irrespective of cell design or frother dosage. A general bubble size of approximately 1 mm was measured in a flotation column, while bubble sizes between 0.3 and 2 mm were measured in a batch cell. The percentage solids in the pulp had a strong influence on the bubble sizes measured in a Jameson cell.

### 2.6.2.2 Bubble Size Estimation

One method used to estimate bubble diameter in flotation columns and mechanical flotation cells is by making use of drift flux analysis [Dobby *et al.*, 1987]. Bubble terminal rise velocity is determined, from which bubble diameter can be calculated using one of several correlations. Bubble diameters estimated using drift flux analysis were found to be within ± 15% of the photographic measurements [Finch and Dobby, 1990]. However, it has been claimed by some researchers [Keuhn Walker *et al.*, 1991] that the use of drift flux analysis cannot give an acceptable estimation of bubble size in co-current downwards flotation columns. The two main reasons for this are that drift flux analysis assumes bubbles to act as solid spheres, which is not always the case [24], and that the effect of frother type and dosage has not been taken into account. A model developed more recently is the one by Zhou *et al.* [1993], which applies to flotation columns [25] only. A good agreement between the prediction from the model and literature data, as well as data from direct photographic measurement was obtained. The model is summarized below.

The upward velocity, $U_{ba}$ in a counter-current two-phase flow system can be written as

$$U_{ba} = U_{bd} + J_g - J_l \tag{66}$$

or

$$U_{ba} = \frac{J_g}{\epsilon_g} \tag{67}$$

where $U_{bd}$ is the bubble drift velocity, which can be determined by

$$U_{bd} = A \frac{[(1 + 3.36\ C_c\ R_v^2)^{0.5} - 1]^2}{(2\ C_c\ R_v)^2} \frac{(1 - k_g\ \epsilon_g)^2}{1 - (k_g\ \epsilon_g)^{5/3}} \tag{68}$$

in which $R_v$ is the bubble radius, $\epsilon_g$ is the gas holdup and $k_g$ is the gas holdup coefficient, related to the bubble arrangements in the column. A is a constant, given as

$$A = \frac{g\ (\rho_l - \rho_g)}{9\ \mu} \tag{69}$$

24. See Figure 4 on page 32 and the discussion of the shape of bubbles at different air flow rates.
25. This method applies to both co-current and counter-current columns.

where $\rho_l$ and $\rho_g$ are the densities of liquid and gas, respectively, g is gravitational acceleration and $\mu$ is the bulk liquid viscosity. $C_c$ is a contamination factor which is a function of frother type and concentration. For Dowfroth 250 solutions of concentration up to 3 cc/100 litres, $C_c$ can be determined as

$$C_c = 110 + 280\ [1 - \exp(-0.55\ C^{0.5})] \tag{70}$$

where C denotes the concentration of frother in the system. For gas holdups less than 30%, $k_g = 0.7$ and Equation (68) can be simplified as

$$U_{bd} = A\ \frac{[(1 + 3.36\ C_c\ R_v^2)^{0.5} - 1]^2}{(2\ C_c\ R_v)^2}\ (1 - 1.06\ \epsilon_g) \tag{71}$$

Substituting Equations (67) and (71) into (66) gives the bubble radius as

$$R_v = \frac{B_c^{0.5}}{(0.84 - C_c\ B_c)} \tag{72}$$

where $B_c$ is a coefficient and can be determined as

$$B_c = \frac{J_g\ (1 - \epsilon_g)/\epsilon_g + J_l}{A\ (1 - 1.06\ \epsilon_g)} \tag{73}$$

for gas holdups less than 30%.

In the case of co-current downward flotation columns, such as Jameson cells, the same approach is followed as in counter-current flow, except that the superficial liquid velocity is larger than the bubble rise velocity, hence relative movement of the bubbles is downwards. Therefore the following relationship can be used to determine the bubble upward velocity

$$-U_{ba} = -J_g + U_{bd} - J_l \tag{74}$$

The minus sign in the equations means that the direction of motion is downward. Using the same analytical treatment as in counter-current flotation columns, the bubble size can be estimated as

$$R_v = \frac{B_d^{0.5}}{(0.84 - C_c\ B_d)} \tag{75}$$

where $B_d$ is determined as

$$B_d = \frac{J_l - J_g\ (1 - \epsilon_g)/\epsilon_g}{A\ (1 - 1.06\ \epsilon_g)} \tag{76}$$

### 2.6.3 Particle Hydrophobicity

The hydrophobicity of particles can be varied by altering the collector dosage or the extent of conditioning. An overview of the effect of particle hydrophobicity on the collection process has been given above [26]. The rate of flotation and therefore the collection efficiency is affected by hydrophobicity through the $E_A$ and $E_S$-terms in Equation (21) on page 13 and therefore also Equation (20) on page 12.

### 2.6.4 Air Flow Rate

Air flow rate is a variable of major importance in flotation kinetics. However, the actual mechanisms by which air flow rate influences flotation kinetics are still incompletely understood [Laplante *et al.*, 1983]. King [1972, 1973b] proposed the following equation for the flotation rate constant

$$K = K_2 A S \phi(D) \tag{77}$$

where $K_2$ is the mass transfer rate constant, A is the bubble surface area per unit volume of pulp, S is the fraction of the bubble surface not covered by adhering particles and $\phi$(D) is a particle size correction factor. A can be given as

$$A = \frac{\sigma \tau G}{V} \tag{78}$$

where $\sigma$ is the bubble surface area per unit volume of air, $\tau$ is the bubble average residence time in the slurry, G is the volumetric air flow rate and V is defined as the pulp volume as before ($\sigma$ and $\tau$ will both vary with G). According to this model, air flow rate affects flotation kinetics because of its influence on the parameter A. Another way of looking at it would be to consider the influence of $J_g$ (which is a linear function of air flow rate) on the first order rate constant in Equation (20) on page 12.

Hydrophobic particles form aggregates with rising air bubbles in the collection zone, after which the particle-bubble aggregates are transported to the froth zone. Because the mass of hydrophobic particles transported to the froth depends on the size and number of bubbles available, it is important to know the air flow rate on which these two variables depend. Unfortunately air rate and bubble size are inseparable from each other [27] in normal flotation applications. The bubble diameter increases with increased gas rate [Dobby and Finch, 1986c]. As air flow rate increases, the total

26. See section 2.3 page 5.
27. A discussed in section 2.6.2 on page 31.

bubble surface also increases, which should increase the flotation rate. However, as mentioned before, higher air flow rate also increases the average bubble diameter, which causes a decrease in the flotation rate. At low air flow rates, the first effect dominates, while the second one is dominant at higher air flow rates. If a system without a froth phase (as used by de Bruyn and Modi [1956] and in this investigation) is considered, a maximum rate of flotation is obtainable at an intermediate air flow rate [Laplante *et al.*, 1983], when the two effects are of equal magnitude. Around this maximum, the effect of changes in air flow rate on flotation recovery is limited.

### 2.6.5 Contacting Intensity

It is possible to vary the contacting intensity between bubbles and particles in certain flotation cell designs. This is achievable in mechanically agitated cells by controlling the impeller speed, while it is possible in a Jameson cell to have conditions of more intense particle-bubble contact by varying the pulp and air flow rates in the downcomer tube [28]. Both of these changes go hand in hand with differences in turbulence. The effect of turbulence has previously been discussed [29].

## 2.7 DESIGN AND OPERATION OF FLOTATION CELLS

It not possible to pin down the "invention" of the flotation process to any single person or date (*any more than the first cuckoo triggers the arrival of Spring* [Kitchener, 1984]). In one of the first papers to be written on flotation, T.J. Hoover [1912] made the following remark:

> *"A new metallurgical process never springs fully developed from the brain of one person, but it is the result of patient investigation, application, and improvement by many minds, during many years."*

He then named 57 people who had made significant contributions to flotation development up until 1912 [Kitchener, 1984]. A better understanding of the fundamentals of the process over the years has led to a shift in interest from fundamental research to that of flotation machine development.

Flotation machines are designed to produce optimum recovery of minerals at as high product grades as possible. An attempt is made for each specific application to reach the most favourable combination of $E_A$, $E_C$ and $E_S$, *i.e.* to produce the most suitable hydrodynamic conditions in the flotation cell. Hydrodynamic conditions include the size of bubbles

28. A discussion of the design and operation of Jameson cells is given in section 2.7.3 on page 44.
29. See the discussion in section 2.4.2 on page 11.

produced, the extent of mixing in the cell, and the intensity of contacting between particles and bubbles.

A wide range of flotation machine designs are now available and most of these are of the mechanical type, but over the past 20 years, many new ideas have been introduced and much activity has gone into the development and demonstration of new types of flotation machines, many of which are column-type devices.

A brief description of the design, operation, and industrial application of some old and novel flotation machines is given in subsequent sections.

### 2.7.1 Mechanical Flotation Cells

Mechanical flotation machines are characterized by a motor-driven impeller that agitates the pulp, suspends the solids and disperses air into the pulp. In normal practice, this machine appears as a vessel having a number of impellers in series. Mechanical machines have an "open" flow of pulp between each impeller or are of "cell-to-cell" designs which have weirs between each impeller. The procedure by which air is introduced into a mechanical cell falls into two broad categories: "self aerating", where the machine uses the depression created by the impeller to induce air, and "supercharged" or "turbocharged", where air is generated from an external blower. The incoming slurry feed to the mechanical flotation machine is usually introduced in the lower portion of the machine [Klimpel, 1987].

The major feature which distinguishes mechanically agitated cells from other cell-types is the high degree of turbulence in the pulp. High intensity of contacting between particles and bubbles promotes the recovery of relatively fine particles, while the solids suspension function of the impeller results in high recoveries of relatively coarse material. Nevertheless, grades are poor due to entrainment of gangue particles.

#### 2.7.1.1 Mechanical Flotation Machine Design

Mechanical flotation machines can be characterised by [Barbery, 1984]:

1) Geometric structure (*e.g.* parallelepiped, cylinder) which defines the overall shape of the cell,
2) Impeller design (impellers are often surrounded by a stator and a diffuser), and
3) Means of air introduction in the cell (diaphragm, diffuser, hollow impeller shaft, pipe located beneath the impeller, *etc.*).

Typical cell geometries are shown in Figure 5 [Barbery, 1984].

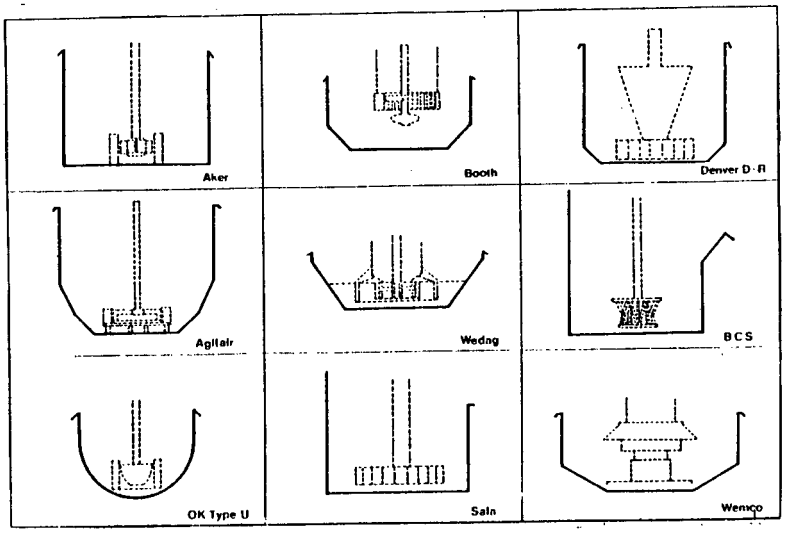


Figure 5 : Cell Tank geometries in Typical Open Flow Mechanically Agitated Flotation Cells.

Some impeller designs which are industrially in use are shown in Figure 6 [Barbery, 1984].

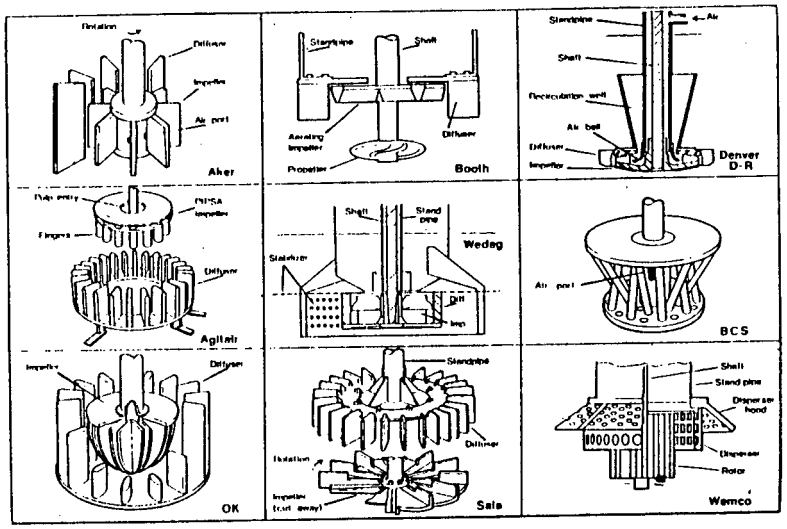


Figure 6 : Impeller Geometries in Typical Mechanically Agitated Cells.

The degree of turbulence created by each impeller type is a function of its specific geometry, the geometry of the cell, rotational speed and air flow rate. Turbulence in mechanical flotation cells is sometimes quantified by the mixing Reynolds number, $Re_m$, which is defined as [Karolat and Hill, 1988]

$$Re_m = \frac{D_i^2 \rho_l \omega}{\mu_l} \tag{79}$$

where $D_I$ is the impeller diameter, $\rho_l$ is the liquid density, $\omega$ is the rotational speed of the impeller (rpm) and $\mu_l$ is the liquid viscosity. It is clear from Equation (79) that specific impeller geometry is not included in this relationship and each impeller type will thus have a correlation of its own.

Different mechanical flotation machines often give plant performances very similar to each other in terms of grade and recovery, independent of their designs and geometry [Klimpel, 1987].

#### 2.7.1.2 Industrial Application of Mechanical Flotation Machines

Mechanical flotation machines are by far the most widely used in the minerals industry [Barbery, 1984]. Novel flotation technology has only recently started taking the place of the mechanical cell in certain applications. It is an open question whether the mechanical cell will ever be completely replaced by novel technology, and it can be expected to continue finding an application in the minerals industry amongst all the new developments a significant period of time.

### 2.7.2 The Column Flotation Cell

The history of column flotation machines apparently began with an invention by two Canadians, Boutin and Tremblay, in the early 1960's [Boutin and Tremblay, 1964]. The column flotation cell is a tall column, usually about 12 m in height, into which conditioned pulp is fed about a fifth of the way down from the top. Air is blown into the column through a diffuser at the base, and wash water is fed above or inside the froth phase.

Column flotation cells have the advantage of high grades which are achievable by proper drainage of entrained [30] gangue particles in the froth due to a high bias rate of wash water. In addition to this, the quiescent contacting environment promotes stability of particle-bubble aggregates which are easily broken up in more turbulent cell environments such as mechanically agitated cells. Despite the high grades and high $E_S$ in these cells, fine particles are difficult to recover because of low contacting intensity between particles and bubbles. On the other hand, coarse particles are lost in the tailings stream due to rapid solid settling, while the action of the impeller in mechanical flotation cells helps to suspend coarse particles. A schematic diagram of a flotation column is shown below in Figure 7 [Finch and Dobby, 1990].

30. A discussion of entrainment has been given in section 2.4.3 on page 23.

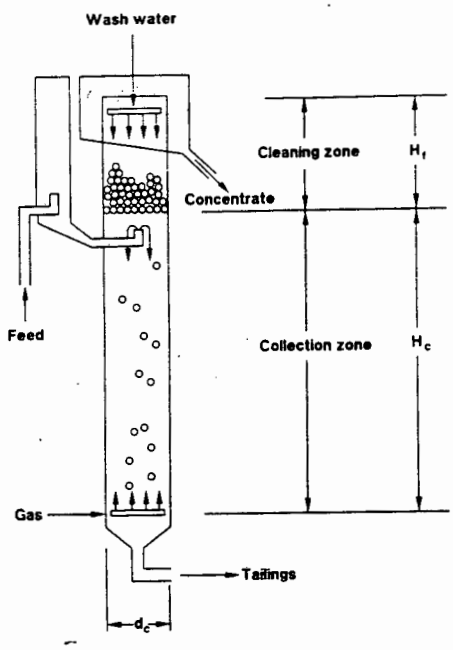


Figure 7 : Schematic Diagram of a Counter-current Flotation Column.

Commercial units were initially constructed as tall rectangular columns, but cylindrical units are now in use as well. Column flotation cells are characterised by a quiescent collection zone, as opposed to the turbulent conditions in a mechanically agitated cell.

Frother is used sparingly in flotation columns in amounts necessary to control bubble size, and a thick froth bed is not desired. The inventors [Boutin and Tremblay, 1964] claim that rising bubbles collect fine gangue particles as a tail (essentially particles that follow in the turbulent wake of the bubble) that would be mechanically entrapped in the froth bed if one were allowed to form. This tail is said to be washed away by the counter-current wash water to give a high-grade concentrate. This unique feature makes columns ideal for cleaning applications [Dobby and Finch, 1986c; Brzezina and Sablik, 1988], although other applications are possible as well. The versatile nature of flotation columns is summed up by Wheeler [1988]:

> *"When used as a rougher-scavenger, the column is excellent; when used as a cleaner, the results can be spectacular".*

### 2.7.2.1 Column Flotation Cell Design

A range of information on the subject of column flotation is available in the literature, but no precise technical data are available for the design and construction of such columns on an industrial scale. For this reason a considerable proportion of the column machines installed on preparation plants are built to suit local conditions, based primarily on the experience and intuition

of the constructor and the plant personnel [Brzezina and Sablik, 1991]. In the proposed designs, the shape of the flotation columns and the point of input of feed and of take-off of concentrate and waste are all very similar. A proposed criterion of length-to-diameter ratios of 10 : 1 typically applies to industrial units [Dobby and Finch, 1986a], although some as low as 5 : 1 have been constructed. The principle difference distinguishing them relates to the method of air dispersion employed [Brzezina and Sablik, 1991].

The objective of bubble generation in column flotation, as in any froth flotation system, is to produce relatively small bubbles at a moderate air rate (typically, superficial gas velocity $J_g$ = 0.5 to 2.0 cm/s). The size of bubbles produced is determined by the type of bubble generation system. Thus, the optimum performance of a flotation column depends to a large extent on the design of the air sparger. Different ways of air sparging have been employed in flotation columns, some of which are listed below [Dobby and Finch, 1991]:

1) Static shear contacting. High velocity contacting of slurry or water and air in an appropriate manner will generate small bubbles. Examples of this mechanism are the use of a pipe containing in-line mixers (patented by Yoon *et al.* [1988]) and the Cominco and USBM turbo-spargers [Tucker *et al.*, 1991].
2) Sparging through porous media without high external shear. This method has been most commonly used in column flotation up to the recent development of other novel methods. Industrial sparging material has typically been pierced rubber or fabric such as filter cloth. Porous spargers unfortunately result in very wide bubble size distributions and an optimum bubble size is therefore difficult to obtain.
3) Sparging through porous media with high external shear. The porous medium is placed in a high velocity slurry line and bubble generation is controlled by both the nature of the medium and the shear action created by the flowing slurry. Examples are the Bahr cell [31] and the Air Sparged Hydrocyclone [Ye *et al.*, 1988].

The intensity of the worldwide research effort devoted to column flotation design is evidenced by the fact that 80 patents were taken out from 1964 up until 1991 [Brzezina and Sablik, 1991].

31. The Bahr cell is discussed in section 2.7.4.6, page 51.

### 2.7.2.2 Industrial Application of Column Flotation Cells

Column flotation took a long time to become accepted by the international mining community. It was only 18 years after the invention of the column that Mines Gaspe' installed the first two commercial units for cleaning of their molybdenum byproduct [Cienski and Coffin, 1981]. They were 18 and 36 inches in diameter, respectively. These two columns replaced 13 stages of conventional cell cleaning [Wheeler, 1988].

The Mount Isa concentrator in Australia serves as another good example of the industrial success of flotation columns as cleaners. In 1986, Mount Isa Mines Limited (M.I.M.) conducted extensive test work with a 50 mm diameter pilot scale column to compare column technology with conventional mechanical flotation machines [Espinosa-Gomez *et al.*, 1988a and Espinosa-Gomez *et al.*, 1988b]. The favourable comparisons led M.I.M. to replace the conventional machines at the lead/zinc concentrator with flotation columns (2.5 m in diameter and 13 m high) to upgrade low grade middlings rougher concentrate to final concentrate (47% Pb + Zn). The commissioning of the columns took place in December, 1987, and an improvement of 2% in overall zinc recovery was obtained, which represented a payback time of one year [Espinosa-Gomez and Johnson, 1989].

Many other applications of column flotation in industry have taken place over the last few years. It has been claimed that when used in copper as a rougher-scavenger, a column will produce a rougher concentrate grade double that of the conventional rougher cells and produce a tailing equal to those of the scavenger cells. One pass in the column equals 2 to 5 stages of conventional copper cleaning [Wheeler, 1988]. Substantial capital and operating cost savings have been reported after replacing conventional mechanical flotation cells with column technology in industry [Nevell, 1990; Jacobi *et al.*, 1991].

## 2.7.3 The Jameson Cell

The Jameson cell (or short column cell) has been hailed as a major breakthrough in flotation technology. Jameson [1988] noticed that a very large portion of the volume of flotation columns is taken up by liquid (typical column cells are up to 13 m high, with a froth layer of less than 1 m). He invented a new column cell in which the froth zone is very similar to that of normal flotation columns, but in which the volume occupied by the liquid has been reduced to the absolute minimum [Jameson, 1988].

### 2.7.3.1 Jameson Cell Design

A diagram of a Jameson cell is shown in Figure 8 [Kennedy, 1990]. The cell is divided into two main zones, one for contacting and the other for concentrate cleaning. Contacting takes place in the downcomer where the feed slurry and air are intimately mixed. This is achieved by supplying a high pressure feed to the cell. This pressurised input provides the motive energy for mixing and is let down through an orifice plate into the downcomer.

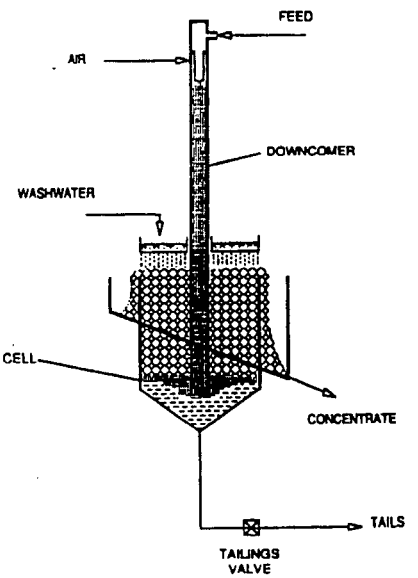


Figure 8 : Schematic Diagram of the Jameson Cell.

The resultant plunging jet of liquid shears and then entrains air that is naturally drawn into the cell. The froth produced is characterised as having a 60% voidage and a mean bubble size of about one third that achieved in a conventional column.

Owing to a high mixing velocity and a large interfacial area, there is rapid contact and capture of particles by the bubbles. The concentrate laden froth is discharged from the bottom of the downcomer where it enters the quiescent portion of the cell. As the froth rises it is washed by a counter-current flow of water supplied from the top of the cell. A high purity concentrate is collected and overflows the top weir lip. Tailings flow to the base of the cell from which they are discharged [Jameson and Manlapig, 1991].

In a conventional flotation column, the liquid descends quite slowly whereas the bubbles are free to rise upwards. In the case of the Jameson cell, the downward velocity in the downcomer is chosen such that all bubbles have to descend in the

downcomer and emerge at the bottom. The orifice plate and hole diameter are critical parameters in the design of the downcomer tube. The effect of chamber volume and diameter on bubble formation at plate orifices has been investigated by Antonaidis *et al.* [1992].

Jameson cells are much shorter than column cells because of the decrease in pulp volume. Instrumentation required to operate the cell is limited to an air rotameter at the air inlet line and a level controller to maintain a constant pulp level. Another advantage is the lack of moving parts in the Jameson cell, which makes it easy to maintain [Jameson and Manlapig, 1991].

#### 2.7.3.2 Industrial Application of Jameson Cells

The Jameson cell is used in full scale plant operations in lead, zinc, copper and coal flotation, with installations scheduled for nickel [Jameson and Manlapig, 1991]. A significant increase in concentrate grade was obtained without a major increase in recovery at Peko Mines, where Jameson cells replaced mechanical cells. The Jameson cells outperformed column cells during pilot plant test work. It also meant shorter construction and installation times and lower capital cost, compared to that of column flotation cells [Jameson, 1991].

### 2.7.4 Other Cell Designs and Flotation Technologies

Many important new developments have taken place in the field of cell design, some of which have been industrially exploited, while others are still in a laboratory test work phase. A few of these novel developments are discussed below.

#### 2.7.4.1 The Deister Flotaire Column

The Deister Flotaire Column was invented by Hollingsworth and Sapp of Phoslab, Inc. [Brezezina and Sablik, 1988]. Flotaire columns are categorized as "first generation" and "second generation" columns. First generation Flotaire columns employ high pressure water, in which frother is dissolved, to generate air bubbles by aspiration into surface tension lowered water. The bubbles are less than 50 $\mu$m in diameter. No froth washing water is generally used. The first generation columns were commercialized in 1979 to recover coarse and hard-to-float phosphate minerals [Zipperian and Svensson, 1988] because of the poor performance of column flotation cells in the coarse particle region. A diagram of a first generation Flotaire cell is given below in Figure 9 [Miller, 1988].

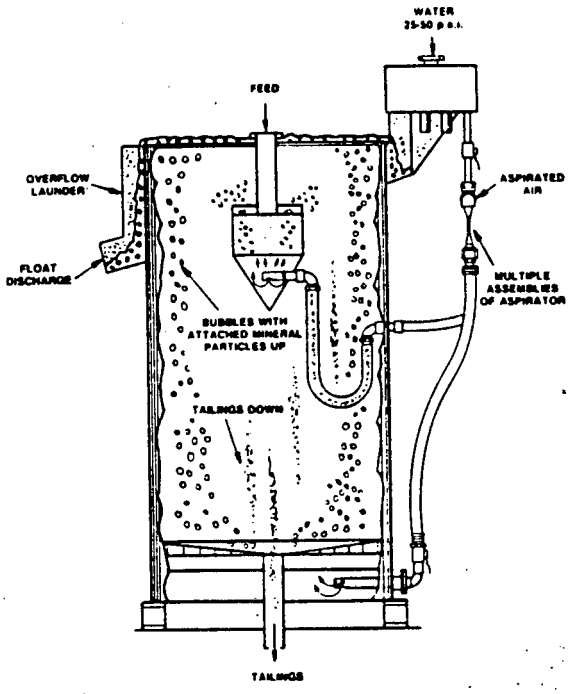


Figure 9 : Schematic Diagram of a First Generation Flotaire Cell.

Second generation Flotaire cells employ dual aeration systems. Some of the bubbles are generated by aspirating surface tension lowered water into air, and are less than 50 $\mu$m in diameter, while additional plus 100 $\mu$m bubbles are supplied by micro diffusers [Zipperian and Svensson, 1988]. A diagram of a second generation Flotaire cell is shown in Figure 10 [Miller, 1988].

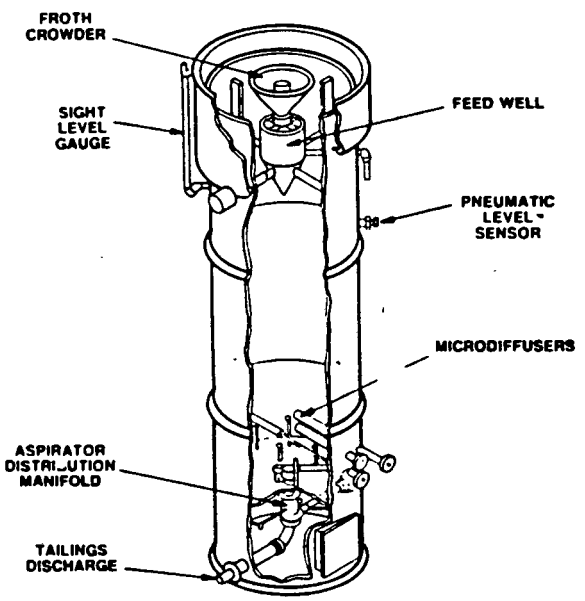


Figure 10 : Schematic Diagram of a Second Generation Flotaire Cell.

Froth washing water is generally used at a rate equal to the froth overflow water. Several commercial second generation Flotaire column flotation machines started

operation in 1986 for flotation of sulphide, coal and metallic oxide minerals [Zipperian and Svensson, 1988].

### 2.7.4.2 The Packed Column

The packed column (or static tube flotation system) was originally conceived in the late 1970's to treat finely ground iron ores and was later developed by David Yang of Michigan Technological University. The unique feature of this column is its packed-bed design permitting an unlimited froth bed height with counter-current water washing for effective processing of fine particles [Yang, 1988]. The system functions efficiently because intimate bubble-particle contact is achieved by the packing design which has no moving parts and requires no ancillary bubble generator. The packing enhances the probability of collision of fine particles with bubbles, which is normally much lower than for coarse particles in normal flotation operations [32]. A schematic diagram of the packed column is shown in Figure 11 [Miller, 1988]

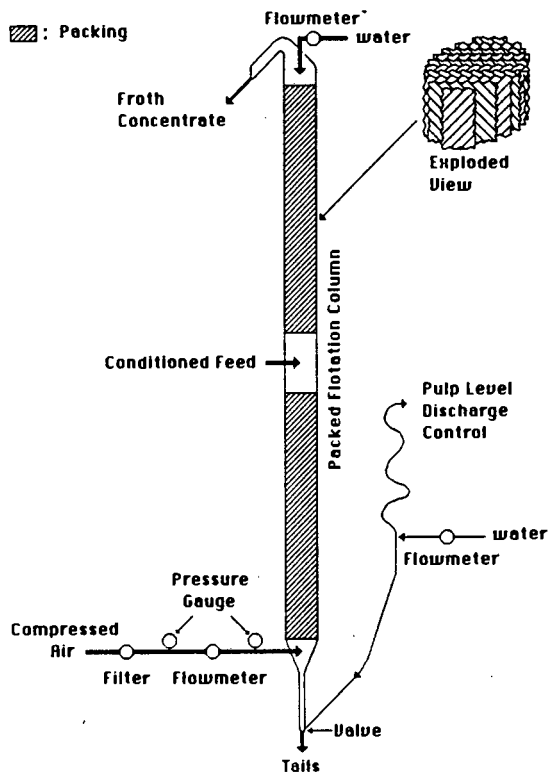


Figure 11 : Packed Flotation Column.

To date, the packed column has been successfully used on a pilot scale for flotation of iron ores, coal, copper ores and other non-metallics [Yang, 1988].

32. A discussion of the collision efficiency is given in section 2.2 on page 5 and section 2.4.2.1 on page 13.

### 2.7.4.3 The Wemco/Leeds Column

The Wemco/Leeds Column was conceived at Leeds University in England, in the early 1950's for the purpose of improving the "release" analysis technique for flotation [Degner and Sabey, 1988]. It was mainly designed to improve the poor grades that are typical of mechanically agitated cells. In contrast to the open rectangular (or square) and cylindrical columns, the Leeds column contains a series of horizontal tubular barriers or baffles designed to strip away the gangue material from the air bubbles as they rise to the top of the column. Typically, four to six horizontal baffle sets are arranged above a mechanical agitator or impeller, although the impeller is not an essential feature of the invention [Miller, 1988]. The arrangement is shown in Figure 12 [Miller, 1988]

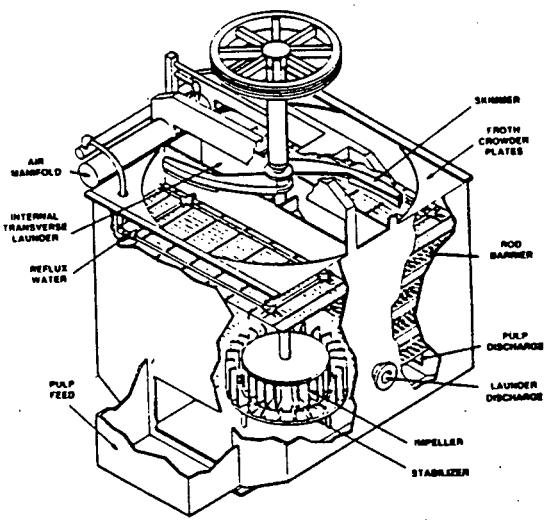


Figure 12 : The Wemco/Leeds Flotation Cell.

In each rod barrier set, the top rod has a density slightly greater than that of slurry, while the lower rod has a density slightly lower than that of slurry. Therefore, when the chamber is full of slurry, the two sets of bars are pushed together by their buoyancy (or lack of it), which results in a hydraulic pinching force between the rods, with the resulting effect of stripping the lightly held gangue material from the air bubbles as they pass through the oscillating and rotating rod sets. Wash water added above the top baffle percolates downward through each baffle set, carrying the disengaged material towards the rotor and from the cell. The Wemco/Leeds column is not much taller than the conventional flotation machine. This technology has been used in industry for the flotation of coal and produced high-grade concentrates [Degner and Sabey, 1988].

#### 2.7.4.4 The Hydrochem Flotation Column

Hydrochem Developments Ltd. has developed and put into full scale operation a novel type of flotation column, which is likened to a bank of mechanical flotation cells turned on end with a common shaft down the centre and with concentrate being produced only off the first cell lip. It is claimed that this arrangement results in a great degree of agitation simplicity and space economy. Also, the so-called hydrofoil impeller ensures low power consumption. Other characteristics of this flotation column include a low height to diameter ratio and the possibility of modifying impeller geometry and operation to suit specific flotation requirements. The design of the Hydrochem column is sensitive to variations in the flotation requirements down the length of the column: impellers of different designs may be housed in each unique zone in the column.

The Hydrochem cell outperforms conventional mechanical machines by far [Schneider and van Weert, 1988]. A commercial unit is currently handling up to 100 tonnes per day rougher concentrate at Dickenson Mines Limited, Balmertown, Ontario.

#### 2.7.4.5 The Pneumatic Flotation Column

The pneumatic flotation column has a cylindrical shape with a tapered bottom. The upper part of the column is equipment for preliminary physicochemical preparation of the feed and for delivering it to the flotation machine, while a system of cyclone aerators serving to provide suitable aeration of the pulp in the machine, is situated in the lower part.

An internal circulation pump recycles a fraction of the tailings to the aerators, while compressed air is fed to the aerators through a special pipe section. After preliminary aeration and mixing with flotation agents, the feed is delivered to the column at a point about 1/3 of its length from the top of the cell. The concentrate overflows over the cell lip, while tailings is removed at the bottom of the cell [Brzezina and Sablik, 1991].

The unique design of this cell addresses the problem of low recoveries in the ultrafine particle size region, while selectivity is still reasonably good.

A diagram of a pneumatic flotation cell is shown below in Figure 13.

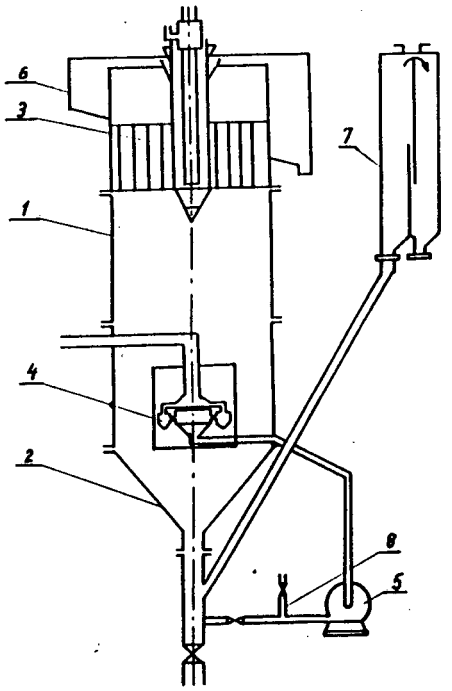


Figure 13 : Diagram of the Pneumatic Flotation Column.

#### 2.7.4.6 The Bahr Cell

The Bahr cell is essentially a column cell with a modified air sparging system. Slurry is passed through many cylindrical, porous plastic elements. High shear is created using small diameter sparging elements and thereby developing a very high slurry line velocity. The small bubbles created in this cell enhance the recovery of fines. It has been introduced as industrial units for coal flotation in Germany and phosphate flotation in Brazil [Dobby and Finch, 1991].

### 2.7.5 Combination of Cell Technologies

The cell designs which have been reviewed have very different geometries and ways of operation. The particle-bubble contacting environments in these cells have unique properties which address different problematic aspects of particle-bubble contacting. To house different cell technologies, each of which has unique advantages, optimally in one single vessel is an impossible task. A possible solution is to combine the most prominent feature of each type of cell into one workable unit. Such flotation devices have been designed and, although mostly used on a pilot plant scale, some of them have been used industrially for some time now. A brief discussion of such systems is given below.

The Hydrochem cell [33] is a good example of a "hybrid cell" which has had industrial success.

A novel agitated bubble column was designed by Karolat and Hill [1988] for the purpose of potash flotation. The laboratory scale column had one double blade impeller at the bottom of the column, which was baffled in this section. A diagram of this cell is shown in Figure 14.

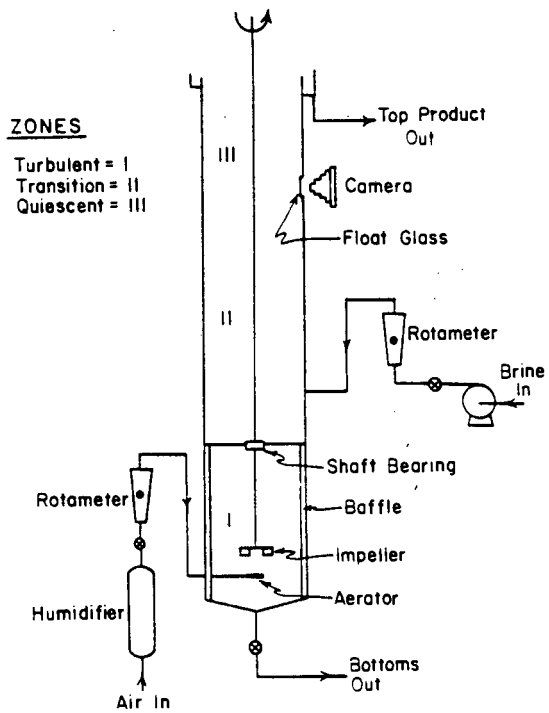


Figure 14 : Agitated Column for Potash Flotation.

It was found that the mean diameter of bubbles which were produced in the column could be predicted from gas holdup using empirical correlations which apply to aerated, agitated tanks. The column produced both high recoveries (>90%) and grades (>97%).

Harris *et al.* [1992] compared the performance of different cell technologies with the emphasis on the recovery of different particle sizes in the respective cells. They compared the performance of a conventional laboratory batch flotation cell and a laboratory scale column cell with that of a hybrid cell, which was essentially a combination of the first two, *i.e.* an agitated stage (laboratory batch cell) was connected to a quiescent stage (column cell) by installing the column cell on top of the batch cell. A diagram of these different systems is shown below in Figure 15.

33. The design and operation of the Hydrochem cell has been discussed in section 2.7.4.4 on page 50.

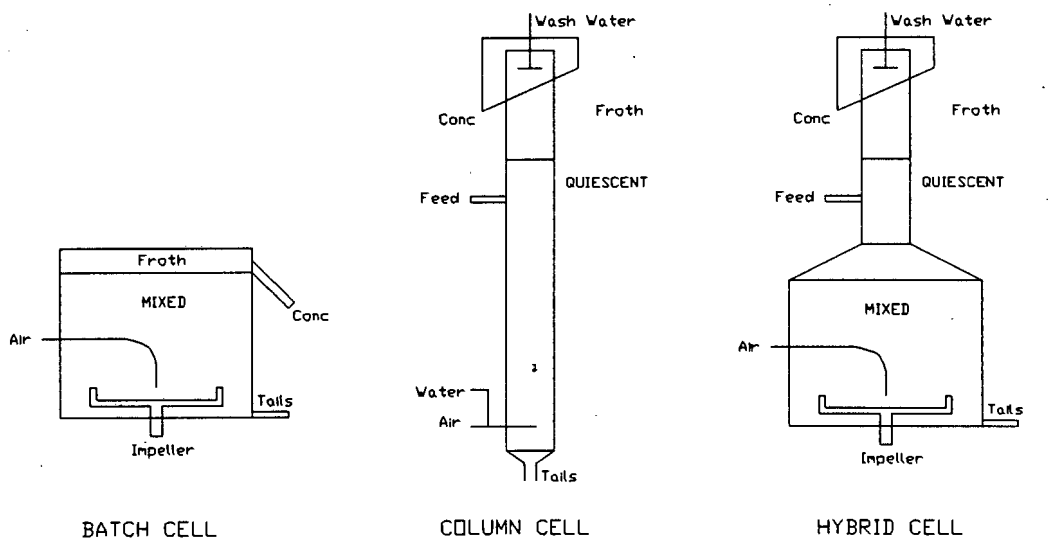


Figure 15 : Schematic Diagram of the Different Cell Configurations used by Harris *et al.* [1992].

This thesis was essentially an extension of the work of Harris *et al.*, although the flotation experiments were done with a shallow froth to be able to concentrate on the collection zone during this work, while their flotation experiments were carried out with a deeper froth bed. Although Harris *et al.* floated coal, which is a more complex ore than quartz because of variations in ash content, their results and findings which were relevant to this thesis are summarized below.

Good performance with respect to recovery of particles was obtained for both coarse (+150 $\mu$m) and fine (-25 $\mu$m) particles with a conventional batch laboratory cell. Selectivity was found to be poor in the fine particle region owing to the entrainment of fine gangue particles, resulting in concentrates with high ash contents. On the other hand, the column cell achieved excellent recoveries and high grades with particles finer than 150 $\mu$m, at the cost of high losses in recovery in the coarse +150 $\mu$m particle size range.

It was demonstrated that the addition of an agitated stage to a column cell significantly improved the recovery of coarse particles in comparison with the conventional column cell, while maintaining good selectivity in the fine particle region. The improved recovery of coarse particles in the agitated cell relative to the column cell was explained by an increase in the residence time of these particles due to the action of the impeller. The increased grades relative to the laboratory batch flotation cell was attributed to better drainage of entrained particles by washing of the froth.

## 2.8 SUMMARY

The performance of a flotation cell is influenced by many variables, such as particle size, the degree of hydrophobicity of the particles, air flow rate and bubble size, to name but a few. The collection zone recovery is influenced by the first order rate constant, conditions of mixing and the mean residence time of pulp inside the vessel. The rate constant is a function of the bubble size, the air flow rate, and the particle collection efficiency. Particle collection efficiency, in turn, is influenced by three factors

1) The collision efficiency, $E_C$,
2) The attachment efficiency, $E_A$, and
3) The fraction of particles which stay attached to a bubble throughout the entire collection process, $E_S$.

Each of these three efficiency terms is again dependent on some or all of the variables mentioned above, which may explain why different flotation machine designs, which employ *different particle-bubble contacting environments*, perform differently.

The success of the column flotation cell, which produces higher product grades than conventional mechanical cells for equivalent recoveries has led to the design of a wide variety of new cell types that have typically sought to improve one or more aspects of the conventional column cell design. These devices utilize different particle-bubble contacting environments which were tailored for different applications. Some of these machines are in operation on plants in industry, while others are still applied on a pilot plant scale.

A hybrid cell which combines the essential features of a conventional mechanical cell and a flotation column has been developed and found to produce the best features of each system when operated individually.. The remainder of this thesis will investigate the effect of different particle-bubble contacting environments, produced using different flotation cell technologies, on flotation performance (and more specifically particle collection efficiency).

# CHAPTER 3
# DESIGN AND OPERATION OF EXPERIMENTAL EQUIPMENT

## 3.1 INTRODUCTION

This Chapter describes the equipment used and the way in which it was operated during the experimental work which was done for this thesis. Details of the design of the equipment are given first, after which the way in which it was operated and the data were analyzed, is discussed.

## 3.2 HYBRID FLOTATION COLUMN

A multipurpose laboratory scale flotation column was designed and constructed for this investigation. It could be run as a standard column flotation cell, a mechanically agitated column cell [34], or a Jameson-type flotation cell [35]. A series of flotation tests, representing a wide spectrum of flotation conditions, was carried out using each of the three cell configurations. Comparative tests were done in a laboratory batch subaeration flotation cell.

### 3.2.1 Design of the Hybrid Column Flotation Cell

The hybrid column cell was 2 m long and had an inside diameter of 100 mm. It was designed to be easily interchangeable between the three different cell configurations by utilising specific equipment. Poly Vinyl Chloride (PVC) was chosen as the chief material of construction because of its low cost, relative ease of machining and transparency. The column comprised three sections:

1) a top froth launder section,
2) a middle section, and
3) a bottom section containing a removable air sparger system.

#### 3.2.1.1 Top Froth Launder Section

The top froth launder section was manufactured as a separate, replaceable unit. A larger launder could be installed if a more stable froth than that of the quartz-amine system was obtained, for example in the flotation of fine coal [Harris *et al.*, 1992]. This section was bolted onto the rest of the column by means of

---

34. A column cell containing an agitator shaft and impellers to provide turbulence in the column.
35. See section 2.7.3 on page 44 for a description of the design and operation of Jameson Cells.

flanges, with rubber o-rings in-between to keep the column water tight [36]. A diagram of this section is shown in Figure 16.

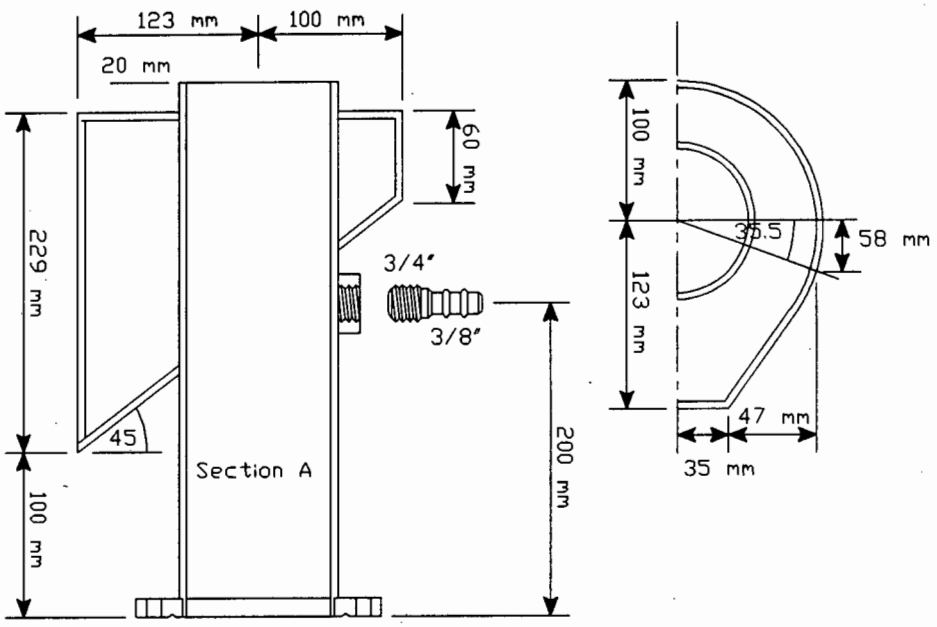


Figure 16 : Top Section of the Hybrid Column and Froth Launder Design.

The pulp feed point to the column was located in the top froth launder section, positioned as close as possible to the top of the cell to maximize the pulp residence time in the column. This placed a limit on the achievable froth depth. The maximum froth depth of 130 mm was more than sufficient for the purposes of this investigation, since a froth depth of 20 mm was maintained throughout the test work. Unlike the rest of the column, the froth launder was manufactured out of perspex. The slide angle was 45° which was relatively steep compared to other flotation columns of this scale. The increased slide angle reduced froth residence time in the launder by enhancing the movement of froth down the launder after overflow, and eliminated the need for wash water during sampling. The shape of the launder was modified to have straight walls up to the point of froth exit to prevent the usual problem of accumulation of froth in corners.

### 3.2.1.2 Middle Baffled Section

The middle section consisted of two cylindrical sections, which were held together with flanges as were all other sections of the column cell. A diagram of the two middle sections is shown below in Figure 17.

36. See Figure 18 on page 58 for a diagram of the design of a flange and the positioning and dimensions of the rubber o-ring.

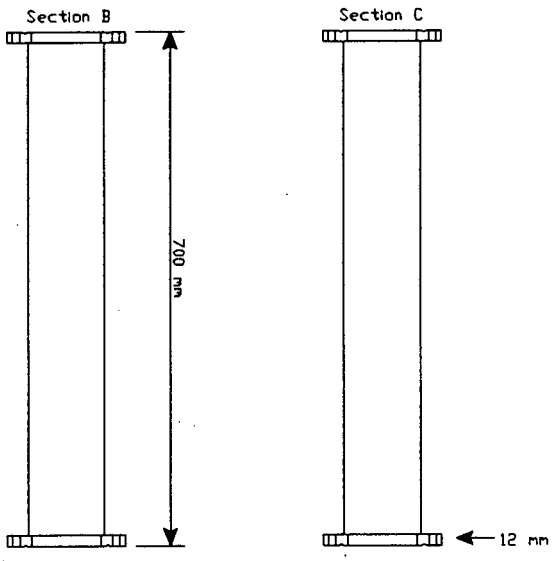


Figure 17 : Middle Sections of the Hybrid Column (Baffles not shown).

The middle section was divided in two so as to have an additional point of support for the impeller shaft when the agitated cell mode was used (impeller shaft supports were positioned between the flanges). The steel shaft was heavy and instability at a high rotational speed would have resulted in damage or destruction of the column [37]. Three points of support down the length of the column were adequate to ensure stable operation at all levels of agitation speed.

Four baffles were built into both middle sections of the column at 90° angles to improve mixing and to prevent a spinning motion of pulp in the column when the agitator was in use. The baffles were 10 mm wide and 1 mm thick stainless steel strips. They were bolted onto the column walls with stainless steel bolts. The baffles covered the entire length of the middle section in which the impellers were positioned and were not removed if the cell configuration was changed from the agitated to the column or Jameson cell mode. The baffles were assumed to have no disrupting effect on the pulp and bubble streams which moved counter-currently in a vertical direction, *i.e.* they were assumed not to interfere with the operation of the column or Jameson cell configurations.

### 3.2.1.3 Bottom Air Sparger Section

The bottom section of the column housed the air sparger mechanism, which was removed when the Jameson cell configuration was operated, and the sparger point

37. PVC is brittle and shatters on impact.

(top port) closed with a PVC plug [38]. The lower port was used for tailings removal. A diagram of the bottom section of the column is shown in Figure 18.

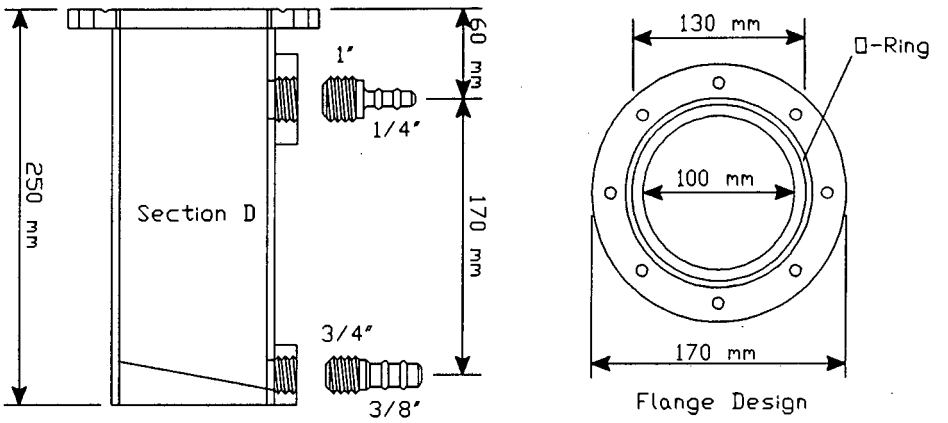


Figure 18 : Bottom Section of the Column and Flange Design.

The bottom of this section was inclined to prevent the build-up of solids, due to solid settling, in the bottom of the column. Solid settling was significant with the flotation of coarser particles and the tubes easily blocked up if the pump rate of pulp was not high enough.

### 3.2.1.4 Column Internals

#### 3.2.1.4.1 Air Sparger Systems

A filter cloth sparger was manufactured out of copper tubing and filter cloth material. The filter cloth was wrapped around the perforated tube, sewed into an envelope and glued into position. The tube was welded onto a 1 inch copper plug which fitted into the top port of the bottom section of the column cell. A glass disc air sparger system was designed in addition to the filter cloth sparger. Glass discs aerators produce narrower bubble size distributions than filter cloth spargers, and are preferable if bubble size measurement is to be done. Discs with five different porosities (0-4) were glass-welded into custom-made glass casings which were attached to glass tubes. The glass tubes were fitted into a 1 inch PVC fitting which screwed into the same position as the filter cloth sparger. This PVC fitting had two rubber o-rings on the inside to keep the system water tight [39].

38. Air and pulp was fed to the column through the downcomer tube and not through the usual feed point.
39. The rubber o-rings in the PVC fitting are not shown in Figure 19 on the next page.

The filter cloth sparger was used throughout the investigation, as bubble size was not one of the key manipulated variables.

A diagram of these two air sparger systems is shown in Figure 19.

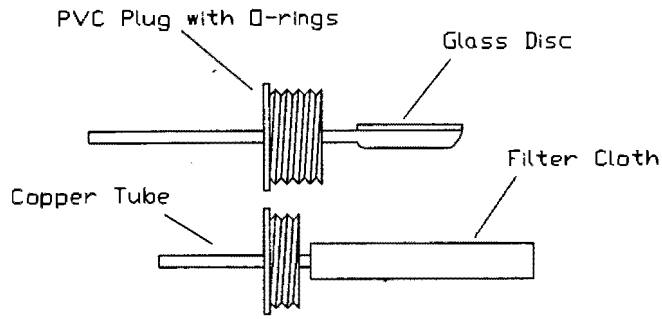


Figure 19 : Air Sparger Systems Designed for use in the Hybrid Column Cell.

### 3.2.1.4.2 Impeller System

The impeller system used in the agitated column mode of operation consisted of a 2 m long stainless steel shaft to which impellers could be attached. The impellers could be positioned at any point along the length of the 2 m long shaft. To avoid a pulp pumping action in an axial direction, the impeller blades were not of the classical propeller type, but were of similar design to those normally used in laboratory batch flotation cells. The sole purpose of the impeller system was to provide a particular degree of turbulence in the cell, and not to suspend the solids. The pulp moved counter-current to the air bubbles in a downwards direction and suspension of solids was consequently unnecessary in the hybrid column cell. Pulp suspension, along with the creation of turbulent conditions are both functions of impellers in mechanical flotation cells [40]. The impeller blades were removable from the stainless steel collars which they were fixed to by simply unscrewing them, and were replaceable with any other design. This allowed versatility of impeller design (*e.g.* flat blade or propeller) and number of blades per impeller (2 or 4). Five impellers were made, but only four were used during the investigation: two impellers per middle section [41], equally spaced along the length of the section. A diagram of the impeller design and their positioning relative to the baffles is shown below in Figure 20.

40. See section 2.7.1 on page 39 for a background on mechanical cell operation.
41. See section 3.2.1.2 on page 56 for a description of this section.

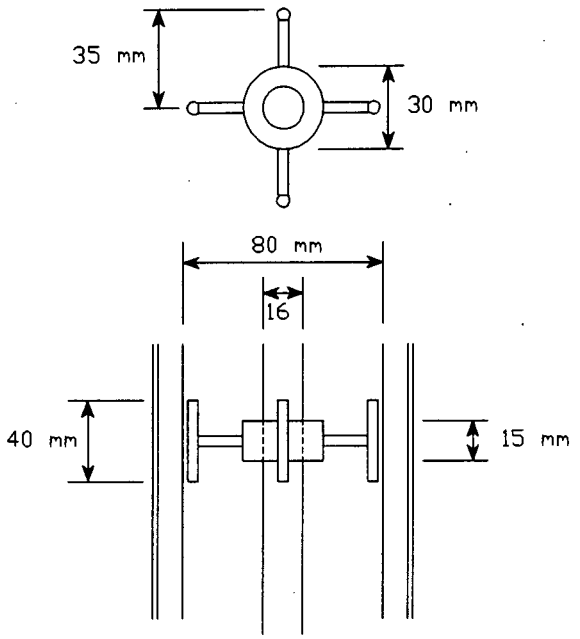


Figure 20 : Impeller Design and Positioning in the Baffled Column Sections.

### 3.2.1.4.3 Agitator Supports

The agitator shaft was supported at three points down the length of the column by means of nylon [42] collars which were fitted inside stainless steel supports. The nylon collars were replaceable after being worn out due to solid grinding between them and the agitator shaft. A diagram of the design and dimensions of the stainless steel supports and nylon collars is shown in Figure 21.

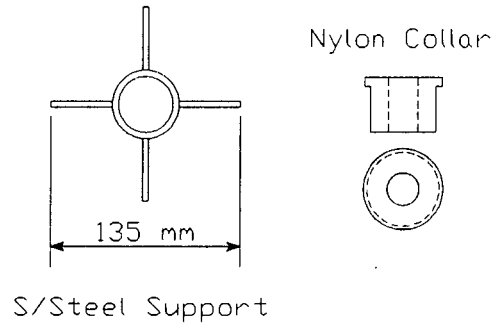


Figure 21 : Design of Nylon Collars and Steel Supports.

The steel supports were secured in position by clamping them between the flanges of the different sections of the column. Slots were made in the flanges for the four steel rods of the agitator supports, so that the column was still kept water tight by the rubber o-rings between the flanges. They

42. Nylon is a relatively hard material and was therefore suitable for this application.

were not removed when the Jameson cell configuration was used, although the nylon collars were removed. The Jameson downcomer tube was positioned inside the rings of the steel supports, which ensured that the Jameson downcomer tube was centred in the column [43]. The supports were removed when the column cell configuration was in use.

### 3.2.1.4.4 Jameson Downcomer Tube

The Jameson cell downcomer tube was designed to provide proper mixing of air and pulp at the conditions under which the column was operated. A diagram of the Jameson downcomer tube design is shown in Figure 22.

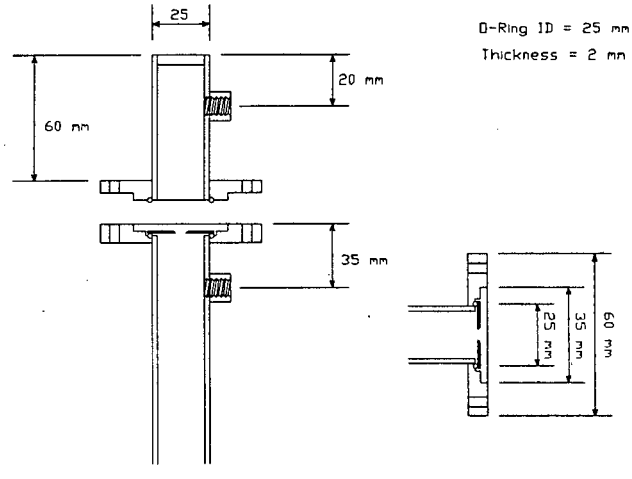


Figure 22 : Jameson Downcomer Tube.

The dimensions of the orifice plate and hole, as well as the positioning of the pulp and air feed points, were adapted from a system of similar scale used previously in on-site test work [Harris *et al.*, 1994]. The orifice plate was clamped in-between two flanges and was kept water tight with two rubber o-rings, one on either side of it. Apart from the orifice plate and o-ring, the downcomer tube was made out of PVC because transparency of the tube was a requirement for operation of the Jameson cell. The downcomer tube was positioned inside the column in such a way that the exit of the tube was at exactly the same height as the air sparger position. Although the Jameson cell represented a totally different mechanism of particle-bubble contacting, it was attempted to design the hybrid cell to maintain similar geometry as far as possible. A diagram of the length and positioning of the tube is shown below in Figure 23.

43. The downcomer had an outside diameter slightly smaller the inside diameter of the steel supports.

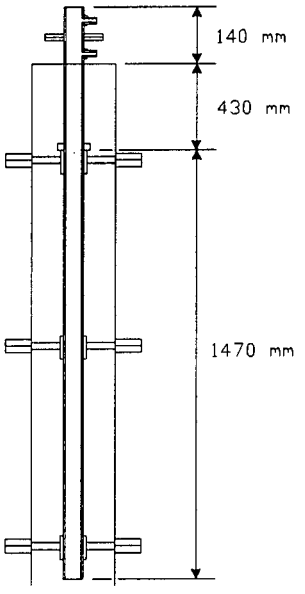


Figure 23 : Length and Positioning of the Jameson Downcomer Tube in the Column.

### 3.2.2 Column Accessories

A description of column accessories and the auxiliary equipment necessary to run the hybrid column cell is given in subsequent sections.

#### 3.2.2.1 Level Control System

The column cell was equipped with an electronic PI level control system [44] which was able to maintain a constant pulp level very effectively, irrespective of the degree of turbulence or the chemical conditions in the column. The conductivity of the pulp was measured and converted to a level signal by the controller. The conductivity was measured with two resistance wires which were placed along the entire length of the column. The level controller wires were attached to two stainless steel rod extensions at the top of the column to keep them taut and to prevent them from getting entangled with the agitator blades when the mechanical agitator was in use. In addition to its automatic control function, the controller facilitated manual control of the pulp level in situations where the conductivity of the pulp or liquid in the column changed during a specific flotation experiment, *e.g.* when electrolyte tracer was injected into the column feed line during residence time distribution measurements.

44. This system was an in-house development of the Chemical Engineering Department at the University of Cape Town.

### 3.2.2.2 Agitator System

An electric motor was mounted above the column to drive the agitator system when the agitated cell configuration was in use. It could be removed from its steel frame when the other cell configurations were in use. The motor was driven by an electronic frequency controller [45], with a maximum agitation speed of 1500 rpm. Agitation speed could be selected by using a calibration curve which transformed the digital frequency reading to rounds per minute (rpm).

### 3.2.2.3 Column Extension

A 2 m extension was manufactured out of PVC to enable the column volume to be doubled if a higher pulp residence time was required. This extension could be inserted between the lower middle and bottom sections of the column cell to still have the three points of support for the agitator shaft and the Jameson cell downcomer tube. The level controller wires would have to be extended when the extension was in use. It was not used during this investigation, as the influence of cell volume was not investigated.

### 3.2.2.4 Other Auxiliary Equipment

Two Watson Marlow peristaltic pumps were used as feed and tailings pumps. A 50 l plastic tank, which was equipped with a mounted electric motor with a two-blade agitator was used as a feed tank. The mounted agitator had a fixed agitation speed of 1470 rpm. A large plastic tank was used as a discharge tank.

### 3.2.2.5 Hybrid Column Rig

An experimental rig was constructed which housed the hybrid column cell with all its auxiliary equipment. Rubber tubing was used to connect the column cell, pumps, ball valves and tanks to each other. It was possible to run any of the three cell configurations by choosing different combinations of valves.

Compressed air was fed to the hybrid column through a rotameter, while the desired amount of water was fed to the feed tank prior to each flotation experiment. A diagram of the rig is shown below in Figure 24.

45. The frequency controller was supplied by Telemechanique and electronically simulated three phase power from two phase supply.

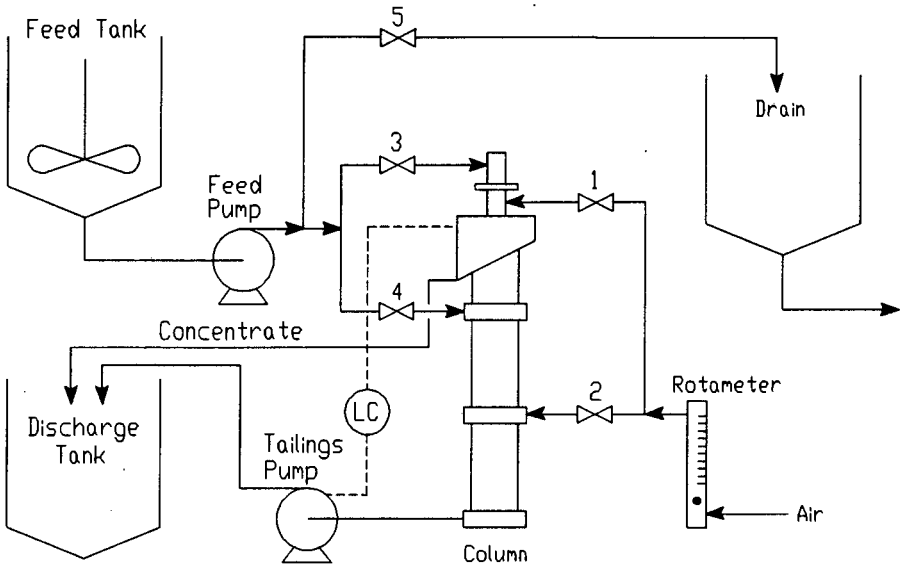


Figure 24 : Diagram of the Hybrid Column Rig.

## 3.3 LABORATORY BATCH FLOTATION CELL

The laboratory batch cell was of the "open-top" Leeds-type, with a volume of 3 litres. It was equipped with a variable speed agitator system. Air was fed at the bottom of the cell through a stainless steel tube and was dispersed by the impeller. Air flow could be varied with a rotameter. Froth removal was done with a scraper. Pulp level in the cell could be kept constant, even with sample removal, by a constant head device. A detailed description of the laboratory batch cell has been given elsewhere [Franzidis *et al.* [1991].

## 3.4 BUBBLE SIZE ANALYZER

The bubble size analyzer which was developed at the University of Cape Town [46] was used to measure bubble size during some of the column and Jameson cell flotation experiments. It was able to measure bubble size in two and three phase systems. Measurement in three phase was done by adding a sampling column to the measurement device. A description of its design and operation has been given elsewhere [Tucker *et al.*, 1994].

## 3.5 AUXILIARY EQUIPMENT

Equipment which was not directly used in flotation experiments, *i.e.* for measurement and ore preparation is described in the following sections. The procedures employed when using this equipment are described in Appendix B on page 163.

46. A discussion of the application of this system has been given in section 2.6.2.1 on page 34.

### 3.5.1 Equipment used for Sizing and Preparation of Quartz

1) A 300 mm diameter Polaris laboratory scale mill was used when size reduction of quartz was necessary. The milling media was either steel balls of different sizes (ranging from 20 mm to 60 mm) or steel rods of uniform size (25 mm in diameter). The rods weighed approximately 1.1 kg each. This mill was also used to establish milling curves.
2) A laboratory scale screening machine was used to divide quartz into four different particle size fractions. 500 mm diameter screens were used in the machine.
3) An Eriez Magnetics 10-cup rotary sample splitter was used to split quartz samples and to prepare representative samples.
4) A root two series Tyler sieve configuration was used to determine the size distributions of different quartz particle size fractions. An Eriez Magnetics rotating sieve shaker was used in conjunction with the sieves.
5) A Malvern particle size analyzer was used to determine the particle size distributions of particles smaller than 106 $\mu$m. Quartz was calcined in a Carbolite laboratory furnace.

### 3.5.2 Equipment used for Measurement

1) A Hanna digital electronic pH meter was used to determine the pH of flotation pulp or other solutions. It was calibrated using buffers of pH 4, 7 or 10, depending on the measured pH range.
2) The rotational speed of equipment like the mill and agitators in the different cell types was measured with an electronic Veeder Root optical tachometer.
3) A two digit Mettler laboratory scale was used to determine the mass of samples and to weigh the quartz which was to be floated, while a four digit Mettler laboratory balance was used to measure the mass of chemicals.
4) The absorption of clear liquid samples was measured with a Cary UV-visible spectrometer.
5) Temperature was measured during the calcination of quartz by a thermocouple inside the furnace.

## 3.6 OPERATION OF THE HYBRID COLUMN FLOTATION CELL

Froth phenomena are complex [Goodall *et al.*, 1988], and it was decided to concentrate on the collection zone alone by keeping the froth depth shallow (20 mm). It was assumed that the dropback of particles from the froth to the pulp would be negligible if the froth depth was

as small as 1% of the column length. This assumption is discussed in detail on page 12 where the significance of Equation (19) is discussed.

It was initially proposed to run the cell in semi-batch mode [47] by recycling the tailings and concentrate streams to the feed tank. The motivation behind this would be to minimize the consumption of ore, and to reach steady state, after which additional changes could be made to the system (*e.g.* to add more collector or to change the air flow rate). Two flotation experiments were carried out in the column cell configuration using the recycle configuration. The +106 -150 $\mu$m particle size fraction was floated and 10 second samples of the flotation concentrate were taken at 10 minute intervals. The absorbance of the liquid phase was measured (at 290 nm) using ultraviolet spectroscopy. The wet sample mass and absorbance as a function of flotation time are displayed in Figure 25. The collector dosage used in this experiment was initially 150 g/t, but a further 50 g/t was added after 110 minutes to give a total dosage of 200 g/t in the system.

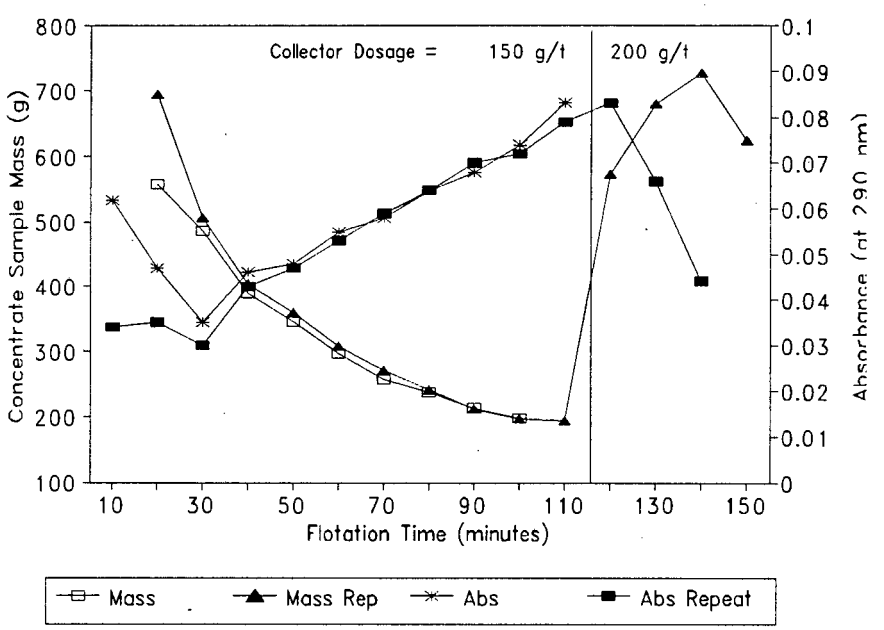


Figure 25 : Flotation Response with Recycle Configuration.

It is clear from this Figure that the system approached steady state only after a flotation time of approximately 2 hours. The repeat run shows that the system gave reproducible results. The continuous decrease in sample mass can probably be attributed to the following factors:

1) The cumulative mass of solids removed in the concentrate via sampling was not a negligible amount compared to the total mass of solids in the system as was initially assumed (approximately 13% of the solids was removed),
2) Mixing of the recycled tailings and concentrate streams with the pulp in the feed

47. Such an arrangement was used by Mular and Musara [1991].

tank was ineffective. Air was entrained by the incoming concentrate stream and a thick layer of froth formed inside the feed tank. This effectively led to a decrease in solids concentration of the pulp in the feed tank, and

3) The collector molecules were removed from the particle surfaces owing to very intense mixing in the feed tank [48]. The increase in absorbance in Figure 25 supports this hypothesis. After the extra collector was added, the absorbance decreased sharply when the additional collector adsorbed, as was the case with the initial conditioning period during the first 30 minutes.

It was therefore decided to run the hybrid column in continuous mode. Using the continuous arrangement as shown in Figure 24 on page 64, it was found that it was possible for the system to reach steady state in as short a time as 3.5 minutes. This was with as little as 40 l of total pulp. At a solids concentration of 100 g/l, this required 4 kg of ore per run. At the standard pulp feed rate of 3 l/min, the system reached steady state after only 1.2 retention times. The total time available for each flotation experiment was between 6 and 7 minutes. The flotation response from a typical run [49] and a repeat run is shown in Figure 26.

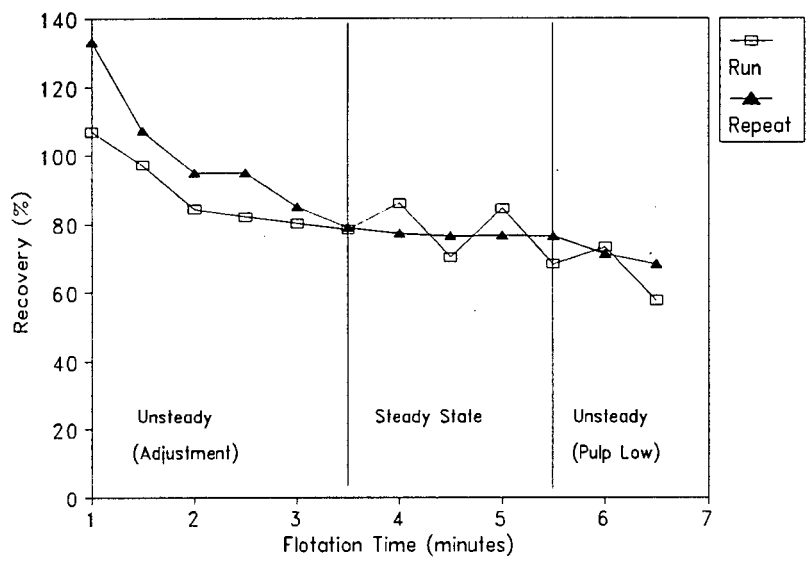


Figure 26 : Typical Flotation Response of the Hybrid Column Cell.

The response curve can be divided into three regions:

1) an unsteady region where the system approached steady state (0 - 3.5 minutes),
2) a steady state region (between 3.5 and 5.5 minutes), and
3) a final unsteady region where the recovery decreased again.

48. The agitator in the feed tank had a rotational speed of 1470 rpm and the impeller blades had sharp edges.
49. The column cell configuration was used during this run, and particles of size +75 -106 $\mu$m were floated with both the collector and frother dosages being 80 g/t. The quartz was not calcined beforehand.

The unsteady behaviour in the first region was probably due to the level controller being adjusted and possibly to the pulp being displaced by the air bubbles which started entering the cell at t = 0. The unsteady behaviour after 5.5 minutes was probably caused by improper mixing in the feed tank due to the pulp level which decreased to such an extent that it was below the impeller level. This led to a decrease in pulp density and air bubbles being drawn into the feed tube and fed to the column. The repeat run again shows that results were reproducible, although the level controller was very unstable during this experiment and led to a variation in pulp level which influenced recovery. It is important to note that the marked variation in recovery was not due to froth phenomena at different froth depths, but to a froth accumulation effect. Figure 26 also illustrates how data from runs in which the level controller had not yet stabilized were interpreted: a linear regression was done on those points which lay in the steady state region. Increasing the pulp feed rate with the chosen conditions was not a viable option because of practical considerations: the retention time of pulp in the column would be less and steady state would therefore probably not be reached.

The period of conditioning of ore which was used during all the subsequent experiments with the hybrid column cell was chosen using the data from Figure 25 on page 66. The pulp was conditioned for a minimum period of 25 minutes during all experiments. An air rate of 3 l/min was chosen as standard. This corresponds to a superficial gas velocity of 0.64 cm/s which may seem low if it is compared with the suggested value of 1 - 2 cm/s [Yianatos *et al.*, 1988]. This might imply that the column cell was not run optimally. It was not the idea of this thesis to operate each of the three cell configurations at optimum conditions, but to compare the relative collection efficiencies at similar operating conditions. The operating conditions chosen were practical, workable levels of operation, and are discussed in more detail in section 4.4 on page 80. A description of the experimental work carried out is given in that section.

## 3.7 SUMMARY

A laboratory scale hybrid column flotation cell was designed for this investigation. It could be modified to house three totally different particle-bubble contacting environments. The column was operated in continuous mode and practical levels for operating parameters were determined. Comparative work was done in a laboratory subaeration batch flotation cell. A description of experimental equipment has been given.

# CHAPTER 4
# EXPERIMENTAL DETAILS

## 4.1 INTRODUCTION

The aim of this thesis was to investigate the effect of different particle-bubble contacting environments on particle collection efficiency in flotation. The contacting environment in a column cell is quiescent, while a much more turbulent environment prevails in mechanical cells like the laboratory batch and agitated column cells. The mechanism used in a Jameson-type cell to contact particles and bubbles is far removed from those employed in column and agitated cells. The environment in a Jameson downcomer tube is turbulent, while in the rest of the cell (the disengagement zone) it is quiescent.

A series of tests was carried out in each of the three hybrid column cell configurations, and in the laboratory batch cell, at various collector dosages and particle sizes. The influence of particle-bubble contacting environment on particle collection efficiency was investigated by comparing the flotation recoveries and performances so obtained.

The choice of ore and the way in which it was pre-treated is discussed in the first part of this Chapter. Reasons for the choice of the ore are given, after which its sizing into different particle size fractions is discussed. The chemical reagents that were used are discussed in the second part of this Chapter, along with a motivation for the choice of flotation pH. The specific flotation parameters that were investigated, which resulted in distinctly different particle-bubble contacting environments, are discussed in the next section. The choice of constant operating conditions is motivated and the operating procedures which were used during the experimental work in the different column cell configurations are described. The Chapter concludes with a description of the experiments were carried out with respect to every flotation variable.

## 4.2 ORE DETAILS

### 4.2.1 Choice of Ore [50]

Adsorption of collector molecules onto silicate minerals occurs via physisorption. This mechanism is relatively simple compared to chemisorption which is most common in

---

50. Also see the discussion of the quartz-amine system in section 2.3.4 on page 9.

typical industrial flotation operations. Quartz is one of the most abundant silicate minerals and is often regarded as an impurity in ore mixtures. It is a high volume, low value commodity and purification is often done by reverse flotation [Crozier, 1992]. Quartz of high purity (> 99.6% $SiO_2$), a raw product for glass manufacturing, was chosen for use as ore in this investigation. Two of the products offered by the retailers, Consol Industrial Minerals in Cape Town, were suitable for this project. They were (called by their trade names):

1) 12DA, a coarse product, and
2) No. 2 Foundry Sand, a finer product.

The size distributions of these two products were obtained from the supplier, and are given in Appendix C on page 169.

### 4.2.2 Particle Sizing

Particle size is an important variable in flotation [51] and a proper investigation of collection efficiency of particles in different cell environments requires the use of more than one particle size fraction. The two quartz products were therefore sized into four different particle size fractions, as shown in Table 2.

Table 2 : Quartz Particle Size Fractions.

| Particle Size ($\mu$m) | Description |
|---|---|
| -106 | Multiple Fraction (Separate Size Analysis) |
| +106 -150 | Single Fraction |
| +150 -300 | Single Fraction |
| +300 | Single Fraction |

The -106 $\mu$m size fraction is described as multiple because it had a very wide size distribution, containing a high percentage of fines as well as particles of intermediate size. Although it was floated as a single fraction, the concentrates were analyzed for size after flotation. The other three fractions were considered as single fractions, although the +150 -300 $\mu$m fraction covers two sizes in the normal root two Taylor series. The first three particle size fractions were obtained from the finer No. 2 Foundry Sand product, and the +300 $\mu$m fraction from the 12DA product in the following way:

51. The influence of particle size on flotation is discussed in section 2.6.1 on page 28.

The -106 $\mu$m size fraction was prepared by milling the entire No. 2 Foundry Sand Product down to 55% passing 106 $\mu$m [52]. The milling time was determined via milling curves: two types of milling media were tried (rods and balls) with balls giving the best performance [53]. The milling was consequently done using balls, and every batch was milled for a period of 30 minutes. The material larger than 106 $\mu$m was screened out afterwards by bulk screening [54]. The +106 -150 $\mu$m and +150 -300 $\mu$m size fractions were obtained by screening out the material coarser than 300 $\mu$m and finer than 106 $\mu$m out of the (unmilled) No. 2 Foundry Sand Product, and separating the two by screening. The +300 $\mu$m size fraction was obtained by screening out the material smaller than 300 $\mu$m from the coarse 12DA product.

Like most processes, screening is not perfect and it was desired to have as small an overlap as possible on each side of the distribution of the single particle size fractions, as well as on the coarse side of the -106 $\mu$m fraction. To check this, size distributions of all size fractions coarser than 106 $\mu$m were obtained by means of dry sieving [55], while the -106 $\mu$m size fraction was analyzed with a Malvern particle size analyzer (the Malvern analysis is further discussed in section 5.4.2 on page 107). The results of the particle size analyses of all four size fractions are shown in Table 3.

Table 3 : Particle Size Distributions of the Quartz Fractions used in the Flotation Test Work.

| Particle Size ($\mu$m) | Particle Size Distribution (%) | | | |
|---|---|---|---|---|
| | -106 | +106 -150 | +150 -300 | +300 |
| -25 | 32.02 | | | |
| +25 -38 | 13.76 | | | |
| +38 -53 | 9.71 | | | |
| +53 -75 | 19.35 | | | |
| +75 -106 | 19.72 | 16.74 | 1.82 | |
| +106 -150 | 5.44 | 72.95 | 19.16 | |
| +150 -212 | | 10.31 | 57.46 | 0.25 |
| +212 -300 | | | 20.52 | 17.83 |
| +300 -425 | | | 1.04 | 63.11 |
| +425 -500 | | | | 13.30 |
| +500 | | | | 5.51 |
| Total | 100.00 | 100.00 | 100.00 | 100.00 |

52. Details of the milling process are given in Appendix B2 on page 163.
53. The establishment of the milling curves and the results are given in Appendix D on page 171.
54. The screening technique is described in Appendix B3 on page 164.
55. The experimental procedure which was used is described in Appendix B4 on page 164.

A graphical illustration of the relative positions of the size fractions in the global particle size range is shown in Figure 27.

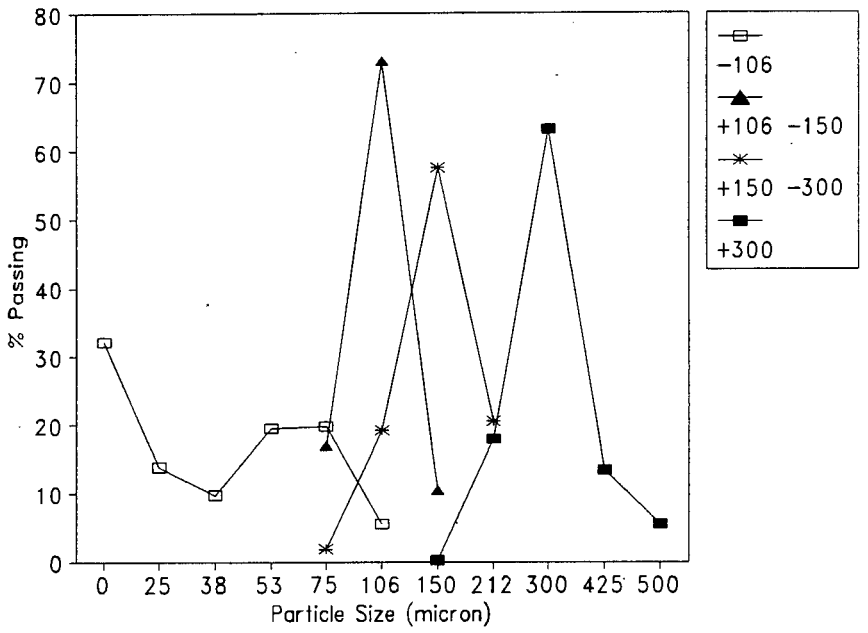


Figure 27 : Particle Size Distributions of the Prepared Size Fractions.

Although the percentage overlap between size fractions was in some cases as high as 20%, it is clear from Figure 27 that the distributions of the fractions coarser than 106 $\mu$m all had pronounced peaks in the desired size range. Furthermore, the mean particle diameters of the size fractions (which are calculated in the next section) are distinctly different. The size distribution of the -106 $\mu$m size fraction had a double peak probably because the raw product, No. 2 Foundry Sand also had a double peak in its distribution, or because the mechanism of milling resulted in a high fines percentage due to attrition between the balls.

#### 4.2.2.1 Determination of the Mean Particle Diameter of the Four Particle Size Fractions

The mean particle diameters of the four particle size fractions used during the flotation experiments were calculated from their respective particle size distributions. These mean diameters were calculated for use in calculations in which particle diameter was required as a parameter. It was assumed that all the particle size fractions had gamma distributions, and the mean particle diameters were therefore calculated using an expression similar to Equation (55) on page 25, which applies to mean residence time. The calculated mean diameters are presented below in Table 4.

Table 4 : Calculated Mean Particle Diameters of Particle Size Fractions.

| Particle Size Fraction ($\mu$m) | Mean Particle Diameter ($\mu$m) |
|---|---|
| -106 | 73.69 |
| +106 -150 | 129.38 |
| +150 -300 | 194.25 |
| +300 | 370.34 |

### 4.2.3 Pre-Treatment

The surface of the quartz obtained from the glass manufacturer appeared to be contaminated. It had a dark brown colour and small black particles were present in the quartz. The particle surface was analyzed with infrared spectroscopy and the contamination was found to be of an organic nature. The organic material was probably from a reverse flotation step used to separate the quartz from other materials after mining it. It was crucial to clean the surface of the quartz for two reasons:

1) To avoid the possibility of varying degrees of contamination on the particle surface (organic coating of the quartz particles would decrease the available area for collector molecules to adsorb onto), and
2) To ensure that the pH of the pulp stayed constant during all the flotation experiments [56].

Three different methods of cleaning of the quartz particle surface were investigated, and are discussed in subsequent sections:

1) Attritioning,
2) Hydrochloric acid wash, and
3) Calcination at 500 °C.

#### 4.2.3.1 Attritioning

Contaminated quartz from the No. 2 Foundry Sand product was screened to remove the material coarser than 106 $\mu$m, and was attritioned in the feed tank of the hybrid column rig [57]. After each stage of attritioning, the water was decanted and fresh water added. The absorbance of the decanted water was measured with ultraviolet spectroscopy after every wash (or attritioning session)

56. The flotation of quartz is extremely pH sensitive, as is discussed in section 4.3.2 on page 78.
57. The experimental procedure used is described in Appendix B6 on page 165.

and the results are shown in Figure 28, in which the absorbance of the wash water is plotted against the number of washes.

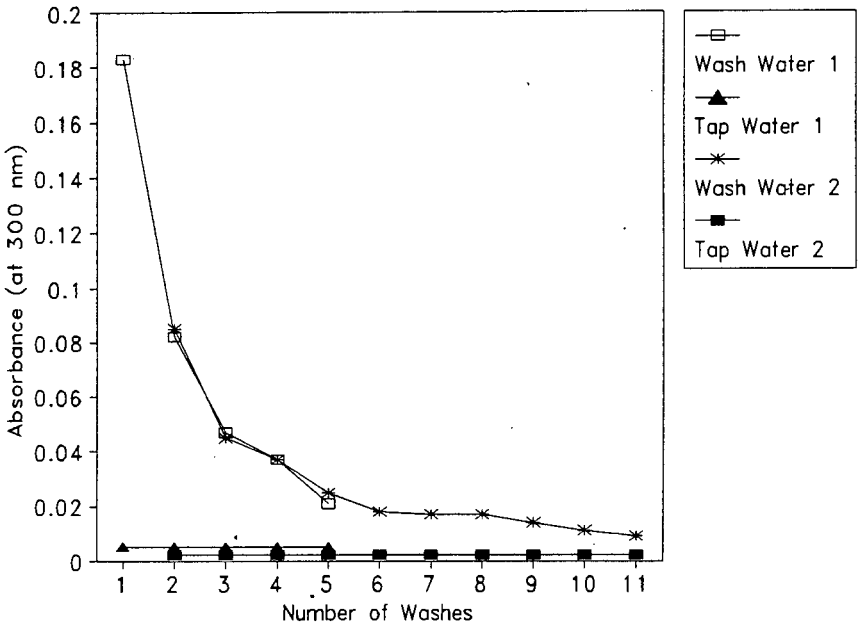


Figure 28 : Quartz Cleaning by means of Attritioning - Absorbance Effect.

The reproducibility of these results may be seen to be good if the repeat run (numbered 2) is compared with the first run. It is clear from Figure 28 that the attritioning treatment did have a cleaning effect on the quartz surface, since the absorbance of the wash water (the dirty water which was removed after every wash) ultimately approached that of tap water. Attritioning also had a marked effect on the pH of the wash water, as is shown in Figure 29.

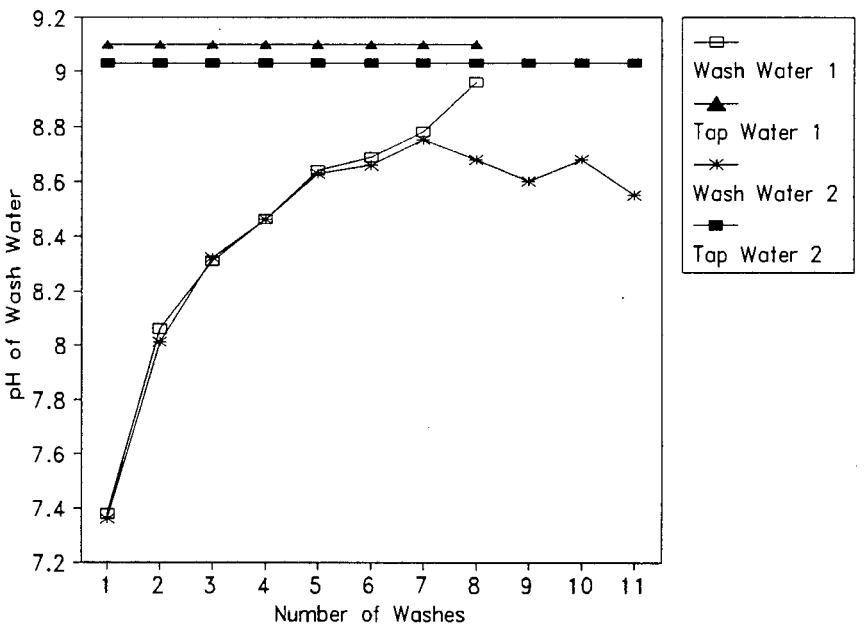


Figure 29 : Quartz Cleaning by means of Attritioning - pH Effect.

These results again were reproducible, and the fact that the wash water pH approached the tap water pH again showed the cleaning effect of attritioning. The observed asymptotic offset in pH between tap and wash water could be expected, since the presence of quartz in water has an effect on the pH of the pulp.

Although it was found that attritioning did have a cleaning effect on the quartz surface, it was not possible to conclude that the quartz surface was completely clean after this treatment, since a plateau in absorbance could only imply a limit of the current washing method, *i.e.* it was possible that attritioning only removed part of the contamination. It can well be imagined that if the intensity of agitation had been increased, the quartz surface would end up being cleaner. Keeping this in mind, as well as the fact that this method was very labour intensive, it was decided to investigate two other methods, *viz.* acid washing and calcination. These two methods are described in the following sections.

#### 4.2.3.2 Acid Washing

This method of cleaning the surface of quartz has been used by many researchers in the past, specifically prior to methylation [58], and the procedure of Smith and Rajala [1989] was selected for this investigation [59]. This method of cleaning of the quartz surface was even more labour intensive than the attrition method, since the surface had to be washed repeatedly until all the acid was removed from the surface. The success of this method of quartz cleaning was evaluated with batch flotation in which the final recovery of quartz particles which had been acid washed was compared with that of calcined quartz. This is further discussed in the following section.

#### 4.2.3.3 Calcination

Most organic compounds can be cracked under atmospheric conditions at a temperature of about 500 °C [Emmett, 1960]. The possibility of cleaning the surface of the quartz by means of calcination (roasting the quartz in a furnace at 500 °C for two hours) was therefore investigated [60]. A distinct change in colour was observed after this treatment: the quartz particles were white and free of black particles after calcination.

---

58. A discussion of the use of this process has been given in section 2.3.4 on page 9.
59. This method is described in Appendix B7 on page 166.
60. This procedure is discussed in Appendix B8 on page 166.

In an attempt to evaluate the success of this method, thermogravimetric analysis (TGA) was done on the quartz surface, but the loss in mass with temperature showed a continuing downward trend; no plateau was reached as could be expected. However, it was found that the pH of the pulp containing quartz which was cleaned by calcination remained constant during the flotation experiments in the hybrid column. The quartz particles were still being attritioned in the feed tank during the run. In addition to this, the pH of the pulp was measured as between 8.6 and 8.8 for most of the flotation runs done in the hybrid column cell. If this is compared with the data in Figure 29 on page 74, it is reasonable to assume that the quartz surface was clean after calcination.

The flotation of quartz particles which were treated by acid washing and calcination was compared with that of raw, contaminated quartz. The flotation experiments were done in a laboratory batch flotation cell (at pH = 7) and the results are shown in Figure 30.

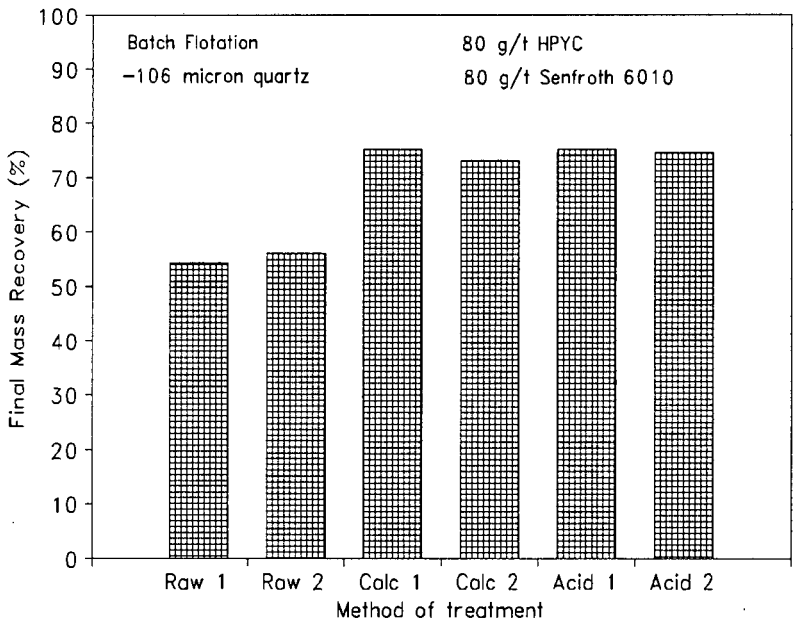


Figure 30 : Comparison of Quartz Cleaning Methods.

In this Figure, Raw denotes contaminated quartz, Calc denotes raw quartz which had been calcined and Acid means raw quartz which had been acid washed. It is evident from Figure 30 that cleaning the quartz surface resulted in an increase in final flotation recovery of approximately 20%, probably because of a higher collector coverage on the cleaned quartz particles. Acid washing and calcination resulted in more or less the same increase in recovery. Reproducibility was within 5%, even though some of the runs were done with long time intervals between them. The cleaning method chosen was calcination at 500 °C because of its relative simplicity and good reproducibility.

## 4.3 CHEMICAL CONDITIONS USED

### 4.3.1 Choice of Reagents

The cationic collectors most widely used in industry are the amines which exist in the cationic form below certain pH values. As with many of the anionic salts, these collectors will attach to mineral surfaces of opposite charge and are frequently used in conjunction with modifiers and depressants, although every attempt is usually made to adjust both pH and the type and concentration of other ions in solution to ensure that only the mineral to be collected has a negative surface charge. Primary, secondary and tertiary amines are weak bases, whereas quaternary amines are strong bases. Quaternary amines are completely ionized at all values of pH, while ionization of primary, secondary and tertiary amines is pH dependent [King, 1982].

A quaternary pyridinium salt (hexadecyl pyridiniumchloride) was chosen as collector to render the quartz particles hydrophobic. Hexadecyl pyridiniumchloride (HPYC) is readily soluble in water and stable in solution [61]. It has the advantage over the classical choice of dodecylammonium acetate (used by de Bruyn and Modi [1956] and Smith and Scott [1990]) of being detectable by ultraviolet spectroscopy.

Frothers are surface-active, usually non-ionic molecules whose function in the flotation system is to provide a large air-water interface (by lowering the surface tension of the water) of sufficient stability to ensure that a floated particle will not fall back into the flotation pulp before it can be removed. Frothers also have an influence on the kinetics of the attachment of the particle to the bubble. In the flotation of non-sulphide minerals such as quartz, the collectors are normally strongly surface-active and thereby provide their own frothing action. A Senmin product, Senfroth 6010 [62] was chosen as frothing agent.

A dispersant was used in some of the flotation experiments to break up flocs which formed with particles of a certain size, at high collector dosages. The dispersant chosen was tetra-Sodium Pyrophosphate ($Na_4P_2O_7.10\ H_2O$). An alternative would have been Sodium Silicate ($Na_2.SiO_2$). It has to be kept in mind that Na acts as a depressant in quartz flotation [Crozier, 1992] and the dosage consequently had to be chosen such that it was sufficient to disperse the flocs, but not so high as to cause heavy depression, resulting in poor recoveries.

61. Amines are known to undergo chemical changes if left in solution for a period of time.
62. A blend of 90% dimethyl phthalate and 10% polyglycol ether.

### 4.3.2 Choice of Flotation pH

Quartz flotation is strongly pH dependent. An investigation of the effect of pH on the zeta potential of quartz in the presence of $FeCl_2$ was done by Fuerstenau [1975] and a diagram of his results is shown in Figure 31.

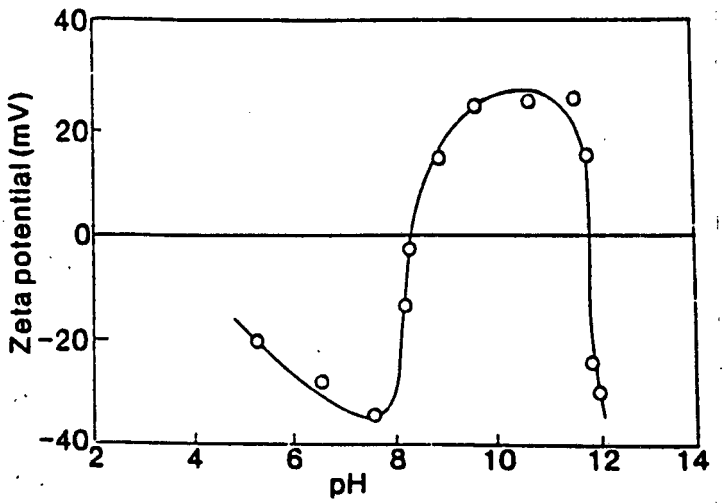


Figure 31 : Zeta Potential of Quartz as a Function of pH.

The charge on the surface of the quartz should have the inverse response to the zeta potential, *i.e.* at a pH just above 8, surface charge should become drastically more negative. This will lead to increased collector (cationic) adsorption, making the particles more hydrophobic, and consequently result in a marked increase in flotation recovery. This is clearly shown in Figure 32, which shows a correlation between zeta potential, collector adsorption density, contact angle and flotation recovery [Fuerstenau, 1976].

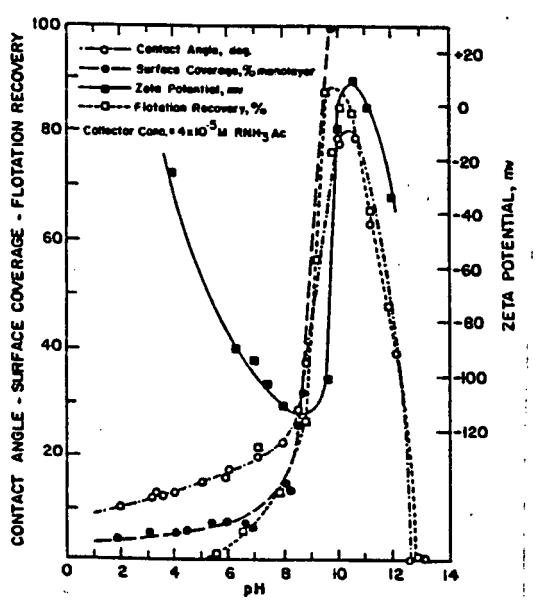


Figure 32 : Correlation between Contact Angle, Adsorption Density, Zeta Potential and Flotation Recovery of Quartz [Fuerstenau, 1976].

Although a primary amine was used here as collector, the same theory applies to a quaternary pyridinium salt such as HPYC [Fuerstenau, 1976].

From Figure 31 and Figure 32, flotation recovery can be expected to become very labile in the region of pH = 8 and above, while pH = 7 would be a more stable point of operation. This was confirmed experimentally with batch flotation as displayed in Figure 33, in which the sensitivity of recovery with pH is clearly illustrated. Raw, uncleaned ore was used for this investigation.

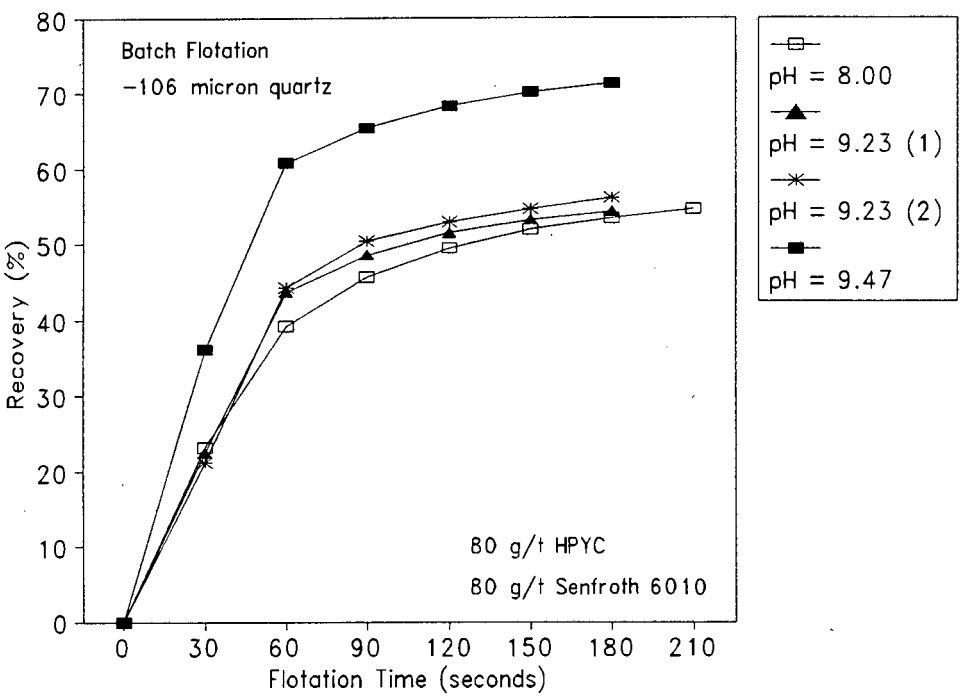


Figure 33 : Effect of pH on Quartz Recovery.

It is clear from this Figure that flotation recovery increased significantly with only a small increase in pH from 9.23 to 9.47, although the recoveries at pH = 8 and 9.23 were very similar. The flotation curve at pH = 9.23 and its repeat run (numbered 2) shows that the reproducibility was good, and the substantial increase in recovery with a very small change in pH must therefore be attributed to quartz surface phenomena.

It was decided to do all flotation the flotation experiments at pH = 7, since experimental error in pH adjustment should have little effect on flotation recovery at this level. Flotation was done in tap water. $H_2SO_4$ and NaOH were used as pH modifiers [63] [Crozier, 1992].

63. The method of addition of these modifiers, the concentration used and the amount added is described in section 4.5 on page 82.

## 4.4 FLOTATION PARAMETERS

### 4.4.1 Choice of Flotation Parameters

The experiments were designed to subject one ore type (quartz) to a wide variety of particle-bubble contacting environments. Different cell configurations were used to float quartz particles of different size and degree of hydrophobicity. Furthermore, conditions in the cells (*e.g.* the contacting intensity) were sometimes varied while keeping the particle size and degree of hydrophobicity constant. The variables which were investigated, with limiting values where applicable, are listed in Table 5.

Table 5 : Flotation Variables which were Investigated.

| Variable | Description |
|---|---|
| Flotation cell type | Column, Jameson, Agitated and Laboratory Batch Cells<br>(Different Particle-Bubble Contacting Environments) |
| Particle Size | Four Size Fractions: See Table 2 on page 70<br>(Size finer than 25 $\mu$m to as coarse as 500 $\mu$m) |
| Particle Hydrophobicity | Collector Dosage (0-500 g/t) |
| Contacting Intensity | Impeller Speed (0-1570 rpm) |
| Air Flow Rate | 0-7 l/min (Residence Time Distribution Investigation) |

In addition to the flotation experiments, residence time distribution (RTD) studies were carried out in the hybrid column cell to investigate characteristics of mixing in the different cell configurations. This test work was not carried out using pulp, but with tap water. Air flow rate was listed as a variable in Table 5 because it was varied during the RTD investigation.

A detailed description of the way in which the experiments were carried out with reference to the experimental procedures which were used is given in section 4.6 on page 86. Some of the operating parameters were kept constant during the experimental work, and are discussed in the next section.

### 4.4.2 Choice of Constant Operating Parameters

#### 4.4.2.1 Pulp Density

Industrial quartz flotation operations are carried out with pulps containing between 20 and 40% solids [Crozier, 1992]. A solids concentration of 10% (100

grams of quartz per litre of pulp) was used in all the flotation experiments in this thesis. This relatively low solids concentration was chosen to minimize the amount of quartz consumed during the experimental work, as well as to have first order kinetics. The rate of flotation is not first order for very concentrated pulps, as discussed in section 2.4 on page 10.

#### 4.4.2.2 Frother Type and Concentration

Synergism between collector and frother exists [Leja and Schulman, 1954]. A frother dosage which would be small enough not to hinder the effect of the collector, but sufficient to result in bubbles of an intermediate size had to be chosen. The froth phase was kept shallow, and froth stability was therefore not a major factor to consider. It has been shown by Tucker *et al.* [1994] that bubble size decreases with increased frother dosage in a laboratory batch flotation cell. A point is reached after which the bubble size is not affected by further addition of frother, and stays constant. This was shown to hold for five different types of frother.

Senfroth 6010, which was the frother chosen for this investigation, was shown to result in bubbles of constant size (less than 1.60 mm) at frother dosages of 10 ppm and higher if the collector dosage was kept constant. Bubble coalescence or slugging was also not noticed during an experiment with water and 80 g/t collector and frother. A constant frother dosage of 80 g/ton of ore, which corresponds to 8 ppm at 10 % solids, was chosen and used during all the flotation experiments. This dosage lay within the boundaries of 50 to 100 g/t which is typical in industrial quartz flotation plants [Crozier, 1992].

#### 4.4.2.3 pH

Quartz flotation can be done under acidic, neutral or basic conditions. If the acidic route is followed, flotation is done at approximately pH = 2, while basic flotation is normally carried out at a pH of approximately 9.5 [Crozier, 1992]. Neutral pH was chosen for this investigation, as discussed in section 4.3.2 on page 78, and all the flotation work was carried out at pH = 7.

#### 4.4.2.4 Froth Depth

A constant froth depth of 20 mm was used during all the experiments in the hybrid column cell (see section 2.4.2 on page 11 and in section 3.6 on page 65).

#### 4.4.2.5 Pulp Conditioning

Mixing conditions in the feed tank were kept constant for all the flotation experiments carried out in the hybrid column cell, irrespective of particle size or level of hydrophobicity. An impeller speed of 1470 rpm was used at all times, and was assumed to result in the same extent of conditioning during all the experiments. Conditioning time also depended on the time which it took the column to fill up during the flotation runs, which in turn was a function of the particle settling velocity [64], but it was kept as constant as possible.

## 4.5 OPERATING PROCEDURES

The procedures employed during the flotation experiments with each of the cell types are described in subsequent sections.

### 4.5.1 Column Cell Configuration

(A diagram of the experimental rig is shown in Figure 24 on page 64).

4.4 kg of quartz of a chosen size was deposited into the feed tank. 40 litres of pulp was made up by adding tap water (of which the pH had been measured in a glass beaker) to the feed tank. The pulp mixture was stirred at 1470 rpm while the pH of the pulp was measured [65] with the pH probe placed at a fixed position in the feed tank. The pH of the pulp was adjusted to 7 during the next 5 minutes by adding 0.1 mol/dm$^3$ $H_2SO_4$ or 0.1 mol/dm$^3$ NaOH as pH modifiers.

The desired amount of reagents (frother, collector and sometimes dispersant) was added and a period of 5 minutes was allowed for conditioning and proper mixing with the pulp in the feed tank. The pH of the pulp was monitored after reagent addition and was readjusted to pH = 7 if it had changed during this period of conditioning.

Both the feed and tailings pumps were started (valve 4 open), with the tailings stream being recycled to the feed tank. The feed pump was calibrated beforehand to deliver the chosen pulp feed rate. The tailings pump speed was adjusted to a level sufficient to prevent blockage of the tubes due to settling of solids in the column, with the level controller on manual. The column normally took between 7 and 15 minutes to fill up

64. See the operating procedure for the column cell configuration in section 4.5.1 on page 82.
65. $pH_{pulp}$ was noted down after it had stabilized, or alternatively after a period of 5 minutes.

and the fill-up time was recorded for calculation of total conditioning time [66].

The air valve (valve 2) was opened when the pulp level was approximately 10 cm from the top of the column. Valve 1 was opened at first to release the built-up pressure in the air line, after which valve 2 was opened, and valve 1 was slowly closed. This procedure prevented the pulp from blowing out over the top of the column due to built-up pressure in the air line. Timing was started directly after the air valve was opened, and the tailings hose outlet was redirected to the discharge tank to render the operation continuous. A period of 1 minute was allowed for level controller adjustment, during which the air flow rate was adjusted to the desired level by adjusting the air rotameter.

Concentrate samples were taken after this period of one minute, at the outlet of the froth launder in pre-weighed glass bottles. Sampling was done for a period of 10 seconds at 30 second intervals. Twelve samples were taken per experiment, as the total available flotation time had been determined as between 6 and 7 minutes [67]. Tailing samples were not taken during any of the experiments.

Both pumps were stopped after the run, the air valve (2) was closed and the decrease in level was recorded. Gas holdup was calculated from the decrease in pulp level. The tailings pump was restarted to empty out the column after opening valve 5 and closing valve 4: settling solids blocked the tubes if the pulp was left stagnant inside the column.

The solids from both the feed and discharge tanks were pumped into a filter press. The water was removed under air pressure, and the solids were dried and stored. The sampling bottles, containing the wet concentrate samples, were weighed and dried in a microwave oven. The dry mass was determined afterwards. Dry quartz samples of both concentrate and tailings streams were kept. Particle size analysis was carried out on the combined concentrate sample if the -106 $\mu$m particle size fraction was floated. This analysis was done using a Malvern particle size analyzer according to the experimental procedure in Appendix B5 on page 165.

### 4.5.2 Jameson Cell Configuration

The same operating procedure as for the column cell configuration was used to run the Jameson cell, except that the pulp was fed through valve 3 instead of valve 4, and air

66. The pulp underwent further conditioning during fill-up of the column.
67. See the discussion in section 3.6 on page 65.

was fed through valve 1 instead of valve 2 during operation. The operating procedure for the column cell has been described in the previous section (4.5.1). Furthermore, column fill-up was done through the feed point used during the operation of the column cell (valve 4 open) to prevent excessive solid settling, especially when coarse particles were floated [68]. The pulp feed was redirected to the Jameson downcomer tube when the column was approximately 75% full. The pulp level in the Jameson cell was constantly monitored to ensure that air accumulation did not occur in the downcomer tube when the air rate was too high. Air drawn into the Jameson downcomer tube caused pulp level fluctuations in the column and resulted in very unstable operation. The air was released by opening an external valve on the Jameson downcomer tube if air build-up occurred. Gas holdup measurement was done in a similar way to the column cell configuration, except that the decrease in level in the Jameson downcomer tube was measured instead of in the surrounding column vessel. The downcomer tube was lifted out of the column to see the pulp interface if it was below the pulp level in the surrounding column disengagement zone. The pulp level in the downcomer did not change by lifting it out, since the downcomer tube was a closed system after all the valves had been closed.

### 4.5.3 Agitated Cell Configuration

The same operating procedure as for the column cell configuration was used to run the agitated cell, except that the agitator was started and checked for the correct rotational speed when the column was approximately 75% full. The operating procedure for the column cell has been described in section 4.5.1 on page 82. Rotational speed was measured with a Veeder Root optical tachometer. The agitator was switched off along with the feed and tailings pumps and air flow prior to gas holdup measurement.

### 4.5.4 Laboratory Batch Cell [69]

Water at the desired pH was prepared by adding approximately 3.2 l of tap water to a plastic bucket, mildly stirring it with a laboratory agitator, and adding 0.1 mol/dm$^3$ $H_2SO_4$ or 0.1 mol/dm$^3$ NaOH until the desired pH [70] was reached. pH measurement was carried out with the pH probe at a fixed position in the bucket. Approximately 1 litre of this water was added to the laboratory batch cell and the agitator was started

68. The pulp was fed through the downcomer tube when the Jameson cell was in operation. The pulp exited virtually at the bottom of the cell, leaving the rest of the column as clear liquid if air was not fed into the column.
69. This procedure was adopted from Stonestreet [1991] and modified.
70. pH was normally adjusted to 7, except when the effect of pH on batch flotation was investigated.

at the desired rotational speed [71]. Rotational speed was calibrated with a tachometer.

The cell was filled to just below the 3 litre mark and the constant head device was activated to control the pulp level. It was assumed that the water added to the cell in this way would have a negligible effect on the pH of the water in the cell (tap water pH was normally measured as being higher than 7). Addition of quartz to the prepared pH-adjusted water did not change the pH of the pulp significantly, and it was assumed that $pH_{pulp} = pH_{water,adjusted}$.

It normally took about 1 minute for the constant head device to adjust the pulp level to a level which would correspond to exactly 3 litres of pulp, had the agitator and air been switched off. This normally resulted in a froth depth of 1 - 1.5 cm. The pulp was agitated for a further minute (including the above mentioned fill-up time) after which the desired amounts of frother, collector and dispersant, if desired, were added to the pulp. A period of 3 minutes was allowed for conditioning, after which aeration at 3 l/min was commenced. The air rotameter was accurately calibrated using a simple gas-water displacement technique [72].

Timing was started as soon as the air valve was opened and 10 seconds was allowed before scraping at 5 second intervals started. Samples were collected every 30 seconds, after which the 10 second period was again allowed to remove the pan and wash the cell lip and scraper with a wash bottle (*i.e.* 5 scrapes per sample). Wash bottles were weighed before and after floats and the mass of wash water used was calculated and subtracted from the total mass of water in the samples. Concentrate samples were collected in metal pans, which were weighed while still dry.

The wet sample masses were recorded, and the samples dried in a laboratory oven at 60 °C and weighed again to get the dry sample mass. In some cases the wet samples were transferred to pre-weighed glass bottles and dried in a microwave oven. The samples were recombined with the quartz left behind in the cell, and the total mass was determined again if the quartz was subject to further treatment. Samples of the combined concentrate were kept and stored. The combined concentrate samples were analyzed for size with a Malvern particle size analyzer if the -106 $\mu$m particle size fraction was floated.

---

71. The normal rotational speed was 1200 rpm, except where the influence of agitation speed on quartz recovery was investigated.

72. A 2 l measuring cylinder was filled with water and placed upside down in a pan containing water. The air was allowed to flow through the rotameter into the water-filled measuring cylinder. The volume of air per minute was determined using a stop watch and monitoring the water level in the cylinder.

## 4.6 THE EXPERIMENTAL PROGRAM

The experimental work which was carried out is discussed in subsequent sections. The operating procedures, experimental procedures and experimental conditions used during the investigation of every flotation variable and the residence time distribution (RTD) investigation are described under relevant headings. Although the particle hydrophobicity, particle size and cell type investigations are discussed as separate entities, they were essentially one investigation in which the different particle size fractions were floated at different collector dosages in the different contacting environments. They have been treated separately here because the results obtained from the experimental work are presented separately in Chapter 5.

### 4.6.1 Flotation Cell Type

A discussion of the different cell types which were used during the bulk of the flotation experiments has been given in Chapter 3. They were the three different configurations of the hybrid column flotation cell, *viz.* a standard column cell, an agitated column cell, and a Jameson cell, and a laboratory batch flotation cell. The design of the hybrid cell has been discussed in section 3.2 on page 55, while a description of the laboratory batch cell has been given in section 3.3 on page 64.

The four cell types represented different particle-bubble contacting environments. Pulp was fed counter-current to air in the column and agitated cells. If a particle was therefore not collected during the first encounter with a bubble or if it was separated from a bubble, it had many other opportunities to be collected or re-collected until it was finally recovered in the froth phase or discarded as part of the tailings stream. Particle collection in the Jameson cell took place in the downcomer tube; the rest of the column was simply used as a disengagement zone for the collected particles to separate from the tailings stream. The pulp was discharged from the downcomer tube virtually at the bottom of the Jameson cell and a particle probably did not have a second chance of being collected once it had exited the downcomer tube. Because of co-current flow of pulp and air in the downcomer tube, the particle-bubble aggregates which formed during intense mixing in the top part of the tube were probably not disrupted by a counter current stream of pulp or turbulent eddies, as could be expected in the column and agitated column cell configurations. The laboratory batch cell did not have a flow of pulp, but solids were present in the same cell volume until they were collected and recovered in the froth phase. In addition to the different ways of pulp-air contacting in the different cell types, mixing characteristics of the pulp could be expected to be totally different in each case.

Particles of different sizes and degrees of hydrophobicity were subjected to the four cell environments. The specific particle size fractions and collector dosages which were used in the different cell types are discussed in the next two sections.

### 4.6.2 Particle Hydrophobicity

The degree of particle hydrophobicity in the flotation cells was assumed to be directly proportional to the amount of collector added to the pulp, as discussed in section 2.3 on page 5. The dosage of amines used in industrial quartz flotation operations at neutral pH is between 50 and 200 g/t [Crozier, 1992]. Table 6 shows the range of collector dosages used during this investigation in which the four cell configurations (column, Jameson, agitated and batch) are abbreviated as C, J, A and B, respectively.

Table 6 : Collector Dosages used in Different Cell Types.

| Collector Dosage (g/t) | Cell Type |
|---|---|
| 0 | C J A B |
| 25 | C J A B |
| 50 | B |
| 80 | C J A B |
| 160 | B |
| 200 | C J A B |
| 300 | C |
| 400 | C |
| 500 | C |

The shaded areas in this Table represent the bulk of the experimental work which was carried out for this thesis. All four particle size fractions were floated at these shaded collector dosages shown in Table 6, except at collector dosages greater that 200 g/t, at which only the -106 $\mu$m and +106 - 150 $\mu$m size fractions were floated. These high dosages were used to investigate the effect of collector overdose on particle collection efficiency, and only the column cell configuration was used. Additional experiments were carried out in the batch cell at intermediate collector dosages (50 and 160 g/t), during which all four particle size fractions were again floated. Tetra-Sodium Pyrophosphate ($Na_4P_2O_7.10\ H_2O$) was added to the pulp in repeat runs of experiments in which the +300 $\mu$m particle size fraction was floated at a collector dosage of 200 g/t. This dispersant was added to break up flocs which formed at high collector dosages with the flotation of coarse particles. A dosage of 40 g/t of dispersant was added to the pulp in all three hybrid column cell configurations during these experiments. The operating procedures used are described in section 4.5 on page 82.

### 4.6.3 Particle Size

Four particle size fractions were chosen to investigate the effect of particle size on collection efficiency in the different particle-bubble contacting environments. A detailed discussion of the particle size fractions and their distributions has been given in section 4.2.2 on page 70. The four particle size fractions represented a wide distribution of particle sizes from finer than 25 $\mu$m to as coarse as 500 $\mu$m. The optimum particle size range for quartz flotation is generally regarded as being between 10 and 50 $\mu$m [de Bruin and Modi, 1956]. The chosen particle size range may thus seem far too wide, but the fact that the flotation of particles as coarse as 700 $\mu$m has been investigated by Soto and Barbery [1991] and other workers, adds credibility to the practical significance of this choice.

The finest particle size fraction (-106 $\mu$m fraction) was used directly from storage after it had been milled, and was not calcined prior to flotation, as calcination was done before the milling step in the preparation of this fraction [73]. The three coarsest fractions (+106 -150 $\mu$m, +150 - 300 $\mu$m and +300 $\mu$m) were calcined [74] prior to flotation as there was no milling step involved.

All four size fractions were floated in the three hybrid column cell configurations and in the laboratory batch flotation cell. Each particle size fraction was floated at a number of collector dosages in all of the cells to investigate the effect of the degree of hydrophobicity on particle collection (see section 4.6.2 above). The pulp and air feed rates used were both 3 l/min. An agitation speed of 500 rpm was used in the agitated column cell, while 1200 rpm was used in the batch flotation cell. The operating procedures which were used during the particle size investigation have been described in sections 4.5.1 to 4.5.4 on pages 82 to 84.

### 4.6.4 Contacting Intensity

The intensity of contacting between ore particles and bubbles can be varied by changing the impeller speed in the agitated column and batch cells. It is possible to vary the contacting intensity in the Jameson cell by adjusting the pulp and air feed rates, thereby forcing the pulp through the orifice plate at different linear velocities and creating varying degrees of turbulence in the downcomer tube. This option was not pursued because of practical limitations of the experimental setup [75], and only the agitated

73. The milling procedure is described in Appendix B2 on page 163.
74. The calcination process is described in Appendix B8 on page 166.
75. This aspect has been discussed in section 3.6 on page 65.

column configuration and laboratory batch cell were used in the contacting intensity investigation.

The +106 -150 $\mu$m particle size fraction was chosen to investigate the effect of contacting intensity on particle collection efficiency. This size fraction proved to be coarse enough to illustrate the expected decrease in particle collection at high impeller speeds due to a decrease in $E_S$, but still fine enough for increased flotation recovery with increased agitation, due to an increase in $E_C$ [Ahmed and Jameson, 1985], to be expected. A constant collector dosage of 80 g/t was used, which was low enough not to cause flocculation of particles, as was often the case with collector dosages of 200 g/t and higher [76].

Practical levels of agitation speed were selected for the agitated column and laboratory batch cells, and are shown in Table 7.

Table 7 : Chosen Levels of Agitation Speed (rpm).

| Agitated Column Cell | Batch Cell |
|---|---|
| 0 | 800 |
| 300 | 1000 |
| 500 | 1200 |
| 800 | 1400 |
| 1200 | 1570 |

The maximum agitation speed in the agitated column cell was limited by its design: although the frequency controller-electrical motor combination was capable of impeller speeds as high as 1500 rpm, the safest upper limit was found to be approximately 1200 rpm. The column started vibrating vigorously at higher agitation speeds when the nylon collars which supported the shaft became slightly worn. The lower limit of 0 rpm corresponds to the column cell configuration, although the agitator was not present in the column cell. The minimum agitation speed in the batch cell was limited by solid suspension phenomena, while the upper limit was a design limit of 1570 rpm. An air flow rate of 3 l/min was used during all the tests in both cell types. The pulp was fed to the agitated column cell at the standard rate of 3 l/min.

The operating procedures used during the investigation of contacting intensity have been described in sections 4.5.3 and 4.5.4 on page 84.

76. A discussion of the flocculation phenomenon is given in section 5.3.5 on page 105.

### 4.6.5 Residence Time Distribution (RTD)

The hydrodynamic conditions in flotation cells with different designs can be expected to be distinctly different. Column cells have quiescent contacting environments, mechanical cells employ very turbulent contacting environments, while a combination of turbulent and quiescent environments are found in Jameson-type cells. Different cell types will exhibit different mixing characteristics, which can be quantified by a mixing parameter as discussed in section 2.5 on page 24.

Residence time distribution (RTD) measurements were carried out in all three configurations of the hybrid column cell to quantify the extent of mixing in each cell environment. A salt tracer (saturated KCl solution) was injected into the feed line of the cell in each case and the concentration of tracer in the tailings stream was measured with time. These measurements were done using a conductivity probe which was connected to a computer. The conductivity-time results were used to establish RTD curves and to determine the mean residence time of the liquid in each configuration at different modes of operation. The investigation was carried out on the liquid phase, using tap water which contained the standard dosage of 80 g/t of frother. Ideally, mixing of the solid and gas phases should also have been investigated, but it was assumed that the solid mixing characteristics were similar to that of the liquid [77].

The tracer tests were carried out in the three hybrid column configurations. Air feed rate was varied during the experiments with the column cell configuration. It was not varied during experiments with the Jameson cell, since the size of the mixing tank did not allow pulp feed rate to be increased. The standard liquid feed rate of 3 l/min was used in all tests. The chosen variables and their levels of operation are summarized in Table 8, in which the numerical values refer to volumetric flow rates in l/min.

Table 8 : Variables in the RTD Experiments.

| Column Cell Configuration | Agitated Cell Configuration | Jameson Cell Configuration |
|---|---|---|
| Air = 0<br>Air = 3<br>Air = 5<br>Air = 7 | Air = 3, 500 rpm | Air = 3 |

77. A discussion of this assumption has been given in section 2.5.2 on page 25.

The experimental procedure used during the RTD investigation is described in Appendix B9 on page 167.

## 4.7 SUMMARY

High purity quartz was chosen as ore for the flotation test work. It was sized into four particle size fractions ranging from finer than 25 $\mu$m to as coarse as +300 $\mu$m. The ore was found to be contaminated with organic matter. Three different methods of cleaning of the quartz surface were investigated. Calcination at 500 °C was chosen because of the simplicity of the method.

A pyridinium salt, hexadecyl pyridimiumchloride, was chosen as collector, and a mixture of dimethyl phtalate and polyglycol ether was selected as frothing agent. The flotation of quartz is strongly pH sensitive, and a suitable level of operation was found to be pH = 7.

Flotation experiments were carried out in three different column-type flotation cell configurations and in a laboratory batch cell. The hybrid column configurations were a column cell, an agitated column cell and a Jameson cell. Four particle size fractions were floated in these different flotation cell environments at different degrees of hydrophobicity (levels of collector addition). The influence of agitation speed was investigated in the agitated column cell configuration and batch cells. The aim of these flotation experiments was to investigate the effect of particle-bubble contacting environment on particle collection efficiency. Residence time distribution studies were carried out in the liquid phase to quantify the extent of mixing in the three hybrid column cell configurations.

# CHAPTER 5
# RESULTS AND DISCUSSION

## 5.1 INTRODUCTION

The results obtained during the experimental work are presented in this Chapter, along with a discussion of their significance to particle collection efficiency. The detailed flotation results are given in Appendix I on page 187, while the detailed residence time distribution results are presented in Appendix E on page 173. The data which are relevant to the investigation of each aspect of this study have been taken from these two Appendices, and are presented and discussed under appropriate headings in this Chapter.

The results from the bulk of the flotation experiments [78] are presented first, followed by a brief discussion of this data. This is followed by a more in-depth discussion of these results in which the effect of specific variables on particle collection efficiency is considered. The influence of particle hydrophobicity is discussed first, after which the same data are analyzed for the effect of particle size by including additional data obtained from Malvern particle size analyses of the flotation concentrates [79]. A comparison is then drawn between the flotation behaviour of the different cell types, and possible explanations for differences in particle collection are discussed. This discussion includes the data which were obtained from the contacting intensity investigation in the agitated column and batch cells.

Following this, bubble size data which were determined from gas holdup measurements during the flotation experiments in the column and Jameson cell configurations are presented and discussed. The residence time distribution results are then presented along with a discussion of the mixing characteristics in the different cell environments, which in turn contributes to the explanation of the differences in flotation behaviour in the different cell types. The collection efficiency of the -106 $\mu$m particle size fraction is then calculated as a function of hydrophobicity for the column cell by making use of the flotation results, bubble size data and mixing characteristics.

The Chapter concludes with a summary of the results which were obtained, in which a general discussion of the findings obtained from this work is given.

---

78. See the shaded areas in Table 6 on page 87, as well as the discussion following this Table.
79. The concentrates from the experiments with the -106 $\mu$m particle size fraction were analyzed because this fraction represented the size range used in typical industrial flotation operations, as well as the fact that it contains particles of the optimum size for quartz flotation.

## 5.2 FLOTATION RESULTS

The results from the bulk of the flotation experiments are summarized below in Table 9 to Table 12. Quartz and water recoveries are shown for the four particle size fractions at four levels of hydrophobicity (collector dosage). Experiments which were repeated with dispersant added to the pulp are denoted with (D) in the particle size columns of the Tables.

Table 9 : Quartz and Water Recovery in the **Column Cell** Configuration with Different Particle Size Fractions Floated at Different Collector Dosages.

| Particle Size ($\mu$m) | Collector Dosage (g/t) | | | |
|---|---|---|---|---|
| | 0 | 25 | 80 | 200 |
| | Quartz Recovery (%) | | | |
| -106 | 0.00 | 14.17 | 43.60 | 82.69 |
| +106 -150 | 0.00 | 0.00 | 12.61 | 60.72 |
| +150 -300 | 0.00 | 0.00 | 14.47 | 50.10 |
| +300 | 0.00 | 0.05 | 17.53 | 5.20 |
| +300 (D) | | | | 37.23 |
| | Water Recovery (%) | | | |
| -106 | 0.00 | 4.85 | 8.69 | 17.80 |
| +106 -150 | 0.00 | 0.00 | 1.26 | 6.40 |
| +150 -300 | 0.00 | 0.00 | 3.42 | 7.84 |
| +300 | 0.00 | 0.05 | 2.95 | 8.90 |
| +300 (D) | | | | 5.99 |

Table 10 : Quartz and Water Recovery in the **Agitated Cell** Configuration with Different Particle Size Fractions Floated at Different Collector Dosages.

| Particle Size ($\mu$m) | Collector Dosage (g/t) | | | |
|---|---|---|---|---|
| | 0 | 25 | 80 | 200 |
| | Quartz Recovery (%) | | | |
| -106 | 0.00 | 26.93 | 66.95 | 97.38 |
| +106 -150 | 0.00 | 3.71 | 38.12 | 86.35 |
| +150 -300 | 0.00 | 0.48 | 7.11 | 76.50 |
| +300 | 0.00 | 3.14 | 52.18 | 3.34 |
| +300 (D) | | | | 30.94 |
| | Water Recovery (%) | | | |
| -106 | 0.00 | 11.03 | 16.92 | 27.95 |
| +106 -150 | 0.00 | 0.90 | 5.68 | 12.81 |
| +150 -300 | 0.00 | 2.56 | 5.92 | 17.56 |
| +300 | 0.00 | 2.06 | 11.12 | 10.97 |
| +300 (D) | | | | 19.42 |

Table 11 : Quartz and Water Recovery in the **Jameson Cell** Configuration with Different Particle Size Fractions Floated at Different Collector Dosages.

| Particle Size ($\mu$m) | Collector Dosage (g/t) | | | |
|---|---|---|---|---|
| | 0 | 25 | 80 | 200 |
| | Quartz Recovery (%) | | | |
| -106 | 0.00 | 18.43 | 68.79 | 96.53 |
| +106 -150 | 0.00 | 2.00 | 38.77 | 90.07 |
| +150 -300 | 0.00 | 0.97 | 51.24 | 71.98 |
| +300 | 0.00 | 8.44 | 65.52 | 66.25 |
| +300 (D) | | | | 68.41 |
| | Water Recovery (%) | | | |
| -106 | 0.00 | 5.85 | 14.08 | 24.02 |
| +106 -150 | 0.00 | 0.20 | 4.28 | 13.23 |
| +150 -300 | 0.00 | 3.41 | 9.92 | 12.21 |
| +300 | 0.00 | 0.83 | 15.31 | 16.26 |
| +300 (D) | | | | 14.41 |

Table 12 : Quartz and Water Recovery in the Laboratory **Batch Cell** with Different Particle Size Fractions Floated at Different Collector Dosages.

| Particle Size ($\mu$m) | Collector Dosage (g/t) | | | | | |
|---|---|---|---|---|---|---|
| | 0 | 25 | 50 | 80 | 160 | 200 |
| | Quartz Recovery (%) | | | | | |
| -106 | 0.00 | 17.08 | 43.76 | 73.10 | 85.66 | 91.25 |
| +106 -150 | 0.00 | 0.00 | 12.28 | 57.38 | 88.10 | 91.15 |
| +150 -300 | 0.00 | 0.00 | 6.68 | 35.44 | 89.50 | 94.16 |
| +300 | 0.00 | 0.00 | 31.19 | 65.68 | 86.75 | 86.55 |
| | Water Recovery (%) | | | | | |
| -106 | 0.00 | 3.28 | 5.65 | 7.99 | 12.76 | 17.34 |
| +106 -150 | 0.00 | 0.00 | 1.94 | 4.74 | 13.92 | 19.19 |
| +150 -300 | 0.00 | 0.00 | 1.43 | 4.42 | 13.21 | 16.83 |
| +300 | 0.00 | 0.00 | 2.87 | 8.08 | 21.35 | 27.68 |

The detailed results of the flotation experiments are presented in Appendix I on page 187. Although additional experiments were carried out to investigate certain aspects resulting from analysis of the above data, the results of these runs are not shown here. Rather, these data will be presented and discussed further on in this Chapter.

The data from Table 9 to Table 12 above are displayed graphically below in Figure 34 to Figure 37, in which quartz recovery is plotted against collector dosage for each of the four particle size fractions investigated. Water recoveries are not plotted since this thesis focussed on particle collection.

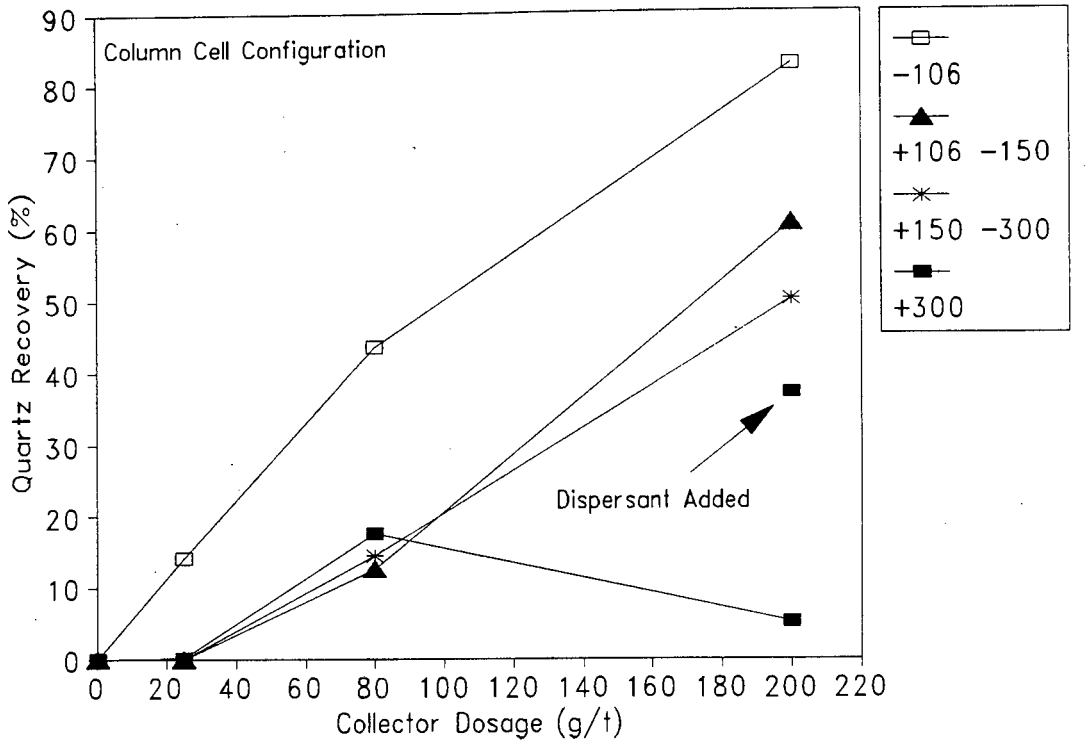


Figure 34 : The Effect of Hydrophobicity on Quartz Recovery in the **Column Cell** Configuration.

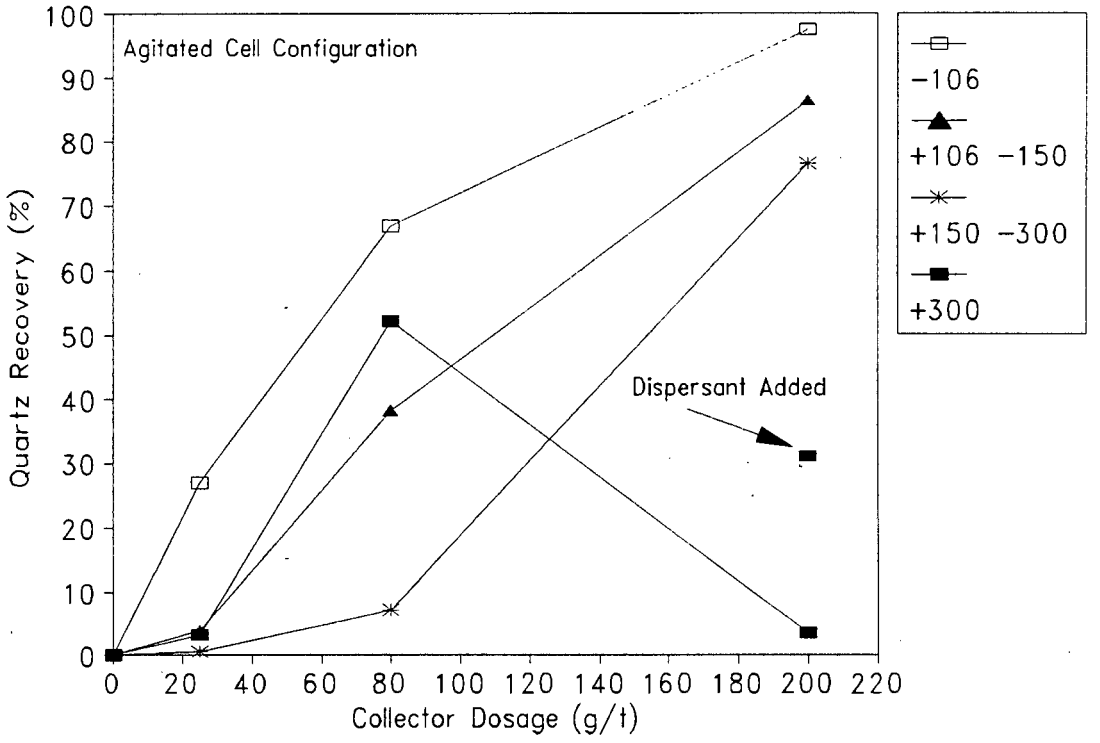


Figure 35 : The Effect of Hydrophobicity on Quartz Recovery in the **Agitated Cell** Configuration.

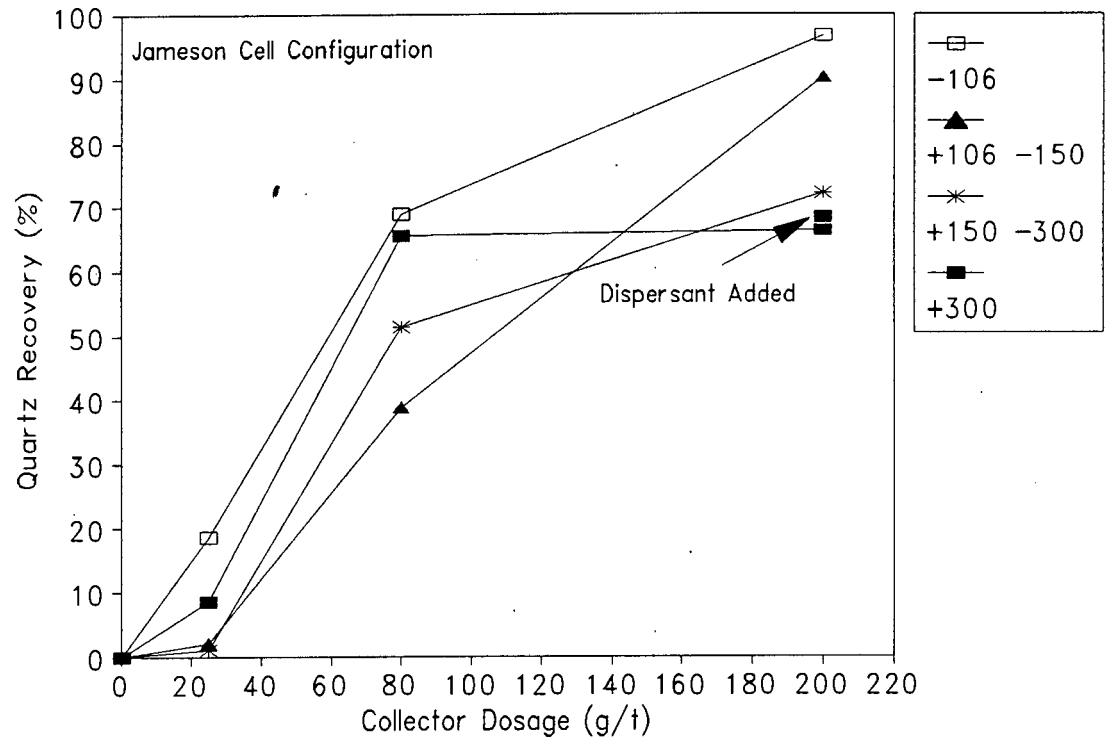


Figure 36 : The Effect of Hydrophobicity on Quartz Recovery in the **Jameson Cell** Configuration.

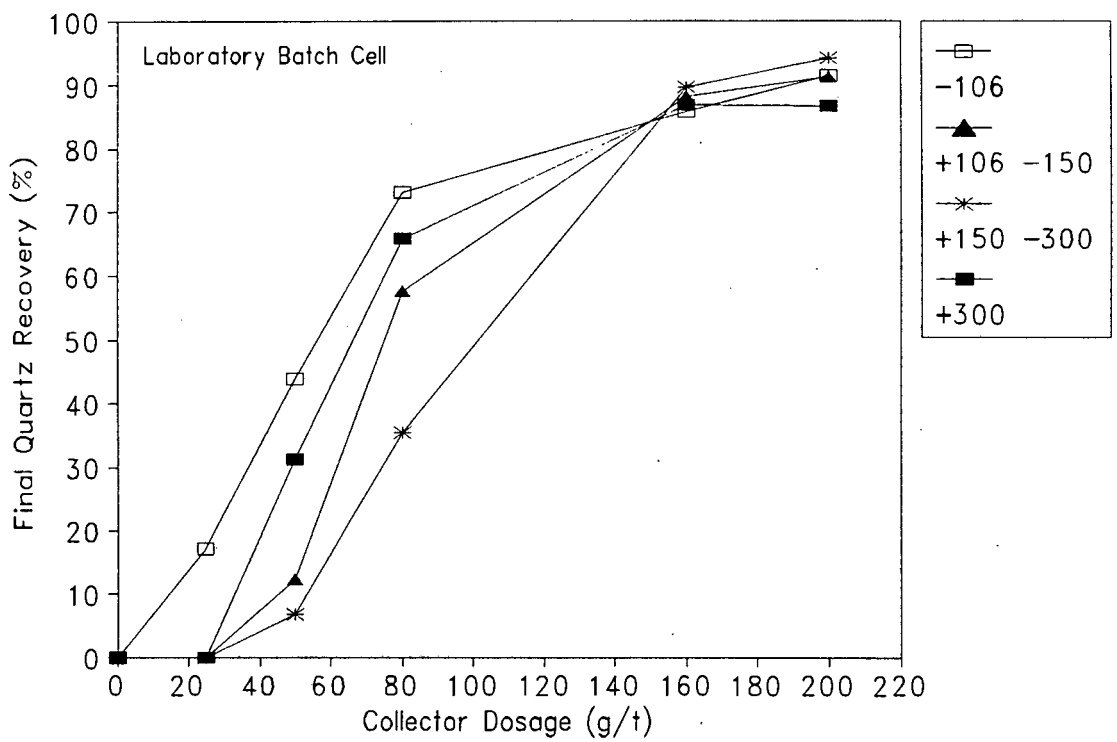


Figure 37 : The Effect of Hydrophobicity on Quartz Recovery in the Laboratory **Batch Cell.**

It is clear from these Figures that the different cell types performed quite differently with respect to particle size and hydrophobicity. If the column and agitated cell results (Figure 34 and Figure 35) are compared, they can be seen to be quite similar in appearance, although the relative positions of the particle size curves are different. However, the results from the Jameson and batch cells (Figure 36 and Figure 37) look quite different to the other two cells. The general differences in appearance of these graphs already show that the different particle contacting environments resulted in marked differences in efficiency of particle collection.

It is also clear from these Figures that the different particle size fractions exhibited distinctly different flotation behaviour. The finest size fraction (-106 $\mu$m) generally gave the highest recovery throughout the range of collector dosages used. An exception was the batch cell experiments, in which the +150 -300 $\mu$m fraction floated better at collector dosages of 150 g/t and higher. Although it could be expected that recovery would decrease with increasing particle size [80] in the size range used during these experiments, this was not always the case: the +300 $\mu$m fraction resulted in higher recoveries than the two immediately finer fractions with all the cell types at a collector dosage of 80 g/t. This was also the case at a dosage of 50 g/t in the batch cell and at 25 g/t in the Jameson cell. Despite the high recoveries of this fraction at 80 g/t, recovery proved to be poor at 200 g/t in the column and agitated cells. An interesting phenomenon is the fact that the three coarsest particle size fractions were recovered at the low collector dosage of 25 g/t in the agitated and Jameson cells, although no collection of these particles took place in the column and batch cells. A more detailed discussion of these results is given under the particle size and particle hydrophobicity discussions in sections 5.3 and 5.4 on pages 99 and 107.

It can also be seen in these Figures that none of the particle size fractions floated without collector added to the pulp in any of the cells. Increased hydrophobicity (collector dosage) generally resulted in increased particle collection, with the -106 $\mu$m particle size fraction approaching 100% recovery at 200 g/t collector dosage in all the cell types, except in the column cell: the final quartz recovery at 200 g/t collector was only approximately 83% in this cell. The +300 $\mu$m particle size fraction showed a distinct maximum in recovery in the column and agitated cells, while recovery remained relatively constant in the Jameson cell. These unexpected results are discussed below in section 5.3.

This brief discussion of the results will be expanded in subsequent sections when the effect of various factors on particle collection efficiency will be discussed. The effect of particle hydrophobicity on particle collection efficiency is discussed first.

80. See the classical n-curve for particle size in Figure 3 and the discussion in section 2.6.1 on page 28.

## 5.3 PARTICLE HYDROPHOBICITY

The function of the collector in flotation pulps is to render selected particles hydrophobic to enable them to become attached to bubbles and be recovered as a concentrate in the froth. Hydrophobicity is therefore a prerequisite for particles to be floatable, as discussed in section 2.2 on page 5. A brief review of the relationship between particle hydrophobicity, particle collection and particle collection efficiency is given in the following section.

### 5.3.1 Particle Hydrophobicity and Particle Collection Efficiency

The floatability of ore particles is strongly dependent upon the hydrophobicity of the particles. An increased dosage of collector added to the slurry should result in a higher degree of hydrophobicity via reduction of the contact angle between liquid and solid at the interface [81]. Physically, the efficiency of collision between particles and bubbles, $E_C$, is regarded as being independent of the hydrophobicity of the particles, although reduced bubble size due to synergistic effects between collector and frother (see the discussion in section 5.3.6) could influence $E_C$. The dependence of $E_C$ on bubble size is illustrated by Equations (22) to (24) on pages 13 and 14, as well as the model of Finch and Dobby for column cells (Equations (27) to (37) on pages 15 to 18).

Secondly, an increased collector dosage increases the attachment efficiency of particles to bubbles, $E_A$, by reducing the induction time, $t_i$, as is clear from the expression of Yoon and Luttrell [1989] (Equation (38) on page 18) and the model of Finch and Dobby for prediction of attachment efficiency (Equations (39) to (46) on pages 20 to 21). An increased collector dosage should also increase the fraction of particles that remain attached to a bubble, $E_S$, via stronger repulsion forces out of the water phase due to a higher degree of hydrophobicity (see Equation (49) on page 23).

Increased hydrophobicity should consequently result in increased collection efficiency, $E_K$, via the above mentioned changes in the three terms $E_C$, $E_A$ and $E_S$ (see Equation (21) on page 13). This increase in $E_K$ will in turn affect the flotation rate constant, k (see Equation (20) on page 12), which, for a fixed residence time, should result in increased recovery, depending on the mixing characteristics prevailing in the cell.

A discussion of the flotation results which were presented above in section 5.2 is given below with reference to this brief theoretical background. Results from additional experiments which were carried out are also presented and discussed.

81. See the discussion of contact angle and hydrophobicity in section 2.3.1 on page 6.

### 5.3.2 Discussion of the Flotation Results with respect to Hydrophobicity

The flotation results which were presented in section 5.2 on page 94 clearly show that increased hydrophobicity generally resulted in increased particle collection (recovery) and water recovery within the range of collector dosage used. The plot of quartz recovery in the column cell (Figure 34 on page 96) shows the recovery of the finest (-106 $\mu$m) particles increasing from 0% up to approximately 83% as the collector dosage was increased from 0 to 200 g/t, while in the other cell types (Figure 35 to Figure 37) the recovery of the same size fraction increased from 0% to close to 100% under the same conditions. The coarser particle size fractions followed the same trend, except for the coarsest (+300 $\mu$m) fraction, for which recovery was poor at 200 g/t. This general increasing trend in recovery with collector dosage agrees with the theory which was summarized in the previous section (increased $E_K$ and k owing to higher $E_A$ and $E_S$). However, the unexpected decrease in recovery with the +300 $\mu$m size fraction contradicts what was explained there. This phenomenon can not easily be explained in terms of hydrophobicity and was further investigated with additional experiments in the column cell configuration. The findings from this work are discussed in sections 5.3.3 to 5.3.5 on page 101 to 105 below.

It is also clear from this data that particle collection did not occur without collector added to the pulp in any of the cell types. This confirms that particle hydrophobicity is a prerequisite for particle collection since quartz is naturally hydrophilic. Although $E_C$ is independent of hydrophobicity, $E_A$ and $E_S$ would in this case be zero.

Although particle size effects are discussed elsewhere [82], an interesting phenomenon from this data is that the +300 $\mu$m particle size fraction floated better than the two finer size fractions (+106 -150 $\mu$m and +150 -300 $\mu$m) at intermediate collector dosages (80 g/t in all the cell types, as well at 50 g/t in the batch cell). Coarse particles should generally be collected at a rate smaller than that of fine particles due to lower $E_S$. It is difficult to try to explain this phenomenon in terms of collection efficiency and an attempt to do so will not be made here.

Despite the fact that a relatively wide range of collector dosages was used during these experiments, a valid question would be what the effect of increasing the dosage of collector to beyond the maximum of 200 g/t [83] would be on particle collection? This and other aspects following from this work are discussed in subsequent sections.

---

82. See the discussion in section 5.4 on page 107.
83. Collector dosages used during quartz flotation are typically lower than 200 g/t [Crozier, 1992].

### 5.3.3 The Effect of Addition of Excess Collector on Particle Collection

The recovery of the -106 $\mu$m particle size fraction in the column cell would be expected to increase further with addition of more collector than 200 g/t (which was the maximum collector dosage used during the bulk of the experiments) until 100% is eventually approached. To assess whether this would be the case, three more dosages of collector (300 g/t, 400 g/t and 500 g/t) were investigated during experiments that were carried out in the column cell configuration. The two finest particle size fractions (the -106 $\mu$m and +106 -150 $\mu$m fractions) were floated during these experiments, while the rest of the flotation conditions were kept the same as in the original experiments.

Quartz and water recoveries obtained from these experiments are shown in Table 13 as a function of collector dosage for each of the four particle size fractions. The data that were already presented in Table 9 on page 94 are included in this Table. A repeat experiment with the +300 $\mu$m particle size fraction at a collector dosage of 200 g/t was also carried out in which dispersant was added to the pulp: this run is denoted with (D) in the particle size column of the Table.

Table 13 : Recovery of Quartz and Water in the Column Cell Configuration with Different Particle Size Fractions Floated at Different Levels of Hydrophobicity.

| Particle Size ($\mu$m) | Collector Dosage (g/t) | | | | | | |
|---|---|---|---|---|---|---|---|
| | 0 | 25 | 80 | 200 | 300 | 400 | 500 |
| | Quartz Recovery (%) | | | | | | |
| -106 | 0.00 | 14.17 | 43.60 | 82.69 | 87.94 | 92.36 | 95.97 |
| +106 -150 | 0.00 | 0.00 | 12.61 | 60.72 | 82.01 | 69.16 | 50.20 |
| +150 -300 | 0.00 | 0.00 | 14.47 | 50.10 | | | |
| +300 | 0.00 | 0.05 | 17.53 | 5.20 | | | |
| +300 (D) | | | | 37.23 | | | |
| | Water Recovery (%) | | | | | | |
| -106 | 0.00 | 4.85 | 8.69 | 17.80 | 19.28 | 24.36 | 26.22 |
| +106 -150 | 0.00 | 0.00 | 1.26 | 6.40 | 9.52 | 9.82 | 6.07 |
| +150 -300 | 0.00 | 0.00 | 3.42 | 7.84 | | | |
| +300 | 0.00 | 0.05 | 2.95 | 8.90 | | | |
| +300 (D) | | | | 5.99 | | | |

A graphical illustration of this data is given below in Figure 38. The expected increasing trend of quartz recovery [84] with collector dosage is evident for the -106 $\mu$m particle size fraction. The +106 -150 $\mu$m fraction showed a decrease in recovery at

84. Water recovery also showed an increasing trend with collector dosage, as is clear from Table 13.

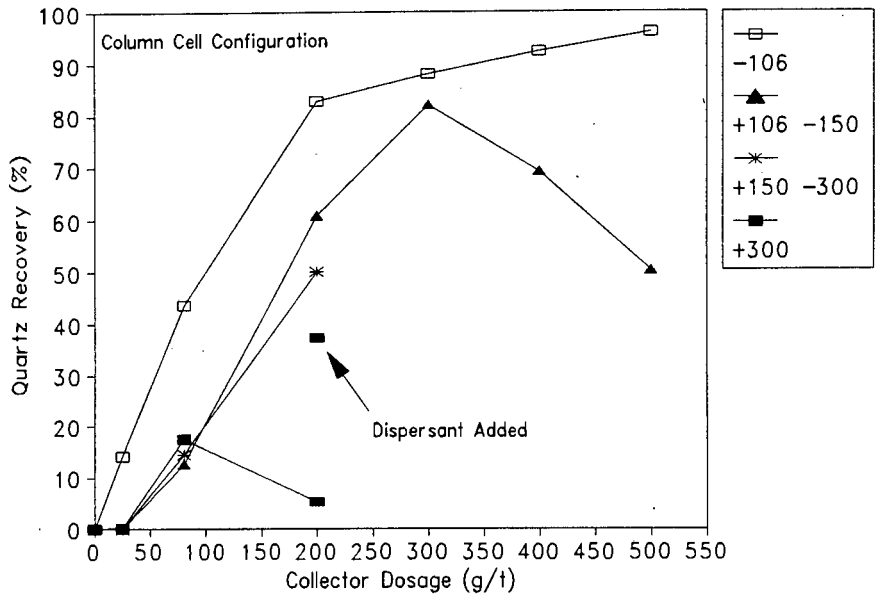


Figure 38 : The Effect of Hydrophobicity on Quartz Recovery in the Column Cell Configuration.

collector dosages greater than 300 g/t, while a poor recovery was obtained with the +300 $\mu$m size fraction at a collector dosage of 200 g/t.

If the curves of the +106 -150 $\mu$m and +300 $\mu$m size fractions are considered, it is clear that the decrease in recovery occurred at a lower collector dosage for the coarser particle size fraction. A possible explanation for this phenomenon could be that smaller particles have larger surface area to mass ratios than large particles, and the potential for collector adsorption can consequently be expected to be greater for small particles than for the same mass of large particles. The recovery of the finest (-106 $\mu$m) size fraction probably did not decrease with increased collector addition because of high collector uptake owing to larger surface area, but could be expected to decrease (similar to the coarser fractions) at a collector dosage greater than 500 g/t. If this is so, it would be reasonable to expect the +150 -300 $\mu$m particle size fraction to reach its maximum recovery in this system (before recovery starts decreasing) at a collector dosage which is somewhere between 80 and 300 g/t.

The next section takes a closer look at this data by analyzing it more comprehensively.

### 5.3.4 Mechanism of Adsorption of Collector onto the Quartz Surface

The flotation results that were presented in the previous section were further interpreted by calculating the percentage of the quartz particle surface area that was covered with

collector molecules. The total projected area of the collector molecules [85] was divided by the total available surface area of the quartz particles. The mean particle diameters of each particle size fraction (calculated in section 4.2.2.1 on page 72) was used in the calculation of the pseudo coverage of particles with collector molecules. The particles were assumed to be spherical during these calculations. It was further assumed that all the collector molecules present in the pulp were attached to the quartz surface during flotation (*i.e.* complete conditioning). The results of these calculations are presented in Table 14.

Table 14 : Pseudo Coverage of the Particle Surface with Collector Molecules (%).

| Particle Size Fraction ($\mu$m) | Collector Dosage (g/t) | | | | | | |
|---|---|---|---|---|---|---|---|
| | 0 | 25 | 80 | 200 | 300 | 400 | 500 |
| -106 | 0.00 | 4.25 | 13.62 | 34.04 | 51.06 | 68.08 | 85.10 |
| +106 -150 | 0.00 | 7.47 | 23.91 | 59.77 | 89.65 | 119.53 | 149.42 |
| +150 -300 | 0.00 | 11.22 | 35.89 | 89.73 | | | |
| +300 | 0.00 | 21.38 | 68.43 | 171.08 | | | |

The surface coverage can be seen from the Table to be below 100% for all the experiments with the -106 $\mu$m particle size fraction, while it exceeded 100% with the +106 -150 $\mu$m fraction for collector dosages greater than 300 g/t. The calculated surface coverage of the +150 -300 $\mu$m size fraction was below 100 % for all the collector dosages used, while it was much greater than 100% for the +300 $\mu$m particle size fraction at a collector dosage of 200 g/t. If it is assumed that monolayer coverage of the particle surface with collector molecules took place, there must have been collector molecules in excess in the cases where the calculated surface coverage exceeded 100%. These molecules could then either be present as free ions in solution, or could have been adsorbed onto the quartz surface as a second (double) layer.

If the calculated particle surface coverages are compared with the flotation recoveries in Table 13 on page 101 and Figure 38 on page 102, it becomes clear that the points at which the +106 -150 $\mu$m and +300 $\mu$m size fractions started showing a decrease in recovery correspond to particle surface coverages of more than 100%. It is therefore proposed that the excess collector molecules formed a second layer on the particle surface with the particles having an orientation opposite to those present in the first layer, and that they were not present in solution. It is further proposed that the

85. The hydrophilic head of the collector used during this investigation (HPYC - see section 4.3.1 on page 77) comprised a pyridinium ring. The diameter (bond length) of pyridinium rings is given as 1.85 Å [Weast, 1976].

hydrophobic tails of the molecules in the two respective layers became entangled, leaving the hydrophilic heads of the outer layer of molecules facing outwards. Although the particles should have been entirely covered with collector molecules when the proposed second layer started forming (maximum degree of hydrophobicity reached), they would become less hydrophobic to a degree which depended on the extent of double layer coverage. This hypothesis is supported if flotation recovery is plotted against the percentage available hydrophobic quartz surface [86] for the experiments with the +106 -150 $\mu$m particle size fraction. The results are shown in Figure 39. The points at which the double layer of collector molecules is proposed to have formed, are also indicated on this Figure.

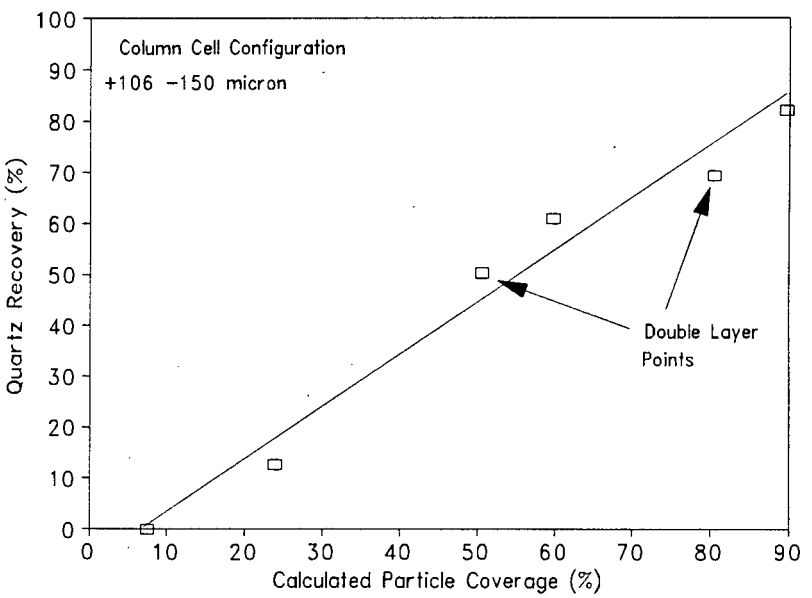


Figure 39 : Calculated Percentage Available Hydrophobic Quartz Surface *vs.* Quartz Recovery in the Column Cell Configuration.

It is evident from this Figure that there is a linear relationship between the percentage available hydrophobic surface and flotation recovery. A linear regression was used to obtain the line through these points, and a correlation coefficient of 0.97 was obtained for this fit. It has to be noted that the points which represent the cases where the surface coverage was greater than 100% fell on the same line with the other data points. This supports the theory of the formation of a second layer of collector.

It would therefore be reasonable to conclude that, with only one exception, the adsorption of collector molecules onto particles never exceeded monolayer coverage

86. The percentage available hydrophobic quartz surface was calculated for cases in which the particle surface coverages exceeded 100% by subtracting the percentage by which it exceeded 100%, from 100%.

for any of the particle size fractions floated in the range of collector dosage used during the bulk of the flotation experiments (0 - 200 g/t). The exception was the experiments with the +300 $\mu$m particle size fraction at a collector dosage of 200 g/t, during which the particles were covered more than 100%, as was shown above in Table 14.

Although it is tempting to contribute the poor recovery of the +300 $\mu$m particle size fraction at 200 g/t collector solely to this collector double layer effect, the formation of small flocs was noticed during the flotation experiments with this size fraction. The presence of these flocs could be another possible cause for the poor recovery of these particles. A discussion of this is given in the following section.

### 5.3.5 Flocculation of Coarse Particles at High Collector Dosages

The formation of small flocs was noticed during flotation of the +300 $\mu$m size fraction at a collector dosage of 200 g/t [87]. It seemed that the flocs were formed during conditioning in the feed tank, and that they were pumped to the column cell without being disrupted in the connecting rubber tubes. It is therefore possible that the poor recovery of this size fraction was due to these flocs being too heavy to be recovered in the column cell (*i.e.* poor recovery owing to low $E_S$).

To determine which one of the two effects (flocculation or the collector double layer formation, which was discussed in the previous section) was responsible for the poor recovery during this experiment, it was repeated with dispersant added to the pulp in all three of the hybrid column cell configurations [88]. If the results from the two experiments in the column cell (Figure 38) are compared, it is clear that a significant increase in recovery from 5.20% to 37.23% occurred. It is therefore proposed that the addition of dispersant inhibited the formation of flocs in the feed tank, and that the increase in recovery was due to the unflocculated particles being light enough to be recovered (flocs were not noticed during the repeat run). Furthermore, the point which represents this second experiment lies at a position where one would have expected it to be if the general trend from the other data points is considered.

It can therefore be proposed that a combination of the two effects was responsible for the poor recovery. It is clear from Figure 38 that the +300 $\mu$m size fraction gave a greater quartz recovery than the two finer (+150 -300 $\mu$m and +106 -150 $\mu$m) particle size fractions at a collector dosage of 80 g/t, which is contrary to what one would

87. Just as large particles have a high efficiency of collision with bubbles, $E_C$, and efficiency of attachment to bubbles, $E_A$, they should easily collide and attach to each other (with collector tails interacting).

88. The type of dispersant and the dosage used have been discussed in section 4.6.2 on page 87.

expect, since the coarse particles are heavier and should therefore be more difficult to recover. It could be argued that this relatively small difference between the recoveries of the three fractions can be attributed to experimental error, but this fraction floated better at this collector dosage in all the cell configurations without exception, as discussed in section 5.2 on page 94. One might therefore have expected the recovery of the +300 $\mu$m particle size fraction to be greater than the two finer fractions at a collector dosage of 200 g/t too, but it was smaller, even with dispersant added to the pulp. While this does not explain why the recovery of the coarser size fraction should be greater at 80 g/t, the observation does support the hypothesis that a combination of the above mentioned two effects (flocculation and double layer formation) occurred. This seems reasonable if the fact that formation of flocs was not noticed during flotation of the +106 -150 $\mu$m particle size fraction at collector dosages greater than 300 g/t (in which double layer formation is postulated to have occurred) is considered.

With this additional information on the mechanism of collector adsorption and other side effects at hand, the choice of the number and range of collector dosages used may be evaluated. This is discussed in the following section.

### 5.3.6 Evaluation of the Choice of the Range and Dosages of Collector

It is clear from the discussion in the previous section that the choice of the range of collector dosages used was a sensible one, since side effects became clear within this range, *e.g.* collector double layer formation and flocculation. The experiments in the batch cell were carried out at smaller increments of collector dosage, which provided more information on aspects which might normally have been attributed to experimental error. An example is the unexpected high recovery of the +300 $\mu$m size fraction at an intermediate collector dosage (80 g/t), which was confirmed by the same effect at 50 g/t collector (see Figure 37 on page 97). It is therefore recommended that this work be extended, but at smaller increments of collector dosage to get more comprehensive data. Experiments with the +300 $\mu$m size fraction could for example determine at which collector dosage floc formation starts.

### 5.3.7 Summary

Increased hydrophobicity (collector dosage) generally led to increased particle collection in all the cell types. Decreased recovery with increased collector was shown to be due to the formation of a double layer of collector on the particle surface with an opposite orientation to the first, or to a combination of this effect and flocculation phenomena.

## 5.4 PARTICLE SIZE

Particle size is considered to play a vital role in the flotation process, as is evidenced by the intensity of the research effort which has been devoted to this aspect in the past. Particle size has therefore been identified as one of the most important variables which were investigated in this thesis [89]. Its effect on particle collection efficiency will be discussed in subsequent sections with reference to the flotation results which were obtained.

A brief review of the theoretical aspects of the effect of particle size on particle collection efficiency is given in the following section.

### 5.4.1 Particle Size and Particle Collection Efficiency

Collection efficiency, $E_K$, is influenced by particle size, $d_p$, via the three terms on the right hand side of Equation (21) on page 13. The dependence of collision efficiency, $E_C$, upon $d_p$ is quantified by Equations (22) to (24) on pages 13 to 14, as well as the model of Finch and Dobby in section 2.4.2.1.1 on page 15. $E_C$ increases with $d_p$ due to geometrical considerations: larger particles have a greater chance of colliding with bubbles than small ones. $E_A$ is affected by $d_p$ in that $E_A$ increases with increasing $d_p$ (see Equation (38) on page 18 and Finch and Dobby's model in section 2.4.2.2.1 on page 19). Finally, increased $d_p$ results in a decrease in the fraction of particles which stay attached to bubbles, $E_S$ (see Equations (48) and (49) on pages 22 and 23). This can mainly be attributed to a momentum effect: larger particles are more easily detached from bubbles owing to increased mass. $E_K$ is therefore strongly dependent upon $d_p$, amongst other factors such as mixing in the cell and particle hydrophobicity.

Proper analysis of the flotation results in terms of particle size requires more comprehensive information on the flotation behaviour of particles within the relatively wide -106 $\mu$m size fraction. This is given in subsequent sections.

### 5.4.2 Particle Size Analysis of the -106 $\mu$m Size Fraction

In order to investigate the effect of the particle-bubble contacting mechanism on the recovery of quartz by particle size, particle size analyses were carried out on the concentrates obtained in the experiments with the -106 $\mu$m size fraction in the different cell configurations [90]. Size analysis was also carried out on the feed used in each of

89. See the discussion in section 2.6.1 on page 28.
90. The results of the flotation experiments were presented in section 5.2 on page 94.

these experiments in order to calculate the recovery of each particle size sub-fraction. These analyses were made using a Malvern particle size analyzer and the detailed results are presented in Appendix G on page 181. This instrument was able to detect particles as small as 1.93 $\mu$m, and could measure the distribution of particles at very small increments of particle size. The reproducibility of measurements was tested by carrying out two repeat analyses of the -106 $\mu$m feed fraction. These results are presented in Table 15, in which the distributions of the particle size sub-fractions were summed to obtain Tyler distributions.

Table 15 : Particle Size Analysis of the -106 $\mu$m Feed Fraction with the Malvern Particle Size Analyzer.

| Particle Size ($\mu$m) | % Passing | | |
|---|---|---|---|
| | Run 1 | Run 2 | Run 3 |
| 2 | 31.78 | 32.39 | 32.02 |
| 25 | 46.08 | 46.29 | 45.78 |
| 38 | 55.38 | 56.10 | 55.48 |
| 53 | 74.80 | 75.10 | 74.83 |
| 75 | 94.93 | 94.41 | 94.55 |

This Table shows that the reproducibility of the measurements with the Malvern was very good and it was therefore assumed that the analyses of the concentrates would be equally reproducible.

Although only the total recoveries of the experiments with the -106 $\mu$m size fraction were measured during flotation experiments, it was possible to calculate the recoveries of the sub-fractions within this fraction from the size analysis results. The recovery of the total fraction for the specific experiment was multiplied by the ratio of the mass of particles in the specific size range in the concentrate over that present in the feed.

These calculated recoveries provide much more comprehensive information on particle size effects and are presented and discussed in the following section.

### 5.4.3 Discussion of the Flotation Results with respect to Particle Size

The calculated recoveries of sub-fractions within the -106 $\mu$m particle size fraction are presented below in Table 16 to Table 19 for the different cell types at varying collector dosages. The results from experiments with the three coarser particle size fractions (which were presented in Table 9 to Table 12 on pages 94 to 95 along with the recoveries of the complete -106 $\mu$m size fraction) are included in these Tables for the sake of completeness.

Table 16 : Quartz Recovery (%) of Size Fractions in the **Column Cell** Configuration at Different Collector Dosages.

| Particle Size Fraction ($\mu$m) | Collector Dosage (g/t) | | | | | | |
|---|---|---|---|---|---|---|---|
| | 0 | 25 | 80 | 200 | 300 | 400 | 500 |
| +1.93 -25 | 0.00 | 24.86 | 52.21 | 61.65 | 62.89 | 75.74 | 80.14 |
| +25 -38 | 0.00 | 17.25 | 59.30 | 83.32 | 87.41 | 87.04 | 83.27 |
| +38 -53 | 0.00 | 18.64 | 62.34 | 97.78 | 95.46 | 93.10 | 92.81 |
| +53 -75 | 0.00 | 7.48 | 40.69 | 94.00 | 95.56 | 96.34 | 86.56 |
| +75 -106 | 0.00 | 1.94 | 13.57 | 92.43 | 99.50 | 98.60 | 96.34 |
| +106 -150 | 0.00 | 0.00 | 12.61 | 60.72 | 82.01 | 69.16 | 50.20 |
| +150 -300 | 0.00 | 0.00 | 14.47 | 50.10 | | | |
| +300 | 0.00 | 0.05 | 17.53 | 5.20 | | | |

Table 17 : Quartz Recovery (%) of Size Fractions in the **Agitated Cell** Configuration at Different Collector Dosages.

| Particle Size Fraction ($\mu$m) | Collector Dosage (g/t) | | | |
|---|---|---|---|---|
| | 0 | 25 | 80 | 200 |
| +1.93 -25 | 0.00 | 47.87 | 72.54 | 95.84 |
| +25 -38 | 0.00 | 34.66 | 77.97 | 96.23 |
| +38 -53 | 0.00 | 33.65 | 87.09 | 99.12 |
| +53 -75 | 0.00 | 15.03 | 80.73 | 96.23 |
| +75 -106 | 0.00 | 3.35 | 62.22 | 89.54 |
| +106 -150 | 0.00 | 3.71 | 38.12 | 86.35 |
| +150 -300 | 0.00 | 0.48 | 7.11 | 76.50 |
| +300 | 0.00 | 3.14 | 52.18 | 3.34 |

Table 18 : Quartz Recovery (%) of Size Fractions in the **Jameson Cell** Configuration at Different Collector Dosages.

| Particle Size Fraction ($\mu$m) | Collector Dosage (g/t) | | | |
|---|---|---|---|---|
| | 0 | 25 | 80 | 200 |
| +1.93 -25 | 0.00 | 36.75 | 60.80 | 80.54 |
| +25 -38 | 0.00 | 21.24 | 79.10 | 97.62 |
| +38 -53 | 0.00 | 22.12 | 83.20 | 99.80 |
| +53 -75 | 0.00 | 6.11 | 73.57 | 99.80 |
| +75 -106 | 0.00 | 2.06 | 61.56 | 99.44 |
| +106 -150 | 0.00 | 2.00 | 38.77 | 90.07 |
| +150 -300 | 0.00 | 0.97 | 51.24 | 71.98 |
| +300 | 0.00 | 8.44 | 65.52 | 66.25 |

Table 19 : Quartz Recovery (%) of Size Fractions in the Laboratory **Batch Cell** at Different Collector Dosages.

| Particle Size Fraction ($\mu$m) | Collector Dosage (g/t) | | | |
|---|---|---|---|---|
| | 0 | 25 | 80 | 200 |
| +1.93 -25 | 0.00 | 21.02 | 65.35 | 92.56 |
| +25 -38 | 0.00 | 31.11 | 72.67 | 94.35 |
| +38 -53 | 0.00 | 36.08 | 88.26 | 98.12 |
| +53 -75 | 0.00 | 16.93 | 83.25 | 99.22 |
| +75 -106 | 0.00 | 5.03 | 75.22 | 93.15 |
| +106 -150 | 0.00 | 0.00 | 57.38 | 91.15 |
| +150 -300 | 0.00 | 0.00 | 35.44 | 94.16 |
| +300 | 0.00 | 0.00 | 65.68 | 86.55 |

The results from these Tables are plotted along with the actual experimental recoveries of the three coarser particle size fractions as a function of particle size in Figure 40 to Figure 43. In these Figures, the data points on the left of the dividing line represent the calculated recoveries of the smaller sub-fractions, while the data points on the right represent the experimental recoveries of the three coarser particle size fractions. It was assumed here that no interaction took place between particles of different sizes within the -106 $\mu$m particle size fraction when constructing these graphs. The validity of this assumption is discussed below.

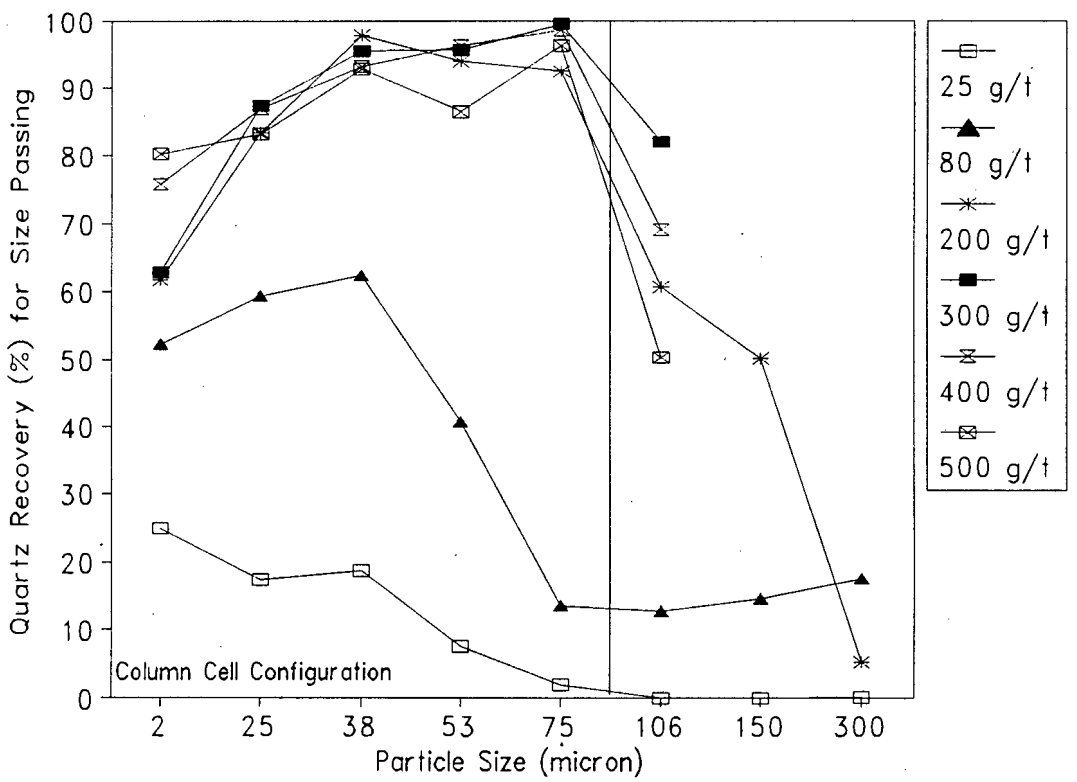


Figure 40 : Variation of Flotation Recovery with Particle Size in the **Column Cell** Configuration at Different Collector Dosages.

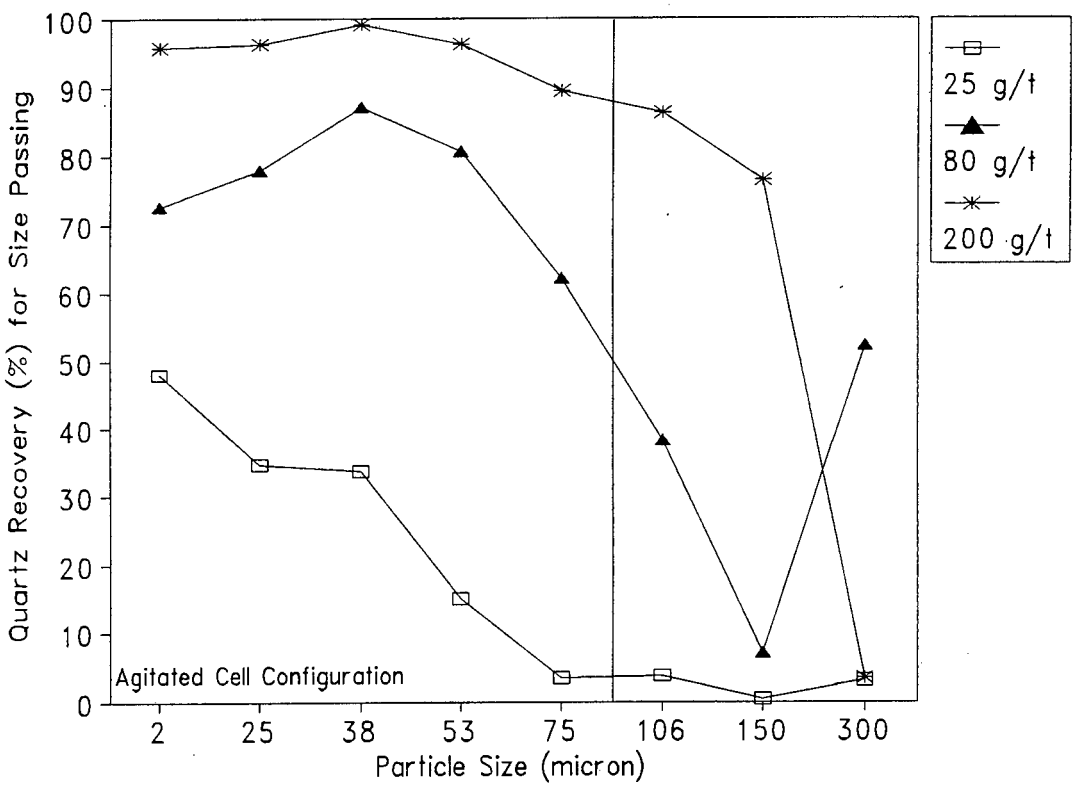


Figure 41 : Variation of Flotation Recovery with Particle Size in the **Agitated Cell** Configuration at Different Collector Dosages.

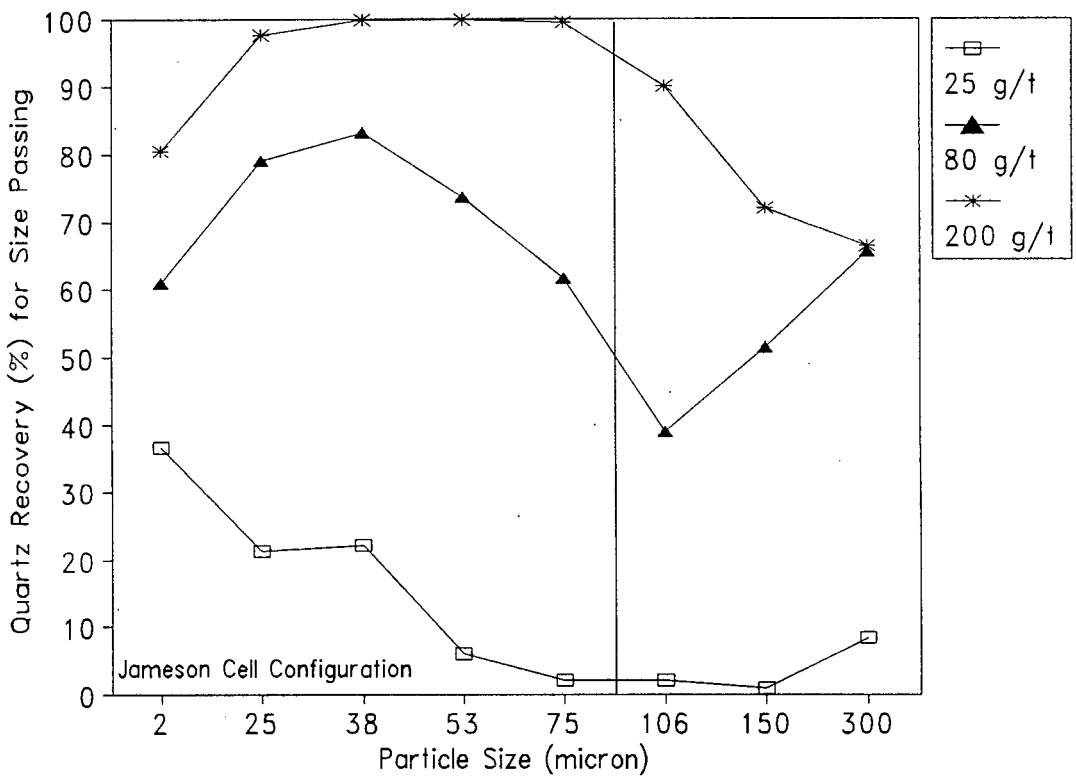


Figure 42 : Variation of Flotation Recovery with Particle Size in the **Jameson Cell** Configuration at Different Collector Dosages.

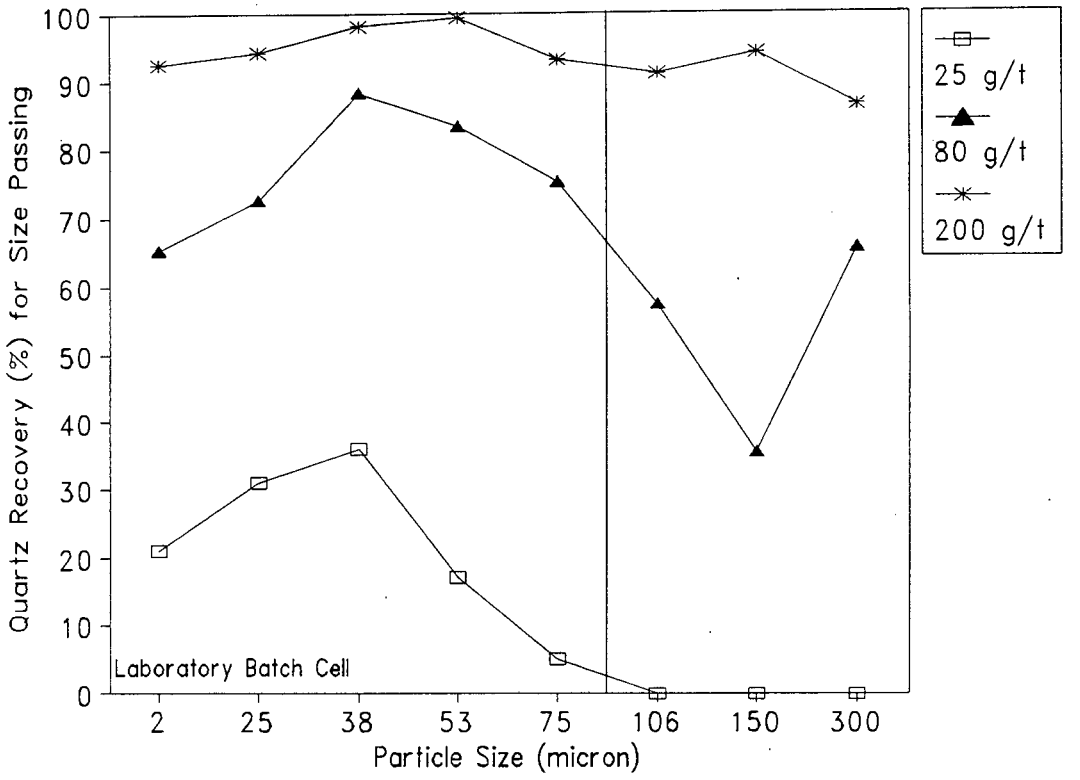


Figure 43 : Variation of Flotation Recovery with Particle Size in the Laboratory **Batch Cell** at Different Collector Dosages.

It is possible that different size particles within the -106 $\mu$m size fraction could interact with each other [91]. The fact that this size fraction comprised a relatively wide distribution of particle sizes could therefore lead to the question whether it is scientifically correct to plot the calculated recoveries of the sub-fractions within this fraction together with the recoveries of the other (narrower) size fractions. However, it is clear from the Figures above that the transition across the dividing line between the calculated and experimental recoveries was generally smooth, which supports the assumption made above that no interaction took place between particles. The calculated recoveries of the sub-fractions could therefore rightfully be compared to the experimental recoveries of the three coarser size fractions.

The first observation that can be made from these Figures is that collector dosage (hydrophobicity) had a significant effect on particle size behaviour in the different cell environments. This becomes clear if the particle size curves of experiments at 25 g/t collector are compared to those at higher dosages: the expected n-curved response [92] of recovery with particle size did not occur at this low collector dosage, but a general

91. For example, it is well known that the presence of fines in a flotation feed can have a detrimental effect on flotation recovery (see the discussion in section 2.6.1.1 on page 31).

92. See Figure 3 and the discussion in section 2.6.1 on page 28.

decreasing trend in flotation recovery with increased particle size was obtained (except in the batch cell). This is probably due to the relatively high $E_S$ of fine particles owing to smaller momentum: hydrophobic repulsion should be low at this collector dosage which would result in only particles with low momentum remaining attached to bubbles, while coarse particles would easily detach from the bubbles. The particle size curves at 80 g/t collector showed the expected trend of relatively poor recovery in the coarse and fine particle regions (n-curve), as discussed in section 2.6.1 on page 28. A further increase in hydrophobicity caused the curves to move up further, while the n-shape was in some cases even more pronounced. However, the recovery curve in the batch cell at 200 g/t was almost flat, which shows that the batch cell was not as sensitive to particle size as the other cells at this collector dosage. Despite the marked change in particle size behaviour with increased collector dosage, the shape of the curves did not change significantly with collector dosages of up to 300 g/t and more in the column cell. However, very fine (-25 $\mu$m) particles showed increased recovery with increased collector dosage at dosages greater than 200 g/t, while the recovery of intermediate (+106 -150 $\mu$m) particles decreased with further addition of collector at these dosages. It is therefore proposed that very fine particles were preferentially recovered at high collector dosages. The unexplained high recovery of coarse particles at 80 g/t collector noted in section 5.3.2 above is evident in these Figures.

It is also clear that the different cell types exhibited different flotation behaviour with particle size. The recovery of very fine (-25 $\mu$m) particles at high collector dosages was much greater in the agitated and batch cells than in the column and Jameson cell configurations. This is proposed to be due to greater contacting intensity owing to agitation (increased $E_C$ and $E_A$). Furthermore, recovery of coarse (+300 $\mu$m) particles at a collector dosage of 200 g/t was much smaller in the column and agitated cells than in the Jameson and batch cells. Flocculation of particles occurred during these experiments, as discussed in section 5.3.5 on page 105, which probably caused the poor recovery. Particle collection did not occur without collector added to the pulp, irrespective of the size of the particles, and these results were therefore not shown in these Figures. Coarse (+300 $\mu$m) particles were not collected in the column and batch cells at the low collector dosage of 25 g/t. However, collection of coarse particles did occur in the agitated and Jameson cell configurations at this dosage. A more comprehensive discussion of these phenomena is given in section 5.5.2 on page 116 in which the effect of cell type on particle collection efficiency is discussed.

The optimum particle size range for quartz flotation was found by de Bruyn and Modi [1956] to be between 10 and 50 $\mu$m for a continuous laboratory flotation cell and between 9 and 50 $\mu$m for a laboratory batch cell. These findings are confirmed by the

recovery results of the -106 μm size fraction at collector dosages of 80 g/t and more.

The choice of the number and range of the particle size fractions used during the experimental work may be questioned at this point. A discussion of this is given in the following section.

### 5.4.4 Evaluation of the Choice of Particle Size Fractions

The four particle size fractions that were used in the flotation experiments during this investigation represented a wide range of particle size. However, the fact that this wide distribution of size was contained within only four particle size fractions may be questioned. Stated differently, should more particle size fractions with narrower fractions not have been used instead? It would have been ideal to have had as many narrow size fractions as possible to determine the effect of particle size in detail, but the practical implication of this made it difficult to achieve: screening becomes increasingly more difficult as particles become finer, with the result that there is a physical limit to the separation of very fine particles from a batch of milled ore. Furthermore, industrial screens are manufactured in standard mesh sizes, which limits the size of fractions that can obtained via screening. If the additional information that was obtained from particle size analysis of the -106 μm size fraction is compared with the labour-intensive task of preparing separate fractions within this size range, it is evident that the former method of operation is to be preferred. However, it is recommended that the size fractions which are treated in this way should still be as narrow as possible to avoid possible interaction of particles of different size within the fraction. It is therefore recommended that the method of flotation of a size fraction with particle size analysis afterwards be used by future workers. Coarser size fractions can also be subjected to this method. The +150 -300 μm size fraction, which was considered as being one single fraction, although it comprised two Tyler fractions (+150 -212 μm and +212 -300 μm) could also have been analyzed in this way.

### 5.4.5 Summary

Particle size phenomena were strongly influenced by the collector dosage used. Low collector dosages resulted in fine particles being collected first, while higher collector dosages resulted in classical n-shaped curves of recovery with collector dosage. Fine particles were collected preferentially at high collector dosages. The different cell types exhibited different particle size behaviour with the agitated and Jameson cells promoting the recovery of coarse particles at low collector dosages. The agitated and batch cells enhanced fine particle collection at high collector dosages.

## 5.5 FLOTATION CELL TYPE

The aim of this thesis was to investigate the effect of *different contacting environments* on particle collection efficiency. The effect of the different cell types which were chosen to result in different contacting environments was therefore a crucial variable in this investigation. The flotation results which were presented in the sections above are discussed with respect to cell type in this section. A description of the contacting environments in the four different cell types is given below. The discussion includes a brief review of the expected effect of these different contacting environments on particle collection efficiency.

### 5.5.1 Particle Contacting Environment (Cell Type) and Particle Collection Efficiency

The contacting environment in the column cell configuration is essentially quiescent, although air bubbles still create a certain degree of turbulence in the cell [93]. The contacting environment in the agitated cell configuration is identical to that of the column cell, except that turbulence is added in the form of agitation. Pulp is fed counter-current to air in these two cells, so that if a particle is not collected during the first encounter with a bubble or if it is separated from a bubble, it will have many other opportunities to be collected or re-collected until it is finally recovered in the froth phase or discarded as part of the tailings stream. Collection in the Jameson cell takes place in the downcomer tube; the rest of the column is simply used as a disengagement zone for the collected particles to separate from the tailings stream. The co-current stream of pulp and air is discharged from the downcomer virtually at the bottom of the cell and a particle will probably not have a second chance of being collected once it has exited the downcomer tube. The Jameson cell is further characterised by intense contacting between particles and bubbles across the orifice, after which the pulp enters the relatively quiescent downcomer tube. Although both the agitated and Jameson cell configurations can be regarded as devices which employ intense conditions of contacting, it is difficult to compare these two cells with respect to the intensity of contacting between particles and bubbles. The batch cell represents a different contacting environment in that it is a process in which the concentration of solids decrease with time as solids are removed in the froth. The batch cell also employs intense conditions of contacting owing to agitation as is the case with the agitated cell.

93. See the discussion of the effect of air flow rate on the mixing characteristics and pulp residence time in the column cell in section 5.7.3.1 on page 138.

These different contacting environments can be expected to result in marked differences in the efficiency of particle collection. The environment in the column cell configuration can be expected to result in relatively high $E_S$ due to the absence of turbulence in this cell, which should lead to increased recovery of particles that are easily detached from bubbles (such as coarse particles). However, $E_C$ should be low due to a relatively small number of collisions compared to more turbulent environments. $E_A$ can also be expected to be low owing to low impact between particles and bubbles, with the effect that the liquid film between particles and bubbles should not easily be ruptured. Fine particles which attach with more difficulty owing to low $E_C$ and $E_A$ could therefore be expected not to be easily recovered in the column cell.

Addition of agitation in the agitated cell should result in higher $E_C$ because of an increased number of collisions per volume of pulp, while $E_A$ should be higher owing to increased impact between particles and bubbles. Despite these factors, $E_S$ can be expected to be significantly lower because of turbulent forces which should detach particles from bubbles. The recovery of fine particles (which have low $E_C$ and $E_A$, but high $E_S$) can therefore be expected to be more efficient in the agitated cell. The same arguments should apply to the contacting environment in the batch cell, although the characteristics of mixing will be totally different.

The Jameson cell should also result in high $E_C$ and $E_A$ owing to intense contacting across the orifice, although $E_S$ can be expected to be greater than in the agitated cell because of the quiescent conditions in the disengagement zone, as well as the absence of a counter-current stream of pulp which could detach particles from bubbles. However, the fact that particles do not have a second chance of being collected once they have exited the downcomer tube may counter the possible gain in collection via high $E_S$. The Jameson cell could therefore be expected to collect both coarse and fine particles efficiently. With this brief theoretical background in mind, the flotation results are discussed with respect to cell type in the following section.

### 5.5.2 Discussion of the Flotation Results with respect to Flotation Cell Type (Particle-Bubble Contacting Environment)

The flotation results which were presented in the particle size discussion in section 5.4 above are discussed with respect to cell type in this section. Differences in particle collection between these cell types can best be illustrated by plotting quartz recovery against particle size. These results are shown below in Figure 44 to Figure 46 in which the particle size behaviour at the different collector dosages is shown.

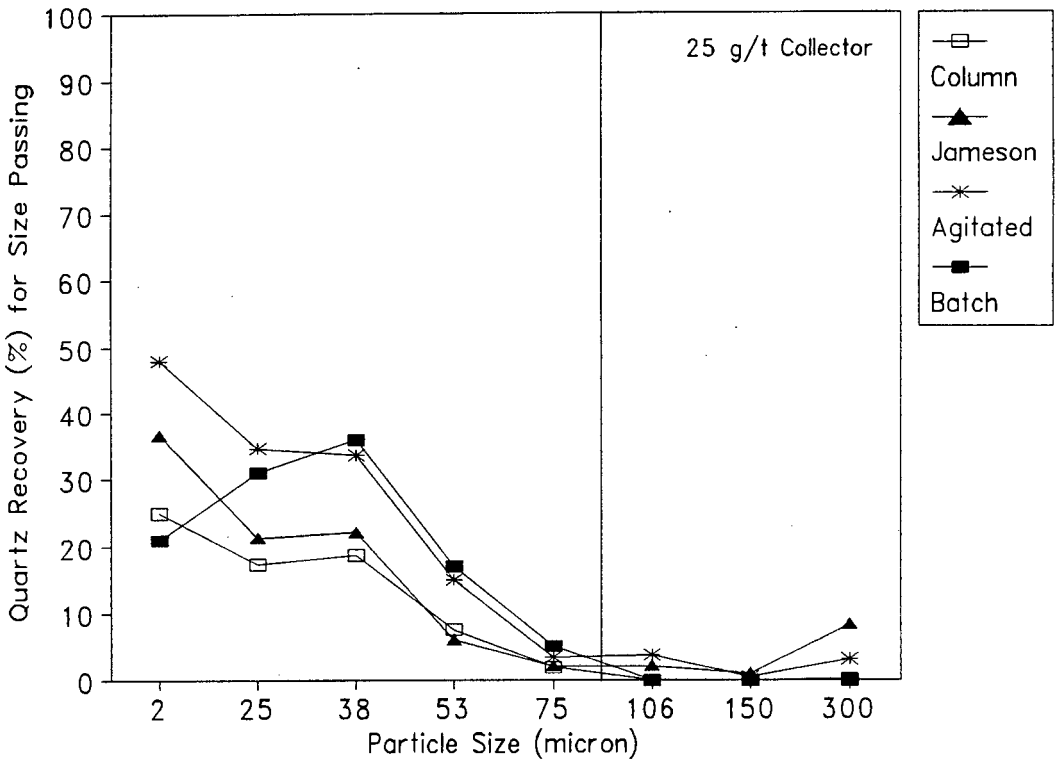


Figure 44 : Variation of Flotation Recovery with Particle Size for the Different Cell Configurations at a Collector Dosage of **25 g/t**.

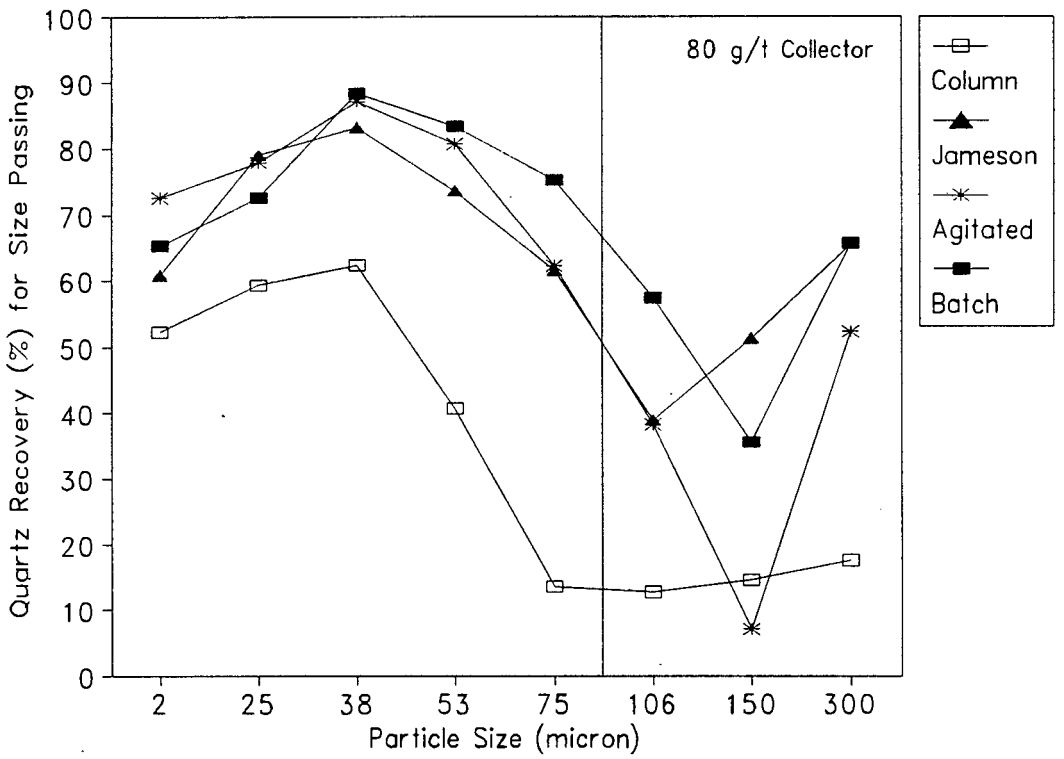


Figure 45 : Variation of Flotation Recovery with Particle Size for the Different Cell Configurations at a Collector Dosage of **80 g/t**.

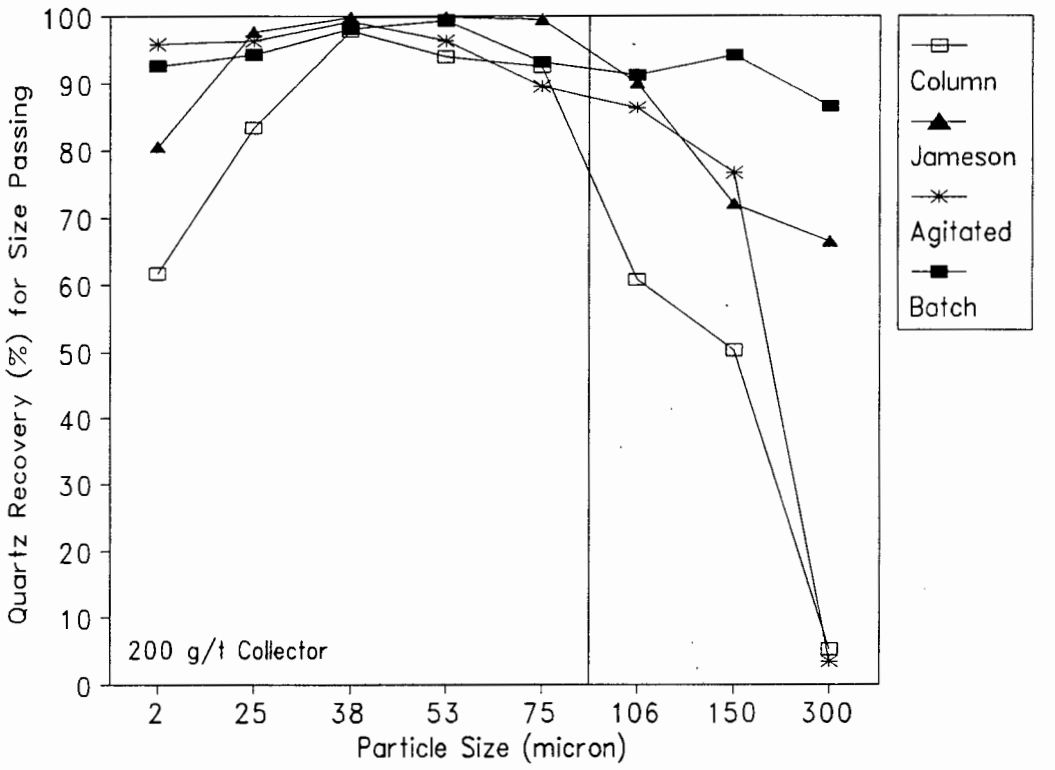


Figure 46 Variation of Flotation Recovery with Particle Size for the Different Cell Configurations at a Collector Dosage of **200 g/t**.

It is evident from these Figures that the column cell was outperformed by the other two hybrid cell configurations and the batch cell almost without exception. The column cell configuration might have been mistreated in this investigation due to the low air flow rate used in the column [94]. It is therefore recommended that future workers conduct a sensitivity analysis of recovery with respect to air flow rate to determine the optimum air flow rate to be used in the hybrid column. Nevertheless, due to the comparative nature of this investigation, as well as the possibility that the three hybrid cell configurations may have exhibited optimum performance at different air flow rates, it was assumed to be a suitable level of operation. The poor performance of the column cell can probably be attributed to low $E_C$ and $E_A$, as discussed in section 5.5.1 above. The relatively poor recovery of -25 $\mu$m particles at 200 g/t illustrates this effect very clearly, since fine particles are known to exhibit poor recovery owing to the above mentioned effect. Although increased recovery of coarser particles was expected owing to high $E_S$, this did not seem to occur, as the performance of the column cell was poor irrespective of the particle size fraction which was floated. This poor performance became especially clear at a collector dosage of 80 g/t, while the column gave a more similar (poor) performance to the other cells at 25 g/t.

94. The superficial gas velocity, $J_g$, in flotation columns should ideally be between 1 and 2 cm/s, while $J_g$ was calculated as 0.64 cm/s for the flotation conditions used during experiments in the hybrid column.

It was proposed in the discussion in section 5.5.1 above that increased intensity of contacting would benefit the collection of fine particles. The fact that fine (-25 $\mu$m) particles were collected more efficiently in the other three cell types at 200 g/t collector shows that this was indeed the case. This is illustrated even more clearly if the calculated recoveries of particles within the -106 $\mu$m size fractions (prior to summation to Tyler fractions) are plotted against particle size for the four different cell environments at a collector dosage of 80 g/t. This is shown in Figure 47.

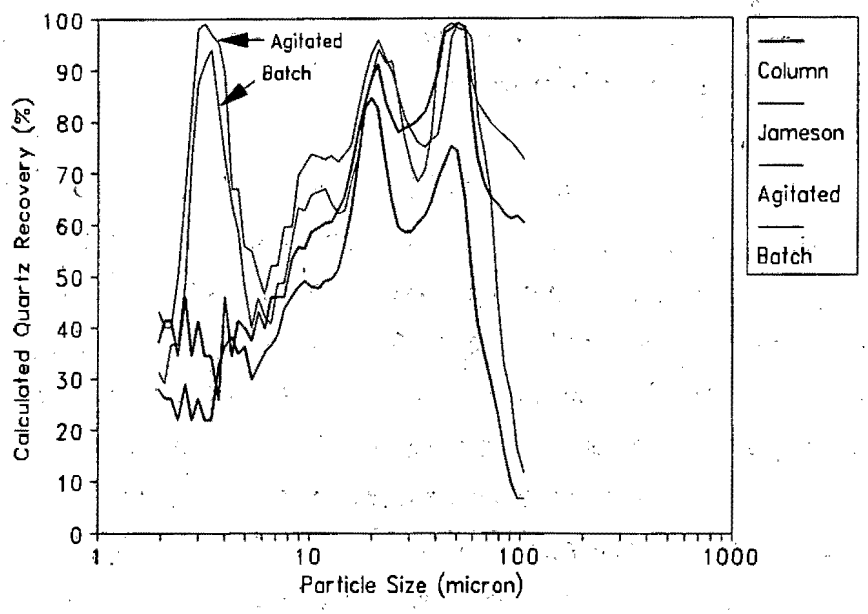


Figure 47 : Comparison of the Calculated Recoveries of Segments of the -106 $\mu$m size fraction in the Different Cell Environments at a Collector Dosage of 80 g/t.

It is clear from this Figure that agitation enhanced the recovery of very fine (approximately 2 - 3 $\mu$m) particles. This was probably due to increased collision efficiency, $E_C$, and attachment efficiency, $E_A$, as was expected. Added turbulence via agitation probably did not decrease the fraction of particles which remained attached to bubbles, $E_S$, since it is regarded as approaching unity [95] for particles as fine as these. However, coarser (+70 $\mu$m) particles proved to have been recovered more poorly in the agitated cell, and it is proposed that this can be attributed to directly decreased $E_S$.

Now that it has been established that agitation increased the collection of fine particles, while coarser particles were detached from bubbles, the question may be asked what the effect of variation in agitation speed (contacting intensity) would be on particle collection efficiency. This aspect is discussed in the following section.

95. See the discussion in section 2.4.2.3 on page 22.

### 5.5.2.1 The Effect of Agitation Speed (Contacting Intensity) on Particle Collection Efficiency

It was possible to vary the intensity of contacting between particles and bubbles in some of the flotation cell types. One way of achieving different degrees of contacting intensity is by varying the impeller speed in mechanically agitated cells like the agitated and batch cells. It is also possible to vary contacting intensity in the Jameson cell by increasing the pulp and air feed rates, but this option was not pursued due to physical limitations of the equipment that was used during the flotation experiments [96].

The agitated cell configuration and the laboratory batch cell were used to float the +106 -150 $\mu$m particle size fraction at different impeller speeds. A discussion of the experimental conditions and levels of agitation used during this investigation may be found in section 4.6.4 on page 88. The detailed results can be found in Appendix I on page 187. The flotation conditions (*e.g.* air flow rate, collector dosage and solids concentration) were similar in these cell types, but different levels of agitation speed were used in the batch cell because of practical considerations [97]. The results obtained from this investigation are presented below in Table 20, in which quartz recovery in the two cell types is shown with agitation speed.

Table 20 : Quartz and Water Recovery *vs.* Contacting Intensity (Impeller Speed).

| Agitation Speed (rpm) | Quartz Recovery (%) | Water Recovery (%) |
|---|---|---|
| Agitated Column Configuration | | |
| 0 | 12.61 | 1.26 |
| 300 | 27.13 | 3.41 |
| 500 | 38.12 | 5.68 |
| 800 | 45.09 | 11.13 |
| 1200 | 33.15 | 6.49 |
| Laboratory Batch Cell | | |
| 800 | 65.07 | 4.85 |
| 1000 | 53.59 | 5.21 |
| 1200 | 57.38 | 4.74 |
| 1400 | 50.24 | 5.49 |
| 1570 | 38.98 | 4.21 |

96. See the discussion in section 4.4.1 on page 80.
97. See section 4.6.4 on page 88 for a discussion of this.

Graphical illustrations of these results is shown in Figure 48 and Figure 49, in which quartz recovery is plotted against agitation speed.

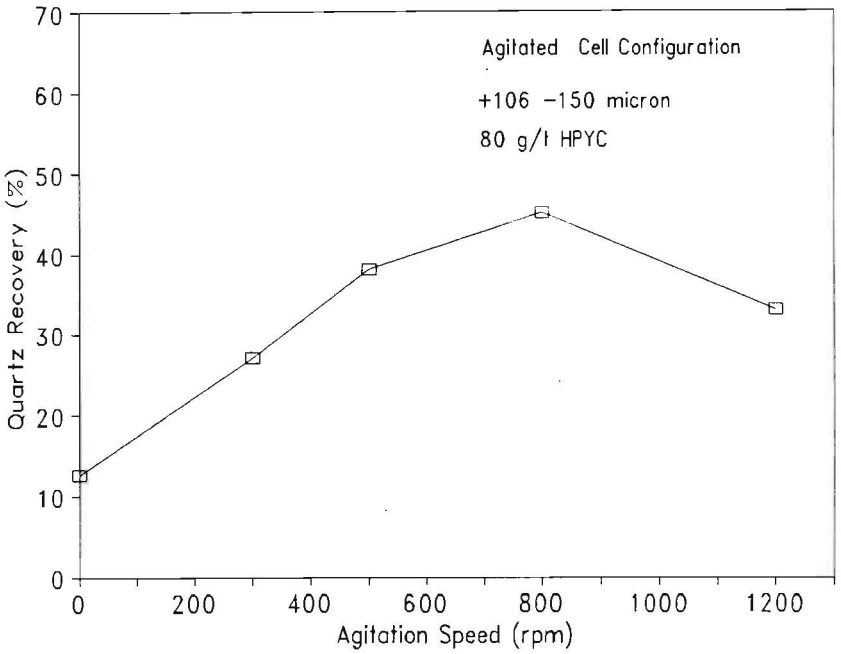


Figure 48 : Effect of Contacting Intensity (Agitation Speed) on Recovery in the **Agitated Cell** Configuration.

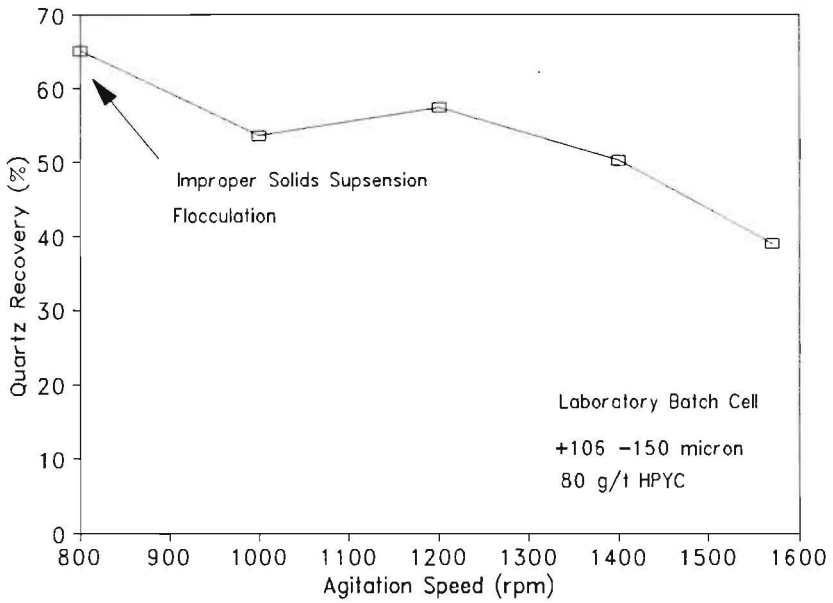


Figure 49 : Effect of Contacting Intensity (Agitation Speed) on Recovery in the **Batch Cell**.

It is clear from Figure 48 that increased agitation speed in the agitated cell led to increased recovery of the +106 -150 $\mu$m size fraction up to a point where it reached a maximum (800 rpm). Further increase in agitation speed caused a

decrease in recovery. The batch cell showed similar behaviour although improper solid suspension occurred at 800 rpm, and maximum recovery was obtained at 1200 rpm.

The initial increase in recovery can probably be attributed to increased collision efficiency, $E_C$, and attachment efficiency, $E_A$, owing to more intense contacting between particles and bubbles with increased agitation speed. Detachment of particles from bubbles should only become significant at higher levels of agitation speed and $E_S$ is therefore not considered to be a significant a factor at low agitation speed. These results confirm the findings of Ahmed and Jameson [1985] who showed that increased agitation rate increases the recovery of particles with a density close to that of water without decrease in recovery due to decreased $E_S$.

A further increase in agitation resulted in reduced recovery in both cell types. Decreased collection is proposed to have been due to increased detachment of particles from bubbles (lower $E_S$). $E_C$ and $E_A$ should become less dependent on agitation rate at high agitation, and decreased collection must therefore be attributed to lower $E_S$.

The contribution of the effect of bubble size may be questioned here. Bubbles are generally broken up by agitation [Prince and Blanch, 1990] and bubble size can therefore be expected to become independent of agitation speed at high levels of agitation. However, it has recently been found that bubble size in agitated columns may remain constant with increased agitation [Harris, 1995], probably because of equal rates of bubble breakup and coalescence. The effect of bubble size should therefore not influence collection efficiency.

The results also show that the choice of 500 rpm as standard agitation rate during the experiments with agitated cell was relatively close to the optimum level of operation (800 rpm). Furthermore, 1200 rpm proved to be at the optimum in the batch cell. Although only the +106 -150 $\mu$m particle size fraction was used during the agitation rate investigation (and particles of different size will most probably show different optima), it is clear that the choice of 500 rpm and 1200 rpm respectively was not totally unrealistic.

Now that the effect of varying contacting intensity on particle collection efficiency has been discussed, the flotation results from Figure 44 to Figure 46 above (pages 117 to 118) can be further discussed.

It is clear from these Figures that coarse (+300 $\mu$m) particles were not collected at the low collector dosage of 25 g/t in the column and batch cells. Collection of these particles in the agitated cell is an unexpected result, since it is clear from the discussion above that coarse particles should easily detach from bubbles with agitation. A possible explanation is greater residence time in the agitated column compared to the other cells. The recovery of these particles in the Jameson cell is proposed to be due to the unique contacting mechanism of this cell: particles are intensely contacted with bubbles, after which the aggregates are probably not disrupted in the quiescent disengagement zone. Also, a disrupting counter-current stream does not exist as with the column and agitated cells.

The high intensity of contacting in the Jameson cell can be illustrated by the data in Figure 36 on page 97. Flocs which formed in the feed tank with flotation of the +300 $\mu$m size fraction at 200 g/t collector dosage were apparently broken up when they were pumped through the orifice of the Jameson cell. This is shown by the fact that the point which represents the repeat experiment with dispersant added to the pulp to break up the flocs almost coincides with the point of the original experiment. Recovery in the column and agitated cells at the same conditions was significantly lower when flocs were formed. Although it is evident from this that the contacting intensity in the Jameson cell must have been quite substantial, this still does not give any indication of the relative intensity of the agitated cell environment.

It could be expected from the discussion in section 5.5.1 above that agitation in the batch cell should also have promoted fine particle collection, as was the case with the agitated and Jameson cells. Despite increased collection of fine particles at the collector dosage of 25 g/t in these cells, the batch cell did not result in increased collection of fine particles at this dosage. However, coarse particles were collected efficiently at 80 g/t and 200 g/t. Recovery in the batch cell also showed low sensitivity towards particle size at 200 g/t, as discussed in section 5.4.3 on page 108. It is proposed that this cell promoted coarse particle collection due to the relatively shallow collection zone in which particle dropback would be less significant.

### 5.5.3 Summary

The four cell types showed different characteristics of collection efficiency. The column cell performed poorly compared to other cells in which contacting was more intense. The agitated cell promoted fine particle collection, while the Jameson cell collected coarse and fine particles efficiently. At high collector dosages coarse particles in the batch cell were generally collected more efficiently than in the other cells.

## 5.6 BUBBLE SIZE

Up to this point, the effect of bubble size on particle collection efficiency has not been considered during the discussion. Bubble size is an important parameter in flotation operations, as is evidenced by active ongoing research on sparging mechanisms. It was not listed as one of the flotation variables in Table 5 on page 80 because it was not independently manipulated during the flotation experiments. However, knowledge of the size of bubbles which were generated in the different cell environments under different flotation conditions was crucial in this investigation. The way in which bubble size was determined in two of the cell configurations and the size of bubbles in these cells are discussed in subsequent sections.

A brief review of the effect of bubble size on particle collection efficiency, flotation rate and recovery is given in the following section.

### 5.6.1 Bubble Size and Particle Collection Efficiency

Particle collection efficiency, $E_K$, is strongly dependent upon the size of bubbles in flotation slurries. Collision efficiency, $E_C$, decreases with increased bubble size, $d_b$ as is clear from Equations (22) to (24) on pages 13 to 14 and the model of Finch and Dobby [1990] in section 2.4.2.1.1 on page 15. The efficiency of attachment of particles to bubbles, $E_A$, is also dependent upon $d_b$ (see Equation (38) on page 18 and the Finch and Dobby model in section 2.4.2.2.1 on page 19) and decreases with increased $d_b$. The fraction of particles which remain attached to bubbles, $E_S$, increases with increased $d_b$ (see Equation (49) on page 23). Furthermore, the first order rate constant, k, is affected by $d_b$ in that it decreases with increased $d_b$. The mixing characteristics in a cell will also be dependent upon $d_b$ because different air flow rates (which should alter $d_b$) generally result in differences in mean residence time, $\tau$, and vessel dispersion number, $N_d$. The sum total of these factors contributes to a strong dependence of collection zone recovery, $R_c$, on $d_b$.

In order to have an idea of mean bubble size during the flotation experiments, $d_b$ was estimated from gas holdup in the column and Jameson cell configurations. Gas holdup was also measured in the agitated cell, but $d_b$ could not be determined in the same way as with the other two cell types, since the theory which was used only applies to quiescent systems. The contacting environment in the downcomer tube of the Jameson cell can also be regarded as being quiescent, although contacting over the orifice is turbulent. A more comprehensive discussion of this follows in subsequent sections in which the bubble size results are also given and discussed.

### 5.6.2 Gas Holdup Measurement

Bubble size can be estimated from the gas holdup in column-type flotation cells [98]. Gas holdup in column cells is normally estimated from pressure differences at different heights in the column if it is run on a continuous basis [Yianatos and Levy, 1991]. However, direct measurement of gas holdup was carried out during experiments in the hybrid column by measuring the decrease in pulp level after the air, feed and tailings pumps were shut off after each experiment (and the agitator when it was used). The collection zone in the column and agitated column cell configurations is defined as the volume of aerated pulp in the column cell above the air sparger, while the collection zone in the Jameson cell is the volume of aerated pulp in the downcomer tube. The results of these measurements are shown in Table 21.

Table 21 : Measured Gas Holdup (%) in the Different Cell Configurations.

| Collector Dosage (g/t) | Column Cell Configuration | Jameson Cell Configuration | Agitated Cell Configuration |
|---|---|---|---|
| -106 μm Particle Size Fraction | | | |
| 0 | 3.87 | 3.87 | 5.52 |
| 25 | 4.14 | 4.42 | 6.63 |
| 80 | 4.70 | 5.52 | 8.01 |
| 200 | 5.25 | 6.34 | 8.84 |
| 300 | 5.52 | | |
| 400 | 5.80 | | |
| 500 | 6.08 | | |
| +106 -150 μm Particle Size Fraction | | | |
| 0 | 3.87 | 4.42 | 6.35 |
| 25 | 4.14 | 4.97 | 6.91 |
| 80 | 4.42 | 5.25 | 7.73 |
| 200 | 5.54 | 5.83 | 9.12 |
| 300 | 8.30 | | |
| 400 | 9.43 | | |
| 500 | 10.50 | | |
| +150 -300 μm Particle Size Fraction | | | |
| 0 | 3.59 | 4.42 | 7.46 |
| 25 | 3.87 | 6.08 | 8.01 |
| 80 | 4.42 | 7.22 | 8.29 |
| 200 | 4.97 | 11.05 | 10.50 |
| +300 μm Particle Size Fraction | | | |
| 0 | 3.31 | 3.87 | 7.46 |
| 25 | 4.42 | 4.42 | 7.99 |
| 80 | 7.19 | 6.10 | 8.87 |
| 200 | 8.29 | 12.16 | 9.96 |
| 200 (Dispersant) | 6.06 | 12.15 | 15.47 |

98. Estimation of bubble diameter from gas holdup has been discussed in section 2.6.2.2 on page 35.

It was not necessary to take the diameter of the collection zone or the dimensions of equipment present in the collection zone (*e.g.* the agitator shaft) into account during the calculation of gas holdup, since it was calculated as the linear distance with which the pulp level decreased, divided by the total length of the collection zone.

Gas holdup was not measured in the laboratory batch cell because of practical reasons: the decrease in pulp level with air and agitator switched off was not as significant as in the hybrid column cell, and the geometry of the batch cell complicated the calculation of gas holdup. Gas holdup measurement was therefore limited to the three hybrid column configurations. It is clear from this Table that gas holdup generally increased with increased collector dosage. Gas holdup in the agitated cell was generally greater than in the column and Jameson cells, while the lowest values were measured in the column cell configuration.

The calculation of mean bubble diameter from the measured gas holdup values in the column and Jameson cell configurations is described in the following section.

### 5.6.3 Calculation of Bubble Size from Gas Holdup

A number of methods have been used to estimate bubble size from gas holdup. The model of Zhou *et al.* [1993] was chosen to analyze the gas holdup data obtained in this thesis. The theory behind this method of bubble size estimation, along with a discussion of other available methods and their applicability, has been presented in section 2.6.2.2 on page 35. The model of Zhou *et al.* applies to gas holdups of less than 30%. It is clear from Table 21 above that gas holdup never exceeded 30% in any of the cell configurations, which made it possible to use the model with a number of simplifications. In this model bubble diameter, $d_b$, is not only a function of the gas holdup, $\epsilon_g$, but also of the superficial liquid and gas velocities, $J_l$ and $J_g$, the density of the liquid and gas, $\rho_l$ and $\rho_g$, the bulk liquid viscosity, $\mu$, and the frother type and dosage. The fact that the effects of frother type and dosage on bubble size are included in this model distinguishes it from other methods of bubble size estimation used previously [99]. Zhou *et al.* developed correlations for three different frother types, namely pine oil solutions, Dowfroth 250 and MIBC solutions. The characteristics of Dowfroth 250 were closest to that of Senfroth 6010 [Senmin, 1994], which was the frother used during this investigation. It was therefore assumed that the small differences which existed between these two frothers would not have a great effect.

99. Different types of frother often result in different size bubbles with the same dosage, as was shown by Tucker *et al.* [1994].

As discussed in section 5.6.1 above, this method of bubble size estimation only applies to quiescent contacting environments. It could therefore not be used to predict bubble size in the agitated column and batch cells owing to the turbulent conditions in these cells. It was assumed that the conditions in the downcomer of the Jameson cell was quiescent enough to allow prediction of bubble size using this method. Alternatively, gas holdup could have been measured in the outer column region of the Jameson cell, and bubble size could have been estimated by regarding the exit point of the downcomer tube as a sparger. However, measurement of the gas holdup inside the downcomer tube was considered more correct because of the absence of a counter-current stream of pulp in the outer region (disengagement zone) of this cell.

Details of the parameters which were used in the calculation of bubble size are given in Appendix F1 on page 179. The calculated bubble sizes in the column and Jameson cell configurations are presented in Table 22.

Table 22 : Calculated Bubble Size (mm) in the Different Cell Configurations.

| Collector Dosage (g/t) | Column Cell Configuration | Jameson Cell Configuration |
|---|---|---|
| -106 μm Particle Size Fraction | | |
| 0 | 1.643 | 1.495 |
| 25 | 1.521 | 1.292 |
| 80 | 1.339 | 1.041 |
| 200 | 1.207 | 0.922 |
| 300 | 1.154 | |
| 400 | 1.107 | |
| 500 | 1.066 | |
| +106 -150 μm Particle Size Fraction | | |
| 0 | 1.643 | 1.292 |
| 25 | 1.521 | 1.231 |
| 80 | 1.422 | 1.167 |
| 200 | 1.150 | 1.058 |
| 300 | 0.846 | |
| 400 | 0.778 | |
| 500 | 0.727 | |
| +150 -300 μm Particle Size Fraction | | |
| 0 | 1.796 | 1.391 |
| 25 | 1.643 | 1.019 |
| 80 | 1.422 | 0.880 |
| 200 | 1.268 | 0.632 |
| +300 μm Particle Size Fraction | | |
| 0 | 1.994 | 1.620 |
| 25 | 1.422 | 1.391 |
| 80 | 0.936 | 1.016 |
| 200 | 0.847 | 0.589 |
| 200 (Dispersant) | 1.068 | 0.589 |

It is clear from these results that cell environment, particle size and collector dosage had an effect on the size of bubbles which were formed in the collection zone during the flotation experiments. The bubble size results are further discussed in section 5.6.5 below. The accuracy of these estimated bubble sizes was evaluated by comparing them to measured bubble size in the column and Jameson cells. This is discussed in the following section.

### 5.6.4 Bubble Size Measurements and Evaluation of Predicted Values

In addition to the predicted bubble sizes from gas holdup data, bubble size was measured in the column and Jameson cell configurations. The measurements were carried out during some of the flotation experiments in which the -106 $\mu$m particle size fraction was floated. The UCT Bubble Size Analyzer was used to measure the bubble size in the pulp [100]. At the time, measurements could not be carried out in the agitated column configuration since the electrical motor which drove the agitator was in the way of the bubble sizer. The operational success of the UCT Bubble Size Analyzer has been reported in numerous publications [Tucker *et al.*, 1993a, 1993b, 1994]. The bubble sizer could be equipped with a sampling column, which made it possible to carry out bubble size measurements in three phase systems. The sampling column was only used during some of the measurements, while the rest were done without the sampling column. Repeat runs were carried out at certain collector dosages. The actual measured mean bubble diameters with standard deviations are given in Appendix F2 on page 180. A summary of the measured mean bubble diameters, or averages in the case of multiple measurements, is given in Table 23.

Table 23 : Measured Mean Bubble Size in the Column and Jameson Cell Configurations during Experiments with the -106 $\mu$m Particle Size Fraction.

| Collector Dosage (g/t) | Column Cell Configuration | | Jameson Cell Configuration | |
|---|---|---|---|---|
| | $d_b$ (mm) | Std. Dev. (mm) | $d_b$ (mm) | Std. Dev. (mm) |
| 0 | 1.543 | 0.813 | 1.085 | 0.864 |
| 25 | 1.573 | 0.893 | 1.313 | 0.735 |
| 80 | 0.823 | 0.501 | 0.956 | 0.529 |
| 200 | 1.100 | 0.648 | 0.870 | 0.756 |
| 300 | 0.671 | 0.505 | | |
| 400 | 0.837 | 0.478 | | |
| 500 | 0.768 | 0.578 | | |

100. A description of the UCT Bubble Size Analyzer has been given in section 2.6.2.1 on page 34.

The measured bubble size data are compared with the calculated data in Figure 50, in which the data from the column and Jameson cells were plotted together to evaluate the success of the prediction of mean bubble size from gas holdup.

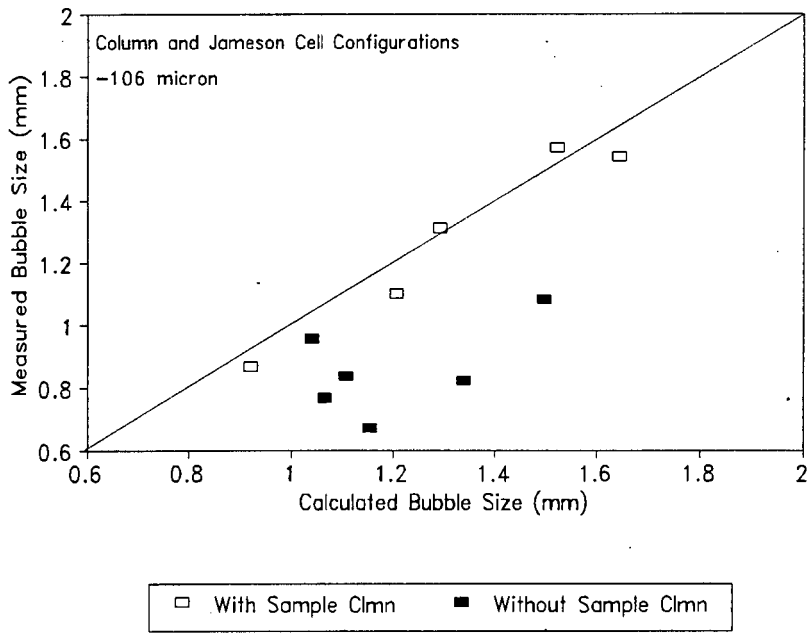


Figure 50 : Measured *vs.* Calculated Bubble Size in the Hybrid Column Cell.

It is clear from this Figure that bubble sizes measured without the sampling column were smaller than the estimated values. A possible explanation for this is that particles might have been sucked through the capillary along with the liquid, and that they were interpreted by the analyzer as very small bubbles. The mean bubble diameter which was calculated by computer would thus have been affected by this. However, bubble size values which were measured with the sampling column compared well with the estimated values with this particle size fraction. The calculated values (determined on the basis of gas holdup values) were consequently assumed to be accurate and were used during the rest of the thesis.

The bubble size results which were presented in section 5.6.3 above are discussed in the following section with respect to the effect of collector dosage (hydrophobicity) and cell type.

### 5.6.5 Discussion of Bubble Size Results with Respect to Particle Collection Efficiency

The bubble sizes which were predicted from gas holdup and were presented in Table 22 above are plotted below in Figure 51 to Figure 54. These Figures show the values for each cell type, and collector dosage.

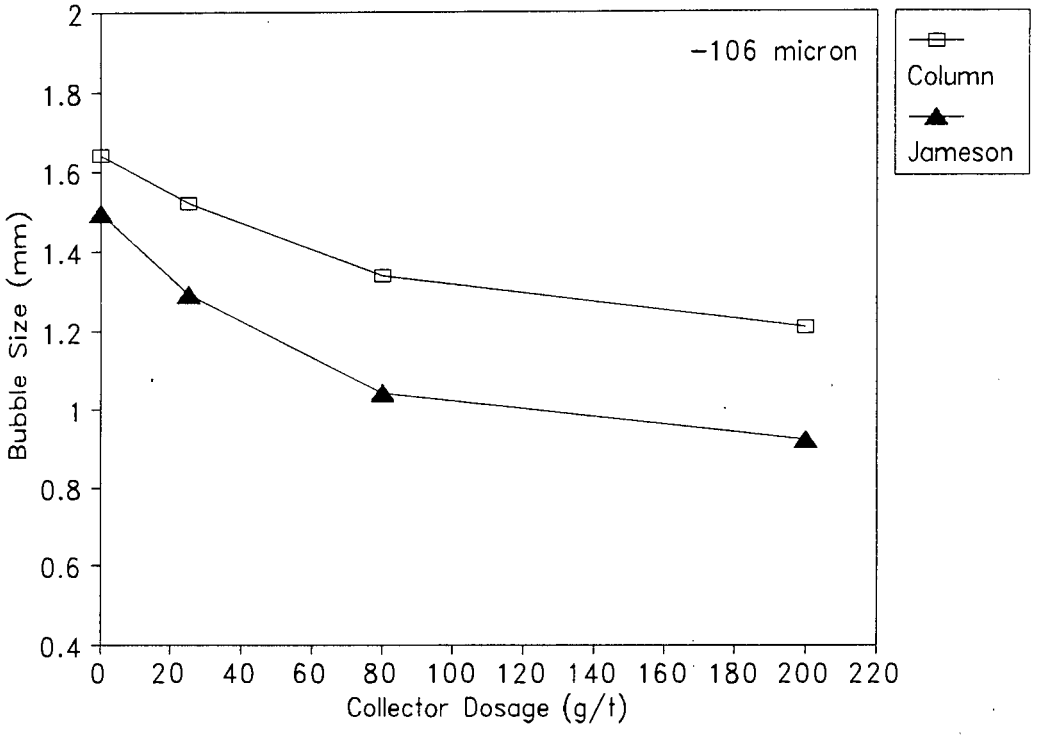


Figure 51 : Variation of Bubble Size with Collector Dosage in the Different Cell Configurations for the **-106 μm** Particle Size Fraction.

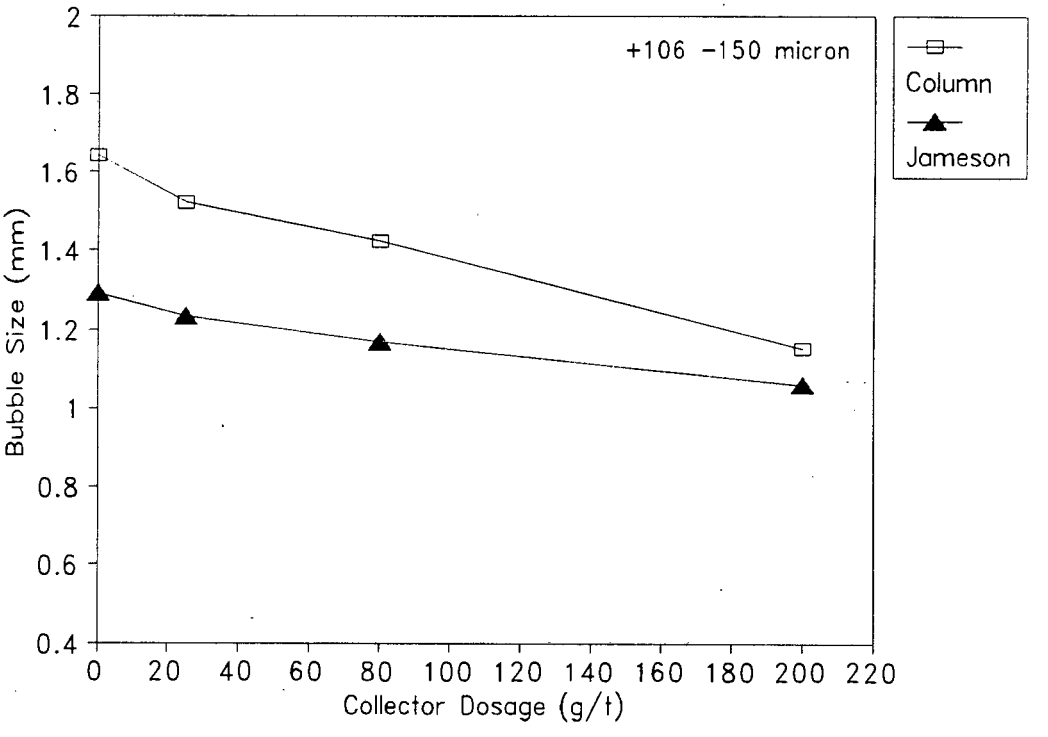


Figure 52 : Variation of Bubble Size with Collector Dosage in the Different Cell Configurations for the **+106 -150 μm** Particle Size Fraction.

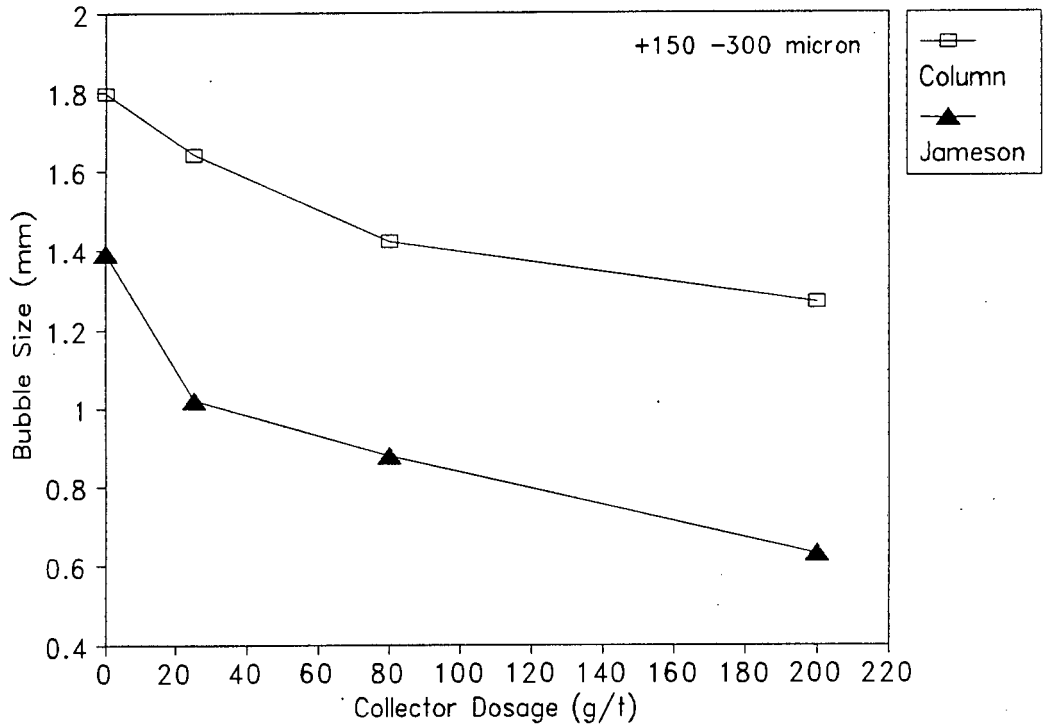


Figure 53 : Variation of Bubble Size with Collector Dosage in the Different Cell Configurations for the **+150 -300 μm** Particle Size Fraction.

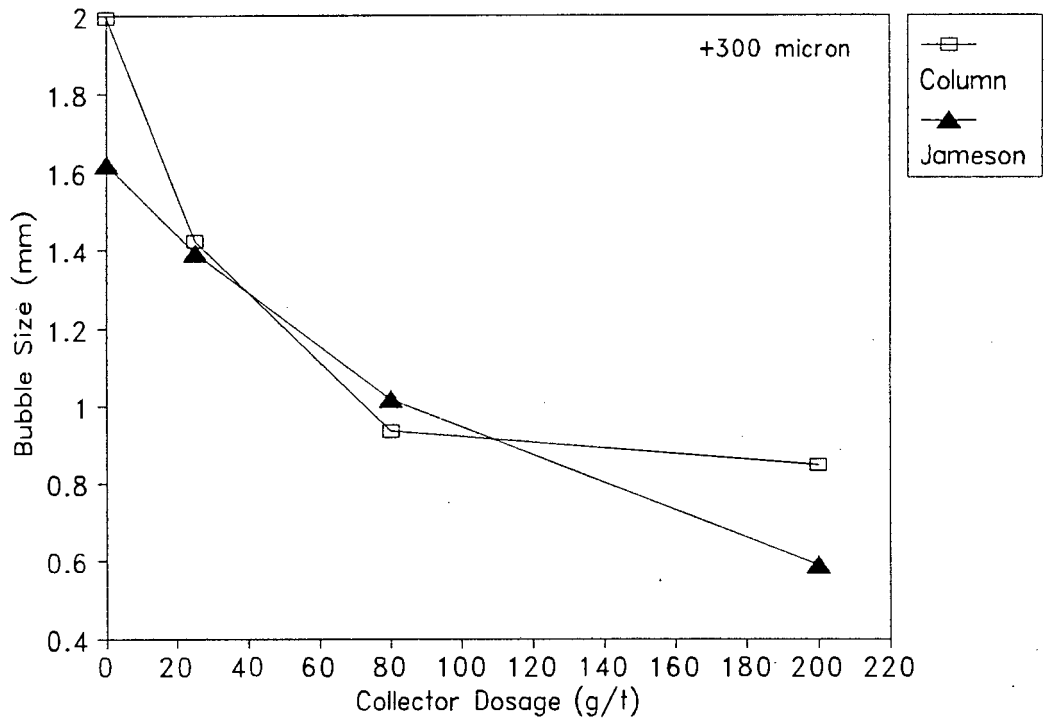


Figure 54 : Variation of Bubble Size with Collector Dosage in the Different Cell Configurations for the **+300 μm** Particle Size Fraction.

The effect of collector dosage is clear from these Figures: increased collector dosage resulted in smaller bubbles, which shows that this collector has the same effect as frother on bubble size. This is proposed to be due to collector and frother having similar structures. The addition of frother to flotation slurries results in reduced surface tension, which inhibits bubble coalescence, resulting in smaller bubbles. Furthermore, it is clear that bubble size was not affected by collector after a certain dosage had been reached. The same phenomenon has been found by Tucker *et al.* [1994] [101] for a suite of different frothers in a laboratory batch cell.

These Figures also illustrate the effect of cell type (contacting environment) on bubble size. The column cell generally produced bigger bubbles than the Jameson cell under the same conditions. Whether this is to be explained in terms of differences in the mechanism of bubble generation or to bubble breakup can not easily be determined. Very little is currently known about the mechanism of bubble formation at an orifice [Antonaidis *et al.*, 1992]. An interesting phenomenon is that bubbles in the Jameson cell became significantly smaller as particle size increased, as is clear from Figure 53 and Figure 54. Although air holdup was greater in the agitated cell than in the column and Jameson cells, bubble size can be expected to be similar to that in the column cell [Harris, 1995]. Similar bubble size with increased gas holdup implies a longer collection zone residence time of bubbles. It is therefore proposed that the agitator mechanism caused the bubbles to follow the turbulent streams around the impellers, and that they did not rise uniformly as in a quiescent system.

It is clear from the discussion in section 5.6.1 on page 124 that flotation rate should increase with reduction in bubble size. This could give an additional explanation for effective particle collection of coarse particles (+150 -300 $\mu$m and +300 $\mu$m) in the Jameson cell, as was discussed in section 5.5.2 on page 116.

Bubble size in the column cell became increasingly sensitive to collector with increased particle size, as is clear from the increased downward trend in bubble size with collector of the +150 -300 $\mu$m and +300 $\mu$m particle size fractions in Figure 53 and Figure 54. The combined effect of collector dosage and particle size on bubble size in the column and Jameson cell is illustrated in Figure 55 to Figure 56 below in which the same data as above were plotted in a different way. In these Figures the legends refer to the four different particle size fractions in microns. The repeat experiments in which dispersant was added to the pulp (+300 $\mu$m size fraction floated at 200 g/t) are also shown.

101. See the discussion in section 4.4.2.2 on page 81.

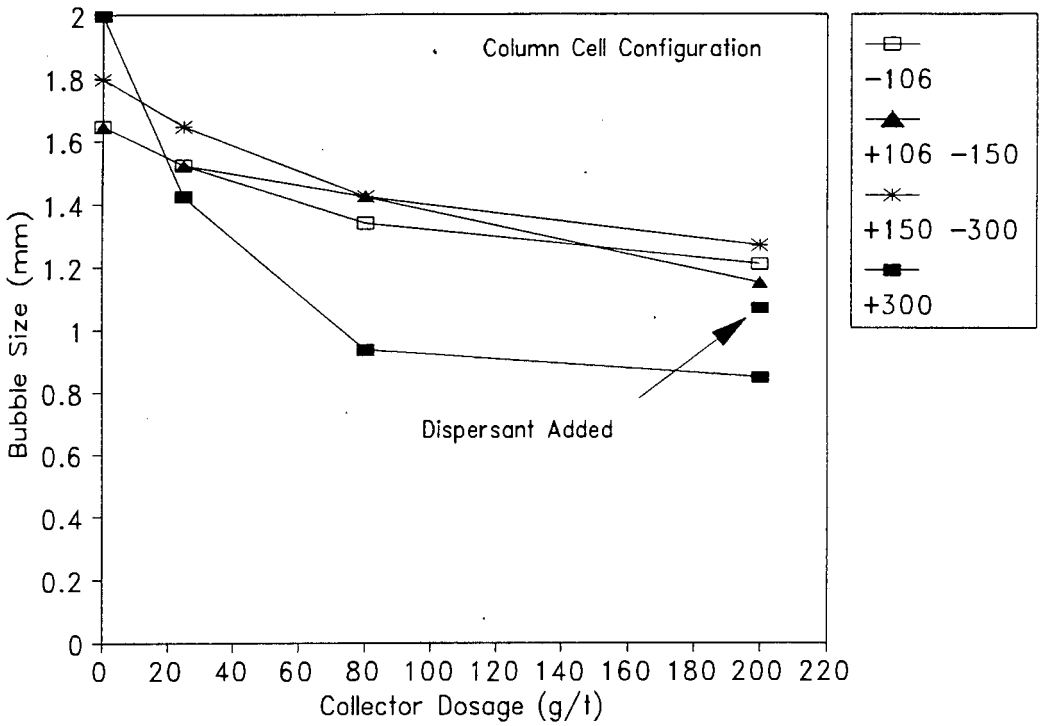


Figure 55 : The Effect of Feed Particle Size and Collector Dosage on Bubble Size in the **Column Cell Configuration.**

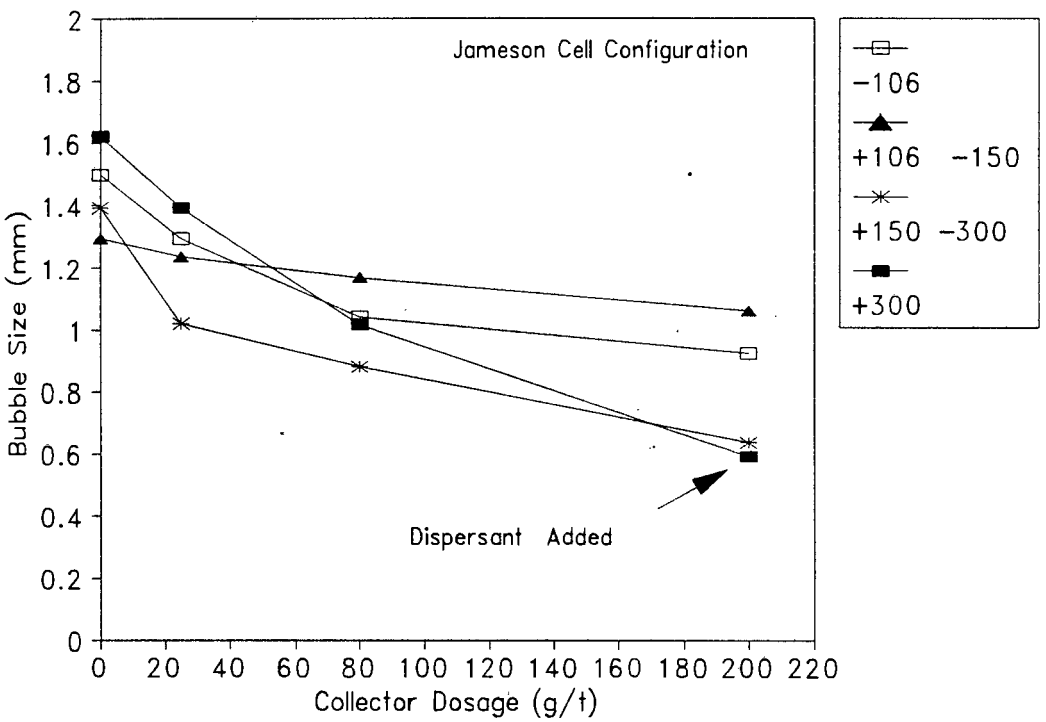


Figure 56 : The Effect of Feed Particle Size and Collector Dosage on Bubble Size in the **Jameson Cell Configuration.**

It is clear from these Figures that bubble size in the column cell was significantly reduced with flotation of coarse particles (+300 $\mu$m), while the finer particle size fractions did not seem to have such a big influence. Bubble size varied significantly with collector dosage during flotation experiments with the +300 $\mu$m size fraction in the Jameson cell. Bubble formation at an orifice was shown to be strongly affected by the viscosity of the liquid [Antonaidis *et al.*, 1992]. Although this work was carried out in a two phase system, and findings from it may possibly not be extrapolated to three phase systems, it is still proposed that changes in particle size altered the slurry viscosity, with the result that bubble size changed significantly.

Finally, it is clear that bubble size in both these cell configurations was between 0.5 and 2 mm, which compares well with the observations of Tucker *et al.* [1993b] as discussed in section 2.6.2.1 on page 34. They found that all bubbles in three different cell configurations that were used during their work were smaller than 2 mm, while an average size of approximately 1 mm was found in a laboratory column flotation cell.

### 5.6.6 Summary

The differences in bubble size in the two flotation cell types showed that the hydrodynamic conditions inside them were significantly different. Bubble size was shown to be affected by collector dosage, particle size and cell environment. Increased collector dosage generally reduced bubble size, probably owing to reduced coalescence, similar to frothing agents. Bubble size in the column cell reduced significantly when particle size was increased from +150 -300 $\mu$m to +300 $\mu$m. The column cell produced the largest bubbles, while smaller bubbles were found in the Jameson cell. Unexpectedly fine bubbles were formed in the Jameson cell when relatively coarse (+150 -300 $\mu$m and +300 $\mu$m) particles were floated at high collector dosages.

## 5.7 RESIDENCE TIME DISTRIBUTION (RTD)

Tracer tests were carried out in the column, agitated and Jameson cell configurations to determine the residence time distribution of pulp in each of the cell environments. This was done in order to investigate (quantify) the differences in the extent of mixing in the different cells. Although air flow rate was kept constant at 3 l/min in the agitated and Jameson cell configurations, it was varied in the column cell configuration. The tests were carried out in the liquid phase only, using a salt tracer (saturated KCl solution) in water with frother added to it. It was assumed that the residence time distribution of the liquid approached that of the pulp [Dobby and Finch, 1985]. The tracer concentration in the water of the tailings stream was determined by means of conductivity measurements.

### 5.7.1 Characterization of the Pulse Input Signal

Before commencement of the tests, the shape of the input pulse was determined. Three experiments were carried out in which the standard volume of tracer solution was injected into the feed line. The conductivity was measured with the probe positioned at the feed inlet, 5 cm away from the injection point. The conductivity of the feed was measured with time and this data was converted to an E(t) distribution, using Equation (57) on page 25, thereby normalizing the data. These data are presented in Appendix E1 on page 173. A graphical illustration of the pulse input curves is shown in Figure 57, in which conductivity of the water is plotted against time for three consecutive experiments.

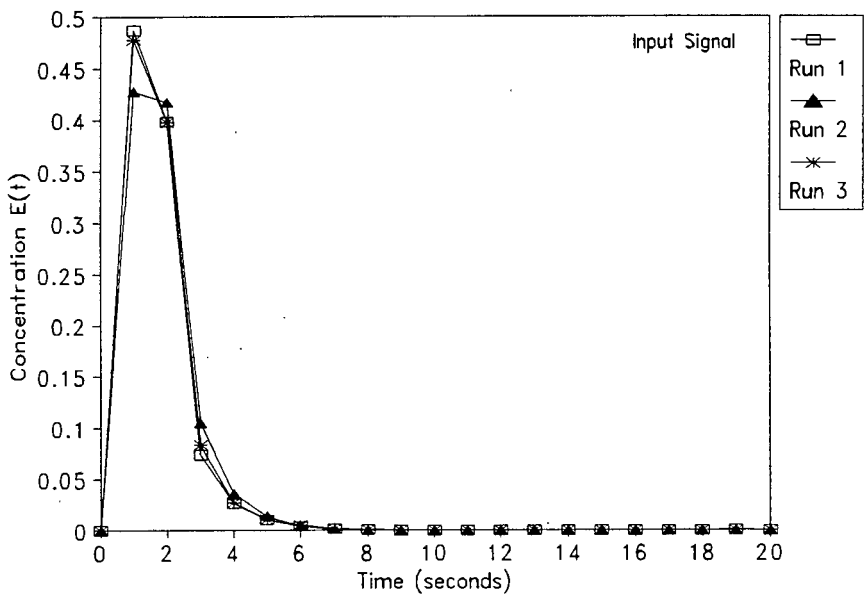


Figure 57 : Salt Tracer Pulse Input Curve.

The input time of about 4 seconds was considered negligible compared to typical calculated mean residence times in the three cell configurations (presented in section 5.7.3 below). The shape of the input was close to delta input and it was assumed that it was a perfect Dirac delta function [102]. It is clear that the results were reproducible.

### 5.7.2 Treatment of Data and Models Used

Residence time distribution curves were established by subtracting the average of the measured baseline readings from the conductivity readings [103]. The resulting values

102. The Dirac delta function is described in Levenspiel [1972] on page 262.
103. The conductivity of the water was not always zero probably due to tracer still left inside the hybrid column from previous conductivity measurements, or inaccurate calibration of the electronic interface.

were normalized to obtain E(t) curves, using Equation (57) on page 25. The mean residence time was determined using Equation (55), after which the E(t) data were converted to E($\theta$) distributions, and the different models were fitted to these RTD curves ($\theta$ is dimensionless residence time, calculated using Equation (58) on page 26).

The numerical solution to the axial dispersion model has been reported in the literature to give the best fit to RTD curves in flotation columns if used with least squares fitting, as discussed in section 2.5.2.1 on page 26. This model was fitted to all the RTD curves which resulted from the different experiments. The tanks in series model was also fitted for the sake of comparison. These two models have been discussed in section 2.5.2.1 and 2.5.2.2 on page 26 to 28 above. The model for small extents of dispersion (Equation (64) on page 27) was fitted to some of the RTD curves in which the dispersion was low (*e.g.* where air was not fed to the cells). The applicability of these different models to fitting the RTD data obtained from these experiments is illustrated below by considering two examples.

The RTD curve and fitted models for the column cell configuration with no air fed to the column are shown in Figure 58.

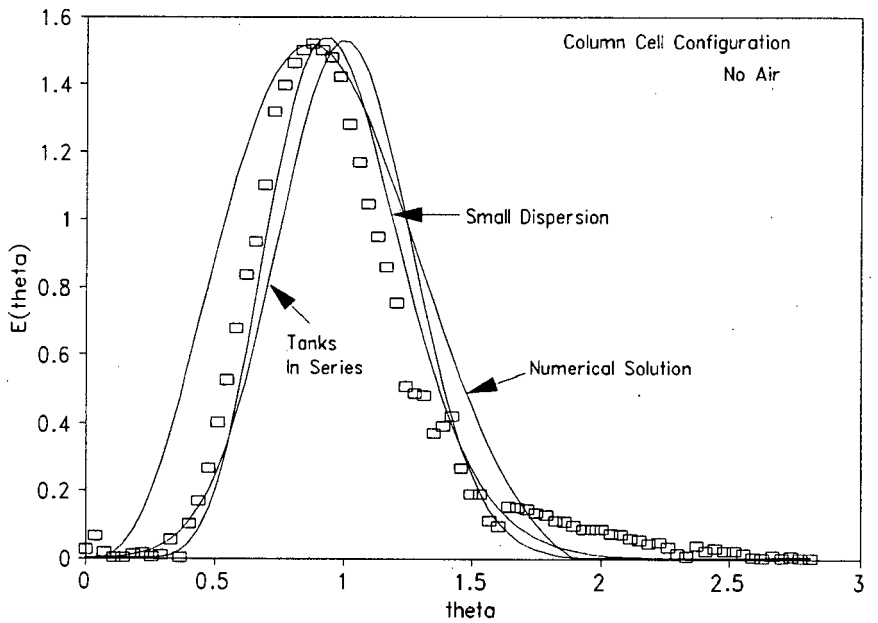


Figure 58 : RTD Curve and Model Fits for the Column Cell Configuration with No Air Fed to the Column and a Liquid Feed Rate of 3 l/min.

In this Figure, Small Dispersion denotes the axial dispersion model solution for small extents of dispersion. Data for the same experiment, but with air fed to the column at 3 l/min are illustrated below in Figure 59.

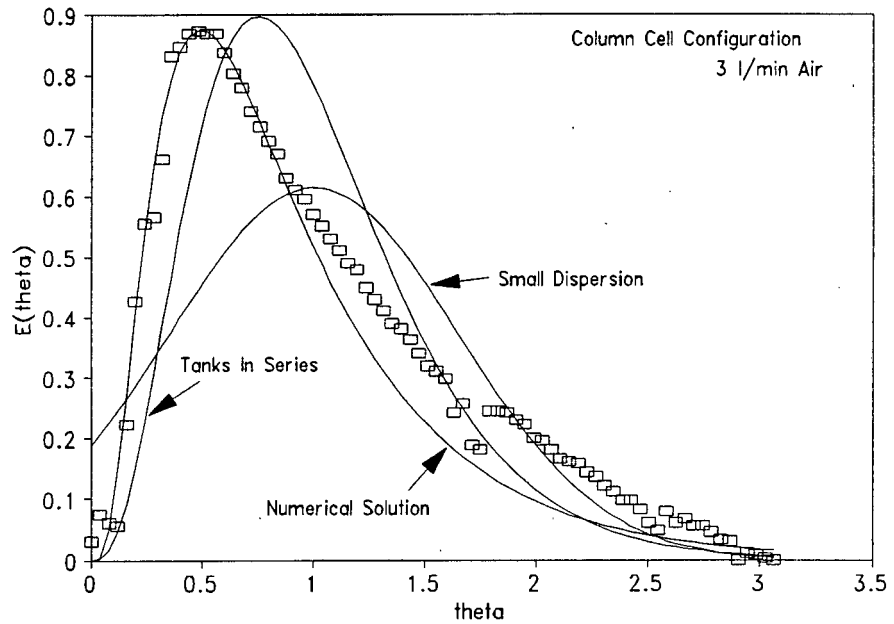


Figure 59 : RTD Curve and Model Fits for the Column Cell Configuration with Air and Liquid Feed Rates of 3 l/min.

It is clear from these two Figures that the solution for small extents of dispersion provided the best fit out of the three models for the liquid-filled column without air flowing (Figure 58), but it gave very poor results for the mixed system in which air was flowing (Figure 59). Although the tanks in series model resulted in good fits in both cases, it was not as good as with the mixed case. The numerical solution to the axial dispersion model gave a very good fit to the RTD data in the mixed case, while it was relatively poor when no air was fed to the column.

The small dispersion model was therefore used when no air was fed to the specific cell configuration, while the numerical solution and the tanks in series model were both used to quantify the extent of mixing in cases where air was introduced into the column.

The RTD data and model fits are presented in the following section. A least squares procedure was used to for the fits and errors are given along with the data. If the errors seem to be extremely large compared to the values of $N_d$, it is because the squares of the errors of each reading taken during the RTD tests were summed [104]. The errors should therefore only be compared to each other, and not to the values of vessel dispersion number, $N_d$.

104. Tests typically comprised of over 70 measurements, the errors of which should add up to a great number.

### 5.7.3 Discussion of Residence Time Distribution Results

The detailed results from the RTD experiments are presented in Appendix E2 on page 173. The different models were fitted to this data, and the vessel dispersion number, $N_d$, from either the correlation for small dispersion, or the numerical solution to this model, is presented. The vessel dispersion coefficient was also determined using the correlation from Manqiu and Finch [1993] [105], and was compared to the results from the solutions of this model. The number of tanks from the tanks in series model is also presented. The errors of the least squares method resulting from the respective fits are presented to create an idea of the success of the fit. As discussed above, if these errors seem particularly large, it is because the errors from each of the many points were summed to give the final error. This error should therefore not be compared to the absolute value of $\tau$.

#### 5.7.3.1 Effect of Air Flow Rate

The data from the RTD experiments in the column cell configuration, which were conducted at a number of air flow rates, are presented in Table 24 to illustrate the effect of air flow rate.

Table 24 : The Effect of Air Flow Rate on the Mixing Characteristics in the Column Cell Configuration.

| Air Flow Rate (l/min) | $\tau$ (min) | $N_d$ | Error | N |
|---|---|---|---|---|
| 0 | 4.57 | 0.034 | 10.27 | 14.0 |
| 3 | 4.19 | 0.230 | 5.86 | 4.2 |
| 5 | 4.80 | 0.350 | 6.64 | 3.4 |
| 7 | 4.02 | 0.390 | 7.37 | 3.0 |

It is clear from this Table that the flow of air through the column contributed significantly to the mixing in the column, if $N_d$ of the case in which air was not flowing is compared to the experiments during which air was flowing. Higher air flow rates resulted in more turbulent conditions in the pulp, which is to be expected. Despite this increase in $N_d$ due to higher air flow rate, the collection was still relatively quiescent compared to the agitated, Jameson and batch cells.

A comparison of the characteristics of mixing in the different cell configurations is given in the following section.

105. See Equation (63) on page 27.

### 5.7.3.2 Mixing in the Different Cell Configurations

Detailed results from the RTD experiments in the three hybrid cell configurations at the liquid and air feed rates used during the flotation experiments (3 l/min liquid, and 3 l/min air) are presented in Appendix E2 on page 173. The mixing parameters which were determined from fits of the axial dispersion model to these data are presented in Table 25.

Table 25 : Comparison of the Mixing Parameters in the Hybrid Cell Configurations.

| Cell Type | $\tau$ (min) | $N_d$ | Error | N |
|---|---|---|---|---|
| Column | 4.19 | 0.230 | 5.86 | 4.2 |
| Agitated | 3.71 | 0.518 | 4.39 | 3.2 |
| Jameson | 2.52 | - | 57.57 | - |

The mixing parameters of the Jameson cell are not given in this Table, since none of the models could be fitted to the experimental RTD data. The collection zone of the Jameson cell is defined as the inside of the downcomer tube, which implies that sampling should have been done at the exit of the tube. This was physically impossible in the current system. Further workers may want to devise a method of achieving this. The conductivity measurements in this cell were carried out at the tailings point, as was the case with the other cells.

It is clear from Table 25 that the agitated cell exhibited much more turbulent conditions of mixing than the column cell. In the light of the discussion in section 5.5.1 on page 115 and most of the results presented thus far, this is to be expected. The more intense conditions of mixing in the agitated cell can directly be attributed to agitation, which is principally the only difference between the differences in collection zone mixing between the two cell types.

The vessel dispersion number, $N_d$, can also be estimated by using the correlation of Manqiu and Finch [1991] (Equation (63) on page 27). This correlation gives a value of 0.282 for conditions used in the column cell experiments, which compares relatively well with the value of 0.230 from Table 25. The difference between these two values can especially be seen to be very small if the value obtained in the agitated cell of 0.518 is compared to them. This illustrates that the values which were determined from the RTD tests are realistic. This correlation can not be used to calculate $N_d$ for the agitated cell configuration,

since it only applies to quiescent systems such as the column cell. The shortcomings of the Jameson cell which prevented the calculation of $N_d$ is unfortunate, sine it would have been meaningful to have an idea of mixing in this cell configuration.

A graphical illustration of the RTD curves obtained from the conductivity measurements in the different cells is given in Figure 60.

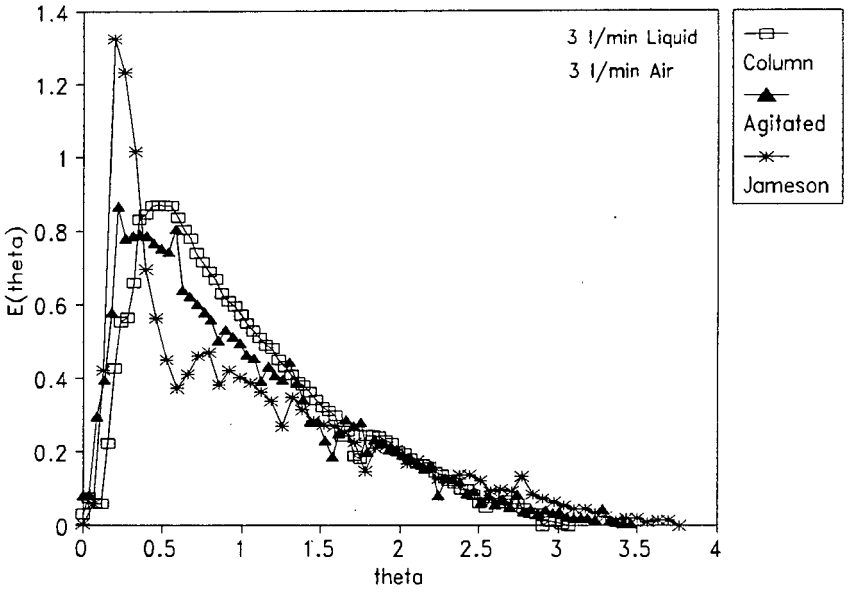


Figure 60 : Comparison of RTD Curves for the Different Hybrid Column Configurations at Air and Water Flow Rates of 3 l/min.

It is clear from this Figure that the Jameson cell exhibited mixing behaviour that was significantly different from the other two cell configurations. The tests were repeated at different liquid and air flow rates to confirm this irregular behaviour, and although the results are not presented here, they were reproducible and the same patterns were obtained.

### 5.7.4 Summary

The characteristics of mixing in the column and agitated cells were quite different to each other, as could be expected. The agitated cell was more mixed than the column cell and a shorter residence time was obtained in the agitated cell compared to the column cell. The residence time in the Jameson was even shorter, although the vessel dispersion number could not be determined in this cell. Vessel dispersion number was greater in the agitated cell than in the column. Air rate was shown to increase mixing in the column cell.

## 5.8 CALCULATION OF PARTICLE COLLECTION EFFICIENCY IN THE COLUMN AND AGITATED COLUMN CELL CONFIGURATIONS

The aim of this thesis was to investigate the effect of particle-bubble contacting environment on particle collection *efficiency*, $E_K$. Up to this point, the results have only been interpreted with respect to particle collection efficiency in a qualitative way. However, it is possible to calculate particle collection efficiency if the mixing parameters (vessel dispersion number, $N_d$, and mean residence time, $\tau$), bubble size, $d_b$, superficial gas velocity, $J_g$, and flotation recovery, R, is known. The success of this calculation is dependent upon certain assumptions:

1) Flotation recovery, R, is equal to the recovery in the collection zone, $R_c$ (*i.e.* the recovery in the froth zone, $R_f$, is unity) [106], and
2) Particle residence time approaches that of the liquid if particles are sufficiently fine [Dobby and Finch, 1985].

The equations used during the calculation of $E_K$ are Equation (20) on page 12 and Equation (52) and (53) on page 25.

Using this method, collection efficiency could only be calculated accurately for the column cell configuration since bubble size could not be determined in the agitated cell, and the geometry of the Jameson cell did not allow the determination of the vessel dispersion number in this cell. However, as discussed in section 5.6.5 above, bubble size in the agitated cell can be expected to be similar to that in the column cell, despite the addition of agitation. Collection efficiency was therefore calculated for the agitated cell by assuming the same bubble size as in the column cell configuration. $E_K$ was calculated with varying collector dosage for the experiments with the -106 $\mu$m particle size fraction in these two cells and the results are displayed in Table 26.

Table 26 : Collection Efficiency in the Column and Agitated Cell Configurations with Varying Collector Dosage.

| Collector Dosage (g/t) | Column Cell | Agitated Cell |
|---|---|---|
| 0 | 0.000 | 0.000 |
| 25 | 0.036 | 0.088 |
| 80 | 0.127 | 0.338 |
| 200 | 0.419 | 1.706 |

106. The hybrid column was operated with a shallow froth depth (1% of the length of the column) during the flotation experiments, and it can therefore be assumed that $R = R_c$.

The detailed parameters which were necessary to calculate $E_K$ are presented in Appendix H on page 185. A graphical illustration of the data from this Table is given in Figure 61, in which $E_K$ is plotted against collector dosage.

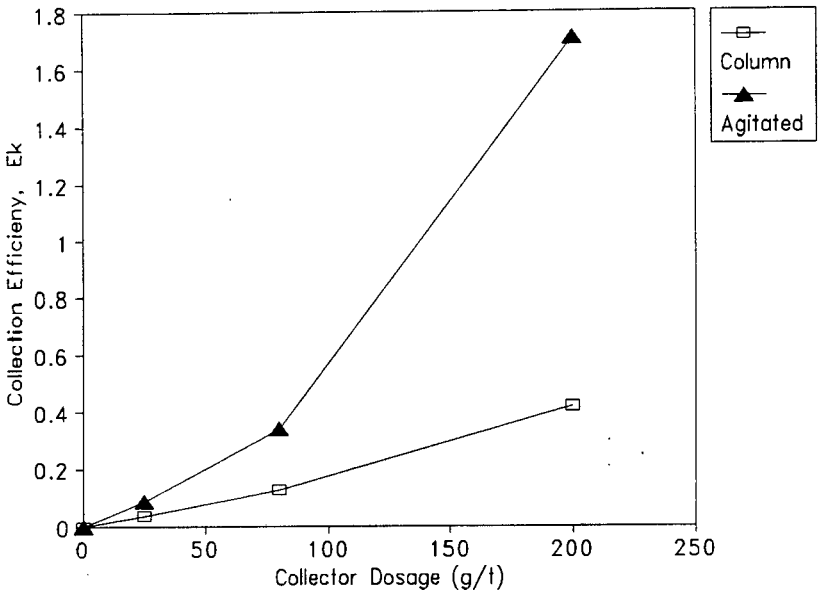


Figure 61 : Variation of Collection Efficiency with Collector Dosage in the Column Cell and Agitated Cell Configurations.

As could be expected, the particle collection efficiency increased with increased hydrophobicity (collector dosage). $E_K$ was zero with no collector added to the pulp, which explains why particles were not collected with collectorless flotation, irrespective of the bubble size or mixing in the pulp. $E_K$ for the column cell increased to 0.419 at a collector dosage of 200 g/t, while it exceeded unity in the agitated cell. It is not possible for $E_K$ to be greater than unity, and the assumption that the column and agitated cell configurations resulted in the same bubble size may therefore be questioned. It is also possible that the vessel dispersion number, $N_d$, may have been incorrectly determined in the agitated cell configuration. An attempt will not be made here to explain this unexpected result, but it is proposed that $E_K$ must have been close to unity during this experiment. If this is true, the earlier assumption that $E_S$ was unity for the -106 $\mu$m size fraction is supported. The environment of contacting the agitated cell was relatively turbulent compared to that in the column cell, and this size fraction could easily have been detached from bubbles.

It is further clear that the relationship between hydrophobicity (collector dosage) and $E_K$ is almost linear for the column cell, while the relationship in the agitated cell configuration is very non-linear. It would therefore be reasonable to propose that the addition of an agitated stage increases the particle collection efficiency, since the only difference between the

column and agitated cells is the addition of turbulence in the form of agitation. It is further proposed that, had it been possible to determine the mixing parameters of the Jameson cell, its curve would lie somewhere between these two curves for this particle fraction due to the differences in bubble size (recovery of this particle size fraction was very similar in all three these cells).

### 5.8.1 Summary

Particle collection efficiency increased with particle hydrophobicity (collector dosage) in both the column and agitated cell configurations, as could be expected. The column cell showed collection efficiencies that were lower than that in the agitated cell. This was probably owing to agitation which was present in the agitated cell.

## 5.9 OVERALL SUMMARY AND DISCUSSION

The flotation experiments were carried out in four different contacting environments *viz.* the three hybrid column cell configurations (quiescent column, agitated column and Jameson cell) and the sub-aeration laboratory batch cell. The performance of the three hybrid column configurations (which were operated on a continuous basis) can not easily be compared to the performance of the laboratory batch cell (batchwise operation). The reason for this is that recovery in continuous systems gives an indication of an equilibrium flotation rate under the specific flotation conditions, while the recovery in the batch system changes with time and the recovery which is normally quoted is the recovery after infinite flotation time. Nevertheless, comparison of the results from experiments in the continuous hybrid column configurations and the batch cell did provide some valuable information on the effect of contacting environment on particle collection efficiency, $E_K$.

It is clear from the flotation results reported and discussed in this Chapter that differences in the environment in which contacting between particles and bubbles took place resulted in different particle collection efficiencies. The addition of agitation to the column cell resulted in a significant increase in $E_K$ with flotation of relatively fine particles, which was attributed to increased efficiency of collision between particles and bubbles and efficiency of attachment of particles to bubbles. This finding is not limited to the mere addition of agitation, since increased agitation speed had the same effect on flotation recovery (and consequently $E_K$ [107]). Furthermore, the cell environments which were characterized by intense contacting between particles and bubbles generally produced increased recovery, especially in the fine

107. Although $E_K$ could only be calculated in the column and agitated cell configurations, flotation recovery in the different cells gave a good indication of the particle collection efficiency during the experiment.

particle range. It would thus appear that increased intensity of contacting generally resulted in increased particle collection efficiency.

Intense contacting between particles and bubbles followed by relatively quiescent disengagement (such as the mechanism employed in the Jameson cell configuration) proved to be beneficial to collection of both fine and coarse particles. Coarse particles probably benefitted by the absence of detachment forces once aggregates were formed, while fine particle collection was possibly enhanced by the intense conditions of contacting across the orifice.

Increased particle hydrophobicity (which was altered by changing the collector dosage) generally led to increased collection of particles. However, very high collector dosages led to decreased recovery, probably as a result of the formation of a second layer of molecules on the quartz particle surface and flocculation of coarse particles.

Particle size exhibited classical n-curve behaviour at intermediate levels of particle hydrophobicity (collector dosage), while fine particles were preferentially collected when the level of hydrophobicity was low.

Finer bubbles were formed in the Jameson cell than in the column cell configuration. A more comprehensive investigation of bubble size in this system is recommended.

It would be dangerous to try and generalize these findings since the flotation experiments were carried out using a pure ore (quartz) without a gangue component. Selectivity and grade could therefore not be taken into account during the analysis of the flotation results. Harris *et al.* [1992], whose work was along the same lines as the work carried out during this investigation, found that reduced selectivity accompanies any increase in recovery owing to more intense contacting. One of the limitations of the work during this thesis is therefore the absence of a gangue component in the ore, despite the advantages of working with a pure ore system such as quartz. It is therefore recommended that this work be extended to a "real ore" system to address this shortcoming.

The fact that the experiments in the hybrid column cell configurations were carried out with a shallow froth enabled one to focus on the collection zone; thus ignoring froth phenomena. An advantage of this approach is that particle collection efficiency, $E_K$, could be determined from quartz recovery and other parameters. Despite this advantage, "real" flotation cells do have a relatively deep froth bed, and it is therefore recommended that testwork be undertaken using a deeper froth bed as a follow-up to this thesis.

# CHAPTER 6
# CONCLUSIONS AND RECOMMENDATIONS

The aim of this thesis was to determine the effect of particle-bubble contacting environment on particle collection efficiency. In order to do this, flotation experiments were carried out with high purity quartz in four different cell types. The quartz was divided into four different particle size fractions which were floated at a wide range of collector dosages added to the pulp. Frother dosage was kept constant during all the experiments. Additional experiments were carried out during which agitation speed was varied in two of the cell types. The conclusions which may be drawn from this work are summarized in this Chapter and some recommendations for further work are given.

## 6.1 CONCLUSIONS

(1) The efficiency of collection of particles is strongly dependent upon the characteristics of the contacting environment in which flotation occurs. Thus, flotation behaviour of the same ore in different cell types can be expected to be significantly different. In addition to cell type, these differences are affected by the size and the degree of hydrophobicity of particles contained in the ore.

(2) Collection efficiency, $E_K$, of relatively fine particles is enhanced by more intense conditions of contacting. Increased contacting intensity can be brought about by the addition of an agitated stage to a quiescent cell such as a column cell, or by increasing the intensity of agitation in a cell which already employs agitation.

(3) Increased agitation speed causes increased particle collection up to a maximum point, after which a further increase in agitation causes decreased collection. Bubble size becomes smaller with increased agitation owing to bubble breakup.

(4) The quiescent column cell is outperformed by other more turbulent cell configurations. Collection of coarse particles is enhanced by the Jameson cell configuration at low collector dosages and it was shown that the contacting conditions in this cell are very turbulent. The column and agitated cells are much more sensitive to particle size at intermediate and high collector dosages than the Jameson and batch cells. The agitated cell results in the best recovery of fine particles at high collector dosages owing to increased collection efficiency.

(5) Flotation of fine particles generally results in higher recovery than that of coarser particles, irrespective of cell environment or the hydrophobicity of particles. Coarse particle collection can be unexpectedly low at high collector dosages owing to a combination of flocculation and formation of a second layer of collector molecules on the ore surface with opposite orientation to the first. The optimum particle size range for quartz flotation (found by de Bruyn and Modi [1956] to be between 10 and 50 $\mu$m for a continuous laboratory flotation cell and between 9 and 50 $\mu$m for a laboratory batch cell) is again confirmed by the results obtained in this thesis for intermediate collector dosages.

(6) Hydrophobicity is a prerequisite for particle collection, as is evidenced by the fact that collectorless flotation resulted in no collection of particles. Increased hydrophobicity (collector dosage) generally results in increased particle collection up to the point of formation of a second layer of inverted collector molecules. Particle collection then decreases at a rate proportional to the coverage of the particle surface with molecules within the second layer.

(7) Bubble size is affected by collector dosage, particle size and cell environment [108]. Increased collector dosage causes smaller bubbles, while increased particle size generally has the same effect. The Jameson cell promotes the formation of bubbles which are significantly smaller than those in the column cell at high collector dosages. Bubble size in the column cell becomes increasingly sensitive to collector dosage with increased particle size.

(8) The characteristics of mixing is also a strong function of the cell environment in which flotation takes place. Although the contacting environment in the column cell is generally regarded as being quiescent, the introduction of air causes a drastic increase in mixing. Increased turbulence via agitation causes mixing to move away from plug flow conditions and to become more mixed. The intensity of mixing in the Jameson cell is proposed to be between that of the column and agitated cells.

## 6.2 RECOMMENDATIONS FOR FURTHER WORK

This thesis was only concerned with the sub-processes which occur in the collection zone of flotation cells. However, a key feature of the operation of column cells is the cleaning action of wash water through a deep froth bed. This implies that the cleaning zone cannot be

108. Frother dosage was kept constant during this investigation, but would lead to decreased bubble size if it were increased.

ignored when practical systems are considered. It is therefore recommended that this work be extended using the hybrid column cell with a deeper froth than 1% of the column length. The cleaning action in deep froth beds affects the grade of flotation products, and the use of a complex (real) ore is therefore recommended during this work.

The mixing characteristics of the Jameson cell could not be determined during the experimental work owing to its unique contacting environment. More comprehensive knowledge of the mechanism of contacting across orifices is currently lacking in the literature and it is recommended that a separate study be conducted to address this aspect using the existing equipment.

The hybrid column cell was operated in continuous mode during this investigation. Another way of operation is to run it in recycle (semi-batch) mode by recycling the tails back to the feed point. This will result in considerable savings in ore consumption, which should be ideal if a valuable ore type is floated. This way of operation should be explored by future workers.

# REFERENCE LIST


Abrahamson, J., 1975, Collision Rates of Small Particles in a Vigorously Turbulent Fluid, Chem. Eng. Sci., Vol. 30, pp. 1371-1379, in Yoon, 1993, *op cit.* . . . . . 14

Ahmed, N. and Jameson, G.J., 1985, The Effect of Bubble Size on the Rate of Flotation of Fine Particles, International Journal of Mineral Processing, Vol. 14, pp. 195-215. . . 22

Antonaidis, D., Mantzavinos, D. and Stamatoudis, M., 1992, The Effect of Chamber Volume and Diameter on Bubble Formation at Plate Orifices, Trans. Inst. Chem. Eng., Vol. 70, Part A, March, pp. 161-165. . . . . 46

Arbiter, N., 1951, Flotation Rates and Flotation Efficiency, Mining Engineering, N.Y., Vol. 3, pp. 791-796. . . . . 10

Barbery, G., 1984, Engineering Aspects of Flotation in the Minerals Industry: Flotation Machines, Circuits and their Simulation, The Scientific Basis of Flotation, Proceedings of the NATO Advanced Study Institute on the Scientific Basis of Flotation, Cambridge, England, July, 1982, K.J. Ives (ed.), pp. 289-348. . . . . 39

Blake, P. and Haynes, J.M., 1973, Contact Angle Hysteresis, in Progress in Surface and Membrane Science, J.F. Danielli *et al.*, (ed.), New York, Academic, Vol. 6, pp. 125-138. . . . . .9

Blake, P. and Ralston, J., 1985, Particle Size, Surface Coverage and Flotation Response, Colloids and Surfaces, Vol. 16, pp. 41-53. . . . . 9

Boutin, P. and Tremblay, R.J., 1964, Method and apparatus for the separation and recovery of ores, Canadian Patent No. 694547, September, in Miller, 1988, *op cit.* . . . . . 1

Brown, D.J., 1965, A Photographic Study of Froth Flotation, Fuel Soc. J., Vol. 16, pp. 22-34. . . . . .5

Brzezina, R. and Sablik, J., 1991, Pneumatic Flotation Machine Flokob - 3 Industrial Model, Column '91, Proceedings of an International Conference on Column Flotation, Volume 2, June 2-6, Canada, G.E. Agar, B.J., Huls and D.B. Hyma (ed.), pp. 619-630. . . . . 1

Cienski, T. and Coffin, V.L., 1981, Column Flotation Operation at Mines Gaspe' Molebdynum Circuit, Proc. 13th Annual Meeting of the Canadian Mineral Processors, Vol. 240. . . . . 44

Clift, R., Grace, J.R. and Weber, M.E., 1978, Bubbles, Drops, and Particles, Academic Press, New York. . . . . 31

Crawford, R. and Ralston, J., 1988, The Influence of Particle Size and Contact Angle in Mineral Flotation, International Journal of Mineral Processing, Vol. 23, pp. 1-24. . . . 8

Crawford, R., Koopal, L.K. and Ralston, K., 1987, Contact Angles on Particles and Plates, Colloids Surf. in press, in Crawford and Ralston, 1988, *op cit.* . . . . . 8

Crozier, R.D., 1992, Flotation, Theory, Reagents and Ore Testing, Pergamon Press. . . . . 70

De Bruyn, P.L. and Modi, H.J., 1956, Particle Size and Flotation Rate of Quartz, Mining Engineering, April, pp. 415-419. . . . . 30

Degner, V.R. and Sabey, J.B., 1988, Wemco/Leeds Flotation Column Development, Column '88, Proceedings of an International Conference on Column Flotation, K.V.S. Sastry (ed.), SME Annual Meeting, Phoenix, Arizona, January 25, pp. 267-279. . . . . 49

Dobby, G.S. and Finch, J.A., 1986a, Flotation Scale-up and Modelling, CIM Bull., Vol. 78, No. 89, 1986. . . . . 43

Dobby, G.S. and Finch, J.A., 1986b, A Model of Particle Sliding Time for Flotation Size Bubbles, Journal of Colloid and Interface Science, Vol. 109, No. 2, pp. 493-498. . . . 19

Dobby, G.S. and Finch, J.A., 1986c, Particle Collection in Columns - Gas Rate and Bubble Size Effects, Canadian Metallurgical Quarterly, Vol. 25, No. 1, pp. 9-13. . . . . 34

Dobby, G.S. and Finch, J.A., 1987, Particle Size Dependence in Flotation Derived from a Fundamental Model of the Capture Process, Int. J. Min. Proc., Vol. 21, pp. 241-260. . . . . 21

Dobby, G.S. and Finch, J.A., 1991, Column Flotation: A Selected Review, Part II, Minerals Engineering, Vol. 4, Nos. 7-11, pp. 911-923. . . . . 43

Dobby, G.S., Yianatos, J.B. and Finch, J.A., 1987, Estimation of Bubble Diameter in Flotation Columns from Drift Flux Analysis, Canadian Metallurgical Quarterly, Vol. 25, No. 1, pp. 9-13. . . . . 35

Dunne, R.C., Forbes, A.W., Harris, P.J, Hulse, N.D. and Moys, M., 1976, The Measurement of Bubble Size Distributions in Flotation Pulps, National Institute for Metallurgy, Mineral and Process Division, Technical Memorandum No. 14032. . . . . 34

Elliot, G.E.P. and Riddiford, A.C., 1964, Contact Angles, in Recent Progress in Surface Science, J.F. Danielli *et al.* (ed.), New York, Academic, in Jameson *et al.*, 1977, *op cit.* . . . . . 9

Emmett, P.H. (ed.), 1960, Catalysis, Vol. VII, Reinhold Publishing Corporation, New York, p. 4. . . . . 75

Engelbrecht, J.A. and Woodburn, E.T., 1975, The Effects of Froth Height, Aeration Rate and Gas Precipitation on Flotation, J. S. Afr. Inst. Min. Metall., 1975, Vol. 32, p. 125. . . . . 23

Espinosa-Gomez, R. and Johnson, M.W., 1989, Column Design and Industrial Experience for Cleaning of LGM Concentrates, Column Flotation Workshop, Adelaide, Australia, July. . . . . 44

Espinosa-Gomez, R., Finch, J.A. and Johnson, N.W., 1988a, Column Flotation of Very Fine Particles, Minerals Engineering, Vol. 1, No. 1, pp. 3-18. . . . . 44

Espinosa-Gomez, R., Yianatos, J., Finch, J.A. and Johnson, N.W., 1988b, Carrying Capacity Limitations in Flotation Columns, Column '88, Proceedings of an International Conference on Column Flotation, K.V.S. Sastry (ed.), SME Annual Meeting, Phoenix, Arizona, January 25, pp. 143-148. . . . . 44

Evans, L.F., Ewers, W.E. and Meadows, F., 1962, The Flotation of Cassiterite, Aust. J. Appl. Sci., Vol. 13, pp. 113-146. . . . . 30

Ewers, W.E., 1955, A Retrospective View of Flotation, in Principles of Flotation (Revised Edition), Melbourne: Australasian Institute of Mining and Metallurgy, pp. 57-64. . . . 29

Fichera, M.A. and Chudacek, M.W., 1992, Batch Cell Flotation Models - A Review, Minerals Engineering, Vol. 5, No. 1, pp. 41-55. . . . . 10

Finch, J.A. and Dobby, G.S., 1990, Column Flotation, Pergamon Press. . . . . 1

Flint, L.R. and Howarth, W.J., 1971, Collision Efficiency of Small Particles with Spherical Air Bubbles, Chem. Eng. Sci., Vol. 26, pp. 1155-1168. . . . . 13

Fowkes, F.M., 1967, Attractive Forces at Solid-Liquid Interfaces, "Wetting", Soc. Chem. Industry Monograph No. 25, London, pp. 3-30. . . . . 7

Franzidis, J.P., Harris, M.C. and O'Connor, C.T., 1991, Review of Column Flotation Practice on South African Mines, Column '91, Proceedings of an International Conference on Column Flotation, Volume 2, June 2-6, Canada, G.E. Agar, B.J., Huls and D.B. Hyma (ed.), pp. 479-493. . . . . 64

Fuerstenau, M.C. (ed.), 1976, Flotation, A.M. Gaudin Memorial Volume, Volume 1, American Institute of Mining, Metallurgical and Petroleum Engineers, Inc., pp. 87-147. . . . . 78

Fuerstenau, M.C., 1975, Role of Metal Ion Hydrolysis in Oxide and Silicate Flotation Systems, AICLhE Symp. Series No. 150, Vol. 71, p. 16. . . . . 78

Gaudin, A.M. and Morrow, J.G., 1954, AIME Trans., Vol. 199, p. 1196. . . . . 8

Gaudin, A.M., 1957, Flotation (1st Edition), McGraw-Hill, New York. . . . . 1

Gaudin, A.M., Groh, J.O., and Henderson, H.B., 1931, Effect of Particle Size on Flotation, Am. Inst. Min. Metall. Eng., Tech. Publ. No. 414, in Trahar, 1981, *op cit.* . . . . . 13

Goodall, C.M, Barker, A.M. and O'Connor, C.T, 1988, Investigation of a Pyrite-Quartz Flotation Froth by Use of a Novel Froth-Splitting Apparatus, International Journal of Mineral Processing, Vol. 24, pp. 307-317. . . . . 65

Harris, M.C., 1995, Chemical Engineering Department, University of Cape Town, Personal Communication. . . . . 122

Harris, M.C., Franzidis, J.P., Breed, A.W. and Deglon, D.A., 1994, An On-Site Evaluation of Different Flotation Technologies for Fine Coal Beneficiation, Minerals Engineering, Vol. 7, Nos. 5/6, pp. 699-714. . . . . 61

Harris, M.C., Franzidis, J.P., O'Connor, C.T and Stonestreet, P., 1992, An Evaluation of the Role of Particle Size in the Flotation of Coal using Different Cell Technologies, Minerals Engineering, Vol.5, Nos. 10-12, pp. 1225-1238. . . . . 2

Holtham, P.N. and Cheng, Ta-Wui, 1991, Study of the Probability of Detachment of Particles from Bubbles in Flotation, Trans. Instn. Min. Metall., Vol. 100, September-December, pp. C147-C155. . . . . 23

Hoover, T.J., 1912, Concentrating Ores by Flotation, Mining Magazine, London, in Kitchener, 1984, *op cit.* . . . . . 38

Jacobi, H.P., Murdock, D.J. and Tucker, R.J., 1991, Column Cells *vs.* Conventional Flotation - A Cost Comparison, Column '91, Proceedings of an International Conference on Column Flotation, Volume 2, June 2-6, Canada, G.E. Agar, B.J., Huls and D.B. Hyma (ed.), pp. 645-659. . . . . 44

Jameson, G.J. and Manlapig, E.V., 1991, Applications of the Jameson Flotation Cell, Column '91, Proceedings of an International Conference on Column Flotation, Volume 2, June 2-6, Canada, G.E. Agar, B.J., Huls and D.B. Hyma (ed.), pp. 673-687. . . . . 45

Jameson, G.J., 1984, Physics and Hydrodynamics of Bubbles, The Scientific Basis of Flotation, Proceedings of the NATO Advanced Study Institute on the Scientific Basis of Flotation, Cambridge, England, July, 1982, K.J. Ives (ed.), pp. 53-77. . . . . 31

Jameson, G.J., 1988, A New Concept in Flotation Column Design, Column '88, Proceedings of an International Conference on Column Flotation, K.V.S. Sastry (ed.), SME Annual Meeting, Phoenix, Arizona, January 25, pp. 281-285. . . . . 44

Jameson, G.J., 1991, Operating Experiences with Jameson Cells at Newlands Coal Pty. Ltd., Queensland, Paper D3, Department of Chemical Engineering, University of Newcastle, NSW, pp. 147-158. . . . . 46

Jameson, G.J., Nam, S. and Moo Young, M., 1977, Physical Factors Affecting Recovery Rates in Flotation, Minerals Sci. Engng., Vol. 9, No. 3, July, pp. 103-118. . . . . 1

Johnson, R.E. and Dettre, R., 1969, Wettability and Contact Angles, in Surface and Colloid Science, E. Matijevic (ed.), New York, Wiley, Vol. 2, pp. 85-154, in Jameson *et al.*, 1977, *op cit.* . . . . . 9

Jordan, C.E. and Spears, D.R., 1990, Evaluation of a Turbulent Flow Model for Fine-Bubble and Fine-Particle Flotation, Minerals & Metallurgical Processing, May, pp. 65-73. . . . . 11

Karolat, W.H. and Hill, G.A., 1988, An Agitated Bubble Column for Use in Potash Flotation, The Canadian Journal of Chemical Engineering, Vol. 66, December, pp. 1017-1020. . . . . 40

Kelly, E.G. and Spottiswood, D.J., 1982, Introduction to Mineral Processing, John Wiley and Sons, New York. . . . . 6

Kennedy, A, 1990, Mining Magazine, October, pp. 281-285. . . . . 45

Keuhn Walker, L.A., Cienski, T. and Reynolds, V., 1991, Air Sparging Evaluation Method, In Column '91, Proceedings of an International Conference on Column Flotation, Volume 2, June 2-6, Canada, G.E. Agar, B.J., Huls and D.B. Hyma (ed.), *op cit.* . . . . . 35

King, R.P. (ed.), 1972, Flotation Research Work of the N.I.M. Research Group, and the Department of Chemical Engineering, University of Natal, J. S. Afr. Inst. Min. Metall., Vol. 72, No. 4, pp. 135-145, in Laplante *et al.*, 1983, *op cit.* . . . . . 37

King, R.P., 1973b, A Computer Programme for the Simulation of the Performance of a Flotation Plant, Revised Report, N.I.M. Research Rep. No. 1436, p. 10, in Laplante *et al.*, 1983, *op cit.* . . . . . 37

King, R.P., 1982, Principles of Flotation, South African Institute of Mining and Metallurgy, Johannesburg. . . . . 6

Kitchener, J.A., 1984, The Flotation Process: Past, Present and Future in Brief, The Scientific Basis of Flotation, Proceedings of the NATO Advanced Study Institute on the Scientific Basis of Flotation, Cambridge, England, July, 1982, K.J. Ives (ed.), pp. 3-52. . . . . 38

Klimpel, R.R. and Isherwood, S., 1987, Some Industrial Implications of Changing Frother Chemical Structure, International Journal of Mineral Processing, 33 (1991), pp. 369-381. . . . . 11

Klimpel, R.R., 1984, Use of Chemical Reagents in Flotation, Chemical Engineering, September, pp. 75-79. . . . . 8

Klimpel, R.R., 1987, Mechanical Flotation Machines for the Treatment of Fine Coal, Fine Coal Processing, Chapter 6, S. Mishra and R.R. Klimpel (ed.), The Dow Chemical Company, Noyes Publications, New Jersey, pp. 136-159. . . . . 1

Klimpel, R.R., Hansen, R. and Meyer, W., 1982, The Engineering Characterization of Flotation reagent Behaviour in Sulfide Ore Flotation, Proceedings of the XIV CIM International Mineral Processing Congress, Toronto, Canada, pp. 17.1-17.14. . . . . 10

Laplante, A.R., Toguri, J.M. and Smith, H.W., 1983, The Effect of Air Flow Rate on the Kinetics of Flotation. Part 1: The Transfer of Material from the Slurry to the Froth, International Journal of Mineral Processing, Vol. 11, pp. 203-219. . . . . 37

Laskowski, J. and Iskra, J., 1970, Role of Capillary Effects in Bubble-Particle collision in Flotation, Institution of Mining and Metallurgy, 10 March, pp. C6-C10. . . . . 9

Laskowski, J. and Kitchener, J.A., 1969, The Hydrophilic-Hydrophobic Transition on Silica, J. Coll. Interf. Sci., Vol. 79, pp. 670-679. . . . . 7

Laskowski, J., 1974, Particle-Bubble Attachment in Flotation, Minerals Sci. Engng., Vol. 6, No. 4, pp. 223-235. . . . . 7

Laskowski, J., 1986, The Relationship between Floatability and Hydrophobicity, Advances in Mineral Processing, P. Somasundaran (ed.), AIME, Littleton, pp. 189-208. . . . . 6

Leja, J. and Schulman, J.H., 1954, Flotation Theory: Molecular Interactions between Frothers and Collectors at Solid-Liquid Interfaces, Trans. AIME, Vol. 99, pp. 221-228. . . . . 81

Levenspiel, O., 1972, Chemical Reaction Engineering, Second Edition, Wiley. . . . . 24

Manqiu, Xu and Finch, J.A., 1991, The Axial Dispersion Model in Flotation Column Studies, Minerals Engineering, Vol. 4, No. 5/6, pp. 553-562. . . . . 25

Manqiu, Xu, Finch, J.A. and Laplante, A.R., 1991, Numerical Solution to Axial Dispersion Model in Flotation Column Studies, Canadian Metallurgical Quarterly, Vol. 30, No. 2, pp.71-77. . . . . 27

Miller, K.J., 1988, Novel Flotation Technology - A Survey of Equipment and Processes, Presented at AIME Conference - Industrial Practise of Fine Coal Processing, Hidden Valley, Somerset PA, September, Chapter 33, pp. 347-363. . . . . 41

Mills, P.J.T. and O'Connor, C.T., 1990, The Modelling of Liquid and Solids Mixing in a Flotation Column, Minerals Engineering, Vol. 3, No. 6, pp. 567-576. . . . . 26

Mills, P.J.T., 1992, Modelling of the Mixing Characteristics and Flotation Kinetics of the Collection Zone in Flotation Columns, PhD Thesis, University of Cape Town, South Africa. . . . . 16

Mular, A.L. and Musara, W.T., 1991, Batch Column Flotation: Rate Data Measurement, Column '91, Proceedings of an International Conference on Column Flotation, June 2-6, Canada, G.E. Agar, B.J. Huls and D.B. Hyma (ed.), Volume 1, pp. 63-74. . . . . 11

Nesset, J.E., 1988, The Application of Residence Time Distributions to Flotation and Mixing Circuits, CIM Bulletin, November, pp. 75-83. . . . . 25

Nevell, A. 1990, Column/Conventional Flotation Cost Comparison, Amdel/SAIT/AMF, Proceedings, Austr. IMM, October. . . . . 44

O'Connor, C.T., Randall, E.W. and Goodall, C.M., 1990, Measurement of the Effects of Physical and Chemical Variables on Bubble Size, International Journal of Mineral Processing, Vol. 28, pp. 139-149. . . . . 34

Pope, M.I. and Sutton, D.I., 1971, Collector Adsorption During Froth Flotation, Powder Technology, Vol. 5, pp. 101-103. . . . . 8

Prince, M.J. and Blanch, H.W., 1990, Bubble Coalescence and Break-Up in Air Sparged Bubble Columns, AIChE Journal, Vol. 36, No. 10, pp. 1485-1499. . . . . 33

Reay, D. and Ratcliff, G.A., 1973, Removal of Fine Particles from Water by Dispersed Air Flotation - Effects of Bubble Size and Particle Size on Collection Efficiency, Canadian Journal Chem. Engrg., Vol. 53, No. 178, in Yoon, 1993, *op cit.* . . . . . 13

Schubert, H. and Bischofberger, C., 1979, On the Optimization of Hydrodynamics in Flotation Processes, Proceedings 13th Int. Miner. Process. Cong. Warszawa, Vol. 2, pp. 1261-1287, in Yoon, 1993, *op cit.* . . . . . 14

Schubert, H., 1986, Aufbereitung Fester Mineralisher Rohstoffe, Vol. 2, 3rd Edition, Grundstoffverlag, Leipzig, in Yoon, 1993, *op cit.* . . . . . 15

Schuhmann, R., 1942, Flotation Kinetics, Methods for Steady-State Study of Flotation Problems, J. Phys. Chem. Ithaca., Vol. 46, p. 891. . . . . 11

Schultze, H.J., 1984, Physico-Chemical Elementary Processes in Flotation, Elsevier, Amsterdam, 384 pp. . . . . 11

Senmin, 1994, Private communication between D.J. Bradshaw from the Chemical Engineering Department at the University of Cape Town and J. Aupiais from Senmin. . . . . 126

Sivamohan, R., 1990, The Problem of Recovering Very Fine Particles in Mineral Processing, International Journal of Mineral Processing, Vol. 28, pp. 247-288. . . . . 28

Smith, R.W. and Rajala, J.A., 1989, Temperature Requirements of Dodecyl and Hexadecylsulphate Flotation of Calcium Activated Quartz, Minerals Engineering, Vol. 2, No. 1, pp. 229-234. . . . . 10

Smith, R.W. and Scott, J.L., 1990, Mechanisms of Dodecylamine Flotation of Quartz, Mineral Processing and Extractive Metallurgy Review, Vol. 7, pp. 81-94. . . . . 9

Soto, H. and Barbery, G., 1991, Flotation of Coarse Particles in a Counter-Current Column Cell, Minerals and Metallurgical Processing, February, pp. 16-21. . . . . 30

Stonestreet, P., 1991, Reverse Flotation: A Novel Process for the Beneficiation of Fine Coal, University of Cape Town, RSA. . . . . 84

Sutherland, K.L and Wark, J.W., 1955, Principles of Flotation, Melbourne, Australas. Inst. Min. Metal. . . . . 5

Sutherland, K.L., 1948, Physical Chemistry of Flotation. XI. Kinetics of the Flotation Process, J. Phys. Colloid, Vol. 52, pp. 394-425. . . . . 11

Taggart, A.F., 1945, Handbook of Mineral Dressing, Ores and Industrial Minerals (2nd Edition), Wiley, New York. . . . . 6

Tomlinson, H.S. and Fleming, M.G., 1965, Flotation Rate Studies, 6th International Mineral Processing Congress, Cannes, 1963, A. Roberts (ed.), Oxford, Pergamon, pp. 563-579. . . . . 10

Trahar, W.J. and Warren, L.J., 1976, The Floatability of Very Fine Particles, International Journal of Mineral Processing, Vol. 3, pp. 103-131. . . . . 28

Trahar, W.J., 1981, A Rational Interpretation of the Role of Particle Size in Flotation, International Journal of Mineral Processing, Vol. 8, pp. 289-327. . . . . 29

Tucker, J.P., Deglon, D.A., Franzidis, J.P., Harris, M.C. and O'Connor, C.T., 1994, An Evaluation of a Direct Method of Bubble Size Distribution Measurement in a Laboratory Batch Flotation Cell, Minerals Engineering, Vol. 7, Nos. 5/6, pp. 667-680. . . . . 81

Tucker, J.P., Deglon, D.A., Franzidis, J-P., Harris, M.C. and O'Connor, C.T., 1993a, An Evaluation of a Direct Method of Bubble Size Distribution Measurement in a Batch Flotation Cell, Minerals Engineering, in press. . . . . 34

Tucker, J.P., Deglon, D.A., Franzidis, J-P., Harris, M.C. and O'Connor, C.T., 1993b, A Study of the Effect of Different Physical and Chemical Parameters on the Bubble Size in a Three Phase System, UCT-Genmin Report #23-7/93. . . . . 34

Tucker, J.P., Franzidis, J.P. and O'Connor, C.T., 1991, The Effect of Physical and Chemical Parameters on Bubble Size Distributions in a Cominco Air Sparging Test Rig, Column '91, Proceedings of an International Conference on Column Flotation, Volume 1, June 2-6, Canada, G.E. Agar, B.J. Huls and D.B. Hyma (ed.), pp. 289-302. . . . . 43

Weast, R.C., 1976, Handbook of Chemistry and Physics, 57th Edition, R.C. Weast (ed), p. F-215. . . . . 103

Weber, M.E. and Paddock, D., 1983, Interceptional and Gravitational Collision Efficiencies for Single Collectors at Intermediate Reynolds Numbers, J. Colloid Interf. Sci., Vol. 94, pp. 328-335, in Yoon, 1993, *op cit.* . . . . . 13

Wheeler, D.A., 1988, Historical View of Column Flotation Development, Column '88, Proceedings of an International Conference on Column Flotation, K.V.S. Sastry (ed.), SME Annual Meeting, Phoenix, Arizona, January 25, pp. 3-4. . . . . 42

Yang, D.C., 1988, A New Packed Column Flotation System, Column '88, Proceedings of an International Conference on Column Flotation, K.V.S. Sastry (ed.), SME Annual Meeting, Phoenix, Arizona, January 25, pp. 257-265. . . . . 48

Ye, Y. and Miller, J.D., 1989, International Journal of Mineral Processing, Vol. 25, pp. 199-219. . . . . 18

Ye, Y., Gopalakrishnan, S., Pacquet, E. and Miller, J.D., 1988, Development of the Air Sparged Hydrocyclone: A Swirl-flow Flotation Column, Column '88, Proceedings of an International Conference on Column Flotation, K.V.S. Sastry (ed.), SME Annual Meeting, Phoenix, Arizona, January 25, pp. 305-314. . . . . 43

Yianatos, J.B. and Levy, A.R., 1991, Estimation of Gas Holdup, Diameter and Apparent Density of Mineralized Bubbles in Industrial Flotation Columns, Column '91, Proceedings of an International Conference on Column Flotation, Volume 2, June 2-6, Canada, G.E. Agar, B.J., Huls and D.B. Hyma (ed.), pp. 1-20. . . . . 125

Yianatos, J.B., Finch, J.A. and Laplante, A.R., 1987, Selectivity in Column Flotation Froths, International Journal of Mineral Processing, January, pp. 122-151. . . . . 12

Yianatos, J.B., Finch, J.A., Dobby, G.S. and Xu, M., 1988, Bubble Size Estimation in a Bubble Swarm, Journal of Colloid and Interface Science, Vol. 126, No. 1, pp. 37-44. . . . . 68

Yoon, R.H. and Luttrell, G.H., 1989, The Effect of Bubble Size on Fine Particle Flotation, Mineral Processing and Extractive Metallurgy Review, J.S. Laskowsi (ed.), Gordon and Breach Science Publishers, New York, Vol. 5, pp. 101-122, in Yoon, 1993, *op cit.* . . . . . 14

Yoon, R.H., 1993, Microbubble Flotation, Minerals Engineering, Vol. 6, No. 6, pp. 619-630. . . . . 13

Yoon, R.H., Adel, G.T. and Luttrell, G.H., 1988, U.S. Patent Appl. No. 5761008, in Dobby and Finch, 1991, *op cit.* . . . . . 43

Yordan, J.L. and Yoon, R.H., 1986, Induction Time Measurements for a Quartz-Amine Flotation System, 115th SME Annual Meeting, New Orleans, preprint 86-105, in Yoon, 1993, *op cit.* . . . . . 9

Zhou, Z.A., Egiebor, N.O. and Plitt, L.R., 1993, Frother Effects on Bubble Size Estimation in a Flotation Column, Minerals Engineering, Vol. 6, No. 1, pp.55-67. . . . . 35

Zipperian, D.E. and Svensson, U., 1988, Plant Practice of the Flotaire Column Flotation Machine for Metallic, Non-metallic and Coal Flotation, Column '88, Proceedings of an International Conference on Column Flotation, K.V.S. Sastry (ed.), SME Annual Meeting, Phoenix, Arizona, January 25, pp. 43-54. . . . . 46

# APPENDIX A
# NUMERICAL SOLUTIONS TO SURFACE VORTICIY

**(After Dobby and Finch, 1987)**

Surface vorticity can be estimated by Equation (41) on page 21:

$$\xi_s = a + b\,\theta + c\,\theta^2 + d\,\theta^3$$

where the constants a, b, c and d are related to $Re_b$ in the following way

$$a = -0.01082 - 7.723\times10^{-4}\,Re_b + 1.735\times10^{-6}\,Re_b^2 - 2.046\times10^{-9}\,Re_b^3$$

$$b = +0.0745 + 3.013\times10^{-3}\,Re_b - 7.402\times10^{-6}\,Re_b^2 + 8.931\times10^{-9}\,Re_b^3$$

$$c = -4.276\times10^{-4} - 1.977\times10^{-5}\,Re_b + 5.194\times10^{-8}\,Re_b^2 - 6.520\times10^{-11}\,Re_b^3$$

$$d = -1.103\times10^{-6} - 1.032\times10^{-7}\,Re_b + 1.397\times10^{-10}\,Re_b^2 - 1.334\times10^{-13}\,Re_b^3$$

# APPENDIX B
# EXPERIMENTAL PROCEDURES

## INTRODUCTION

Various procedures were established for the experimental work for this thesis. This Appendix gives a detailed description of these procedures.

## B1 MILLING CURVE

This procedure was used to establish milling curves for two types of milling media, *viz.* rods and balls. The milling curves were established to determine the time the No. 2 Foundry Sand product had to be milled to create a size distribution of 50% passing 106 $\mu$m.

2.5 kg of quartz (No.2 Foundry Sand [109]) was calcined [110] and added to a 300 mm diameter Polaris laboratory scale mill while it was tilted upwards. Approximately 25 kg of milling media (10 kg of media per kg of ore) was loaded into the mill. The milling media was either steel balls of different sizes (ranging from approximately 20 mm to 60 mm) or steel rods of uniform size (25 mm in diameter). The rods weighed approximately 1.1 kg each. The lid was closed and secured in place with the clamp provided and the mill was adjusted to the horizontal position. It was started at a rotational speed of 55 rpm, which was 75% of its critical rotational speed. The critical rotational speed of the mill was determined as 73 rpm by measuring the rotational speed at which all the milling media were forced to the walls of the mill. The mill was stopped after 5 minutes and its contents were carefully removed (the milling media were removed first not to lose any of the milled quartz). After this, the particle size distribution of the milled quartz was determined, using the experimental procedure described in Appendix B4 on page 164. All the quartz was recombined and fed back to the mill after sieving. A milling curve (% finer than 106 $\mu$m *vs.* milling time) was established in this way, assuming that losses of quartz throughout the whole procedure were negligible. The results of these experiments are given in Appendix D on page 171.

## B2 MILL

This procedure was used to mill the No. 2 Foundry Sand product to 50% passing 106 $\mu$m. The resulting size fraction was the fines fraction used in the experiments.

---

109. See section 4.2.1 on page 69 for a description of this product.
110. The Calcination process is described in Appendix B8 on page 166.

2.5 kg of calcined [111] (No. 2 Foundry Sand) quartz was loaded into a laboratory scale mill while it was tilted upwards. Approximately 25 kg of steel balls (10 kg of balls per kg of ore) was added to the mill and the lid was closed and secured in position with the clamp provided. The mill was tilted to the horizontal position and started. It was run at 55 rpm for 30 minutes, as determined from milling curves [112]. The mill was then emptied out and the milled material was stored in plastic buckets for later use. Quartz which was stuck to the balls was removed by dropping the balls onto a coarse wire cloth screen and letting the quartz fall through the screen into a bucket.

## B3 BULK SCREENING

This procedure was used to divide the quartz products obtained from Consol Industrial Minerals into four different particle size fractions by means of screening.

The quartz was divided into different particle size fractions with a laboratory scale screening machine which was located at the University of Stellenbosch. The machine was equipped with 500 mm diameter screens, and screens of different mesh grades were made up to fit onto it. The screening machine was started and enough quartz was poured onto the screen to cover it. The quartz was continuously spread out evenly over the surface of the screen with a scraper. The bottom product was collected in a bucket at the outlet spout of the machine, while the top product was scooped up and deposited into a second bucket. Every screening session was maintained until most of the finer particles passed through the screen, after which the screen was emptied and the next batch was loaded. The order of screening was from coarse to fine particles at all times.

## B4 SIEVING

This procedure was used to determine the size distributions of the three coarsest particle size fractions, *viz.* the +106 -150 $\mu$m, the +150 -300 $\mu$m and the +300 $\mu$m particle size fractions.

A representative sample was prepared in the following way. 2 kg of quartz was weighed out on a laboratory scale and was then split into ten batches with a rotary sample splitter. Five of these batches (every second one) were combined and the resulting batch was again split in the same way to obtain a total sample mass of approximately 500 g. This was again split into ten samples to obtain approximately 50 g per sampling cup. An arbitrary sample cup

111. See footnote 109 *op cit.*
112. The milling curves are given in Appendix D on page 171.

was chosen to obtain a representative sample. Precisely 50 g of the quartz from this sample cup was weighed out and dry sieved with a rotating screen shaker for ten minutes. A root two series Tyler sieve configuration was used at all times. Each of the sieves was cleaned in an ultrasonic bath for a minimum of 15 minutes and allowed to dry prior to sieving. The mass of quartz form each sieve was taken and the size distribution calculated.

## B5 MALVERN

This procedure was used to determine the size distribution of the prepared -106 $\mu$m particle size fraction prior to flotation, as well as the size distributions of the flotation concentrates after flotation experiments using this particle size fraction.

A representative sample was prepared in the following way. All the concentrate samples from the flotation run were combined and split into ten batches with an Eriez Magnetics 10-cup rotary sample splitter. One of these batches was again split into ten in the same way. This procedure was repeated until approximately 25 g of sample was left per sample cup. The Malvern particle size analyzer was set up with the correct lens and was flushed with water to remove any particles from the lens compartment. Approximately two spatulas of the sample was deposited into the mixing compartment of the Malvern analyzer and readings were automatically taken the instrument. This was repeated until reproducible results were obtained.

## B6 ATTRITIONING

This procedure was used to investigate the possibility of cleaning the surface of contaminated quartz via attritioning.

A total mass of 2 kg of contaminated quartz with a size distribution similar to the -106 $\mu$m particle size fraction was weighed out on a laboratory scale. The quartz was deposited into the feed tank of the flotation rig and 12 litres of tap water was added. A sample of the water was taken in a glass beaker and the pH was measured. The same agitator which was used for all the hybrid column flotation runs was used to stir the pulp vigorously for a period of five minutes. Another 10 minutes was allowed for the solids to settle, after which a plastic syringe was used to take a sample of the water. The water was sucked through a piece of filter cloth to prevent solids still left in the water from entering the sample. A further sample was taken from the tank in a glass beaker. The sample from the syringe was kept for ultraviolet spectroscopy analysis, while the pH of the water sample in the beaker was measured directly. The water in the tank was removed via decanting and the same volume of fresh tap water was added, after which the whole procedure was repeated.

## B7 ACID WASHING

This procedure was used to investigate the possibility of cleaning the surface of contaminated quartz particles via acid washing. The quartz treated in this way was either contaminated, or quartz which was floated after it had been treated this way previously.

The quartz was added to a 1 litre glass beaker and 3 minutes was allowed for the solids to settle out. The water was removed through a rubber tube (by siphoning) and 600 ml fresh, cold tap water was added to the wet quartz. The beaker and contents were heated on a gas flame up to boiling point (approximately 100 °C) while continuously stirring with a laboratory stirrer at a rate sufficient to keep the solids properly suspended. At boiling point 6 ml HCl was added to the pulp to give a solution of concentration 0.1 mol/dm$^3$ HCl. This acidic pulp was boiled for 15 minutes while still being stirred continuously. The flame was removed, the agitator was switched off, and 3 minutes solid settling time was allowed. The hot acid solution was removed in the same way as described above and its pH was measured. The quartz was washed by adding approximately 600 ml fresh, cold tap water, agitating the resulting pulp for 5 minutes, allowing 3 minutes for solid settling and again removing the water. The pH of the wash water was again measured. This procedure was repeated until the pH of the wash water asymptotically approached the pH of the tap water, which was measured beforehand [113]. The cleaned quartz was dried in a microwave oven in the same glass beaker and its mass determined with a laboratory scale. The difference in mass due to losses (with water removal) was made up by adding quartz which had been treated in a similar way.

## B8 CALCINATION

This procedure was used to remove a layer of organic contamination from the quartz particle surface prior to floating it.

A rectangular basket was made out of 300 $\mu$m wire cloth. Its dimensions were such that it could just fit into a Carbolite laboratory furnace. The furnace was preheated to 500 °C. The appropriate mass of quartz [114] was put into the foil-lined basket and inserted into the furnace. It was left to calcine for an hour and removed. The heated quartz was stirred with a metal stirrer to ensure proper escape of gases due to the calcination process, as well as to ensure that a maximum surface area of the quartz was exposed to the heat. It was calcined

113. The pH of the wash water did not reach the exact same pH of the tap water as had been suggested in the literature [Smith and Rajala, 1989], but an offset existed which could not be surpassed. This is probably because of the presence of the quartz in the water.

114. 2.5 kg for milling or 4.4 kg in the case of normal column floats.

for another hour after which the basket with quartz was removed from the furnace and left to cool down on a steel grid. The calcined quartz was floated as soon as it reached room temperature. The -106 $\mu$m size fraction was not floated directly after it had been calcined, but was milled, screened and stored afterwards. The milling and screening procedures have been described in Appendices B2 and B3 on pages 163 and 164.

## B9 TRACER TESTS

This procedure was used to determine the liquid phase mixing characteristics of the three hybrid column cell configurations at different operating conditions.

A volume of 40 l of tap water was added to the feed tank of the hybrid column. The feed tank agitator was started and the standard dosage of frother (80 g/t Senfroth 6010 at 100 g/l solid concentration) was added to the water to produce a similar bubble size distribution to that which occurred during normal three phase operation. A period of 10 minutes was allowed for proper mixing of the frother with the water. The feed pump which had been pre-calibrated to 3 l/min was started and the column was allowed to fill up. When the agitated column was in use, the column agitator was started at the desired rotational speed when the column was approximately 75% full. The air was opened at the desired flow rate when the water in the column was at approximately the same level. The level controller was manually adjusted to maintain a 20 mm froth depth after the tailings pump was started and switched to PI control.

A baseline of conductivity for the water with frother was measured while the tailings stream was recycled to the feed tank. A conductivity probe, connected to a computer for data logging at one second intervals, was placed in-line in the tailings hose at a point close to the column. A syringe containing 5 ml of a saturated solution of KCl in water (34.4 g/100 cc) was pushed into the feed line 3 cm away from the pulp feed point (normal or Jameson tube).

The tailings stream was redirected to the discharge tank to render the operation continuous and timing was started the moment the syringe was emptied out into the feed line. Level was controlled manually from this point onwards since the addition of KCl to the water altered its conductivity, resulting in a substantial decrease in pulp level. The conductivity measurements as a function of time were stored onto disc by the computer and were analyzed afterwards. Gas holdup was measured after each run in the same way as had been done during normal hybrid column operation [115].

115. See the experimental procedure in Appendix 4.5.1 on page 82.

# APPENDIX C
# QUARTZ PARTICLE SIZE DISTRIBUTIONS

## Particle Size Distributions of the two Quartz Products used as Flotation Feed

The two raw products obtained from Consol Industrial Minerals had different particle size distributions. The 12DA product was much coarser than the No. 2 Foundry Sand product. The particle size distributions of the two products are given in Table 27.

Table 27 : Particle Size Distribution of the Quartz Products.

| Particle Size ($\mu$m) | % Passing | |
|---|---|---|
| | 12DA | No. 2 |
| +53 -75 | 0.8 | 4.9 |
| +75 -106 | 3.6 | 11.7 |
| +106 -125 | 3.7 | 12.5 |
| +125 -150 | 6.4 | 24.2 |
| +150 -212 | 16.0 | 35.5 |
| +212 -300 | 22.9 | 8.6 |
| +300 -425 | 25.3 | 2.1 |
| +425 -600 | 18.7 | 0.4 |
| +600 -800 | 2.4 | 0.1 |
| +800 | 0.2 | 0.0 |

A graphical illustration of the distribution of these two products is shown in Figure 62.

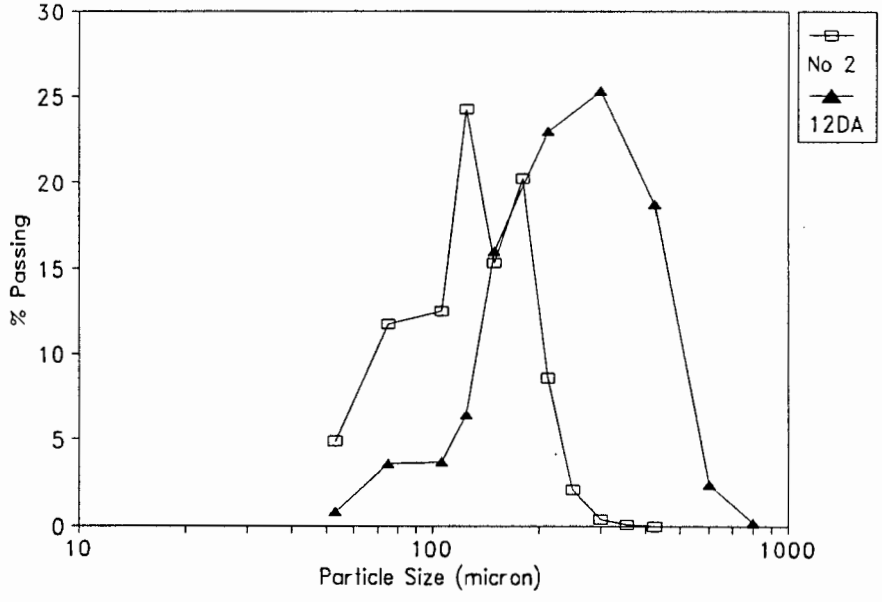


Figure 62 : Particle Size Distributions of Quartz Products.

# APPENDIX D
# MILLING DATA

Rods and balls were tried to determine which medium would ensure the most effective milling. Details of the milling procedure used are given in Appendix B1 on page 163. Figure 63 shows the relative performance of rods and balls.

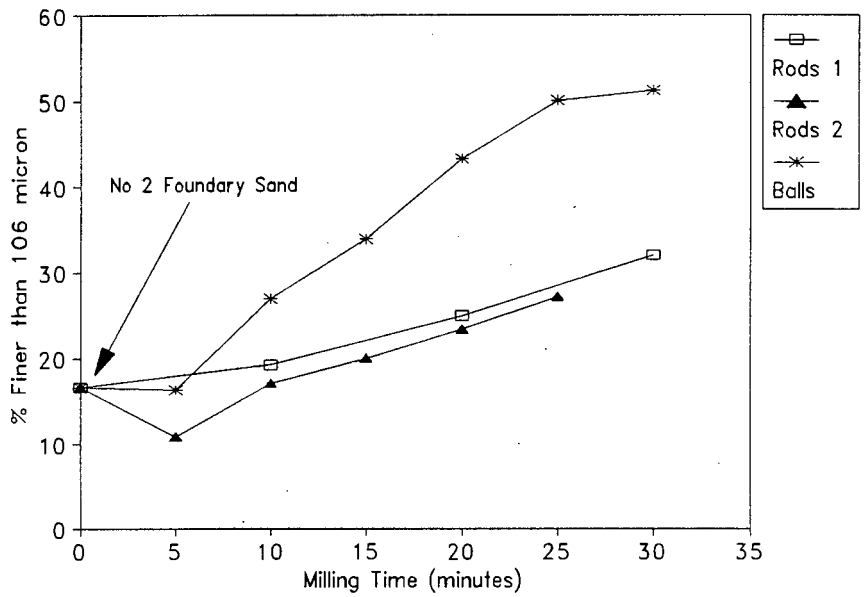


Figure 63 : Milling Curves Resulting from Two Different Milling Media (No. 2 Foundry Sand).

It is clear from Figure 63 that the balls outperformed the rods by far. Not only did the rods result in a poorer performance, but they often became entangled in the mill, which was not possible with the balls. Balls were thus selected as the milling medium.

The milling time was chosen as 30 minutes from the milling curves, after which more than 50% of the quartz was finer than 106 $\mu$m, which was sufficient for separation of the - 106 $\mu$m material for use in the flotation experiments. A repeat run was carried out using rods, and it is clear that the reproducibility with rods was relatively good, if it is kept in mind that run 1 was only screened at 10 minute intervals, with consequently less loss of sample.

The initial decrease in the milling curves after 5 minutes may be due to a different particle size analysis being used at the point where milling time is zero. This point was obtained from the supplier of the quartz.

The numerical values of the milling curves are given below in Table 28.

Table 28 : Milling Curve Data - Comparison of Rods and Balls.

| | % Finer than 106 $\mu$m | | |
|---|---|---|---|
| Milling Time (minutes) | Rods (Run 1) | Rods (Run 2) | Balls |
| 0 (No. 2) | 16.60 | 16.60 | 16.60 |
| 5 | | 10.82 | 16.31 |
| 10 | 19.18 | 16.99 | 26.93 |
| 15 | | 19.94 | 33.89 |
| 20 | 24.90 | 23.35 | 43.19 |
| 25 | | 27.10 | 50.03 |
| 30 | 31.90 | | 51.18 |

# APPENDIX E
# RESIDENCE TIME DISTRIBUTION RESULTS

## E1 RTD Data for the Input Pulse Signal

The measured conductivity and normalized E(t) values for the input signal are presented in Table 29. The conductivity data were not converted to dimensionless units in this case to make use of the practical significance of real time results.

Table 29 : Tracer Input Pulse Data.

| Time (s) | Run 1 | | Run 2 | | Run 3 | |
|---|---|---|---|---|---|---|
| | Conductivity | E(t) | Conductivity | E(t) | Conductivity | E(t) |
| 0 | 0 | 0.0000 | 0 | 0.0000 | 0 | 0.0000 |
| 1 | 4095 | 0.4868 | 4095 | 0.4268 | 4095 | 0.4774 |
| 2 | 3344 | 0.3975 | 3994 | 0.4163 | 6401 | 0.3965 |
| 3 | 617 | 0.0733 | 994 | 0.1036 | 713 | 0.0831 |
| 4 | 219 | 0.0260 | 339 | 0.0353 | 227 | 0.0265 |
| 5 | 86 | 0.0102 | 128 | 0.0133 | 85 | 0.0099 |
| 6 | 35 | 0.0042 | 40 | 0.0042 | 38 | 0.0044 |
| 7 | 13 | 0.0016 | 4 | 0.0004 | 15 | 0.0018 |
| 8 | 3 | 0.0004 | 0 | 0.0000 | 3 | 0.0004 |
| 9 | 0 | 0.0000 | 0 | 0.0000 | 0 | 0.0000 |
| 10 | 0 | 0.0000 | 0 | 0.0000 | 0 | 0.0000 |
| 11 | 0 | 0.0000 | 0 | 0.0000 | 0 | 0.0000 |
| 12 | 0 | 0.0000 | 0 | 0.0000 | 0 | 0.0000 |
| 13 | 0 | 0.0000 | 0 | 0.0000 | 0 | 0.0000 |
| 14 | 0 | 0.0000 | 0 | 0.0000 | 0 | 0.0000 |
| 15 | 0 | 0.0000 | 0 | 0.0000 | 0 | 0.0000 |
| 16 | 0 | 0.0000 | 0 | 0.0000 | 0 | 0.0000 |
| 17 | 0 | 0.0000 | 0 | 0.0000 | 0 | 0.0000 |
| 18 | 0 | 0.0000 | 0 | 0.0000 | 0 | 0.0000 |
| 19 | 1 | 0.0001 | 0 | 0.0000 | 0 | 0.0000 |
| 20 | 0 | 0.0000 | 0 | 0.0000 | 0 | 0.0000 |
| Total | 8413 | 1.0000 | 9594 | 1.0000 | 8577 | 1.0000 |

## E2 RTD Results for the Different Cell Configurations

Although the conductivity measurements were taken at one second intervals, the RTD data are presented here at 10 second intervals. The model calculations and errors are not presented here, but are summarized in the main text.

The data for the column cell configuration are given below in Table 30.

Table 30 : RTD Data for the Column Cell Configuration for Different Air Flow Rates.

| 0 l/min Air 3 l/min Pulp | | 3 l/min Air 3 l/min Pulp | | 5 l/min Air 3 l/min Pulp | | 7 l/min Air 3 l/min Pulp | |
|---|---|---|---|---|---|---|---|
| $\theta$ | E($\theta$) | $\theta$ | E($\theta$) | $\theta$ | E($\theta$) | $\theta$ | E($\theta$) |
| 0.0000 | 0.0239 | 0.0000 | 0.0302 | 0.0000 | 0.0000 | 0.0000 | 0.0069 |
| 0.0365 | 0.0650 | 0.0398 | 0.0755 | 0.0347 | 0.0000 | 0.0415 | 0.0069 |
| 0.0729 | 0.0178 | 0.0796 | 0.0604 | 0.0694 | 0.0000 | 0.0830 | 0.0570 |
| 0.1094 | 0.0020 | 0.1194 | 0.0566 | 0.1041 | 0.0384 | 0.1245 | 0.2315 |
| 0.1459 | 0.0020 | 0.1592 | 0.2227 | 0.1388 | 0.1511 | 0.1660 | 0.4354 |
| 0.1824 | 0.0118 | 0.1990 | 0.4265 | 0.1735 | 0.5798 | 0.2075 | 0.5287 |
| 0.2188 | 0.0142 | 0.2387 | 0.5548 | 0.2082 | 0.5686 | 0.2490 | 0.7326 |
| 0.2553 | 0.0040 | 0.2785 | 0.5661 | 0.2429 | 0.7247 | 0.2904 | 0.8156 |
| 0.2918 | 0.0099 | 0.3183 | 0.6605 | 0.2776 | 0.8139 | 0.3319 | 0.8795 |
| 0.3283 | 0.0554 | 0.2581 | 0.8303 | 0.3123 | 0.8561 | 0.3734 | 0.8330 |
| 0.3647 | 0.0020 | 0.3979 | 0.8460 | 0.3470 | 0.8672 | 0.4149 | 0.6065 |
| 0.4012 | 0.1023 | 0.4377 | 0.8680 | 0.3817 | 0.8883 | 0.4564 | 0.8760 |
| 0.4377 | 0.1682 | 0.4775 | 0.8718 | 0.4165 | 0.5439 | 0.4979 | 0.8588 |
| 0.4742 | 0.2651 | 0.5173 | 0.8680 | 0.4859 | 0.8709 | 0.5394 | 0.6860 |
| 0.5106 | 0.4009 | 0.5571 | 0.8680 | 0.5206 | 0.8462 | 0.5809 | 0.8242 |
| 0.5471 | 0.5246 | 0.5969 | 0.8365 | 0.5553 | 0.8040 | 0.6224 | 0.8087 |
| 0.5836 | 0.6756 | 0.6367 | 0.8025 | 0.5900 | 0.7508 | 0.6639 | 0.7378 |
| 0.6200 | 0.8356 | 0.6765 | 0.7786 | 0.6247 | 0.7867 | 0.7045 | 0.7067 |
| 0.6565 | 0.9336 | 0.7162 | 0.7400 | 0.6594 | 0.7359 | 0.7469 | 0.4579 |
| 0.6930 | 1.1000 | 0.7560 | 0.7150 | 0.6941 | 0.7309 | 0.7883 | 0.6652 |
| 0.7295 | 1.3189 | 0.7958 | 0.6900 | 0.7288 | 0.6839 | 0.8298 | 0.4009 |
| 0.7659 | 1.3961 | 0.8356 | 0.6700 | 0.7635 | 0.5872 | 0.8713 | 0.6428 |
| 0.8024 | 1.4600 | 0.8754 | 0.6305 | 0.7982 | 0.4138 | 0.9128 | 0.2609 |
| 0.8389 | 1.5050 | 0.9152 | 0.6145 | 0.8329 | 0.6504 | 0.9543 | 0.6030 |
| 0.8754 | 1.5203 | 0.9550 | 0.5953 | 0.8676 | 0.6021 | 0.9958 | 0.3179 |
| 0.9118 | 1.5038 | 0.9948 | 0.5712 | 0.9023 | 0.6033 | 1.0373 | 0.5477 |
| 0.9483 | 1.4801 | 1.0348 | 0.5509 | 0.9370 | 0.5538 | 1.0788 | 0.4855 |
| 0.9848 | 1.4288 | 1.0744 | 0.5327 | 0.9717 | 0.5315 | 1.1203 | 0.4838 |
| 1.0212 | 1.2806 | 1.1142 | 0.5108 | 1.0064 | 0.5278 | 1.1618 | 0.4924 |
| 1.0577 | 1.1693 | 1.1539 | 0.4921 | 1.0411 | 0.4596 | 1.2033 | 0.4095 |
| 1.0942 | 1.0485 | 1.1937 | 0.4793 | 1.0758 | 0.3890 | 1.2448 | 0.4441 |
| 1.1307 | 0.9543 | 1.2335 | 0.4513 | 1.1105 | 0.3915 | 1.2862 | 0.4078 |
| 1.2036 | 0.8586 | 1.2733 | 0.4389 | 1.1452 | 0.3072 | 1.3277 | 0.3974 |
| 1.2401 | 0.7524 | 1.3131 | 0.4152 | 1.1799 | 0.4485 | 1.3692 | 0.3940 |
| 0.2766 | 0.5076 | 1.3529 | 0.3845 | 1.2147 | 0.5055 | 1.4107 | 0.3594 |
| 0.3130 | 0.4850 | 1.3927 | 0.3623 | 1.2494 | 0.4348 | 1.4522 | 0.2073 |
| 1.3495 | 0.4816 | 1.4325 | 0.3427 | 1.2841 | 0.4163 | 1.4937 | 0.3352 |
| 1.3860 | 0.3913 | 1.4723 | 0.3258 | 1.3188 | 0.3878 | 1.5352 | 0.3024 |
| 1.4225 | 0.4209 | 1.5121 | 0.3108 | 1.3535 | 0.3556 | 1.5767 | 0.3231 |
| 1.4589 | 0.2671 | 1.5519 | 0.2984 | 1.3882 | 0.3357 | 1.6182 | 0.2903 |
| 1.4954 | 0.1972 | 1.5916 | 0.2415 | 1.4229 | 0.2577 | 1.6597 | 0.2834 |
| 1.5319 | 0.1889 | 1.6314 | 0.2566 | 1.4576 | 0.3432 | 1.7012 | 0.2609 |
| 1.6048 | 0.1105 | 1.6712 | 0.1887 | 1.4923 | 0.3432 | 1.7427 | 0.2696 |
| 1.6413 | 0.0945 | 1.7110 | 0.1812 | 1.5270 | 0.3159 | 1.7841 | 0.2505 |
| 1.6778 | 0.1527 | 1.7508 | 0.2453 | 1.5617 | 0.2726 | 1.8256 | 0.2143 |
| 1.7142 | 0.1499 | 1.7906 | 0.2453 | 1.5964 | 0.2168 | 1.8671 | 0.2091 |
| 1.7507 | 0.1453 | 1.8304 | 0.2415 | 1.6311 | 0.2812 | 1.9086 | 0.2143 |
| 1.7872 | 0.1346 | 1.8702 | 0.2302 | 1.6658 | 0.2639 | 1.9501 | 0.1676 |
| 1.8237 | 0.1288 | 1.9100 | 0.2227 | 1.7005 | 0.2552 | 1.9916 | 0.1935 |
| 1.8601 | 0.1089 | 1.9498 | 0.2013 | 1.7352 | 0.2354 | 2.0331 | 0.1866 |
| 1.8966 | 0.1081 | 1.9896 | 0.1962 | 1.7699 | 0.1945 | 2.0746 | 0.1693 |
| 1.9331 | 0.0966 | 2.0294 | 0.1812 | 1.8046 | 0.2081 | 2.1161 | 0.1402 |
| 1.9695 | 0.0853 | 2.0691 | 0.1661 | 1.8393 | 0.2032 | 2.1576 | 0.1486 |

| | | | | | | | |
|---|---|---|---|---|---|---|---|
| 2.0060 | 0.0853 | 2.1089 | 0.1661 | 1.8740 | 0.2106 | 2.1991 | 0.1486 |
| 2.0425 | 0.0741 | 2.1487 | 0.1623 | 1.9087 | 0.2081 | 2.2406 | 0.1279 |
| 2.0790 | 0.0702 | 2.1885 | 0.1585 | 1.9434 | 0.2032 | 2.2820 | 0.1123 |
| 2.1154 | 0.0588 | 2.2283 | 0.1434 | 1.9781 | 0.1933 | 2.3235 | 0.1210 |
| 2.1519 | 0.0547 | 2.2681 | 0.1359 | 2.0129 | 0.1895 | 2.3650 | 0.1106 |
| 2.1884 | 0.0430 | 2.3079 | 0.1208 | 2.0476 | 0.1809 | 2.4065 | 0.0968 |
| 2.2249 | 0.0461 | 2.3477 | 0.1132 | 2.0823 | 0.1784 | 2.4480 | 0.0950 |
| 2.2613 | 0.0340 | 2.3875 | 0.0981 | 2.1170 | 0.1474 | 2.4895 | 0.0950 |
| 2.2978 | 0.0144 | 2.4273 | 0.0981 | 2.1517 | 0.1586 | 2.5310 | 0.0968 |
| 2.3343 | 0.0058 | 2.4671 | 0.0830 | 2.1864 | 0.1672 | 2.5725 | 0.0639 |
| 2.3708 | 0.0380 | 2.5068 | 0.0604 | 2.2211 | 0.1598 | 2.6140 | 0.0743 |
| 2.4072 | 0.0216 | 2.5466 | 0.0491 | 2.2558 | 0.1598 | 2.6555 | 0.0605 |
| 2.4437 | 0.0312 | 2.5864 | 0.0793 | 2.2905 | 0.1524 | 2.6970 | 0.0691 |
| 2.4802 | 0.0220 | 2.6262 | 0.0604 | 2.3252 | 0.1412 | 2.7385 | 0.0536 |
| 2.5166 | 0.0238 | 2.6660 | 0.0679 | 2.3599 | 0.1313 | 2.7799 | 0.0518 |
| 2.5531 | 0.0144 | 2.7058 | 0.0566 | 2.3946 | 0.1251 | 2.8214 | 0.0294 |
| 2.5896 | 0.0048 | 2.7456 | 0.0566 | 2.4293 | 0.1388 | 2.8629 | 0.0363 |
| 2.6261 | 0.0026 | 2.7854 | 0.0453 | 2.4640 | 0.1251 | 2.9044 | 0.0363 |
| 2.6625 | 0.0099 | 2.8252 | 0.0340 | 2.4987 | 0.1202 | 2.9459 | 0.0276 |
| 2.6990 | 0.0020 | 2.8650 | 0.0302 | 2.5334 | 0.1177 | 2.9874 | 0.0242 |
| 2.7355 | 0.0059 | 2.9048 | 0.0000 | 2.5681 | 0.1090 | 3.0289 | 0.0467 |
| 2.7720 | 0.0020 | 2.9445 | 0.0113 | 2.6028 | 0.0979 | 3.0704 | 0.0173 |
| 2.8084 | 0.0020 | 2.9843 | 0.0075 | 2.6375 | 0.1028 | 3.1119 | 0.0432 |
| | | 3.0241 | 0.0038 | 2.6722 | 0.1016 | 3.1534 | 0.0052 |
| | | 3.0639 | 0.0000 | | | 3.1949 | 0.0000 |

The data for the experiment in the agitated cell configuration are presented in given in Table 31.

Table 31 : RTD Data for the Agitated Cell Configuration.

| 0 l/min Air<br>3 l/min Pulp<br>500 rpm | | | | | | | |
|---|---|---|---|---|---|---|---|
| $\theta$ | E($\theta$) | $\theta$ | E($\theta$) | $\theta$ | E($\theta$) | $\theta$ | E($\theta$) |
| 0.0000 | 0.0790 | 0.7638 | 0.5780 | 1.5276 | 0.1860 | 2.2914 | 0.1252 |
| 0.0449 | 0.0817 | 0.8087 | 0.5585 | 1.5726 | 0.2484 | 2.3364 | 0.1179 |
| 0.0899 | 0.2954 | 0.8537 | 0.5310 | 1.6175 | 0.2856 | 2.3813 | 0.0836 |
| 0.1348 | 0.3953 | 0.8986 | 0.5126 | 1.6624 | 0.2688 | 2.4262 | 0.0931 |
| 0.1797 | 0.5784 | 0.9435 | 0.4943 | 1.7073 | 0.2789 | 2.4712 | 0.0621 |
| 0.2247 | 0.8646 | 0.9885 | 0.4625 | 1.7523 | 0.1980 | 2.5161 | 0.0784 |
| 0.2696 | 0.7807 | 1.0334 | 0.4543 | 1.7972 | 0.2315 | 2.5610 | 0.0542 |
| 0.3145 | 0.7867 | 1.0783 | 0.3922 | 1.8421 | 0.2245 | 2.6059 | 0.0704 |
| 0.3594 | 0.7891 | 1.1233 | 0.4310 | 1.8871 | 0.2039 | 2.6509 | 0.0471 |
| 0.4044 | 0.7871 | 1.1682 | 0.4057 | 1.9320 | 0.2039 | 2.6958 | 0.0827 |
| 0.4493 | 0.7684 | 1.2131 | 0.3937 | 1.9769 | 0.1897 | 2.7407 | 0.0347 |
| 0.4942 | 0.7522 | 1.2580 | 0.4422 | 2.0219 | 0.1825 | 2.7857 | 0.0440 |
| 0.5392 | 0.7426 | 1.3030 | 0.3860 | 2.0668 | 0.1651 | 2.8306 | 0.0307 |
| 0.5841 | 0.8045 | 1.3479 | 0.3399 | 2.1117 | 0.1545 | 2.8755 | 0.0401 |
| 0.6290 | 0.6404 | 1.3928 | 0.2801 | 2.1566 | 0.1607 | 2.9205 | 0.0328 |
| 0.6740 | 0.6221 | 1.4378 | 0.2808 | 2.2016 | 0.0792 | 2.9654 | 0.0366 |
| 0.7189 | 0.6014 | 1.4857 | 0.2308 | 2.2465 | 0.1258 | 3.0103 | 0.0217 |

The data from the experiments with the Jameson cell configuration are given in Table 32.

Table 32 : RTD Data for the Agitated Cell Configuration under Different Conditions.

| 0 l/min Air 3 l/min Pulp | | 3 l/min Air 3 l/min Pulp | | 5 l/min Air 4 l/min Pulp | | 7 l/min Air 5 l/min Pulp | |
|---|---|---|---|---|---|---|---|
| $\theta$ | E($\theta$) | $\theta$ | E($\theta$) | $\theta$ | E($\theta$) | $\theta$ | E($\theta$) |
| 0.0000 | 0.0005 | 0.0000 | 0.0049 | 0.0000 | 0.0056 | 0.0000 | 0.0000 |
| 0.1773 | 0.0005 | 0.0660 | 0.0589 | 0.0678 | 0.0075 | 0.1014 | 0.0985 |
| 0.3547 | 1.6411 | 0.1321 | 0.4223 | 0.1355 | 1.1585 | 0.2029 | 0.9960 |
| 0.5320 | 1.3631 | 0.1981 | 1.3258 | 0.2033 | 1.2218 | 0.3043 | 1.3100 |
| 0.7094 | 0.4454 | 0.2641 | 1.2325 | 0.2711 | 1.0412 | 0.4057 | 0.9923 |
| 0.8864 | 0.4606 | 0.3301 | 1.0165 | 0.3388 | 0.8325 | 0.5071 | 0.6671 |
| 1.0641 | 0.4346 | 0.3962 | 0.6973 | 0.4066 | 0.6780 | 0.6086 | 0.5537 |
| 1.2414 | 0.3558 | 0.4622 | 0.5647 | 0.4744 | 0.5867 | 0.7100 | 0.4738 |
| 1.4188 | 0.2418 | 0.5282 | 0.4518 | 0.5421 | 0.5513 | 0.8114 | 0.3939 |
| 1.5961 | 0.1752 | 0.5942 | 0.3832 | 0.6099 | 0.5141 | 0.9128 | 0.3605 |
| 1.7735 | 0.1180 | 0.6603 | 0.4125 | 0.6777 | 0.4675 | 1.0143 | 0.6178 |
| 1.9508 | 0.1361 | 0.7263 | 0.4616 | 0.7454 | 0.4638 | 1.1157 | 0.3029 |
| 2.1282 | 0.0695 | 0.7923 | 0.4714 | 0.8132 | 0.4414 | 1.2171 | 0.3601 |
| 2.3055 | 0.0504 | 0.8583 | 0.3830 | 0.8810 | 0.4098 | 1.3185 | 0.3899 |
| 2.4829 | 0.0357 | 0.9244 | 0.4223 | 0.9487 | 0.3911 | 1.4200 | 0.2620 |
| 2.6602 | 0.0225 | 0.9904 | 0.4027 | 1.0165 | 0.3800 | 1.5214 | 0.2490 |
| 2.8375 | 0.0206 | 1.0564 | 0.3879 | 1.0842 | 0.3725 | 1.6228 | 0.2137 |
| 3.0149 | 0.0166 | 1.1224 | 0.3634 | 1.1520 | 0.3576 | 1.7242 | 0.2063 |
| 3.1922 | 0.0117 | 1.1885 | 0.3388 | 1.2198 | 0.3185 | 1.8257 | 0.1988 |
| 3.3696 | 0.0103 | 1.2545 | 0.2701 | 1.2875 | 0.3185 | 1.9271 | 0.1895 |
| 3.5469 | 0.0078 | 1.3205 | 0.3486 | 1.3553 | 0.3576 | 2.0285 | 0.1821 |
| 3.7243 | 0.0078 | 1.3866 | 0.3143 | 1.4231 | 0.2906 | 2.1299 | 0.1635 |
| 3.9016 | 0.0088 | 1.4526 | 0.2848 | 1.4908 | 0.2663 | 2.2314 | 0.1542 |
| 4.0790 | 0.0078 | 1.5186 | 0.2750 | 1.5586 | 0.2291 | 2.3328 | 0.1171 |
| 4.2563 | 0.0069 | 1.5846 | 0.2701 | 1.6264 | 0.2440 | 2.4342 | 0.1134 |
| 4.4337 | 0.0039 | 1.6507 | 0.2553 | 1.6941 | 0.2291 | 2.5356 | 0.1022 |
| 4.6110 | 0.0044 | 1.7167 | 0.2259 | 1.7619 | 0.2310 | 2.6371 | 0.0966 |
| 4.7884 | 0.0044 | 1.7827 | 0.1473 | 1.8297 | 0.1695 | 2.7385 | 0.0911 |
| 4.9657 | 0.0069 | 1.8487 | 0.2112 | 1.8974 | 0.1993 | 2.8399 | 0.0948 |
| 5.1431 | 0.0049 | 1.9148 | 0.2161 | 1.9652 | 0.1769 | 2.9413 | 0.0799 |
| 5.3204 | 0.0044 | 1.9808 | 0.2062 | 2.0330 | 0.1751 | 3.0428 | 0.0762 |
| 5.4977 | 0.0044 | 2.0468 | 0.1370 | 2.1007 | 0.1546 | 3.1442 | 0.0650 |
| 5.6751 | 0.0044 | 2.1128 | 0.1768 | 2.1685 | 0.1546 | 3.2456 | 0.0520 |
| 5.8524 | 0.0044 | 2.1789 | 0.1571 | 2.2363 | 0.1397 | 3.3470 | 0.0780 |
| 6.0298 | 0.0044 | 2.2449 | 0.1277 | 2.3040 | 0.1341 | 3.4485 | 0.0427 |
| 6.2071 | 0.0039 | 2.3109 | 0.1277 | 2.3718 | 0.1173 | 3.5499 | 0.0409 |
| 6.3845 | 0.0034 | 2.3769 | 0.1375 | 2.4396 | 0.1229 | 3.6513 | 0.0334 |
| 6.5618 | 0.0044 | 2.4430 | 0.1375 | 2.5073 | 0.1099 | 3.7527 | 0.0223 |
| 6.7392 | 0.0039 | 2.5090 | 0.1228 | 2.5751 | 0.1062 | 3.8542 | 0.0279 |
| 6.9165 | 0.0059 | 2.5750 | 0.0933 | 2.6429 | 0.0969 | 3.9556 | 0.0242 |
| 7.0939 | 0.0044 | 2.6410 | 0.0982 | 2.7106 | 0.0913 | 4.0570 | 0.0000 |
| 7.2712 | 0.0069 | 2.7071 | 0.0933 | 2.7784 | 0.0875 | 4.1584 | 0.0056 |
| 7.4486 | 0.0029 | 2.7731 | 0.1326 | 2.8462 | 0.0764 | 4.2599 | 0.0093 |
| 7.6259 | 0.0069 | 2.8391 | 0.0835 | 2.9139 | 0.0671 | 4.3613 | 0.0000 |
| 7.8033 | 0.0029 | 2.9052 | 0.0737 | 2.9817 | 0.0615 | 4.4627 | 0.0000 |
| 7.9806 | 0.0034 | 2.9712 | 0.0638 | 3.0494 | 0.0540 | 4.5641 | 0.0000 |
| 8.1579 | 0.0034 | 3.0372 | 0.0540 | 3.1172 | 0.0466 | 4.6656 | 0.0000 |
| 8.3353 | 0.0064 | 3.1032 | 0.0442 | 3.1850 | 0.0410 | 4.7670 | 0.0000 |

| | | | | | | | |
|---|---|---|---|---|---|---|---|
| 8.5126 | 0.0034 | 3.1693 | 0.0442 | 3.2527 | 0.0242 | 4.8684 | 0.0000 |
| 8.6900 | 0.0034 | 3.2353 | 0.0344 | 3.3205 | 0.0317 | 4.9699 | 0.0000 |
| 8.8673 | 0.0034 | 3.3013 | 0.0246 | 3.3883 | 0.0298 | 5.0713 | 0.0000 |
| 9.0447 | 0.0039 | 3.3673 | 0.0147 | 3.4560 | 0.0224 | 5.1727 | 0.0000 |
| 9.2220 | 0.0034 | 3.4334 | 0.0196 | 3.5238 | 0.0112 | 5.2741 | 0.0000 |
| 9.3994 | 0.0024 | 3.4994 | 0.0196 | 3.5916 | 0.0130 | 5.3756 | 0.0000 |
| 9.5767 | 0.0015 | 3.5654 | 0.0098 | 3.6593 | 0.0112 | 5.4770 | 0.0111 |
| 9.7541 | 0.0069 | 3.6314 | 0.0147 | 3.7271 | 0.0075 | 5.5784 | 0.0074 |
| 9.9314 | 0.0039 | 3.6975 | 0.0147 | 3.7949 | 0.0019 | 2.6798 | 0.0019 |
| 10.1088 | 0.0015 | 3.7635 | 0.0000 | 3.8626 | 0.0000 | 5.7813 | 0.0000 |

# APPENDIX F
# BUBBLE SIZE DATA

## F1 Detailed Results from Bubble Size Calculations (After Zhou *et al.*, 1993)

The values in Table 33 were calculated from measured values of gas holdup (Table 21 on page 125) using Equations (66) to (76) in section 2.6.2.2 page 35.

Table 33 : Values of $B_c$, $B_d$ and Final Calculated Bubble Size, $b_d$ for the Different Cell Configurations.

| Collector Dosage (g/t) | -106 $\mu$m Particle Size Fraction | | | |
|---|---|---|---|---|
| | Column Configuration | | Jameson Configuration | |
| | $B_c \times 10^3$ | $d_b$ (mm) | $B_d \times 10^3$ | $d_b$ (mm) |
| 0 | 1.640 | 1.643 | 1.510 | 1.495 |
| 25 | 1.530 | 1.521 | 1.310 | 1.292 |
| 80 | 1.360 | 1.339 | 1.040 | 1.041 |
| 200 | 1.230 | 1.207 | 0.897 | 0.922 |
| 300 | 1.170 | 1.154 | | |
| 400 | 1.120 | 1.107 | | |
| 500 | 1.070 | 1.066 | | |
| Collector Dosage (g/t) | +106 -150 $\mu$m Particle Size Fraction | | | |
| | Column Configuration | | Jameson Configuration | |
| | $B_c \times 10^3$ | $d_b$ (mm) | $B_d \times 10^3$ | $d_b$ (mm) |
| 0 | 1.640 | 1.643 | 1.310 | 1.292 |
| 25 | 1.530 | 0.521 | 1.160 | 1.232 |
| 80 | 1.440 | 1.422 | 1.100 | 1.167 |
| 200 | 1.160 | 1.150 | 0.981 | 1.058 |
| 300 | 0.803 | 0.846 | | |
| 400 | 0.716 | 0.778 | | |
| 500 | 0.651 | 0.727 | | |
| Collector Dosage (g/t) | +150 -300 $\mu$m Particle Size Fraction | | | |
| | Column Configuration | | Jameson Configuration | |
| | $B_c \times 10^3$ | $d_b$ (mm) | $B_d \times 10^3$ | $d_b$ (mm) |
| 0 | 1.760 | 1.796 | 1.310 | 1.391 |
| 25 | 1.640 | 1.643 | 0.938 | 1.019 |
| 80 | 1.440 | 1.422 | 0.780 | 0.880 |
| 200 | 1.290 | 1.268 | 0.485 | 0.632 |
| Collector Dosage (g/t) | +300 $\mu$m Particle Size Fraction | | | |
| | Column Configuration | | Jameson Configuration | |
| | $B_c \times 10^3$ | $d_b$ (mm) | $B_d \times 10^3$ | $d_b$ (mm) |
| 0 | 1.900 | 1.994 | 1.510 | 1.620 |
| 25 | 1.440 | 1.422 | 1.310 | 1.391 |
| 80 | 0.915 | 0.936 | 0.935 | 1.016 |
| 200 | 0.804 | 0.847 | 0.434 | 0.589 |
| 200 disp | 1.070 | 1.068 | 0.435 | 0.589 |

The values of the calculation parameters which were not a function of gas holdup in the different cell configurations are given in Table 34.

Table 34 : Constant Parameters in the Bubble Size Calculations for the Different Cell Configurations.

| Parameter | Value |
|---|---|
| Frother Dosage | 80 g/t |
| Volume Fraction Solids | 0.0402 |
| Pulp Density | 1.066 kg/l |
| Pulp Viscosity | 0.0011 Pa.s |
| C | 0.678 cc/100 litres |
| $C_c$ | 211.97 |
| A | 10477 |

## F2 Measured Bubble Size Data

The results from measurements with the UCT bubble sizer are given in Table 35.

Table 35 : Bubble Size Measurements with the UCT Bubble Size Analyzer.

| Collector Dosage (g/t) | -106 $\mu$m Particle Size Fraction | | | | | |
|---|---|---|---|---|---|---|
| | Column Configuration | | | Jameson Configuration | | |
| | $d_b$ (mm) | Standard Deviation | Sample Column | $d_b$ (mm) | Standard Deviation | Sample Column |
| 0 | 1.543 | 0.813 | Yes | 0.962 | 0.936 | No |
| | | | | 1.041 | 0.831 | No |
| | | | | 1.252 | 0.826 | No |
| 25 | 1.573 | 0.893 | Yes | 1.168 | 0.801 | Yes |
| | | | | 1.388 | 0.714 | Yes |
| | | | | 1.484 | 0.663 | Yes |
| | | | | 1.212 | 0.762 | Yes |
| 80 | 0.823 | 0.501 | No | 0.613 | 0.517 | No |
| | | | | 1.063 | 0.488 | No |
| | | | | 1.219 | 0.581 | No |
| 200 | 1.100 | 0.648 | Yes | 0870 | 0.756 | Yes |
| 300 | 0.671 | 0.505 | No | | | |
| 400 | 0.758 | 0.514 | No | | | |
| | 0.799 | 0.444 | No | | | |
| | 0.784 | 0.436 | No | | | |
| | 1.007 | 0.518 | No | | | |
| 500 | 0.744 | 0.570 | No | | | |
| | 0.719 | 0.547 | No | | | |
| | 0.841 | 0.644 | No | | | |

# APPENDIX G
# MALVERN PARTICLE SIZE ANALYSIS RESULTS

Particle size analysis was done with a Malvern particle size analyzer. Analysis was carried out on the -106 $\mu$m particle size fraction, as well as on the flotation concentrates of the experiments in which this fraction was used as feed. The analysis of the -106 $\mu$m particle size fraction, *i.e.* the feed, is presented in Table 36. Three runs were done to test the reproducibility of the results obtained from this instrument.

Table 36 : Malvern Analysis of the -106 $\mu$m Particle Size Fraction.

| Particle Size ($\mu$m) | % Passing | | | | Particle Size ($\mu$m) | % Passing | | | |
|---|---|---|---|---|---|---|---|---|---|
| | Run 1 | Run 2 | Run 3 | Avg | | Run 1 | Run 2 | Run 2 | Avg |
| 188 | 0.0 | 0.0 | 0.0 | 0.0 | 18.4 | 1.3 | 1.4 | 1.5 | 1.4 |
| 175 | 0.0 | 0.0 | 0.0 | 0.0 | 17.1 | 1.4 | 1.5 | 1.6 | 1.5 |
| 163 | 0.1 | 0.0 | 0.1 | 0.1 | 15.9 | 1.5 | 1.7 | 1.6 | 1.6 |
| 151 | 0.3 | 0.1 | 0.3 | 0.2 | 14.8 | 1.5 | 1.7 | 1.7 | 1.6 |
| 141 | 0.6 | 0.5 | 0.6 | 0.6 | 13.7 | 1.4 | 1.6 | 1.6 | 1.5 |
| 131 | 1.0 | 1.1 | 1.0 | 1.0 | 12.8 | 1.3 | 1.4 | 1.4 | 1.4 |
| 122 | 1.5 | 1.5 | 1.4 | 1.5 | 11.9 | 1.2 | 1.2 | 1.2 | 1.2 |
| 113 | 2.0 | 2.0 | 1.9 | 2.0 | 11.1 | 1.1 | 1.1 | 1.1 | 1.1 |
| 105 | 2.6 | 2.6 | 2.5 | 2.6 | 10.3 | 1.0 | 1.0 | 1.0 | 1.0 |
| 97.8 | 3.2 | 3.3 | 3.2 | 3.2 | 9.56 | 1.0 | 0.9 | 0.9 | 0.9 |
| 90.9 | 4.0 | 4.1 | 3.9 | 4.0 | 8.89 | 0.9 | 0.8 | 0.9 | 0.9 |
| 84.5 | 4.6 | 4.7 | 4.5 | 4.6 | 8.27 | 0.9 | 0.9 | 0.9 | 0.9 |
| 78.6 | 4.9 | 5.0 | 4.8 | 4.9 | 7.69 | 0.9 | 0.9 | 0.9 | 0.9 |
| 73.1 | 5.0 | 5.1 | 4.9 | 5.0 | 7.15 | 0.9 | 0.9 | 0.9 | 0.9 |
| 68.0 | 4.7 | 4.8 | 4.6 | 4.7 | 6.65 | 0.9 | 0.9 | 0.9 | 0.9 |
| 63.2 | 4.1 | 4.1 | 4.0 | 4.1 | 6.18 | 0.8 | 0.9 | 0.9 | 0.9 |
| 58.8 | 3.1 | 3.0 | 3.0 | 3.0 | 5.75 | 0.8 | 0.8 | 0.8 | 0.8 |
| 54.7 | 2.3 | 2.0 | 2.1 | 2.1 | 5.35 | 0.7 | 0.7 | 0.8 | 0.7 |
| 50.8 | 1.9 | 1.5 | 1.7 | 1.7 | 4.97 | 0.6 | 0.6 | 0.6 | 0.6 |
| 47.3 | 1.8 | 1.4 | 1.5 | 1.6 | 4.62 | 0.5 | 0.5 | 0.5 | 0.5 |
| 44.0 | 1.8 | 1.6 | 1.7 | 1.7 | 4.30 | 0.4 | 0.4 | 0.4 | 0.4 |
| 40.9 | 2.0 | 2.0 | 2.1 | 2.0 | 4.00 | 0.3 | 0.3 | 0.3 | 0.3 |
| 38.0 | 2.3 | 2.6 | 2.6 | 2.5 | 3.72 | 0.3 | 0.3 | 0.2 | 0.3 |
| 35.4 | 2.6 | 3.1 | 3.0 | 2.9 | 3.46 | 0.2 | 0.2 | 0.2 | 0.2 |
| 32.9 | 2.7 | 3.2 | 3.1 | 3.0 | 3.21 | 0.2 | 0.2 | 0.2 | 0.2 |
| 30.6 | 2.7 | 3.0 | 2.9 | 2.9 | 2.99 | 0.2 | 0.1 | 0.2 | 0.2 |
| 28.4 | 2.5 | 2.6 | 2.5 | 2.5 | 2.78 | 0.2 | 0.2 | 0.2 | 0.2 |
| 26.4 | 2.3 | 2.1 | 2.1 | 2.2 | 2.59 | 0.3 | 0.3 | 0.3 | 0.3 |
| 24.6 | 2.0 | 1.7 | 1.8 | 1.8 | 2.40 | 0.4 | 0.4 | 0.4 | 0.4 |
| 22.9 | 1.8 | 1.5 | 1.5 | 1.6 | 2.24 | 0.5 | 0.5 | 0.5 | 0.5 |
| 21.3 | 1.5 | 1.3 | 1.4 | 1.4 | 2.08 | 0.5 | 0.5 | 0.5 | 0.5 |
| 19.8 | 1.4 | 1.3 | 1.4 | 1.4 | 1.93 | 0.4 | 0.5 | 0.5 | 0.5 |

The particle size analyses of the flotation concentrates from experiments in the column and

agitated cell configuration are presented in Table 37, in which the collector dosages used during the flotation experiments are indicated.

Table 37 : Malvern Analysis of the -106 μm Flotation Concentrates from the Column and Agitated Cell Configurations.

| Particle Size (μm) | Column Cell | | | | | | Agitated Cell | | |
|---|---|---|---|---|---|---|---|---|---|
| | % Passing | | | | | | | | |
| | 25 g/t | 80 g/t | 200 g/t | 300 g/t | 400 g/t | 500 g/t | 25 g/t | 80 g/t | 200 g/t |
| 188 | 0.2 | 0.4 | 0.0 | 0.4 | 0.3 | 0.5 | 0.0 | 0.6 | 0.7 |
| 175 | 0.2 | 0.4 | 0.0 | 0.4 | 0.4 | 0.5 | 0.0 | 0.6 | 0.7 |
| 163 | 0.2 | 0.4 | 0.2 | 0.6 | 0.6 | 0.7 | 0.0 | 0.6 | 0.7 |
| 151 | 0.2 | 0.4 | 0.5 | 0.8 | 0.8 | 0.9 | 0.0 | 0.6 | 0.7 |
| 141 | 0.2 | 0.4 | 0.8 | 1.1 | 1.1 | 1.2 | 0.0 | 0.6 | 0.7 |
| 131 | 0.2 | 0.4 | 1.2 | 1.5 | 1.5 | 1.5 | 0.0 | 0.7 | 0.7 |
| 122 | 0.2 | 0.5 | 1.7 | 2.0 | 1.9 | 1.9 | 0.0 | 0.7 | 0.8 |
| 113 | 0.2 | 0.4 | 2.3 | 2.5 | 2.4 | 2.4 | 0.0 | 0.7 | 0.7 |
| 105 | 0.2 | 0.4 | 2.9 | 3.1 | 3.0 | 3.0 | 0.0 | 0.5 | 0.5 |
| 97.8 | 0.2 | 0.5 | 3.7 | 3.8 | 3.7 | 3.6 | 0.1 | 0.8 | 0.9 |
| 90.9 | 0.4 | 0.9 | 4.5 | 4.6 | 4.4 | 4.4 | 0.3 | 1.6 | 2.1 |
| 84.5 | 0.7 | 1.7 | 5.2 | 5.2 | 5.0 | 4.9 | 0.7 | 2.3 | 2.9 |
| 78.6 | 1.2 | 2.6 | 5.5 | 5.5 | 5.3 | 5.2 | 1.3 | 3.4 | 4.3 |
| 73.1 | 1.7 | 3.4 | 5.6 | 5.5 | 5.3 | 5.2 | 1.8 | 4.9 | 6.2 |
| 68.0 | 0.9 | 3.8 | 5.4 | 5.3 | 5.1 | 4.9 | 2.1 | 5.2 | 6.5 |
| 63.2 | 2.1 | 3.8 | 4.6 | 4.4 | 4.2 | 4.1 | 2.3 | 4.9 | 5.4 |
| 58.8 | 2.2 | 3.6 | 3.4 | 3.1 | 2.9 | 2.9 | 2.3 | 4.4 | 3.8 |
| 54.7 | 2.2 | 3.2 | 2.7 | 2.5 | 2.3 | 2.2 | 2.2 | 3.7 | 3.0 |
| 50.8 | 2.3 | 2.9 | 2.2 | 2.0 | 1.8 | 1.7 | 2.1 | 2.9 | 2.5 |
| 47.3 | 2.3 | 2.7 | 2.0 | 1.7 | 1.6 | 1.5 | 2.2 | 2.3 | 2.1 |
| 44.0 | 2.5 | 2.8 | 2.1 | 1.9 | 1.7 | 1.7 | 2.3 | 2.2 | 2.2 |
| 40.9 | 2.7 | 3.2 | 2.4 | 2.2 | 2.1 | 1.9 | 2.5 | 2.4 | 2.6 |
| 38.0 | 2.9 | 3.7 | 2.8 | 2.7 | 2.5 | 2.4 | 2.9 | 2.9 | 2.9 |
| 35.4 | 3.0 | 4.1 | 3.1 | 3.1 | 2.8 | 2.7 | 3.2 | 3.3 | 3.2 |
| 32.9 | 3.2 | 4.2 | 3.1 | 3.1 | 2.9 | 2.8 | 3.4 | 3.4 | 3.2 |
| 30.6 | 3.3 | 3.9 | 2.9 | 2.9 | 2.7 | 2.6 | 3.6 | 3.4 | 3.1 |
| 28.4 | 3.4 | 3.4 | 2.5 | 2.5 | 2.4 | 2.3 | 3.6 | 3.1 | 2.8 |
| 26.4 | 3.5 | 3.0 | 2.1 | 2.0 | 2.0 | 1.9 | 3.6 | 2.8 | 2.5 |
| 24.6 | 3.6 | 2.7 | 1.7 | 1.6 | 1.6 | 1.6 | 3.5 | 2.5 | 2.2 |
| 22.9 | 3.7 | 2.7 | 1.5 | 1.4 | 1.4 | 1.4 | 3.4 | 2.2 | 1.9 |
| 21.3 | 3.7 | 2.7 | 1.3 | 1.2 | 1.2 | 1.3 | 3.3 | 2.0 | 1.7 |
| 19.8 | 3.7 | 2.7 | 1.2 | 1.2 | 1.1 | 1.2 | 3.1 | 1.9 | 1.6 |
| 18.4 | 3.5 | 2.7 | 1.2 | 1.2 | 1.2 | 1.2 | 3.1 | 1.9 | 1.6 |
| 17.1 | 3.2 | 2.5 | 1.2 | 1.2 | 1.2 | 1.3 | 3.0 | 1.9 | 1.6 |
| 15.9 | 2.9 | 2.3 | 1.3 | 1.2 | 1.3 | 1.3 | 3.0 | 1.8 | 1.6 |
| 14.8 | 2.7 | 2.1 | 1.2 | 1.2 | 1.3 | 1.3 | 2.9 | 1.8 | 1.5 |
| 13.7 | 2.6 | 1.8 | 1.1 | 1.1 | 1.2 | 1.3 | 2.7 | 1.7 | 1.4 |
| 12.8 | 2.5 | 1.6 | 1.0 | 1.0 | 1.1 | 1.2 | 2.5 | 1.5 | 1.3 |
| 11.9 | 2.4 | 1.4 | 0.9 | 0.9 | 1.0 | 1.1 | 2.3 | 1.3 | 1.2 |
| 11.1 | 2.2 | 1.2 | 0.8 | 0.8 | 0.9 | 1.0 | 2.1 | 1.2 | 1.1 |
| 10.3 | 2.0 | 1.1 | 0.7 | 0.7 | 0.8 | 0.9 | 1.9 | 1.1 | 1.0 |
| 9.56 | 1.8 | 1.1 | 0.6 | 0.6 | 0.7 | 0.8 | 1.7 | 1.0 | 0.9 |
| 8.89 | 1.6 | 1.0 | 0.6 | 0.6 | 0.7 | 0.8 | 1.5 | 0.9 | 0.8 |

| | | | | | | | | | |
|---|---|---|---|---|---|---|---|---|---|
| 8.27 | 1.5 | 1.0 | 0.6 | 0.6 | 0.7 | 0.8 | 1.4 | 0.8 | 0.8 |
| 7.69 | 1.3 | 0.9 | 0.6 | 0.6 | 0.7 | 0.8 | 1.3 | 0.8 | 0.7 |
| 7.15 | 1.2 | 0.8 | 0.6 | 0.6 | 0.7 | 0.8 | 1.3 | 0.7 | 0.7 |
| 6.65 | 1.1 | 0.8 | 0.6 | 0.5 | 0.7 | 0.8 | 1.2 | 0.7 | 0.7 |
| 6.18 | 1.1 | 0.7 | 0.6 | 0.5 | 0.7 | 0.7 | 1.1 | 0.6 | 0.6 |
| 5.75 | 1.0 | 0.6 | 0.5 | 0.5 | 0.6 | 0.7 | 1.1 | 0.6 | 0.6 |
| 5.35 | 0.9 | 0.5 | 0.5 | 0.4 | 0.6 | 0.6 | 1.0 | 0.6 | 0.6 |
| 4.97 | 0.8 | 0.5 | 0.4 | 0.4 | 0.5 | 0.5 | 0.9 | 0.5 | 0.6 |
| 4.62 | 0.7 | 0.4 | 0.3 | 0.3 | 0.4 | 0.5 | 0.8 | 0.5 | 0.5 |
| 4.30 | 0.6 | 0.4 | 0.3 | 0.3 | 0.4 | 0.4 | 0.8 | 0.4 | 0.5 |
| 4.00 | 0.4 | 0.3 | 0.2 | 0.2 | 0.3 | 0.3 | 0.7 | 0.4 | 0.4 |
| 3.72 | 0.3 | 0.2 | 0.2 | 0.2 | 0.2 | 0.2 | 0.6 | 0.4 | 0.4 |
| 3.46 | 0.2 | 0.1 | 0.1 | 0.1 | 0.2 | 0.2 | 0.5 | 0.3 | 0.4 |
| 3.21 | 0.2 | 0.1 | 0.1 | 0.1 | 0.2 | 0.2 | 0.4 | 0.3 | 0.3 |
| 2.99 | 0.2 | 0.1 | 0.1 | 0.1 | 0.2 | 0.2 | 0.4 | 0.3 | 0.3 |
| 2.78 | 0.2 | 0.1 | 0.2 | 0.1 | 0.2 | 0.2 | 0.4 | 0.3 | 0.3 |
| 2.59 | 0.3 | 0.2 | 0.2 | 0.2 | 0.3 | 0.3 | 0.4 | 0.3 | 0.4 |
| 2.40 | 0.3 | 0.2 | 0.3 | 0.3 | 0.3 | 0.4 | 0.4 | 0.3 | 0.4 |
| 2.24 | 0.3 | 0.3 | 0.3 | 0.3 | 0.4 | 0.4 | 0.4 | 0.3 | 0.4 |
| 2.08 | 0.4 | 0.3 | 0.3 | 0.3 | 0.4 | 0.4 | 0.4 | 0.3 | 0.4 |
| 1.93 | 0.3 | 0.3 | 0.3 | 0.3 | 0.4 | 0.4 | 0.4 | 0.3 | 0.3 |

The particle size analyses of the flotation concentrates from experiments in the Jameson cell configuration and the laboratory batch cell are presented in Table 38, in which the collector dosages used during the flotation experiments are indicated.

Table 38 : Malvern Analysis of the -106 μm Flotation Concentrates from the Jameson Cell Configuration and the Laboratory Batch Cell.

| | Jameson Cell | | | Laboratory Batch Cell | | |
|---|---|---|---|---|---|---|
| Particle Size (μm) | % Passing | | | | | |
| | 25 g/t | 80 g/t | 200 g/t | 25 g/t | 80 g/t | 200 g/t |
| 188 | 0.0 | 0.0 | 0.1 | 0.0 | 0.0 | 0.7 |
| 175 | 0.0 | 0.0 | 0.2 | 0.0 | 0.0 | 0.7 |
| 163 | 0.0 | 0.0 | 0.3 | 0.0 | 0.0 | 0.7 |
| 151 | 0.0 | 0.1 | 0.6 | 0.0 | 0.0 | 0.7 |
| 141 | 0.0 | 0.4 | 0.8 | 0.0 | 0.0 | 0.7 |
| 131 | 0.0 | 0.8 | 1.2 | 0.0 | 0.1 | 0.8 |
| 122 | 0.0 | 1.3 | 1.6 | 0.1 | 0.9 | 0.8 |
| 113 | 0.0 | 1.8 | 2.1 | 0.1 | 1.9 | 0.8 |
| 105 | 0.2 | 2.3 | 2.7 | 0.1 | 2.6 | 0.6 |
| 97.8 | 0.3 | 2.9 | 3.4 | 0.5 | 3.3 | 0.9 |
| 90.9 | 0.5 | 3.6 | 4.1 | 1.2 | 4.2 | 1.8 |
| 84.5 | 0.6 | 4.2 | 4.7 | 2.3 | 4.9 | 2.5 |
| 78.6 | 0.7 | 4.6 | 5.1 | 3.5 | 5.3 | 3.5 |
| 73.1 | 0.9 | 4.8 | 5.2 | 4.3 | 5.5 | 5.0 |
| 68.0 | 1.1 | 4.7 | 5.0 | 4.8 | 5.3 | 5.1 |
| 63.2 | 1.3 | 4.3 | 4.3 | 5.1 | 4.7 | 4.5 |
| 58.8 | 1.5 | 3.7 | 2.4 | 5.2 | 3.7 | 3.5 |
| 54.7 | 1.7 | 3.1 | 2.6 | 5.1 | 2.9 | 2.6 |
| 50.8 | 1.9 | 2.6 | 2.1 | 5.2 | 2.5 | 2.1 |
| 47.3 | 2.1 | 2.4 | 2.0 | 5.4 | 2.4 | 2.0 |
| 44.0 | 2.3 | 2.4 | 2.1 | 5.9 | 2.4 | 2.1 |

| | | | | | | |
|---|---|---|---|---|---|---|
| 40.9 | 2.5 | 2.7 | 2.4 | 6.4 | 2.5 | 2.3 |
| 38.0 | 2.7 | 3.1 | 2.8 | 3.4 | 2.7 | 2.6 |
| 35.4 | 2.9 | 3.5 | 3.0 | 3.7 | 2.8 | 2.9 |
| 32.9 | 3.0 | 3.5 | 3.1 | 3.9 | 2.8 | 3.0 |
| 30.6 | 3.1 | 3.3 | 2.9 | 4.0 | 2.8 | 2.9 |
| 28.4 | 3.2 | 2.9 | 2.6 | 3.9 | 2.7 | 2.7 |
| 26.4 | 3.4 | 2.5 | 2.2 | 3.9 | 2.5 | 2.5 |
| 24.6 | 3.5 | 2.2 | 1.9 | 3.7 | 2.3 | 2.3 |
| 22.9 | 3.7 | 2.0 | 1.7 | 3.5 | 2.0 | 2.1 |
| 21.3 | 3.9 | 1.9 | 1.5 | 3.3 | 1.8 | 1.9 |
| 19.8 | 3.9 | 1.8 | 1.4 | 3.1 | 1.7 | 1.8 |
| 18.4 | 3.7 | 1.7 | 1.4 | 3.0 | 1.6 | 1.8 |
| 17.1 | 3.5 | 1.7 | 1.4 | 2.9 | 1.5 | 1.8 |
| 15.9 | 3.2 | 1.7 | 1.4 | 2.9 | 1.5 | 1.9 |
| 14.8 | 3.0 | 1.6 | 1.4 | 2.7 | 1.4 | 1.8 |
| 13.7 | 2.9 | 1.4 | 1.3 | 2.5 | 1.3 | 1.7 |
| 12.8 | 2.8 | 1.2 | 1.2 | 2.3 | 1.2 | 1.6 |
| 11.9 | 2.6 | 1.1 | 1.0 | 2.1 | 1.1 | 1.4 |
| 11.1 | 2.5 | 1.0 | 0.9 | 1.8 | 1.0 | 1.3 |
| 10.3 | 2.4 | 0.9 | 0.8 | 1.6 | 0.9 | 1.2 |
| 9.56 | 2.2 | 0.8 | 0.8 | 1.5 | 0.8 | 1.1 |
| 8.89 | 2.0 | 0.7 | 0.7 | 1.3 | 0.8 | 1.0 |
| 8.27 | 1.9 | 0.7 | 0.7 | 1.2 | 0.7 | 1.0 |
| 7.69 | 1.7 | 0.6 | 0.7 | 1.1 | 0.6 | 0.9 |
| 7.15 | 1.6 | 0.6 | 0.7 | 1.0 | 0.6 | 0.9 |
| 6.65 | 1.4 | 0.6 | 0.6 | 0.9 | 0.5 | 0.9 |
| 6.18 | 1.3 | 0.5 | 0.6 | 0.9 | 0.5 | 0.8 |
| 5.75 | 1.2 | 0.5 | 0.6 | 0.8 | 0.5 | 0.8 |
| 5.35 | 1.1 | 0.4 | 0.5 | 0.8 | 0.4 | 0.7 |
| 4.97 | 1.0 | 0.4 | 0.4 | 0.7 | 0.4 | 0.7 |
| 4.62 | 0.9 | 0.3 | 0.4 | 0.6 | 0.4 | 0.7 |
| 4.30 | 0.7 | 0.2 | 0.3 | 0.5 | 0.4 | 0.6 |
| 4.00 | 0.6 | 0.2 | 0.3 | 0.5 | 0.3 | 0.6 |
| 3.72 | 0.4 | 0.1 | 0.2 | 0.4 | 0.3 | 0.5 |
| 3.46 | 0.3 | 0.1 | 0.2 | 0.4 | 0.3 | 0.5 |
| 3.21 | 0.3 | 0.1 | 0.1 | 0.3 | 0.3 | 0.4 |
| 2.99 | 0.2 | 0.1 | 0.1 | 0.3 | 0.2 | 0.4 |
| 2.78 | 0.3 | 0.1 | 0.2 | 0.3 | 0.2 | 0.4 |
| 2.59 | 0.3 | 0.2 | 0.2 | 0.3 | 0.2 | 0.4 |
| 2.40 | 0.4 | 0.2 | 0.3 | 0.3 | 0.2 | 0.4 |
| 2.24 | 0.4 | 0.3 | 0.4 | 0.3 | 0.3 | 0.4 |
| 2.08 | 0.5 | 0.3 | 0.4 | 0.3 | 0.2 | 0.4 |
| 1.93 | 0.4 | 0.3 | 0.3 | 0.3 | 0.2 | 0.3 |

# APPENDIX H
# PARTICLE COLLECTION EFFICIENCY CALCULATION PARAMETERS

The values of the parameters used during the calculation of collection efficiency, $E_K$, in the column and agitated cell configurations are given in Table 39.

Table 39 : Values of Parameters used during Calculation of Collection Efficiency.

| | Column Cell | | | | Agitated Cell | | | |
|---|---|---|---|---|---|---|---|---|
| | Collector Dosage (g/t) | | | | | | | |
| | 0 | 25 | 80 | 200 | 0 | 25 | 80 | 200 |
| $R_c$ | 0.00 | 14.17 | 43.60 | 82.69 | 0.00 | 26.93 | 66.95 | 97.38 |
| $J_g$ | 1.06 | 1.06 | 1.06 | 1.06 | 1.06 | 1.06 | 1.06 | 1.06 |
| $d_b$ | 1.643 | 1.521 | 1.339 | 1.207 | 1.643 | 1.521 | 1.339 | 1.207 |
| $N_d$ | 0.230 | 0.230 | 0.230 | 0.230 | 0.518 | 0.518 | 0.518 | 0.518 |
| $\tau$ | 4.19 | 4.19 | 4.19 | 4.19 | 3.71 | 3.71 | 3.71 | 3.71 |
| a | 1.000 | 1.070 | 1.257 | 1.770 | 1.000 | 1.308 | 2.023 | 4.277 |
| $R_{c,calc}$ | 0.00 | 14.22 | 43.60 | 82.69 | 0.00 | 26.93 | 66.92 | 97.40 |
| k | 0.0000 | 0.0376 | 0.1508 | 0.5531 | 0.0000 | 0.0925 | 0.4021 | 2.2491 |
| $E_K$ | 0.000 | 0.036 | 0.127 | 0.419 | 0.000 | 0.088 | 0.338 | 1.706 |

# APPENDIX I
# FLOTATION RESULTS

The detailed flotation results from experiments in the three hybrid cell configurations and the laboratory batch cell are presented in this Appendix. The results from the column cell configuration are given in Table 40 on page 187 to Table 62 on page 198. These Tables represent the data from the experiments with the four particle size fractions at different levels of hydrophobicity (collector dosage added). The results from the agitated cell configuration are given in Table 63 on page 199 to Table 83 on page 209. A standard agitation speed of 500 rpm have been used in all the runs with different particle size fractions at different collector dosages. In cases where other levels of agitation speed were used, it is denoted in the captions of these tables. The results from the experiments in the Jameson cell configuration are given in Table 84 on page 209 to Table 100 on page 217. The results from the laboratory batch cell are given in Table 101 on page 218 to Table 128 on page 231. The agitation speed was 1200 rpm during all experiments, unless it is described as different levels in the captions of these Tables.

Table 40 : Flotation Response of the Column Cell Configuration with the -106 $\mu$m Particle Size Fraction with No Collector Added to the Pulp.

| | | | | | | | | |
|---|---|---|---|---|---|---|---|---|
| Pulp Flow Rate | | | 3 | l/min | Water pH | | 8.16 | |
| Air Flow Rate | | | 3 | l/min | Pulp pH | | 7.66 | |
| Measured Froth Depth | | | 20 | mm | Adjusted pH | | 7.00 | |
| Decrease in Pulp Level | | | 70 | mm | Fill-up Time | | 6.5 | min |
| Sample No | Sample Interval (s) | Sample Time (s) | Sample Bottle Mass (g) | Froth + Bottle Mass (g) | Quartz + Bottle Mass (g) | Flotation Time (min) | Quartz Rec (%) | Water Rec (%) |
| 1 | 60 | 10 | 343.65 | 343.65 | 343.65 | 1.0 | 0.00 | 0.00 |
| 2 | 30 | 10 | 346.06 | 346.06 | 346.06 | 1.5 | 0.00 | 0.00 |
| 3 | 30 | 10 | 347.22 | 347.22 | 347.22 | 2.0 | 0.00 | 0.00 |
| 4 | 30 | 10 | 348.21 | 348.21 | 348.21 | 2.5 | 0.00 | 0.00 |
| 5 | 30 | 10 | 345.14 | 345.14 | 345.14 | 3.0 | 0.00 | 0.00 |
| 6 | 30 | 10 | 344.68 | 344.68 | 344.68 | 3.5 | 0.00 | 0.00 |
| 7 | 30 | 10 | 346.86 | 346.86 | 346.86 | 4.0 | 0.00 | 0.00 |
| 8 | 30 | 10 | 348.66 | 348.66 | 348.66 | 4.5 | 0.00 | 0.00 |
| 9 | 30 | 10 | 345.70 | 345.70 | 345.70 | 5.0 | 0.00 | 0.00 |
| 10 | 30 | 10 | 346.55 | 346.55 | 346.55 | 5.5 | 0.00 | 0.00 |
| 11 | 30 | 10 | 345.28 | 345.28 | 345.28 | 6.0 | 0.00 | 0.00 |
| 12 | 30 | 10 | 344.42 | 344.42 | 344.42 | 6.5 | 0.00 | 0.00 |
| Steady State Quartz Recovery | | | **0.00** | % | Air Holdup | | 3.87 | % |
| Steady State Water Recovery | | | **0.00** | % | Conditioning Time | | 11.5 | min |

Table 41 : Flotation Response of the Column Cell Configuration with the -106 μm Particle Size Fraction at a Collector Dosage of 25 g/t.

| | | | | | |
|---|---|---|---|---|---|
| Pulp Flow Rate | 3 | l/min | Water pH | 8.16 | |
| Air Flow Rate | 3 | l/min | Pulp pH | 7.15 | |
| Measured Froth Depth | 20 | mm | Adjusted pH | 7.00 | |
| Decrease in Pulp Level | 75 | mm | Fill-up Time | 7.00 | min |

| Sample No | Sample Interval (s) | Sample Time (s) | Sample Bottle Mass (g) | Froth+ Bottle Mass (g) | Quartz+ Bottle Mass (g) | Flotation Time (min) | Quartz Rec (%) | Water Rec (%) |
|---|---|---|---|---|---|---|---|---|
| 1 | 60 | 10 | 343.65 | 378.87 | 354.06 | 1.0 | 20.82 | 5.16 |
| 2 | 30 | 10 | 346.06 | 375.55 | 353.89 | 1.5 | 15.66 | 4.50 |
| 3 | 30 | 10 | 347.22 | 379.22 | 355.28 | 2.0 | 16.12 | 4.98 |
| 4 | 30 | 10 | 348.21 | 376.93 | 355.34 | 2.5 | 14.26 | 4.49 |
| 5 | 30 | 10 | 345.14 | 372.81 | 351.73 | 3.0 | 13.18 | 4.38 |
| 6 | 30 | 10 | 344.68 | 377.05 | 352.18 | 3.5 | 15.00 | 5.17 |
| 7 | 30 | 10 | 346.86 | 377.88 | 353.85 | 4.0 | 13.98 | 4.99 |
| 8 | 30 | 10 | 348.66 | 380.89 | 355.87 | 4.5 | 14.42 | 5.20 |
| 9 | 30 | 10 | 345.70 | 383.00 | 354.24 | 5.0 | 17.08 | 5.98 |
| 10 | 30 | 10 | 346.55 | 377.01 | 352.97 | 5.5 | 12.84 | 5.00 |
| 11 | 30 | 10 | 345.28 | 384.47 | 353.65 | 6.0 | 16.74 | 6.41 |
| 12 | 30 | 10 | 344.42 | 376.29 | 350.94 | 6.5 | 13.04 | 5.27 |

| | | | | | |
|---|---|---|---|---|---|
| Steady State Quartz Recovery | **14.17** | % | Air Holdup | 4.14 | % |
| Steady State Water Recovery | **4.85** | % | Conditioning Time | 12.0 | min |

Table 42 : Flotation Response of the Column Cell Configuration with the -106 μm Particle Size Fraction at a Collector Dosage of 80 g/t.

| | | | | | |
|---|---|---|---|---|---|
| Pulp Flow Rate | 3 | l/min | Water pH | 8.18 | |
| Air Flow Rate | 3 | l/min | Pulp pH | 7.83 | |
| Measured Froth Depth | 20 | mm | Adjusted pH | 7.00 | |
| Decrease in Pulp Level | 85 | mm | Fill-up Time | 7.00 | min |

| Sample No | Sample Interval (s) | Sample Time (s) | Sample Bottle Mass (g) | Froth+ Bottle Mass (g) | Quartz+ Bottle Mass (g) | Flotation Time (min) | Quartz Rec (%) | Water Rec (%) |
|---|---|---|---|---|---|---|---|---|
| 1 | 60 | 10 | 343.65 | 427.18 | 372.82 | 1.0 | 58.34 | 11.30 |
| 2 | 30 | 10 | 346.06 | 409.26 | 370.62 | 1.5 | 49.12 | 8.03 |
| 3 | 30 | 10 | 347.22 | 400.81 | 369.32 | 2.0 | 44.20 | 6.54 |
| 4 | 30 | 10 | 348.21 | 421.38 | 374.33 | 2.5 | 52.24 | 9.78 |
| 5 | 30 | 10 | 345.14 | 408.38 | 367.53 | 3.0 | 44.78 | 8.49 |
| A6 | 30 | 10 | 346.19 | 406.11 | 368.25 | 3.5 | 44.12 | 7.87 |
| 7 | 30 | 10 | 346.86 | 406.08 | 368.04 | 4.0 | 42.36 | 7.91 |
| 8 | 30 | 10 | 348.66 | 423.76 | 373.08 | 4.5 | 48.84 | 10.53 |
| 9 | 30 | 10 | 345.70 | 406.39 | 364.66 | 5.0 | 37.92 | 8.67 |
| 10 | 30 | 10 | 346.55 | 408.78 | 366.05 | 5.5 | 39.00 | 8.88 |
| 11 | 30 | 10 | 345.28 | 413.75 | 366.79 | 6.0 | 43.02 | 9.76 |
| 12 | 30 | 10 | 344.42 | 396.79 | 362.67 | 6.5 | 36.50 | 7.09 |

| | | | | | |
|---|---|---|---|---|---|
| Steady State Quartz Recovery | **43.60** | % | Air Holdup | 4.70 | % |
| Steady State Water Recovery | **8.69** | % | Conditioning Time | 12.0 | min |

Table 43 : Flotation Response of the Column Cell Configuration with the -106 μm Particle Size Fraction at a Collector Dosage of 200 g/t.

| | | | | | | | |
|---|---|---|---|---|---|---|---|
| Pulp Flow Rate | 3 | l/min | Water pH | 8.16 | | | |
| Air Flow Rate | 3 | l/min | Pulp pH | 7.78 | | | |
| Measured Froth Depth | 20 | mm | Adjusted pH | 7.00 | | | |
| Decrease in Pulp Level | 95 | mm | Fill-up Time | 7.00 | min | | |

| Sample No | Sample Interval (s) | Sample Time (s) | Sample Bottle Mass (g) | Froth+ Bottle Mass (g) | Quartz+ Bottle Mass (g) | Flotation Time (min) | Quartz Rec (%) | Water Rec (%) |
|---|---|---|---|---|---|---|---|---|
| A1 | 60 | 10 | 347.94 | 492.68 | 406.55 | 1.0 | 117.22 | 17.90 |
| A2 | 30 | 10 | 346.96 | 493.72 | 404.52 | 1.5 | 115.12 | 18.54 |
| A3 | 30 | 10 | 346.52 | 499.38 | 404.41 | 2.0 | 115.78 | 19.74 |
| A4 | 30 | 10 | 347.58 | 504.21 | 404.82 | 2.5 | 114.48 | 20.66 |
| A5 | 30 | 10 | 344.77 | 480.41 | 694.52 | 3.0 | 99.50 | 17.85 |
| A6 | 30 | 10 | 346.19 | 498.76 | 398.65 | 3.5 | 104.92 | 20.81 |
| A7 | 30 | 10 | 342.09 | 485.85 | 391.22 | 4.0 | 98.26 | 16.67 |
| A8 | 30 | 10 | 340.84 | 486.80 | 389.72 | 4.5 | 97.76 | 20.18 |
| A9 | 30 | 10 | 341.88 | 466.07 | 383.28 | 5.0 | 82.80 | 17.21 |
| A10 | 30 | 10 | 344.19 | 475.70 | 387.79 | 5.5 | 87.20 | 18.27 |
| A11 | 30 | 10 | 343.79 | 478.49 | 387.64 | 6.0 | 87.70 | 18.88 |
| A12 | 30 | 10 | 341.49 | 459.00 | 378.03 | 6.5 | 73.08 | 16.83 |

| | | | | | |
|---|---|---|---|---|---|
| Steady State Quartz Recovery | **82.69** | % | Air Holdup | 5.25 | % |
| Steady State Water Recovery | **17.80** | % | Conditioning Time | 12.0 | min |

Table 44 : Flotation Response of the Column Cell Configuration with the -106 μm Particle Size Fraction at a Collector Dosage of 300 g/t.

| | | | | | | | |
|---|---|---|---|---|---|---|---|
| Pulp Flow Rate | 3 | l/min | Water pH | 8.18 | | | |
| Air Flow Rate | 3 | l/min | Pulp pH | 7.86 | | | |
| Measured Froth Depth | 20 | mm | Adjusted pH | 7.00 | | | |
| Decrease in Pulp Level | 100 | mm | Fill-up Time | 7.00 | min | | |

| Sample No | Sample Interval (s) | Sample Time (s) | Sample Bottle Mass (g) | Froth+ Bottle Mass (g) | Quartz+ Bottle Mass (g) | Flotation Time (min) | Quartz Rec (%) | Water Rec (%) |
|---|---|---|---|---|---|---|---|---|
| A1 | 60 | 10 | 347.94 | 500.44 | 413.16 | 1.0 | 130.44 | 18314 |
| A2 | 30 | 10 | 346.96 | 496.47 | 408.99 | 1.5 | 124.06 | 18.18 |
| A3 | 30 | 10 | 346.52 | 498.80 | 407.46 | 2.0 | 121.88 | 18.98 |
| A4 | 30 | 10 | 347.58 | 497.25 | 406.88 | 2.5 | 118.60 | 18.78 |
| A5 | 30 | 10 | 344.77 | 493.00 | 400.60 | 3.0 | 111.66 | 19.20 |
| Beaker | 30 | 10 | 124.45 | 271.82 | 178.65 | 3.5 | 108.40 | 19.36 |
| A7 | 30 | 10 | 342.09 | 487.42 | 393.72 | 4.0 | 103.26 | 19.47 |
| A8 | 30 | 10 | 340.84 | 483.36 | 391.54 | 4.5 | 101.40 | 19.08 |
| A9 | 30 | 10 | 341.88 | 473.49 | 385.43 | 5.0 | 87.10 | 18.30 |
| A10 | 30 | 10 | 344.19 | 467.80 | 387.82 | 5.5 | 87.26 | 16.62 |
| A11 | 30 | 10 | 343.79 | 480.21 | 388.52 | 6.0 | 89.46 | 19.06 |
| A12 | 30 | 10 | 341.49 | 470.19 | 382.93 | 6.5 | 82.88 | 18.14 |

| | | | | | |
|---|---|---|---|---|---|
| Steady State Quartz Recovery | **87.94** | % | Air Holdup | 5.52 | % |
| Steady State Water Recovery | **19.28** | % | Conditioning Time | 12.0 | min |

Table 45 : Flotation Response of the Column Cell Configuration with the -106 μm Particle Size Fraction at a Collector Dosage of 400 g/t.

| | | | | | | | | |
|---|---|---|---|---|---|---|---|---|
| Pulp Flow Rate | | | 3 | l/min | Water pH | | 8.18 | |
| Air Flow Rate | | | 3 | l/min | Pulp pH | | 7.91 | |
| Measured Froth Depth | | | 20 | mm | Adjusted pH | | 7.00 | |
| Decrease in Pulp Level | | | 105 | mm | Fill-up Time | | 7.00 | min |
| Sample No | Sample Interval (s) | Sample Time (s) | Sample Bottle Mass (g) | Froth + Bottle Mass (g) | Quartz + Bottle Mass (g) | Flotation Time (min) | Quartz Rec (%) | Water Rec (%) |
| 1 | 60 | 10 | 343.65 | 501.30 | 405.59 | 1.0 | 123.88 | 19.89 |
| 2 | 30 | 10 | 346.06 | 497.58 | 404.32 | 1.5 | 116.52 | 19.38 |
| 3 | 30 | 10 | 347.22 | 483.09 | 395.73 | 2.0 | 138.60 | 25.94 |
| 4 | 30 | 10 | 348.21 | 475.20 | 393.04 | 2.5 | 128.09 | 24.39 |
| 5 | 30 | 10 | 345.14 | 475.30 | 388.97 | 3.0 | 125.23 | 25.63 |
| A6 | 30 | 10 | 346.19 | 475.21 | 386.77 | 3.5 | 115.94 | 26.26 |
| 7 | 30 | 10 | 346.86 | 480.71 | 386.76 | 4.0 | 114.00 | 27.90 |
| 8 | 30 | 10 | 348.66 | 472.87 | 384.59 | 4.5 | 102.66 | 26.21 |
| 9 | 30 | 10 | 345.70 | 466.65 | 380.46 | 5.0 | 99.31 | 25.59 |
| 10 | 30 | 10 | 346.55 | 467.14 | 380.23 | 5.5 | 96.23 | 25.81 |
| 11 | 30 | 10 | 345.28 | 456.10 | 376.92 | 6.0 | 90.40 | 23.51 |
| 12 | 30 | 10 | 344.42 | 462.35 | 377.43 | 6.5 | 94.31 | 25.21 |
| Steady State Quartz Recovery | | | **92.36** | % | Air Holdup | | 5.80 | % |
| Steady State Water Recovery | | | **24.36** | % | Conditioning Time | | 12.0 | min |

Table 46 : Flotation Response of the Column Cell Configuration with the -106 μm Particle Size Fraction at a Collector Dosage of 500 g/t.

| | | | | | | | | |
|---|---|---|---|---|---|---|---|---|
| Pulp Flow Rate | | | 3 | l/min | Water pH | | 8.18 | |
| Air Flow Rate | | | 3 | l/min | Pulp pH | | 7.93 | |
| Measured Froth Depth | | | 20 | mm | Adjusted pH | | 7.00 | |
| Decrease in Pulp Level | | | 110 | mm | Fill-up Time | | 7.00 | min |
| Sample No | Sample Interval (s) | Sample Time (s) | Sample Bottle Mass (g) | Froth + Bottle Mass (g) | Quartz + Bottle Mass (g) | Flotation Time (min) | Quartz Rec (%) | Water Rec (%) |
| A1 | 60 | 7 | 347.94 | 482.84 | 400.93 | 1.0 | 151.40 | 24.32 |
| A2 | 30 | 7 | 346.96 | 485.48 | 398.09 | 1.5 | 146.06 | 25.95 |
| A3 | 30 | 7 | 346.52 | 471.67 | 392.05 | 2.0 | 130.09 | 23.64 |
| A4 | 30 | 7 | 347.58 | 479.04 | 394.39 | 2.5 | 133.74 | 25.13 |
| A5 | 30 | 7 | 344.77 | 475.75 | 387.87 | 3.0 | 123.14 | 26.09 |
| Beaker | 30 | 7 | 124.45 | 246.46 | 164.84 | 3.5 | 115.40 | 24.23 |
| A7 | 30 | 7 | 342.09 | 474.91 | 382.68 | 4.0 | 115.97 | 27.38 |
| A8 | 30 | 7 | 340.84 | 483.34 | 383.46 | 4.5 | 121.77 | 29.66 |
| A9 | 30 | 7 | 341.88 | 477.93 | 380.92 | 5.0 | 111.54 | 28.80 |
| A10 | 30 | 7 | 344.19 | 468.26 | 382.46 | 5.5 | 109.34 | 25.48 |
| A11 | 30 | 7 | 343.79 | 463.54 | 377.72 | 6.0 | 96.94 | 25.48 |
| A12 | 30 | 7 | 341.49 | 465.52 | 374.74 | 6.5 | 95.00 | 26.95 |
| Steady State Quartz Recovery | | | **95.97** | % | Air Holdup | | 6.08 | % |
| Steady State Water Recovery | | | **26.22** | % | Conditioning Time | | 12.0 | min |

Table 47 : Flotation Response of the Column Cell Configuration with the +106 -150 μm Particle Size Fraction with No Collector Added to the Pulp.

| | | | | | | | |
|---|---|---|---|---|---|---|---|
| Pulp Flow Rate | 3 | l/min | Water pH | 8.63 | | | |
| Air Flow Rate | 3 | l/min | Pulp pH | 8.28 | | | |
| Measured Froth Depth | 20 | mm | Adjusted pH | 7.00 | | | |
| Decrease in Pulp Level | 70 | mm | Fill-up Time | 12.00 | min | | |

| Sample No | Sample Interval (s) | Sample Time (s) | Sample Bottle Mass (g) | Froth+ Bottle Mass (g) | Quartz+ Bottle Mass (g) | Flotation Time (min) | Quartz Rec (%) | Water Rec (%) |
|---|---|---|---|---|---|---|---|---|
| A1 | 60 | 10 | 347.94 | 347.94 | 347.94 | 1.0 | 0.00 | 0.00 |
| A2 | 30 | 10 | 346.96 | 346.96 | 346.96 | 1.5 | 0.00 | 0.00 |
| A3 | 30 | 10 | 346.52 | 346.52 | 346.52 | 2.0 | 0.00 | 0.00 |
| A4 | 30 | 10 | 347.58 | 347.58 | 347.58 | 2.5 | 0.00 | 0.00 |
| A5 | 30 | 10 | 344.77 | 344.77 | 344.77 | 3.0 | 0.00 | 0.00 |
| A6 | 30 | 10 | 346.19 | 346.19 | 346.19 | 3.5 | 0.00 | 0.00 |
| A7 | 30 | 10 | 342.09 | 342.09 | 342.09 | 4.0 | 0.00 | 0.00 |
| A8 | 30 | 10 | 340.84 | 340.84 | 340.84 | 4.5 | 0.00 | 0.00 |
| A9 | 30 | 10 | 341.88 | 341.88 | 341.88 | 5.0 | 0.00 | 0.00 |
| A10 | 30 | 10 | 344.19 | 344.19 | 344.19 | 5.5 | 0.00 | 0.00 |
| A11 | 30 | 10 | 343.79 | 343.79 | 343.79 | 6.0 | 0.00 | 0.00 |
| A12 | 30 | 10 | 341.49 | 341.49 | 341.49 | 6.5 | 0.00 | 0.00 |

| | | | | | |
|---|---|---|---|---|---|
| Steady State Quartz Recovery | **0.00** | % | Air Holdup | 3.87 | % |
| Steady State Water Recovery | **0.00** | % | Conditioning Time | 17.0 | min |

Table 48 : Flotation Response of the Column Cell Configuration with the +106 -150 μm Particle Size Fraction at a Collector Dosage of 25 g/t.

| | | | | | | | |
|---|---|---|---|---|---|---|---|
| Pulp Flow Rate | 3 | l/min | Water pH | 9.18 | | | |
| Air Flow Rate | 3 | l/min | Pulp pH | 8.28 | | | |
| Measured Froth Depth | 20 | mm | Adjusted pH | 7.00 | | | |
| Decrease in Pulp Level | 75 | mm | Fill-up Time | 10.50 | min | | |

| Sample No | Sample Interval (s) | Sample Time (s) | Sample Bottle Mass (g) | Froth+ Bottle Mass (g) | Quartz+ Bottle Mass (g) | Flotation Time (min) | Quartz Rec (%) | Water Rec (%) |
|---|---|---|---|---|---|---|---|---|
| 1 | 60 | 10 | 343.69 | 343.69 | 343.69 | 1.0 | 0.00 | 0.00 |
| 2 | 30 | 10 | 347.88 | 347.88 | 347.88 | 1.5 | 0.00 | 0.00 |
| 3 | 30 | 10 | 347.25 | 347.25 | 347.25 | 2.0 | 0.00 | 0.00 |
| 4 | 30 | 10 | 348.24 | 348.24 | 348.24 | 2.5 | 0.00 | 0.00 |
| 5 | 30 | 10 | 345.18 | 345.18 | 345.18 | 3.0 | 0.00 | 0.00 |
| 6 | 30 | 10 | 344.70 | 344.70 | 344.70 | 3.5 | 0.00 | 0.00 |
| 7 | 30 | 10 | 346.88 | 346.88 | 346.88 | 4.0 | 0.00 | 0.00 |
| 8 | 30 | 10 | 348.72 | 348.72 | 348.72 | 4.5 | 0.00 | 0.00 |
| 9 | 30 | 10 | 345.71 | 345.71 | 345.71 | 5.0 | 0.00 | 0.00 |
| 10 | 30 | 10 | 346.57 | 346.57 | 346.57 | 5.5 | 0.00 | 0.00 |
| 11 | 30 | 10 | 345.31 | 345.31 | 345.31 | 6.0 | 0.00 | 0.00 |
| 12 | 30 | 10 | 344.44 | 344.44 | 344.44 | 6.5 | 0.00 | 0.00 |

| | | | | | |
|---|---|---|---|---|---|
| Steady State Quartz Recovery | **0.00** | % | Air Holdup | 4.14 | % |
| Steady State Water Recovery | **0.00** | % | Conditioning Time | 15.5 | min |

Table 49 : Flotation Response of the Column Cell Configuration with the +106 -150 μm Particle Size Fraction at a Collector Dosage of 80 g/t.

| | | | | | | | |
|---|---|---|---|---|---|---|---|
| Pulp Flow Rate | 3 | l/min | Water pH | 9.18 | | | |
| Air Flow Rate | 3 | l/min | Pulp pH | 8.02 | | | |
| Measured Froth Depth | 20 | mm | Adjusted pH | 7.00 | | | |
| Decrease in Pulp Level | 80 | mm | Fill-up Time | 12.50 | min | | |

| Sample No | Sample Interval (s) | Sample Time (s) | Sample Bottle Mass (g) | Froth+ Bottle Mass (g) | Quartz+ Bottle Mass (g) | Flotation Time (min) | Quartz Rec (%) | Water Rec (%) |
|---|---|---|---|---|---|---|---|---|
| 1 | 60 | 10 | 343.69 | 362.68 | 353.59 | 1.0 | 19.80 | 1.89 |
| 2 | 30 | 10 | 347.88 | 365.67 | 357.08 | 1.5 | 18.40 | 1.79 |
| 3 | 30 | 10 | 347.25 | 360.54 | 354.41 | 2.0 | 14.32 | 1.27 |
| 4 | 30 | 10 | 348.24 | 360.47 | 354.75 | 2.5 | 13.02 | 1.19 |
| 5 | 30 | 10 | 345.18 | 359.43 | 352.76 | 3.0 | 15.16 | 1.39 |
| 6 | 30 | 10 | 344.70 | 354.39 | 349.80 | 3.5 | 10.20 | 0.95 |
| 7 | 30 | 10 | 346.88 | 360.06 | 353.51 | 4.0 | 13.26 | 1.36 |
| 8 | 30 | 10 | 348.72 | 359.85 | 354.46 | 4.5 | 11.48 | 1.12 |
| 9 | 30 | 10 | 345.71 | 359.40 | 351.99 | 5.0 | 12.56 | 1.54 |
| 10 | 30 | 10 | 346.57 | 356.13 | 351.02 | 5.5 | 8.90 | 1.06 |
| 11 | 30 | 10 | 345.31 | 359.57 | 352.10 | 6.0 | 13.58 | 1.55 |
| 12 | 30 | 10 | 344.44 | 351.73 | 347.82 | 6.5 | 6.76 | 0.81 |

| | | | | | |
|---|---|---|---|---|---|
| Steady State Quartz Recovery | **12.61** | % | Air Holdup | 4.42 | % |
| Steady State Water Recovery | **1.26** | % | Conditioning Time | 17.5 | min |

Table 50 : Flotation Response of the Column Cell Configuration with the +106 -150 μm Particle Size Fraction at a Collector Dosage of 200 g/t.

| | | | | | | | |
|---|---|---|---|---|---|---|---|
| Pulp Flow Rate | 3 | l/min | Water pH | 9.15 | | | |
| Air Flow Rate | 3 | l/min | Pulp pH | 8.16 | | | |
| Measured Froth Depth | 20 | mm | Adjusted pH | 7.00 | | | |
| Decrease in Pulp Level | 100 | mm | Fill-up Time | 10.50 | min | | |

| Sample No | Sample Interval (s) | Sample Time (s) | Sample Bottle Mass (g) | Froth+ Bottle Mass (g) | Quartz+ Bottle Mass (g) | Flotation Time (min) | Quartz Rec (%) | Water Rec (%) |
|---|---|---|---|---|---|---|---|---|
| 1 | 60 | 10 | 343.69 | 440.84 | 391.07 | 1.0 | 94.76 | 10.34 |
| 2 | 30 | 10 | 347.88 | 412.10 | 382.21 | 1.5 | 68.66 | 6.21 |
| 3 | 30 | 10 | 347.25 | 413.77 | 380.75 | 2.0 | 67.00 | 6.79 |
| 4 | 30 | 10 | 348.24 | 408.77 | 377.96 | 2.5 | 59.44 | 6.40 |
| 5 | 30 | 10 | 345.18 | 404.61 | 375.13 | 3.0 | 59.90 | 6.13 |
| 6 | 30 | 10 | 344.70 | 408.63 | 376.54 | 3.5 | 63.68 | 6.67 |
| 7 | 30 | 10 | 346.88 | 404.98 | 375.76 | 4.0 | 57.76 | 6.07 |
| 8 | 30 | 10 | 348.72 | 412.41 | 380.13 | 4.5 | 62.82 | 6.71 |
| 9 | 30 | 10 | 345.71 | 400.88 | 372.33 | 5.0 | 53.24 | 5.93 |
| 10 | 30 | 10 | 346.57 | 402.71 | 373.93 | 5.5 | 54.72 | 5.98 |
| 11 | 30 | 10 | 345.31 | 397.38 | 370.97 | 6.0 | 51.32 | 5.49 |
| 12 | 30 | 10 | 344.44 | 416.44 | 378.56 | 6.5 | 68.24 | 7.87 |

| | | | | | |
|---|---|---|---|---|---|
| Steady State Quartz Recovery | **60.72** | % | Air Holdup | 5.54 | % |
| Steady State Water Recovery | **6.40** | % | Conditioning Time | 15.5 | min |

Table 51 : Flotation Response of the Column Cell Configuration with the +106 -150 μm Particle Size Fraction at a Collector Dosage of 300 g/t.

| | | | | | | | |
|---|---|---|---|---|---|---|---|
| Pulp Flow Rate | 3 | l/min | Water pH | 9.18 | | | |
| Air Flow Rate | 3 | l/min | Pulp pH | 8.28 | | | |
| Measured Froth Depth | 20 | mm | Adjusted pH | 7.00 | | | |
| Decrease in Pulp Level | 150 | mm | Fill-up Time | 9.50 | min | | |

| Sample No | Sample Interval (s) | Sample Time (s) | Sample Bottle Mass (g) | Froth+ Bottle Mass (g) | Quartz+ Bottle Mass (g) | Flotation Time (min) | Quartz Rec (%) | Water Rec (%) |
|---|---|---|---|---|---|---|---|---|
| 1 | 60 | 10 | 343.69 | 425.28 | 383.83 | 1.0 | 80.28 | 8.62 |
| 2 | 30 | 10 | 347.88 | 442.23 | 391.34 | 1.5 | 86.92 | 10.58 |
| 3 | 30 | 10 | 347.25 | 425.08 | 384.98 | 2.0 | 75.46 | 8.33 |
| 4 | 30 | 10 | 348.24 | 432.48 | 387.83 | 2.5 | 79.18 | 9.28 |
| 5 | 30 | 10 | 345.18 | 434.88 | 386.16 | 3.0 | 81.96 | 10.13 |
| 6 | 30 | 10 | 344.70 | 435.83 | 387.45 | 3.5 | 85.50 | 10.06 |
| 7 | 30 | 10 | 346.88 | 435.57 | 389.26 | 4.0 | 84.76 | 9.63 |
| 8 | 30 | 10 | 348.72 | 450.98 | 397.57 | 4.5 | 97.70 | 11.10 |
| 9 | 30 | 10 | 345.71 | 440.59 | 389.77 | 5.0 | 88.12 | 10.56 |
| 10 | 30 | 10 | 346.57 | 438.00 | 390.22 | 5.5 | 87.30 | 9.93 |
| 11 | 30 | 10 | 345.31 | 449.43 | 393.76 | 6.0 | 96.90 | 11.57 |
| 12 | 30 | 10 | 344.44 | 445.76 | 391.14 | 6.5 | 93.40 | 11.35 |

| | | | | | |
|---|---|---|---|---|---|
| Steady State Quartz Recovery | **82.01** | % | Air Holdup | 8.30 | % |
| Steady State Water Recovery | **9.52** | % | Conditioning Time | 14.5 | min |

Table 52 : Flotation Response of the Column Cell Configuration with the +106 -150 μm Particle Size Fraction at a Collector Dosage of 400 g/t.

| | | | | | | | |
|---|---|---|---|---|---|---|---|
| Pulp Flow Rate | 3 | l/min | Water pH | 8.16 | | | |
| Air Flow Rate | 3 | l/min | Pulp pH | 7.09 | | | |
| Measured Froth Depth | 27 | mm | Adjusted pH | 7.00 | | | |
| Decrease in Pulp Level | 170 | mm | Fill-up Time | 7.50 | min | | |

| Sample No | Sample Interval (s) | Sample Time (s) | Sample Bottle Mass (g) | Froth+ Bottle Mass (g) | Quartz+ Bottle Mass (g) | Flotation Time (min) | Quartz Rec (%) | Water Rec (%) |
|---|---|---|---|---|---|---|---|---|
| A1 | 60 | 10 | 347.94 | 420.10 | 382.76 | 1.0 | 69.64 | 7.76 |
| A2 | 30 | 10 | 346.96 | 417.07 | 382.14 | 1.5 | 70.36 | 7.26 |
| A3 | 30 | 10 | 346.52 | 434.22 | 385.87 | 2.0 | 78.70 | 10.05 |
| A4 | 30 | 10 | 347.58 | 420.81 | 383.62 | 2.5 | 72.08 | 7.73 |
| A5 | 30 | 10 | 344.77 | 421.17 | 382.68 | 3.0 | 75.82 | 8.00 |
| A6 | 30 | 10 | 346.19 | 418.89 | 380.54 | 3.5 | 68.70 | 7.97 |
| A7 | 30 | 10 | 342.09 | 419.75 | 377.65 | 4.0 | 71.12 | 8.75 |
| A8 | 30 | 10 | 340.84 | 417.35 | 374.82 | 4.5 | 67.96 | 8.84 |
| A9 | 30 | 10 | 341.88 | 425.21 | 376.33 | 5.0 | 68.90 | 10.16 |
| A10 | 30 | 10 | 344.19 | 435.39 | 379.29 | 5.5 | 70.20 | 11.66 |
| A11 | 30 | 10 | 343.79 | 433.30 | 377.83 | 6.0 | 68.08 | 11.53 |
| A12 | 30 | 10 | 341.49 | 443.83 | 377.19 | 6.5 | 71.40 | 13.85 |

| | | | | | |
|---|---|---|---|---|---|
| Steady State Quartz Recovery | **69.16** | % | Air Holdup | 9.43 | % |
| Steady State Water Recovery | **9.82** | % | Conditioning Time | 12.5 | min |

Table 53 : Flotation Response of the Column Cell Configuration with the +106 -150 μm Particle Size Fraction at a Collector Dosage of 500 g/t.

| | | | | | | | |
|---|---|---|---|---|---|---|---|
| Pulp Flow Rate | 3 | l/min | Water pH | 8.23 | | | |
| Air Flow Rate | 3 | l/min | Pulp pH | 7.36 | | | |
| Measured Froth Depth | 20 | mm | Adjusted pH | 7.00 | | | |
| Decrease in Pulp Level | 190 | mm | Fill-up Time | 7.25 | min | | |

| Sample No | Sample Interval (s) | Sample Time (s) | Sample Bottle Mass (g) | Froth + Bottle Mass (g) | Quartz + Bottle Mass (g) | Flotation Time (min) | Quartz Rec (%) | Water Rec (%) |
|---|---|---|---|---|---|---|---|---|
| 1 | 60 | 10 | 343.65 | 396.35 | 369.70 | 1.0 | 52.10 | 5.54 |
| 2 | 30 | 10 | 346.06 | 402.10 | 370.65 | 1.5 | 49.18 | 6.54 |
| 3 | 30 | 10 | 347.22 | 398.30 | 371.39 | 2.0 | 48.34 | 5.59 |
| 4 | 30 | 10 | 348.21 | 406.44 | 373.65 | 2.5 | 50.88 | 6.82 |
| 5 | 30 | 10 | 345.14 | 398.64 | 370.40 | 3.0 | 50.52 | 5.87 |
| 6 | 30 | 10 | 344.68 | 404.38 | 371.32 | 3.5 | 53.28 | 6.87 |
| 7 | 30 | 10 | 346.86 | 411.58 | 375.75 | 4.0 | 57.74 | 7.45 |
| 8 | 30 | 10 | 348.66 | 419.98 | 378.82 | 4.5 | 60.32 | 8.55 |
| 9 | 30 | 10 | 345.70 | 417.76 | 377.39 | 5.0 | 63.38 | 8.39 |
| 10 | 30 | 10 | 346.55 | 415.74 | 373.23 | 5.5 | 53.36 | 8.84 |
| 11 | 30 | 10 | 345.28 | 420.51 | 370.49 | 6.0 | 50.42 | 10.40 |
| 12 | 30 | 10 | 344.42 | 411.97 | 365.84 | 6.5 | 42.84 | 9.59 |

| | | | | | |
|---|---|---|---|---|---|
| Steady State Quartz Recovery | **50.20** | % | Air Holdup | 10.50 | % |
| Steady State Water Recovery | **6.07** | % | Conditioning Time | 12.3 | min |

Table 54 : Flotation Response of the Column Cell Configuration with the +150 -300 μm Particle Size Fraction with No Collector Added to the Pulp.

| | | | | | | | |
|---|---|---|---|---|---|---|---|
| Pulp Flow Rate | 3 | l/min | Water pH | 8.22 | | | |
| Air Flow Rate | 3 | l/min | Pulp pH | 8.14 | | | |
| Measured Froth Depth | 20 | mm | Adjusted pH | 7.00 | | | |
| Decrease in Pulp Level | 65 | mm | Fill-up Time | 7.00 | min | | |

| Sample No | Sample Interval (s) | Sample Time (s) | Sample Bottle Mass (g) | Froth + Bottle Mass (g) | Quartz + Bottle Mass (g) | Flotation Time (min) | Quartz Rec (%) | Water Rec (%) |
|---|---|---|---|---|---|---|---|---|
| 1 | 60 | 10 | 343.65 | 343.65 | 343.65 | 1.0 | 0.00 | 0.00 |
| 2 | 30 | 10 | 346.06 | 346.06 | 346.06 | 1.5 | 0.00 | 0.00 |
| 3 | 30 | 10 | 347.22 | 347.22 | 347.22 | 2.0 | 0.00 | 0.00 |
| 4 | 30 | 10 | 348.21 | 348.21 | 348.21 | 2.5 | 0.00 | 0.00 |
| 5 | 30 | 10 | 345.14 | 345.14 | 345.14 | 3.0 | 0.00 | 0.00 |
| 6 | 30 | 10 | 344.68 | 344.68 | 344.68 | 3.5 | 0.00 | 0.00 |
| 7 | 30 | 10 | 346.86 | 346.86 | 346.86 | 4.0 | 0.00 | 0.00 |
| 8 | 30 | 10 | 348.66 | 348.66 | 348.66 | 4.5 | 0.00 | 0.00 |
| 9 | 30 | 10 | 345.70 | 345.70 | 345.70 | 5.0 | 0.00 | 0.00 |
| 10 | 30 | 10 | 346.55 | 346.55 | 346.55 | 5.5 | 0.00 | 0.00 |
| 11 | 30 | 10 | 345.28 | 345.28 | 345.28 | 6.0 | 0.00 | 0.00 |
| 12 | 30 | 10 | 344.42 | 344.42 | 344.42 | 6.5 | 0.00 | 0.00 |

| | | | | | |
|---|---|---|---|---|---|
| Steady State Quartz Recovery | **0.00** | % | Air Holdup | 3.59 | % |
| Steady State Water Recovery | **0.00** | % | Conditioning Time | 12.0 | min |

Table 55 : Flotation Response of the Column Cell Configuration with the +150 -300 μm Particle Size Fraction at a Collector Dosage of 25 g/t.

| | | | | | | | | |
|---|---|---|---|---|---|---|---|---|
| Pulp Flow Rate | | | 3 | l/min | Water pH | | 8.22 | |
| Air Flow Rate | | | 3 | l/min | Pulp pH | | 8.18 | |
| Measured Froth Depth | | | 20 | mm | Adjusted pH | | 7.00 | |
| Decrease in Pulp Level | | | 70 | mm | Fill-up Time | | 6.50 | min |
| Sample No | Sample Interval (s) | Sample Time (s) | Sample Bottle Mass (g) | Froth + Bottle Mass (g) | Quartz + Bottle Mass (g) | Flotation Time (min) | Quartz Rec (%) | Water Rec (%) |
| 1 | 60 | 10 | 343.65 | 343.65 | 343.65 | 1.0 | 0.00 | 0.00 |
| 2 | 30 | 10 | 346.06 | 346.06 | 346.06 | 1.5 | 0.00 | 0.00 |
| 3 | 30 | 10 | 347.22 | 347.22 | 347.22 | 2.0 | 0.00 | 0.00 |
| 4 | 30 | 10 | 348.21 | 348.21 | 348.21 | 2.5 | 0.00 | 0.00 |
| 5 | 30 | 10 | 345.14 | 345.14 | 345.14 | 3.0 | 0.00 | 0.00 |
| 6 | 30 | 10 | 344.68 | 344.68 | 344.68 | 3.5 | 0.00 | 0.00 |
| 7 | 30 | 10 | 346.86 | 346.86 | 346.86 | 4.0 | 0.00 | 0.00 |
| 8 | 30 | 10 | 348.66 | 348.66 | 348.66 | 4.5 | 0.00 | 0.00 |
| 9 | 30 | 10 | 345.70 | 345.70 | 345.70 | 5.0 | 0.00 | 0.00 |
| 10 | 30 | 10 | 346.55 | 346.55 | 346.55 | 5.5 | 0.00 | 0.00 |
| 11 | 30 | 10 | 345.28 | 345.28 | 345.28 | 6.0 | 0.00 | 0.00 |
| 12 | 30 | 10 | 344.42 | 344.42 | 344.42 | 6.5 | 0.00 | 0.00 |
| Steady State Quartz Recovery | | | **0.00** | % | Air Holdup | | 3.87 | % |
| Steady State Water Recovery | | | **0.00** | % | Conditioning Time | | 11.5 | min |

Table 56 : Flotation Response of the Column Cell Configuration with the +150 -300 μm Particle Size Fraction at a Collector Dosage of 80 g/t.

| | | | | | | | | |
|---|---|---|---|---|---|---|---|---|
| Pulp Flow Rate | | | 3 | l/min | Water pH | | 8.16 | |
| Air Flow Rate | | | 3 | l/min | Pulp pH | | 8.09 | |
| Measured Froth Depth | | | 20 | mm | Adjusted pH | | 7.00 | |
| Decrease in Pulp Level | | | 80 | mm | Fill-up Time | | 6.50 | min |
| Sample No | Sample Interval (s) | Sample Time (s) | Sample Bottle Mass (g) | Froth + Bottle Mass (g) | Quartz + Bottle Mass (g) | Flotation Time (min) | Quartz Rec (%) | Water Rec (%) |
| A1 | 60 | 10 | 347.94 | 382.78 | 365.43 | 1.0 | 34.98 | 3.61 |
| A2 | 30 | 10 | 346.96 | 384.53 | 365.64 | 1.5 | 37.36 | 3.93 |
| A3 | 30 | 10 | 346.52 | 380.26 | 363.51 | 2.0 | 33.98 | 3.48 |
| A4 | 30 | 10 | 347.58 | 387.91 | 366.62 | 2.5 | 38.08 | 4.42 |
| A5 | 30 | 10 | 344.77 | 375.46 | 358.77 | 3.0 | 28.00 | 3.47 |
| A6 | 30 | 10 | 346.19 | 379.36 | 360.08 | 3.5 | 27.78 | 4.01 |
| A7 | 30 | 10 | 342.09 | 371.67 | 354.55 | 4.0 | 24.92 | 3.56 |
| A8 | 30 | 10 | 340.84 | 372.95 | 352.83 | 4.5 | 23.98 | 4.18 |
| A9 | 30 | 10 | 341.88 | 386.42 | 357.99 | 5.0 | 32.22 | 5.91 |
| A10 | 30 | 10 | 344.19 | 366.57 | 351.47 | 5.5 | 14.56 | 3.14 |
| A11 | 30 | 10 | 343.79 | 365.08 | 350.96 | 6.0 | 14.34 | 2.93 |
| A12 | 30 | 10 | 341.49 | 368.83 | 348.75 | 6.5 | 15.52 | 4.17 |
| Steady State Quartz Recovery | | | **14.47** | % | Air Holdup | | 4.42 | % |
| Steady State Water Recovery | | | **3.42** | % | Conditioning Time | | 11.5 | min |

Table 57 : Flotation Response of the Column Cell Configuration with the +150 -300 μm Particle Size Fraction at a Collector Dosage of 200 g/t.

| | | | | | | | | |
|---|---|---|---|---|---|---|---|---|
| Pulp Flow Rate | | | 3 | l/min | Water pH | | 8.23 | |
| Air Flow Rate | | | 3 | l/min | Pulp pH | | 8.21 | |
| Measured Froth Depth | | | 20 | mm | Adjusted pH | | 7.00 | |
| Decrease in Pulp Level | | | 90 | mm | Fill-up Time | | 8.25 | min |
| Sample No | Sample Interval (s) | Sample Time (s) | Sample Bottle Mass (g) | Froth+ Bottle Mass (g) | Quartz+ Bottle Mass (g) | Flotation Time (min) | Quartz Rec (%) | Water Rec (%) |
| A1 | 60 | 10 | 347.94 | 424.58 | 386.49 | 1.0 | 77.10 | 7.92 |
| A2 | 30 | 10 | 346.96 | 426.50 | 385.00 | 1.5 | 76.08 | 8.63 |
| A3 | 30 | 10 | 346.52 | 404.70 | 373.74 | 2.0 | 54.44 | 6.43 |
| A4 | 30 | 10 | 347.58 | 413.31 | 377.41 | 2.5 | 59.66 | 7.46 |
| A5 | 30 | 10 | 344.77 | 396.41 | 367.69 | 3.0 | 45.84 | 5.97 |
| A6 | 30 | 10 | 346.19 | 405.48 | 371.33 | 3.5 | 50.28 | 7.10 |
| A7 | 30 | 10 | 342.09 | 397.65 | 365.55 | 4.0 | 46.92 | 6.67 |
| A8 | 30 | 10 | 340.84 | 426.97 | 362.57 | 4.5 | 43.46 | 13.39 |
| A9 | 30 | 10 | 341.88 | 394.97 | 366.72 | 5.0 | 49.68 | 5.87 |
| A10 | 30 | 10 | 344.19 | 398.89 | 368.91 | 5.5 | 49.44 | 6.23 |
| A11 | 30 | 10 | 343.79 | 404.44 | 370.09 | 6.0 | 52.60 | 7.14 |
| A12 | 30 | 10 | 341.49 | 402.20 | 366.30 | 6.5 | 49.62 | 7.46 |
| Steady State Quartz Recovery | | | **50.10** | % | Air Holdup | | 4.97 | % |
| Steady State Water Recovery | | | **7.84** | % | Conditioning Time | | 13.3 | min |

Table 58 : Flotation Response of the Column Cell Configuration with the +300 μm Particle Size Fraction with No Collector Added to the Pulp.

| | | | | | | | | |
|---|---|---|---|---|---|---|---|---|
| Pulp Flow Rate | | | 3 | l/min | Water pH | | 8.63 | |
| Air Flow Rate | | | 3 | l/min | Pulp pH | | 8.36 | |
| Measured Froth Depth | | | 20 | mm | Adjusted pH | | 7.00 | |
| Decrease in Pulp Level | | | 60 | mm | Fill-up Time | | 12.7 | min |
| Sample No | Sample Interval (s) | Sample Time (s) | Sample Bottle Mass (g) | Froth+ Bottle Mass (g) | Quartz+ Bottle Mass (g) | Flotation Time (min) | Quartz Rec (%) | Water Rec (%) |
| A1 | 60 | 10 | 347.94 | 347.94 | 347.94 | 1.0 | 0.00 | 0.00 |
| A2 | 30 | 10 | 346.96 | 346.96 | 346.96 | 1.5 | 0.00 | 0.00 |
| A3 | 30 | 10 | 346.52 | 346.52 | 346.52 | 2.0 | 0.00 | 0.00 |
| A4 | 30 | 10 | 347.58 | 347.58 | 347.58 | 2.5 | 0.00 | 0.00 |
| A5 | 30 | 10 | 344.77 | 344.77 | 344.77 | 3.0 | 0.00 | 0.00 |
| A6 | 30 | 10 | 346.19 | 346.19 | 346.19 | 3.5 | 0.00 | 0.00 |
| A7 | 30 | 10 | 342.09 | 342.09 | 342.09 | 4.0 | 0.00 | 0.00 |
| A8 | 30 | 10 | 340.84 | 340.84 | 340.84 | 4.5 | 0.00 | 0.00 |
| A9 | 30 | 10 | 341.88 | 341.88 | 341.88 | 5.0 | 0.00 | 0.00 |
| A10 | 30 | 10 | 344.19 | 344.19 | 344.19 | 5.5 | 0.00 | 0.00 |
| A11 | 30 | 10 | 343.79 | 343.79 | 343.79 | 6.0 | 0.00 | 0.00 |
| A12 | 30 | 10 | 341.49 | 341.49 | 341.49 | 6.5 | 0.00 | 0.00 |
| Steady State Quartz Recovery | | | **0.00** | % | Air Holdup | | 3.31 | % |
| Steady State Water Recovery | | | **0.00** | % | Conditioning Time | | 17.7 | min |

Table 59 : Flotation Response of the Column Cell Configuration with the +300 μm Particle Size Fraction at a Collector Dosage of 25 g/t.

| | | | | | | | | |
|---|---|---|---|---|---|---|---|---|
| Pulp Flow Rate | | | 3 | l/min | Water pH | | 9.13 | |
| Air Flow Rate | | | 3 | l/min | Pulp pH | | 8.62 | |
| Measured Froth Depth | | | 20 | mm | Adjusted pH | | 7.00 | |
| Decrease in Pulp Level | | | 80 | mm | Fill-up Time | | 12.0 | min |
| Sample No | Sample Interval (s) | Sample Time (s) | Sample Bottle Mass (g) | Froth+ Bottle Mass (g) | Quartz+ Bottle Mass (g) | Flotation Time (min) | Quartz Rec (%) | Water Rec (%) |
| 1 | 60 | 10 | 343.69 | 344.36 | 343.85 | 1.0 | 0.32 | 0.111 |
| 2 | 30 | 10 | 347.88 | 348.29 | 347.96 | 1.5 | 0.16 | 0.07 |
| 3 | 30 | 10 | 347.25 | 347.89 | 347.39 | 2.0 | 0.28 | 0.10 |
| 4 | 30 | 10 | 348.24 | 348.47 | 348.24 | 2.5 | 0.00 | 0.05 |
| 5 | 30 | 10 | 345.18 | 346.01 | 345.38 | 3.0 | 0.40 | 0.13 |
| 6 | 30 | 10 | 344.70 | 345.01 | 344.73 | 3.5 | 0.06 | 0.06 |
| 7 | 30 | 10 | 346.88 | 347.14 | 346.90 | 4.0 | 0.04 | 0.05 |
| 8 | 30 | 10 | 348.72 | 348.97 | 348.74 | 4.5 | 0.04 | 0.05 |
| 9 | 30 | 10 | 345.71 | 346.44 | 345.91 | 5.0 | 0.40 | 0.11 |
| 10 | 30 | 10 | 346.57 | 346.44 | 346.62 | 5.5 | 0.10 | 0.00 |
| 11 | 30 | 10 | 345.31 | 345.91 | 345.40 | 6.0 | 0.18 | 0.11 |
| 12 | 30 | 10 | 344.44 | 345.80 | 344.87 | 6.5 | 0.86 | 0.19 |
| Steady State Quartz Recovery | | | **0.05** | % | Air Holdup | | 4.42 | % |
| Steady State Water Recovery | | | **0.05** | % | Conditioning Time | | 17.0 | min |

Table 60 : Flotation Response of the Column Cell Configuration with the +300 μm Particle Size Fraction at a Collector Dosage of 80 g/t.

| | | | | | | | | |
|---|---|---|---|---|---|---|---|---|
| Pulp Flow Rate | | | 3 | l/min | Water pH | | 9.18 | |
| Air Flow Rate | | | 3 | l/min | Pulp pH | | 8.84 | |
| Measured Froth Depth | | | 22 | mm | Adjusted pH | | 7.00 | |
| Decrease in Pulp Level | | | 130 | mm | Fill-up Time | | 10.0 | min |
| Sample No | Sample Interval (s) | Sample Time (s) | Sample Bottle Mass (g) | Froth+ Bottle Mass (g) | Quartz+ Bottle Mass (g) | Flotation Time (min) | Quartz Rec (%) | Water Rec (%) |
| 1 | 60 | 10 | 343.69 | 365.88 | 352.24 | 1.0 | 17.10 | 2.83 |
| 2 | 30 | 10 | 347.88 | 371.60 | 356.86 | 1.5 | 17.96 | 3.06 |
| 3 | 30 | 10 | 347.25 | 379.70 | 360.45 | 2.0 | 26.40 | 4.00 |
| 4 | 30 | 10 | 348.24 | 375.30 | 359.43 | 2.5 | 22.38 | 3.30 |
| 5 | 30 | 10 | 345.18 | 384.20 | 362.06 | 3.0 | 33.76 | 4.60 |
| 6 | 30 | 10 | 344.70 | 380.82 | 360.50 | 3.5 | 31.60 | 4.22 |
| 7 | 30 | 10 | 346.88 | 392.75 | 367.51 | 4.0 | 41.26 | 5.25 |
| 8 | 30 | 10 | 348.72 | 400.05 | 370.31 | 4.5 | 43.18 | 6.18 |
| 9 | 30 | 10 | 345.71 | 388.51 | 364.51 | 5.0 | 37.60 | 4.99 |
| 10 | 30 | 10 | 346.57 | 418.91 | 373.40 | 5.5 | 53.66 | 9.46 |
| 11 | 30 | 10 | 345.31 | 398.50 | 368.03 | 6.0 | 45.44 | 6.33 |
| 12 | 30 | 10 | 344.44 | 415.14 | 373.06 | 6.5 | 57.24 | 8.75 |
| Steady State Quartz Recovery | | | **17.53** | % | Air Holdup | | 7.19 | % |
| Steady State Water Recovery | | | **2.95** | % | Conditioning Time | | 15.0 | min |

Table 61 : Flotation Response of the Column Cell Configuration with the +300 μm Particle Size Fraction at a Collector Dosage of 200 g/t.

| | | | | | | | |
|---|---|---|---|---|---|---|---|
| Pulp Flow Rate | | 3 | l/min | Water pH | 9.13 | | |
| Air Flow Rate | | 3 | l/min | Pulp pH | 8.60 | | |
| Measured Froth Depth | | 20 | mm | Adjusted pH | 7.00 | | |
| Decrease in Pulp Level | | 150 | mm | Fill-up Time | 16.0 | min | |

| Sample No | Sample Interval (s) | Sample Time (s) | Sample Bottle Mass (g) | Froth + Bottle Mass (g) | Quartz + Bottle Mass (g) | Flotation Time (min) | Quartz Rec (%) | Water Rec (%) |
|---|---|---|---|---|---|---|---|---|
| 1 | 60 | 10 | 343.69 | 372.04 | 352.37 | 1.0 | 34.72 | 8.18 |
| 2 | 30 | 10 | 347.88 | 372.05 | 353.62 | 1.5 | 22.96 | 7.66 |
| 3 | 30 | 10 | 347.25 | 384.10 | 354.43 | 2.0 | 14.36 | 6.17 |
| 4 | 30 | 10 | 348.24 | 367.81 | 351.00 | 2.5 | 11.04 | 6.99 |
| 5 | 30 | 10 | 345.18 | 364.08 | 347.47 | 3.0 | 9.16 | 6.90 |
| 6 | 30 | 10 | 344.70 | 362.06 | 346.08 | 3.5 | 5.52 | 6.64 |
| 7 | 30 | 10 | 346.88 | 367.98 | 348.49 | 4.0 | 6.44 | 8.10 |
| 8 | 30 | 10 | 348.72 | 367.49 | 349.63 | 4.5 | 3.64 | 7.42 |
| 9 | 30 | 10 | 345.71 | 370.98 | 347.04 | 5.0 | 5.32 | 9.95 |
| 10 | 30 | 10 | 346.57 | 371.43 | 347.79 | 5.5 | 4.07 | 8.19 |
| 11 | 30 | 10 | 345.31 | 376.35 | 346.93 | 6.0 | 6.48 | 12.23 |
| 12 | 30 | 10 | 344.44 | 369.16 | 345.68 | 6.5 | 4.96 | 9.76 |

| | | | | | |
|---|---|---|---|---|---|
| Steady State Quartz Recovery | **5.20** | % | Air Holdup | 8.29 | % |
| Steady State Water Recovery | **8.90** | % | Conditioning Time | 21.0 | min |

Table 62 : Flotation Response of the Column Cell Configuration with the +300 μm Particle Size Fraction at a Collector Dosage of 200 g/t (40 g/t Dispersant Added).

| | | | | | | | |
|---|---|---|---|---|---|---|---|
| Pulp Flow Rate | | 3 | l/min | Water pH | 8.43 | | |
| Air Flow Rate | | 3 | l/min | Pulp pH | 7.95 | | |
| Measured Froth Depth | | 15 | mm | Adjusted pH | 7.00 | | |
| Decrease in Pulp Level | | 110 | mm | Fill-up Time | 8.00 | min | |

| Sample No | Sample Interval (s) | Sample Time (s) | Sample Bottle Mass (g) | Froth + Bottle Mass (g) | Quartz + Bottle Mass (g) | Flotation Time (min) | Quartz Rec (%) | Water Rec (%) |
|---|---|---|---|---|---|---|---|---|
| 1 | 60 | 10 | 343.65 | 358.27 | 348.71 | 1.0 | 10.12 | 1.99 |
| 2 | 30 | 10 | 346.06 | 375.71 | 358.81 | 1.5 | 25.50 | 3.51 |
| 3 | 30 | 10 | 347.22 | 388.06 | 364.93 | 2.0 | 35.42 | 4.81 |
| 4 | 30 | 10 | 348.21 | 388.69 | 365.92 | 2.5 | 35.42 | 4.73 |
| 5 | 30 | 10 | 345.14 | 404.05 | 368.87 | 3.0 | 47.46 | 7.31 |
| 6 | 30 | 10 | 344.68 | 382.75 | 359.59 | 3.5 | 29.82 | 4.81 |
| 7 | 30 | 10 | 346.88 | 392.45 | 365.07 | 4.0 | 36.38 | 5.69 |
| 8 | 30 | 10 | 348.66 | 409.26 | 368.10 | 4.5 | 38.88 | 8.55 |
| 9 | 30 | 10 | 345.70 | 404.39 | 361.26 | 5.0 | 31.12 | 8.96 |
| 10 | 30 | 10 | 346.55 | 401.88 | 358.26 | 5.5 | 23.42 | 9.07 |
| 11 | 30 | 10 | 345.28 | 400.54 | 254.12 | 6.0 | 17.68 | 9.65 |
| 12 | 30 | 10 | 344.42 | 397.83 | 351.04 | 6.5 | 13.24 | 9.72 |

| | | | | | |
|---|---|---|---|---|---|
| Steady State Quartz Recovery | **37.23** | % | Air Holdup | 6.06 | % |
| Steady State Water Recovery | **5.99** | % | Conditioning Time | 13.0 | min |

Table 63 : Flotation Response of the Agitated Cell Configuration with the -106 μm Particle Size Fraction with No Collector Added to the Pulp.

| | | | | | | | |
|---|---|---|---|---|---|---|---|
| Pulp Flow Rate | 3 | l/min | Water pH | 8.41 | | | |
| Air Flow Rate | 3 | l/min | Pulp pH | 7.51 | | | |
| Measured Froth Depth | 20 | mm | Adjusted pH | 7.00 | | | |
| Decrease in Pulp Level | 100 | mm | Fill-up Time | 7.00 | min | | |

| Sample No | Sample Interval (s) | Sample Time (s) | Sample Bottle Mass (g) | Froth+ Bottle Mass (g) | Quartz+ Bottle Mass (g) | Flotation Time (min) | Quartz Rec (%) | Water Rec (%) |
|---|---|---|---|---|---|---|---|---|
| 1 | 60 | 10 | 343.65 | 343.65 | 343.65 | 1.0 | 0.00 | 0.00 |
| 2 | 30 | 10 | 346.06 | 346.06 | 346.06 | 1.5 | 0.00 | 0.00 |
| 3 | 30 | 10 | 347.22 | 347.22 | 347.22 | 2.0 | 0.00 | 0.00 |
| 4 | 30 | 10 | 348.21 | 348.21 | 348.21 | 2.5 | 0.00 | 0.00 |
| 5 | 30 | 10 | 345.14 | 345.14 | 345.14 | 3.0 | 0.00 | 0.00 |
| 6 | 30 | 10 | 344.68 | 344.68 | 344.68 | 3.5 | 0.00 | 0.00 |
| 7 | 30 | 10 | 346.86 | 346.86 | 346.86 | 4.0 | 0.00 | 0.00 |
| 8 | 30 | 10 | 348.66 | 348.66 | 348.66 | 4.5 | 0.00 | 0.00 |
| 9 | 30 | 10 | 345.70 | 345.70 | 345.70 | 5.0 | 0.00 | 0.00 |
| 10 | 30 | 10 | 346.55 | 346.55 | 346.55 | 5.5 | 0.00 | 0.00 |
| 11 | 30 | 10 | 345.28 | 345.28 | 345.28 | 6.0 | 0.00 | 0.00 |
| 12 | 30 | 10 | 344.42 | 344.42 | 344.42 | 6.5 | 0.00 | 0.00 |

| | | | | | |
|---|---|---|---|---|---|
| Steady State Quartz Recovery | **0.00** | % | Air Holdup | 5.52 | % |
| Steady State Water Recovery | **0.00** | % | Conditioning Time | 12.0 | min |

Table 64 : Flotation Response of the Agitated Cell Configuration with the -106 μm Particle Size Fraction at a Collector Dosage of 25 g/t.

| | | | | | | | |
|---|---|---|---|---|---|---|---|
| Pulp Flow Rate | 3 | l/min | Water pH | 8.41 | | | |
| Air Flow Rate | 3 | l/min | Pulp pH | 7.33 | | | |
| Measured Froth Depth | 20 | mm | Adjusted pH | 7.00 | | | |
| Decrease in Pulp Level | 120 | mm | Fill-up Time | 7.00 | min | | |

| Sample No | Sample Interval (s) | Sample Time (s) | Sample Bottle Mass (g) | Froth+ Bottle Mass (g) | Quartz+ Bottle Mass (g) | Flotation Time (min) | Quartz Rec (%) | Water Rec (%) |
|---|---|---|---|---|---|---|---|---|
| A1 | 60 | 10 | 347.94 | 433.34 | 366.14 | 1.0 | 36.40 | 13.97 |
| A2 | 30 | 10 | 346.96 | 429.68 | 364.76 | 1.5 | 35.60 | 13.49 |
| A3 | 30 | 10 | 346.52 | 425.06 | 362.95 | 2.0 | 32.86 | 12.91 |
| A4 | 30 | 10 | 347.58 | 429.21 | 364.45 | 2.5 | 33.74 | 13.46 |
| A5 | 30 | 10 | 344.77 | 414.77 | 359.48 | 3.0 | 29.42 | 11.49 |
| A6 | 30 | 10 | 346.19 | 416.93 | 360.92 | 3.5 | 29.46 | 11.64 |
| A7 | 30 | 10 | 342.09 | 407.40 | 355.54 | 4.0 | 26.90 | 10.78 |
| A8 | 30 | 10 | 340.84 | 407.71 | 354.40 | 4.5 | 27.12 | 11.08 |
| A9 | 30 | 10 | 341.88 | 401.81 | 354.44 | 5.0 | 25.12 | 9.85 |
| A10 | 30 | 10 | 344.19 | 413.99 | 357.22 | 5.5 | 26.06 | 11.80 |
| A11 | 30 | 10 | 343.79 | 392.36 | 353.55 | 6.0 | 19.52 | 8.07 |
| A12 | 30 | 10 | 340.60 | 387.99 | 350.41 | 6.5 | 19.62 | 7.81 |

| | | | | | |
|---|---|---|---|---|---|
| Steady State Quartz Recovery | **26.93** | % | Air Holdup | 6.63 | % |
| Steady State Water Recovery | **11.03** | % | Conditioning Time | 12.0 | min |

Table 65 : Flotation Response of the Agitated Cell Configuration with the -106 μm Particle Size Fraction at a Collector Dosage of 80 g/t.

| | | | | | | | | |
|---|---|---|---|---|---|---|---|---|
| Pulp Flow Rate | | | 3 | l/min | Water pH | | 8.41 | |
| Air Flow Rate | | | 3 | l/min | Pulp pH | | 7.65 | |
| Measured Froth Depth | | | 20 | mm | Adjusted pH | | 7.00 | |
| Decrease in Pulp Level | | | 145 | mm | Fill-up Time | | 7.50 | min |
| Sample No | Sample Interval (s) | Sample Time (s) | Sample Bottle Mass (g) | Froth + Bottle Mass (g) | Quartz + Bottle Mass (g) | Flotation Time (min) | Quartz Rec. (%) | Water Rec (%) |
| 1 | 60 | 10 | 343.65 | 524.07 | 396.85 | 1.0 | 106.40 | 26.44 |
| 2 | 30 | 10 | 346.06 | 505.44 | 390.99 | 1.5 | 89.86 | 23.79 |
| 3 | 30 | 10 | 347.22 | 504.13 | 392.32 | 2.0 | 90.20 | 23.24 |
| 4 | 30 | 10 | 348.21 | 492.90 | 387.22 | 2.5 | 97.53 | 27.46 |
| 5 | 30 | 10 | 345.14 | 488.13 | 383.38 | 3.0 | 76.48 | 21.77 |
| 6 | 30 | 10 | 344.68 | 470.72 | 377.87 | 3.5 | 65.98 | 19.30 |
| 7 | 30 | 10 | 346.86 | 485.65 | 382.75 | 4.0 | 71.78 | 21.39 |
| 8 | 30 | 10 | 348.66 | 459.22 | 382.89 | 4.5 | 68.46 | 15.86 |
| 9 | 30 | 10 | 345.70 | 447.31 | 377.67 | 5.0 | 63.94 | 14.47 |
| 10 | 30 | 10 | 346.55 | 446.62 | 380.30 | 5.5 | 67.50 | 13.78 |
| 11 | 30 | 10 | 345.28 | 455.42 | 378.35 | 6.0 | 66.14 | 16.02 |
| 12 | 30 | 10 | 344.42 | 461.57 | 376.35 | 6.5 | 64.88 | 17.61 |
| Steady State Quartz Recovery | | | **66.95** | % | Air Holdup | | 8.01 | % |
| Steady State Water Recovery | | | **16.92** | % | Conditioning Time | | 12.5 | min |

Table 66 : Flotation Response of the Agitated Cell Configuration with the -106 μm Particle Size Fraction at a Collector Dosage of 200 g/t.

| | | | | | | | | |
|---|---|---|---|---|---|---|---|---|
| Pulp Flow Rate | | | 3 | l/min | Water pH | | 8.41 | |
| Air Flow Rate | | | 3 | l/min | Pulp pH | | 7.71 | |
| Measured Froth Depth | | | 20 | mm | Adjusted pH | | 7.00 | |
| Decrease in Pulp Level | | | 160 | mm | Fill-up Time | | 7.50 | min |
| Sample No | Sample Interval (s) | Sample Time (s) | Sample Bottle Mass (g) | Froth + Bottle Mass (g) | Quartz + Bottle Mass (g) | Flotation Time (min) | Quartz Rec (%) | Water Rec (%) |
| A1 | 60 | 5 | 347.94 | 491.71 | 394.47 | 1.0 | 186.12 | 40.42 |
| A2 | 30 | 5 | 346.96 | 471.75 | 383.93 | 1.5 | 147.88 | 36.51 |
| A3 | 30 | 5 | 346.52 | 474.09 | 384.95 | 2.0 | 153.72 | 37.05 |
| A4 | 30 | 5 | 347.58 | 474.63 | 384.02 | 2.5 | 145.76 | 37.67 |
| A5 | 30 | 5 | 344.77 | 458.56 | 377.37 | 3.0 | 130.40 | 33.75 |
| A6 | 30 | 5 | 346.19 | 461.09 | 378.33 | 3.5 | 128.56 | 34.40 |
| A7 | 30 | 5 | 342.09 | 444.60 | 369.98 | 4.0 | 111.56 | 31.02 |
| A8 | 30 | 5 | 340.84 | 439.07 | 367.54 | 4.5 | 106.80 | 29.73 |
| A9 | 30 | 5 | 341.88 | 429.64 | 365.70 | 5.0 | 95.28 | 26.58 |
| A10 | 30 | 5 | 344.19 | 438.45 | 369.09 | 5.5 | 99.60 | 28.83 |
| A11 | 30 | 7 | 343.79 | 475.83 | 377.67 | 6.0 | 96.80 | 29.15 |
| A12 | 30 | 5 | 340.60 | 430.57 | 365.06 | 6.5 | 97.84 | 27.23 |
| Steady State Quartz Recovery | | | **97.38** | % | Air Holdup | | 8.84 | % |
| Steady State Water Recovery | | | **27.95** | % | Conditioning Time | | 12.5 | min |

Table 67 : Flotation Response of the Agitated Cell Configuration with the +106 -150 μm Particle Size Fraction with No Collector Added to the Pulp.

| | | | | | | | | |
|---|---|---|---|---|---|---|---|---|
| Pulp Flow Rate | | | 3 | l/min | Water pH | | 8.97 | |
| Air Flow Rate | | | 3 | l/min | Pulp pH | | 8.54 | |
| Measured Froth Depth | | | 20 | mm | Adjusted pH | | 7.00 | |
| Decrease in Pulp Level | | | 115 | mm | Fill-up Time | | 9.50 | min |
| Sample No | Sample Interval (s) | Sample Time (s) | Sample Bottle Mass (g) | Froth + Bottle Mass (g) | Quartz + Bottle Mass (g) | Flotation Time (min) | Quartz Rec (%) | Water Rec (%) |
| 1 | 60 | 10 | 343.65 | 343.65 | 343.65 | 1.0 | 0.00 | 0.00 |
| 2 | 30 | 10 | 346.06 | 346.06 | 346.06 | 1.5 | 0.00 | 0.00 |
| 3 | 30 | 10 | 347.22 | 347.22 | 347.22 | 2.0 | 0.00 | 0.00 |
| 4 | 30 | 10 | 348.21 | 348.21 | 348.21 | 2.5 | 0.00 | 0.00 |
| 5 | 30 | 10 | 345.14 | 345.14 | 345.14 | 3.0 | 0.00 | 0.00 |
| 6 | 30 | 10 | 344.68 | 344.68 | 344.68 | 3.5 | 0.00 | 0.00 |
| 7 | 30 | 10 | 346.86 | 346.86 | 346.86 | 4.0 | 0.00 | 0.00 |
| 8 | 30 | 10 | 348.66 | 348.66 | 348.66 | 4.5 | 0.00 | 0.00 |
| 9 | 30 | 10 | 345.70 | 345.70 | 345.70 | 5.0 | 0.00 | 0.00 |
| 10 | 30 | 10 | 346.55 | 346.55 | 346.55 | 5.5 | 0.00 | 0.00 |
| 11 | 30 | 10 | 345.28 | 345.28 | 345.28 | 6.0 | 0.00 | 0.00 |
| 12 | 30 | 10 | 344.42 | 344.42 | 344.42 | 6.5 | 0.00 | 0.00 |
| Steady State Quartz Recovery | | | **0.00** | % | Air Holdup | | 6.35 | % |
| Steady State Water Recovery | | | **0.00** | % | Conditioning Time | | 14.5 | min |

Table 68 : Flotation Response of the Agitated Cell Configuration with the +106 -150 μm Particle Size Fraction at a Collector Dosage of 25 g/t.

| | | | | | | | | |
|---|---|---|---|---|---|---|---|---|
| Pulp Flow Rate | | | 3 | l/min | Water pH | | 9.03 | |
| Air Flow Rate | | | 3 | l/min | Pulp pH | | 7.90 | |
| Measured Froth Depth | | | 20 | mm | Adjusted pH | | 7.00 | |
| Decrease in Pulp Level | | | 125 | mm | Fill-up Time | | 7.50 | min |
| Sample No | Sample Interval (s) | Sample Time (s) | Sample Bottle Mass (g) | Froth + Bottle Mass (g) | Quartz + Bottle Mass (g) | Flotation Time (min) | Quartz Rec (%) | Water Rec (%) |
| 1 | 60 | 10 | 345.18 | 360.43 | 366.34 | 1.0 | 12.32 | 1.89 |
| 2 | 30 | 10 | 346.97 | 355.68 | 349.67 | 1.5 | 5.40 | 1.25 |
| 3 | 30 | 10 | 346.53 | 354.23 | 348.41 | 2.0 | 3.76 | 1.21 |
| 4 | 30 | 10 | 347.59 | 351.06 | 348.49 | 2.5 | 1.80 | 0.53 |
| 5 | 30 | 10 | 344.78 | 355.31 | 348.74 | 3.0 | 7.92 | 1.37 |
| 6 | 30 | 10 | 346.20 | 354.06 | 348.04 | 3.5 | 3.68 | 1.25 |
| 7 | 30 | 10 | 342.09 | 350.25 | 344.82 | 4.0 | 5.46 | 1.13 |
| 8 | 30 | 10 | 340.84 | 343.78 | 341.59 | 4.5 | 1.50 | 0.46 |
| 9 | 30 | 10 | 344.15 | 350.69 | 346.02 | 5.0 | 3.74 | 0.97 |
| 10 | 30 | 10 | 44.205 | 348.11 | 345.13 | 5.5 | 1.86 | 0.62 |
| 11 | 30 | 10 | 343.81 | 346.10 | 344.41 | 6.0 | 1.20 | 0.35 |
| 12 | 30 | 10 | 345.62 | 348.09 | 346.16 | 6.5 | 1.08 | 0.40 |
| Steady State Quartz Recovery | | | **3.71** | % | Air Holdup | | 6.91 | % |
| Steady State Water Recovery | | | **0.90** | % | Conditioning Time | | 12.5 | min |

Table 69 : Flotation Response of the Agitated Cell Configuration with the +106 -150 μm Particle Size Fraction at a Collector Dosage of 80 g/t.

| | | | | | | | | |
|---|---|---|---|---|---|---|---|---|
| Pulp Flow Rate | | | 3 | l/min | Water pH | | 8.94 | |
| Air Flow Rate | | | 3 | l/min | Pulp pH | | 7.97 | |
| Measured Froth Depth | | | 20 | mm | Adjusted pH | | 7.00 | |
| Decrease in Pulp Level | | | 140 | mm | Fill-up Time | | 8.00 | min |
| Sample No | Sample Interval (s) | Sample Time (s) | Sample Bottle Mass (g) | Froth+ Bottle Mass (g) | Quartz+ Bottle Mass (g) | Flotation Time (min) | Quartz Rec (%) | Water Rec (%) |
| 1 | 60 | 10 | 343.69 | 466.08 | 393.60 | 1.0 | 99.82 | 15.06 |
| 2 | 30 | 10 | 347.88 | 444.03 | 382.08 | 1.5 | 68.40 | 12.88 |
| 3 | 30 | 10 | 347.25 | 445.36 | 386.98 | 2.0 | 79.46 | 12.13 |
| 4 | 30 | 10 | 348.24 | 441.99 | 387.18 | 2.5 | 77.88 | 11.39 |
| 5 | 30 | 10 | 345.18 | 419.43 | 376.18 | 3.0 | 62.00 | 8.99 |
| 6 | 30 | 10 | 344.70 | 415.44 | 375.55 | 3.5 | 61.70 | 8.29 |
| 7 | 30 | 10 | 346.88 | 422.60 | 376.68 | 4.0 | 59.60 | 9.54 |
| 8 | 30 | 10 | 348.72 | 418.02 | 377.73 | 4.5 | 58.02 | 8.37 |
| 9 | 30 | 10 | 345.71 | 409.58 | 369.62 | 5.0 | 47.82 | 8.31 |
| 10 | 30 | 10 | 346.57 | 402.14 | 368.35 | 5.5 | 43.56 | 7.02 |
| 11 | 30 | 10 | 345.31 | 393.85 | 364.82 | 6.0 | 39.02 | 6.03 |
| 12 | 30 | 10 | 344.44 | 388.71 | 363.05 | 6.5 | 37.22 | 5.33 |
| Steady State Quartz Recovery | | | **38.12** | % | Air Holdup | | 7.73 | % |
| Steady State Water Recovery | | | **5.68** | % | Conditioning Time | | 13.0 | min |

Table 70 : Flotation Response of the Agitated Cell Configuration with the +106 -150 μm Particle Size Fraction at a Collector Dosage of 200 g/t.

| | | | | | | | | |
|---|---|---|---|---|---|---|---|---|
| Pulp Flow Rate | | | 3 | l/min | Water pH | | 8.94 | |
| Air Flow Rate | | | 3 | l/min | Pulp pH | | 8.10 | |
| Measured Froth Depth | | | 20 | mm | Adjusted pH | | 7.00 | |
| Decrease in Pulp Level | | | 165 | mm | Fill-up Time | | 9.00 | min |
| Sample No | Sample Interval (s) | Sample Time (s) | Sample Bottle Mass (g) | Froth+ Bottle Mass (g) | Quartz+ Bottle Mass (g) | Flotation Time (min) | Quartz Rec (%) | Water Rec (%) |
| A1 | 60 | 5 | 345.18 | 439.64 | 386.29 | 1.0 | 164.44 | 22.181 |
| A2 | 30 | 5 | 346.97 | 417.59 | 378.77 | 1.5 | 127.20 | 6.14 |
| A3 | 30 | 5 | 346.53 | 413.77 | 375.63 | 2.0 | 116.40 | 15.85 |
| A4 | 30 | 5 | 347.59 | 411.52 | 3374.14 | 2.5 | 106.20 | 15.54 |
| A5 | 30 | 5 | 344.78 | 411.42 | 373.08 | 3.0 | 113.20 | 15.94 |
| A6 | 30 | 5 | 346.20 | 403.44 | 370.32 | 3.5 | 96.48 | 13.77 |
| A7 | 30 | 5 | 342.09 | 403.16 | 367.31 | 4.0 | 100.88 | 14.90 |
| A8 | 30 | 5 | 340.84 | 393.43 | 363.01 | 4.5 | 88.68 | 12.56 |
| A9 | 30 | 10 | 344.15 | 456.57 | 390.23 | 5.0 | 92.16 | 13.79 |
| A10 | 30 | 10 | 44.205 | 437.66 | 381.84 | 5.5 | 75.28 | 11.60 |
| A11 | 30 | 10 | 343.81 | 449.71 | 389.12 | 6.0 | 90.62 | 12.59 |
| A12 | 30 | 10 | 345.62 | 452.80 | 388.13 | 6.5 | 85.02 | 13.44 |
| Steady State Quartz Recovery | | | **86.35** | % | Air Holdup | | 9.12 | % |
| Steady State Water Recovery | | | **12.81** | % | Conditioning Time | | 14.0 | min |

Table 71 : Flotation Response of the Agitated Cell Configuration with the +150 -300 μm Particle Size Fraction with No Collector Added to the Pulp.

| | | | | | |
|---|---|---|---|---|---|
| Pulp Flow Rate | 3 | l/min | Water pH | 8.49 | |
| Air Flow Rate | 3 | l/min | Pulp pH | 8.31 | |
| Measured Froth Depth | 20 | mm | Adjusted pH | 7.00 | |
| Decrease in Pulp Level | 135 | mm | Fill-up Time | 8.50 | min |

| Sample No | Sample Interval (s) | Sample Time (s) | Sample Bottle Mass (g) | Froth+ Bottle Mass (g) | Quartz+ Bottle Mass (g) | Flotation Time (min) | Quartz Rec (%) | Water Rec (%) |
|---|---|---|---|---|---|---|---|---|
| 1 | 60 | 10 | 343.65 | 343.65 | 343.65 | 1.0 | 0.00 | 0.00 |
| 2 | 30 | 10 | 346.06 | 346.06 | 346.06 | 1.5 | 0.00 | 0.00 |
| 3 | 30 | 10 | 347.22 | 347.22 | 347.22 | 2.0 | 0.00 | 0.00 |
| 4 | 30 | 10 | 348.21 | 348.21 | 348.21 | 2.5 | 0.00 | 0.00 |
| 5 | 30 | 10 | 345.14 | 345.14 | 345.14 | 3.0 | 0.00 | 0.00 |
| 6 | 30 | 10 | 344.68 | 344.68 | 344.68 | 3.5 | 0.00 | 0.00 |
| 7 | 30 | 10 | 346.86 | 346.86 | 346.86 | 4.0 | 0.00 | 0.00 |
| 8 | 30 | 10 | 348.66 | 348.66 | 348.66 | 4.5 | 0.00 | 0.00 |
| 9 | 30 | 10 | 345.70 | 345.70 | 345.70 | 5.0 | 0.00 | 0.00 |
| 10 | 30 | 10 | 346.55 | 346.55 | 346.55 | 5.5 | 0.00 | 0.00 |
| 11 | 30 | 10 | 345.28 | 345.28 | 345.28 | 6.0 | 0.00 | 0.00 |
| 12 | 30 | 10 | 344.42 | 344.42 | 344.42 | 6.5 | 0.00 | 0.00 |

| | | | | | |
|---|---|---|---|---|---|
| Steady State Quartz Recovery | **0.00** | % | Air Holdup | 7.46 | % |
| Steady State Water Recovery | **0.00** | % | Conditioning Time | 13.5 | min |

Table 72 : Flotation Response of the Agitated Cell Configuration with the +150 -300 μm Particle Size Fraction at a Collector Dosage of 25 g/t.

| | | | | | |
|---|---|---|---|---|---|
| Pulp Flow Rate | 3 | l/min | Water pH | 8.80 | |
| Air Flow Rate | 3 | l/min | Pulp pH | 8.64 | |
| Measured Froth Depth | 20 | mm | Adjusted pH | 7.00 | |
| Decrease in Pulp Level | 145 | mm | Fill-up Time | 9.50 | min |

| Sample No | Sample Interval (s) | Sample Time (s) | Sample Bottle Mass (g) | Froth+ Bottle Mass (g) | Quartz+ Bottle Mass (g) | Flotation Time (min) | Quartz Rec (%) | Water Rec (%) |
|---|---|---|---|---|---|---|---|---|
| 1 | 60 | 10 | 343.65 | 391.13 | 345.04 | 1.0 | 2.78 | 9.58 |
| 2 | 30 | 10 | 346.06 | 385.23 | 346.87 | 1.5 | 1.62 | 7.97 |
| 3 | 30 | 10 | 347.22 | 363.28 | 347.72 | 2.0 | 1.00 | 3.23 |
| 4 | 30 | 10 | 348.21 | 373.08 | 348.78 | 2.5 | 1.14 | 5.05 |
| 5 | 30 | 10 | 345.14 | 357.10 | 345.56 | 3.0 | 0.84 | 2.40 |
| 6 | 30 | 10 | 344.68 | 367.14 | 345.10 | 3.5 | 0.84 | 4.58 |
| 7 | 30 | 10 | 346.86 | 354.07 | 346.96 | 4.0 | 0.16 | 1.48 |
| 8 | 30 | 10 | 348.66 | 356.99 | 348.88 | 4.5 | 0.44 | 1.69 |
| 9 | 30 | 10 | 345.70 | 360.36 | 345.87 | 5.0 | 0.34 | 3.01 |
| 10 | 30 | 10 | 346.55 | 352.65 | 346.79 | 5.5 | 0.48 | 1.22 |
| 11 | 30 | 10 | 345.28 | 360.70 | 345.55 | 6.0 | 0.54 | 3.15 |
| 12 | 30 | 10 | 344.42 | 358.87 | 344.52 | 6.5 | 0.20 | 2.98 |

| | | | | | |
|---|---|---|---|---|---|
| Steady State Quartz Recovery | **0.48** | % | Air Holdup | 8.01 | % |
| Steady State Water Recovery | **2.56** | % | Conditioning Time | 14.5 | min |

Table 73 : Flotation Response of the Agitated Cell Configuration with the +150 -300 μm Particle Size Fraction at a Collector Dosage of 80 g/t.

| | | | | | | | | |
|---|---|---|---|---|---|---|---|---|
| Pulp Flow Rate | | | 3 | l/min | Water pH | | 8.67 | |
| Air Flow Rate | | | 3 | l/min | Pulp pH | | 8.15 | |
| Measured Froth Depth | | | 20 | mm | Adjusted pH | | 7.00 | |
| Decrease in Pulp Level | | | 150 | mm | Fill-up Time | | 9.00 | min |
| Sample No | Sample Interval (s) | Sample Time (s) | Sample Bottle Mass (g) | Froth + Bottle Mass (g) | Quartz + Bottle Mass (g) | Flotation Time (min) | Quartz Rec (%) | Water Rec (%) |
| A1 | 60 | 10 | 347.94 | 448.67 | 363.69 | 1.0 | 31.50 | 15.06 |
| A2 | 30 | 10 | 346.96 | 394.36 | 355.97 | 1.5 | 18.02 | 12.88 |
| A3 | 30 | 10 | 346.52 | 386.14 | 353.75 | 2.0 | 14.46 | 12.13 |
| A4 | 30 | 10 | 347.58 | 386.27 | 353.00 | 2.5 | 10.84 | 11.39 |
| A5 | 30 | 10 | 344.77 | 376.79 | 350.98 | 3.0 | 12.42 | 8.99 |
| A6 | 30 | 10 | 346.19 | 378.50 | 349.94 | 3.5 | 7.50 | 8.29 |
| A7 | 30 | 10 | 342.09 | 368.61 | 345.72 | 4.0 | 7.26 | 9.54 |
| A8 | 30 | 10 | 340.84 | 378.15 | 344.133 | 4.5 | 6.58 | 8.37 |
| A9 | 30 | 10 | 344.14 | 366.90 | 346.32 | 5.0 | 4.36 | 8.31 |
| A10 | 30 | 10 | 344.19 | 363.69 | 346.32 | 5.5 | 4.26 | 7.02 |
| A11 | 30 | 10 | 343.79 | 367.75 | 345.85 | 6.0 | 4.12 | 6.03 |
| A12 | 30 | 10 | 341.49 | 351.84 | 342.31 | 6.5 | 1.64 | 5.33 |
| Steady State Quartz Recovery | | | **7.11** | % | Air Holdup | | 8.29 | % |
| Steady State Water Recovery | | | **5.92** | % | Conditioning Time | | 14.0 | min |

Table 74 : Flotation Response of the Agitated Cell Configuration with the +150 -300 μm Particle Size Fraction at a Collector Dosage of 200 g/t.

| | | | | | | | | |
|---|---|---|---|---|---|---|---|---|
| Pulp Flow Rate | | | 3 | l/min | Water pH | | 8.63 | |
| Air Flow Rate | | | 3 | l/min | Pulp pH | | 8.36 | |
| Measured Froth Depth | | | 20 | mm | Adjusted pH | | 7.00 | |
| Decrease in Pulp Level | | | 190 | mm | Fill-up Time | | 9.00 | min |
| Sample No | Sample Interval (s) | Sample Time (s) | Sample Bottle Mass (g) | Froth + Bottle Mass (g) | Quartz + Bottle Mass (g) | Flotation Time (min) | Quartz Rec (%) | Water Rec (%) |
| 1 | 60 | 8 | 343.65 | 459.85 | 384.99 | 1.0 | 103.35 | 19.45 |
| 2 | 30 | 5 | 346.06 | 481.09 | 380.32 | 1.5 | 137.04 | 41.89 |
| 3 | 30 | 8 | 347.22 | 452.80 | 382.94 | 2.0 | 89.30 | 18.15 |
| 4 | 30 | 10 | 348.21 | 449.61 | 379.79 | 2.5 | 63.16 | 14.551 |
| 5 | 30 | 7 | 345.14 | 450.14 | 376.84 | 3.0 | 90.57 | 21.76 |
| 6 | 30 | 10 | 344.68 | 442.35 | 376.02 | 3.5 | 62.68 | 13.79 |
| 7 | 30 | 7 | 346.88 | 452.69 | 377.89 | 4.0 | 88.60 | 22.21 |
| 8 | 30 | 10 | 348.66 | 452.77 | 381.00 | 4.5 | 64.68 | 14.92 |
| 9 | 30 | 10 | 345.70 | 451.45 | 376.09 | 5.0 | 60.78 | 15.66 |
| 10 | 30 | 10 | 346.55 | 457.74 | 379.55 | 5.5 | 66.00 | 16.25 |
| 11 | 30 | 10 | 345.28 | 457.49 | 379.92 | 6.0 | 69.28 | 16.12 |
| 12 | 30 | 10 | 344.42 | 459.43 | 377.89 | 6.5 | 66.94 | 16.95 |
| Steady State Quartz Recovery | | | **76.50** | % | Air Holdup | | 10.50 | % |
| Steady State Water Recovery | | | **17.56** | % | Conditioning Time | | 14.0 | min |

Table 75 : Flotation Response of the Agitated Cell Configuration with the +300 μm Particle Size Fraction with No Collector Added to the Pulp.

| | | | | | | | | |
|---|---|---|---|---|---|---|---|---|
| Pulp Flow Rate | | | 3 | l/min | Water pH | | 8.26 | |
| Air Flow Rate | | | 3 | l/min | Pulp pH | | 8.27 | |
| Measured Froth Depth | | | 20 | mm | Adjusted pH | | 7.00 | |
| Decrease in Pulp Level | | | 135 | mm | Fill-up Time | | 8.50 | min |
| Sample No | Sample Interval (s) | Sample Time (s) | Sample Bottle Mass (g) | Froth + Bottle Mass (g) | Quartz + Bottle Mass (g) | Flotation Time (min) | Quartz Rec (%) | Water Rec (%) |
| A1 | 60 | 10 | 347.94 | 347.94 | 347.94 | 1.0 | 0.00 | 0.00 |
| A2 | 30 | 10 | 346.96 | 346.96 | 346.96 | 1.5 | 0.00 | 0.00 |
| A3 | 30 | 10 | 346.52 | 346.52 | 346.52 | 2.0 | 0.00 | 0.00 |
| A4 | 30 | 10 | 347.58 | 347.58 | 347.58 | 2.5 | 0.00 | 0.00 |
| A5 | 30 | 10 | 344.77 | 344.77 | 344.77 | 3.0 | 0.00 | 0.00 |
| A6 | 30 | 10 | 346.19 | 346.19 | 346.19 | 3.5 | 0.00 | 0.00 |
| A7 | 30 | 10 | 342.09 | 342.09 | 342.09 | 4.0 | 0.00 | 0.00 |
| A8 | 30 | 10 | 340.84 | 340.84 | 340.84 | 4.5 | 0.00 | 0.00 |
| A9 | 30 | 10 | 344.14 | 344.14 | 344.14 | 5.0 | 0.00 | 0.00 |
| A10 | 30 | 10 | 344.19 | 344.19 | 344.19 | 5.5 | 0.00 | 0.00 |
| A11 | 30 | 10 | 343.79 | 343.79 | 343.79 | 6.0 | 0.00 | 0.00 |
| A12 | 30 | 10 | 341.49 | 341.49 | 341.49 | 6.5 | 0.00 | 0.00 |
| Steady State Quartz Recovery | | | **0.00** | % | Air Holdup | | 7.46 | % |
| Steady State Water Recovery | | | **0.00** | % | Conditioning Time | | 13.5 | min |

Table 76 : Flotation Response of the Agitated Cell Configuration with the +300 μm Particle Size Fraction at a Collector Dosage of 25 g/t.

| | | | | | | | | |
|---|---|---|---|---|---|---|---|---|
| Pulp Flow Rate | | | 3 | l/min | Water pH | | 9.07 | |
| Air Flow Rate | | | 3 | l/min | Pulp pH | | 8.52 | |
| Measured Froth Depth | | | 16 | mm | Adjusted pH | | 7.00 | |
| Decrease in Pulp Level | | | 145 | mm | Fill-up Time | | 11.0 | min |
| Sample No | Sample Interval (s) | Sample Time (s) | Sample Bottle Mass (g) | Froth + Bottle Mass (g) | Quartz + Bottle Mass (g) | Flotation Time (min) | Quartz Rec (%) | Water Rec (%) |
| 1 | 60 | 10 | 345.18 | 360.69 | 352.10 | 1.0 | 13.84 | 1.79 |
| 2 | 30 | 10 | 346.97 | 354.49 | 350.06 | 1.5 | 6.18 | 0.92 |
| 3 | 30 | 10 | 346.53 | 352.50 | 349.01 | 2.0 | 4.96 | 0.73 |
| 4 | 30 | 10 | 347.59 | 352.54 | 349.69 | 2.5 | 4.20 | 0.59 |
| 5 | 30 | 10 | 344.78 | 356.57 | 349.75 | 3.0 | 9.94 | 1.42 |
| 6 | 30 | 10 | 346.20 | 350.80 | 346.91 | 3.5 | 1.42 | 0.81 |
| 7 | 30 | 10 | 342.09 | 350.07 | 345.14 | 4.0 | 6.10 | 1.02 |
| 8 | 30 | 10 | 340.84 | 345.54 | 341.36 | 4.5 | 1.04 | 0.87 |
| 9 | 30 | 10 | 344.15 | 370.29 | 346.47 | 5.0 | 4.64 | 4.95 |
| 10 | 30 | 10 | 344.20 | 358.25 | 345.46 | 5.5 | 2.52 | 2.68 |
| 11 | 30 | 10 | 343.81 | 367.06 | 344.69 | 6.0 | 1.76 | 4.65 |
| 12 | 30 | 10 | 345.62 | 351.05 | 346.23 | 6.5 | 1.22 | 1.00 |
| Steady State Quartz Recovery | | | **3.14** | % | Air Holdup | | 7.99 | % |
| Steady State Water Recovery | | | **2.06** | % | Conditioning Time | | 16.0 | min |

Table 77 : Flotation Response of the Agitated Cell Configuration with the +300 μm Particle Size Fraction at a Collector Dosage of 80 g/t.

| | | | | | | | | |
|---|---|---|---|---|---|---|---|---|
| Pulp Flow Rate | | | 3 | l/min | Water pH | | 9.07 | |
| Air Flow Rate | | | 3 | l/min | Pulp pH | | 8.26 | |
| Measured Froth Depth | | | 27 | mm | Adjusted pH | | 7.00 | |
| Decrease in Pulp Level | | | 160 | mm | Fill-up Time | | 11.0 | min |
| Sample No | Sample Interval (s) | Sample Time (s) | Sample Bottle Mass (g) | Froth + Bottle Mass (g) | Quartz + Bottle Mass (g) | Flotation Time (min) | Quartz Rec (%) | Water Rec (%) |
| 1 | 60 | 10 | 343.69 | 475.46 | 390.90 | 1.0 | 94.42 | 17.58 |
| 2 | 30 | 10 | 347.88 | 545.92 | 389.86 | 1.5 | 83.96 | 32.44 |
| 3 | 30 | 10 | 347.25 | 455.01 | 389.13 | 2.0 | 83.76 | 13.69 |
| 4 | 30 | 10 | 348.24 | 439.15 | 384.97 | 2.5 | 73.46 | 11.26 |
| 5 | 30 | 10 | 345.18 | 460.05 | 386.13 | 3.0 | 81.90 | 15.36 |
| 6 | 30 | 10 | 344.70 | 465.93 | 389.39 | 3.5 | 89.38 | 15.91 |
| 7 | 30 | 10 | 346.88 | 469.14 | 392.08 | 4.0 | 90.40 | 16.02 |
| 8 | 30 | 10 | 348.72 | 470.36 | 396.50 | 4.5 | 95.56 | 15.35 |
| 9 | 30 | 10 | 345.71 | 471.65 | 396.71 | 5.0 | 102.00 | 15.58 |
| 10 | 30 | 10 | 346.57 | 463.04 | 397.28 | 5.5 | 101.42 | 13.67 |
| 11 | 30 | 10 | 345.31 | 463.50 | 395.52 | 6.0 | 100.42 | 14.13 |
| 12 | 30 | 10 | 344.44 | 439.89 | 386.40 | 6.5 | 83.92 | 11.12 |
| Steady State Quartz Recovery | | | **80.77** | % | Air Holdup | | 8.87 | % |
| Steady State Water Recovery | | | **18.19** | % | Conditioning Time | | 16.0 | min |

Table 78 : Flotation Response of the Agitated Cell Configuration with the +300 μm Particle Size Fraction at a Collector Dosage of 200 g/t.

| | | | | | | | | |
|---|---|---|---|---|---|---|---|---|
| Pulp Flow Rate | | | 3 | l/min | Water pH | | 9.03 | |
| Air Flow Rate | | | 3 | l/min | Pulp pH | | 8.62 | |
| Measured Froth Depth | | | 23 | mm | Adjusted pH | | 7.00 | |
| Decrease in Pulp Level | | | 180 | mm | Fill-up Time | | 10.5 | min |
| Sample No | Sample Interval (s) | Sample Time (s) | Sample Bottle Mass (g) | Froth + Bottle Mass (g) | Quartz + Bottle Mass (g) | Flotation Time (min) | Quartz Rec (%) | Water Rec (%) |
| 1 | 60 | 10 | 343.69 | 416.94 | 345.11 | 1.0 | 2.84 | 14.93 |
| 2 | 30 | 10 | 347.88 | 454.71 | 347.85 | 1.5 | 0.00 | 22.31 |
| 3 | 30 | 10 | 347.25 | 415.90 | 348.84 | 2.0 | 3.18 | 13.94 |
| 4 | 30 | 10 | 348.24 | 411.82 | 349.75 | 2.5 | 3.02 | 12.90 |
| 5 | 30 | 10 | 345.18 | 363.82 | 345.65 | 3.0 | 0.94 | 3.78 |
| 6 | 30 | 10 | 344.70 | 408.22 | 351.16 | 3.5 | 12.92 | 11.86 |
| 7 | 30 | 10 | 346.88 | 404.65 | 345.19 | 4.0 | 0.00 | 12.36 |
| 8 | 30 | 10 | 348.72 | 427.36 | 357.03 | 4.5 | 16.62 | 16.62 |
| 9 | 30 | 10 | 345.71 | 435.00 | 355.35 | 5.0 | 19.28 | 16.55 |
| 10 | 30 | 10 | 346.57 | 355.88 | 346.96 | 5.5 | 0.78 | 1.8561 |
| 11 | 30 | 10 | 345.31 | 436.58 | 347.43 | 6.0 | 4.24 | 8.53 |
| 12 | 30 | 10 | 341.49 | | | 6.5 | | |
| Steady State Quartz Recovery | | | **3.34** | % | Air Holdup | | 9.96 | % |
| Steady State Water Recovery | | | **10.97** | % | Conditioning Time | | 15.5 | min |

Table 79 : Flotation Response of the Agitated Cell Configuration with the +300 μm Particle Size Fraction at a Collector Dosage of 200 g/t (40 g/t Dispersant Added).

| | | | | | | | | |
|---|---|---|---|---|---|---|---|---|
| Pulp Flow Rate | | | 3 | l/min | Water pH | | 8.25 | |
| Air Flow Rate | | | 3 | l/min | Pulp pH | | 8.19 | |
| Measured Froth Depth | | | 20 | mm | Adjusted pH | | 7.00 | |
| Decrease in Pulp Level | | | 280 | mm | Fill-up Time | | 8.00 | min |
| Sample No | Sample Interval (s) | Sample Time (s) | Sample Bottle Mass (g) | Froth+ Bottle Mass (g) | Quartz+ Bottle Mass (g) | Flotation Time (min) | Quartz Rec (%) | Water Rec (%) |
| A1 | 60 | 10 | 347.94 | 381.72 | 348.68 | 1.0 | 1.48 | 6.87 |
| A2 | 30 | 10 | 346.96 | 424.27 | 348.43 | 1.5 | 2.94 | 15.76 |
| A3 | 30 | 10 | 346.52 | 421.65 | 348.43 | 2.0 | 3.82 | 15.22 |
| A4 | 30 | 10 | 347.58 | 424.15 | 349.88 | 2.5 | 4.60 | 15.44 |
| A5 | 30 | 10 | 344.77 | 419.96 | 348.56 | 3.0 | 7.85 | 14.84 |
| A6 | 30 | 10 | 346.19 | 461.28 | 350.96 | 3.5 | 9.54 | 22.93 |
| A7 | 30 | 8 | 342.09 | 427.25 | 348.56 | 4.0 | 16.18 | 20.44 |
| A8 | 30 | 10 | 340.84 | 436.99 | 350.10 | 4.5 | 18.52 | 18.06 |
| A9 | 30 | 10 | 344.14 | 421.25 | 352.89 | 5.0 | 17.50 | 14.21 |
| A10 | 30 | 10 | 344.19 | 450.96 | 354.93 | 5.5 | 21.48 | 19.96 |
| A11 | 30 | 10 | 343.79 | 448.46 | 355.13 | 6.0 | 22.68 | 19.40 |
| A12 | 30 | 10 | 341.49 | 450.38 | 356.16 | 6.5 | 30.94 | 19.42 |
| Steady State Quartz Recovery | | | **30.94** | % | Air Holdup | | 15.47 | % |
| Steady State Water Recovery | | | **19.42** | % | Conditioning Time | | 13.0 | min |

Table 80 : Flotation Response of the Agitated Cell Configuration with the +106 -150 μm Particle Size Fraction at a Collector Dosage of 80 g/t (Agitation Speed = 300 rpm).

| | | | | | | | | |
|---|---|---|---|---|---|---|---|---|
| Pulp Flow Rate | | | 3 | l/min | Water pH | | 8.49 | |
| Air Flow Rate | | | 3 | l/min | Pulp pH | | 7.17 | |
| Measured Froth Depth | | | 20 | mm | Adjusted pH | | 7.00 | |
| Decrease in Pulp Level | | | 100 | mm | Fill-up Time | | 6.50 | min |
| Sample No | Sample Interval (s) | Sample Time (s) | Sample Bottle Mass (g) | Froth+ Bottle Mass (g) | Quartz+ Bottle Mass (g) | Flotation Time (min) | Quartz Rec (%) | Water Rec (%) |
| 1 | 60 | 10 | 343.65 | 367.67 | 354.97 | 1.0 | 22.64 | 2.64 |
| 2 | 30 | 10 | 346.06 | 384.30 | 362.62 | 1.5 | 33.12 | 4.51 |
| 3 | 30 | 10 | 347.22 | 374.14 | 360.04 | 2.0 | 25.64 | 2.93 |
| 4 | 30 | 10 | 348.21 | 385.44 | 364.61 | 2.5 | 32.80 | 4.33 |
| 5 | 30 | 10 | 345.14 | 374.86 | 358.44 | 3.0 | 26.60 | 3.41 |
| 6 | 30 | 10 | 344.68 | 370.62 | 356.51 | 3.5 | 23.66 | 2.93 |
| 7 | 30 | 10 | 346.88 | 374.70 | 359.60 | 4.0 | 25.44 | 3.14 |
| 8 | 30 | 10 | 348.66 | 368.01 | 356.86 | 4.5 | 16.40 | 2.32 |
| 9 | 30 | 10 | 345.70 | 368.59 | 356.06 | 5.0 | 20.72 | 2.60 |
| 10 | 30 | 10 | 346.55 | 381.24 | 361.21 | 5.5 | 29.32 | 4.16 |
| 11 | 30 | 10 | 345.28 | 366.48 | 355.19 | 6.0 | 19.82 | 2.35 |
| 12 | 30 | 10 | 344.42 | 368.82 | 355.03 | 6.5 | 3.37 | 2.87 |
| Steady State Quartz Recovery | | | **27.13** | % | Air Holdup | | 5.52 | % |
| Steady State Water Recovery | | | **3.41** | % | Conditioning Time | | 11.5 | min |

Table 81 : Flotation Response of the Agitated Cell Configuration with the +106 -150 μm Particle Size Fraction at a Collector Dosage of 80 g/t (Agitation Speed = 800 rpm).

| | | | | | | | |
|---|---|---|---|---|---|---|---|
| Pulp Flow Rate | 3 | l/min | Water pH | 8.45 | | | |
| Air Flow Rate | 3 | l/min | Pulp pH | 7.10 | | | |
| Measured Froth Depth | 15 | mm | Adjusted pH | 7.00 | | | |
| Decrease in Pulp Level | 170 | mm | Fill-up Time | 6.66 | min | | |

| Sample No | Sample Interval (s) | Sample Time (s) | Sample Bottle Mass (g) | Froth+ Bottle Mass (g) | Quartz+ Bottle Mass (g) | Flotation Time (min) | Quartz Rec (%) | Water Rec (%) |
|---|---|---|---|---|---|---|---|---|
| 1 | 60 | 10 | 343.65 | 456.51 | 387.15 | 1.0 | 87.00 | 14.42 |
| 2 | 30 | 10 | 346.06 | 444.58 | 382.86 | 1.5 | 73.60 | 12.83 |
| 3 | 30 | 10 | 347.22 | 463.99 | 380.29 | 2.0 | 66.14 | 17.40 |
| 4 | 30 | 10 | 348.21 | 438.54 | 376.64 | 2.5 | 56.86 | 12.87 |
| 5 | 30 | 10 | 345.14 | 463.55 | 377.93 | 3.0 | 65.58 | 17.80 |
| 6 | 30 | 10 | 344.68 | 437.15 | 373.31 | 3.5 | 57.26 | 13.27 |
| 7 | 30 | 10 | 346.88 | 418.94 | 368.49 | 4.0 | 43.22 | 10.49 |
| 8 | 30 | 10 | 348.66 | 436.15 | 376.31 | 4.5 | 55.30 | 12.44 |
| 9 | 30 | 10 | 345.70 | 415.18 | 365.33 | 5.0 | 39.26 | 10.36 |
| 10 | 30 | 10 | 346.55 | 444.10 | 372.97 | 5.5 | 52.84 | 14.78 |
| 11 | 30 | 10 | 345.28 | 395.34 | 361.64 | 6.0 | 32.72 | 7.00 |
| 12 | 30 | 10 | 344.42 | 424.31 | 368.01 | 6.5 | 47.18 | 11.70 |

| | | | | | |
|---|---|---|---|---|---|
| Steady State Quartz Recovery | **45.09** | % | Air Holdup | 9.37 | % |
| Steady State Water Recovery | **11.13** | % | Conditioning Time | 11.7 | min |

Table 82 : Flotation Response of the Agitated Cell Configuration with the +106 -150 μm Particle Size Fraction at a Collector Dosage of 80 g/t (Agitation Speed = 1200 rpm).

| | | | | | | | |
|---|---|---|---|---|---|---|---|
| Pulp Flow Rate | 3 | l/min | Water pH | 8.36 | | | |
| Air Flow Rate | 3 | l/min | Pulp pH | 7.27 | | | |
| Measured Froth Depth | 15 | mm | Adjusted pH | 7.00 | | | |
| Decrease in Pulp Level | 180 | mm | Fill-up Time | 6.50 | min | | |

| Sample No | Sample Interval (s) | Sample Time (s) | Sample Bottle Mass (g) | Froth+ Bottle Mass (g) | Quartz+ Bottle Mass (g) | Flotation Time (min) | Quartz Rec (%) | Water Rec (%) |
|---|---|---|---|---|---|---|---|---|
| 1 | 60 | 10 | 347.94 | 419.73 | 375.69 | 1.0 | 55.50 | 9.15 |
| 2 | 30 | 10 | 346.96 | 425.01 | 373.00 | 1.5 | 52.08 | 10.81 |
| 3 | 30 | 10 | 346.52 | 416.16 | 370.73 | 2.0 | 48.42 | 9.44 |
| 4 | 30 | 10 | 347.58 | 414.37 | 370.84 | 2.5 | 46.52 | 9.05 |
| 5 | 30 | 10 | 344.77 | 393.94 | 361.93 | 3.0 | 34.32 | 6.65 |
| 6 | 30 | 10 | 346.19 | 389.58 | 362.32 | 3.5 | 32.26 | 5.67 |
| 7 | 30 | 10 | 342.09 | 388.68 | 359.45 | 4.0 | 34.72 | 6.08 |
| 8 | 30 | 10 | 340.84 | 388.10 | 358.30 | 4.5 | 34.92 | 6.19 |
| 9 | 30 | 10 | 344.14 | 385.01 | 359.72 | 5.0 | 31.16 | 5.26 |
| 10 | 30 | 10 | 344.19 | 394.16 | 359.89 | 5.5 | 31.40 | 7.12 |
| 11 | 30 | 10 | 343.79 | 400.06 | 361.59 | 6.0 | 35.60 | 8.00 |
| 12 | 30 | 10 | 341.49 | 390.26 | 356.91 | 6.5 | 30.84 | 6.93 |

| | | | | | |
|---|---|---|---|---|---|
| Steady State Quartz Recovery | **33.15** | % | Air Holdup | 9.92 | % |
| Steady State Water Recovery | **6.49** | % | Conditioning Time | 11.5 | min |

Table 83 : Flotation Response of the Agitated Cell Configuration with the +106 -150 μm Particle Size Fraction at a Collector Dosage of 80 g/t (Pulp Flow Rate = 4 l/min).

| | | | | | | | | |
|---|---|---|---|---|---|---|---|---|
| Pulp Flow Rate | | | 4 | l/min | Water pH | | 8.28 | |
| Air Flow Rate | | | 3 | l/min | Pulp pH | | 7.40 | |
| Measured Froth Depth | | | 15 | mm | Adjusted pH | | 7.00 | |
| Decrease in Pulp Level | | | 150 | mm | Fill-up Time | | 4.50 | min |
| Sample No | Sample Interval (s) | Sample Time (s) | Sample Bottle Mass (g) | Froth + Bottle Mass (g) | Quartz + Bottle Mass (g) | Flotation Time (min) | Quartz Rec (%) | Water Rec (%) |
| 1 | 60 | 10 | 343.65 | 510.61 | 414.60 | 1.0 | 106.43 | 14.97 |
| 2 | 30 | 10 | 346.06 | 516.66 | 411.60 | 1.5 | 98.31 | 16.38 |
| 3 | 30 | 10 | 347.22 | 513.62 | 411.49 | 2.0 | 96.40 | 15.92 |
| 4 | 30 | 10 | 348.21 | 512.37 | 402.46 | 2.5 | 81.38 | 17.13 |
| 5 | 30 | 10 | 345.14 | 505.09 | 407.42 | 3.0 | 93.42 | 15.23 |
| 6 | 30 | 10 | 344.68 | 506.73 | 404.52 | 3.5 | 89.76 | 15.93 |
| 7 | 30 | 10 | 346.88 | 501.13 | 399.51 | 4.0 | 78.95 | 15.84 |
| 8 | 30 | 10 | 348.66 | 478.00 | 395.11 | 4.5 | 69.67 | 12.92 |
| 9 | 30 | 10 | 345.70 | 481.64 | 390.46 | 5.0 | 67.14 | 14.21 |
| 10 | 30 | 10 | 346.55 | 432.26 | 372.52 | 5.5 | 38.95 | 7.91 |
| 11 | 30 | 10 | 345.28 | | | 6.0 | | |
| 12 | 30 | 10 | 344.42 | | | 6.5 | | |
| Steady State Quartz Recovery | | | **79.79** | % | Air Holdup | | 8.29 | % |
| Steady State Water Recovery | | | **14.83** | % | Conditioning Time | | 9.50 | min |

Table 84 : Flotation Response of the Jameson Cell Configuration with the -106 μm Particle Size Fraction with No Collector Added to the Pulp.

| | | | | | | | | |
|---|---|---|---|---|---|---|---|---|
| Pulp Flow Rate | | | 3.2 | l/min | Water pH | | 8.26 | |
| Air Flow Rate | | | 3.0 | l/min | Pulp pH | | 7.82 | |
| Measured Froth Depth | | | 20 | mm | Adjusted pH | | 7.00 | |
| Decrease in Pulp Level | | | 77 | mm | Fill-up Time | | 7.00 | min |
| Sample No | Sample Interval (s) | Sample Time (s) | Sample Bottle Mass (g) | Froth + Bottle Mass (g) | Quartz + Bottle Mass (g) | Flotation Time (min) | Quartz Rec (%) | Water Rec (%) |
| A1 | 60 | 10 | 347.94 | 347.94 | 347.94 | 1.0 | 0.00 | 0.00 |
| A2 | 30 | 10 | 346.96 | 346.96 | 346.96 | 1.5 | 0.00 | 0.00 |
| A3 | 30 | 10 | 346.52 | 346.52 | 346.52 | 2.0 | 0.00 | 0.00 |
| A4 | 30 | 10 | 347.58 | 347.58 | 347.58 | 2.5 | 0.00 | 0.00 |
| A5 | 30 | 10 | 344.77 | 344.77 | 344.77 | 3.0 | 0.00 | 0.00 |
| A6 | 30 | 10 | 346.19 | 346.19 | 346.19 | 3.5 | 0.00 | 0.00 |
| A7 | 30 | 10 | 342.09 | 342.09 | 342.09 | 4.0 | 0.00 | 0.00 |
| A8 | 30 | 10 | 340.84 | 340.84 | 340.84 | 4.5 | 0.00 | 0.00 |
| A9 | 30 | 10 | 344.14 | 344.14 | 344.14 | 5.0 | 0.00 | 0.00 |
| A10 | 30 | 10 | 344.19 | 344.19 | 344.19 | 5.5 | 0.00 | 0.00 |
| A11 | 30 | 10 | 343.79 | 343.79 | 343.79 | 6.0 | 0.00 | 0.00 |
| A12 | 30 | 10 | 341.49 | 341.49 | 341.49 | 6.5 | 0.00 | 0.00 |
| Steady State Quartz Recovery | | | **0.00** | % | Air Holdup | | 3.87 | % |
| Steady State Water Recovery | | | **0.00** | % | Conditioning Time | | 12.0 | min |

Table 85 : Flotation Response of the Jameson Cell Configuration with the -106 μm Particle Size Fraction at a Collector Dosage of 25 g/t.

| | | | | | | | | |
|---|---|---|---|---|---|---|---|---|
| Pulp Flow Rate | | | 3.2 | l/min | Water pH | | 8.26 | |
| Air Flow Rate | | | 3.0 | l/min | Pulp pH | | 7.16 | |
| Measured Froth Depth | | | 22 | mm | Adjusted pH | | 7.00 | |
| Decrease in Pulp Level | | | 88 | mm | Fill-up Time | | 6.50 | min |
| Sample No | Sample Interval (s) | Sample Time (s) | Sample Bottle Mass (g) | Froth+ Bottle Mass (g) | Quartz+ Bottle Mass (g) | Flotation Time (min) | Quartz Rec (%) | Water Rec (%) |
| A1 | 60 | 10 | 347.94 | 388.22 | 359.53 | 1.0 | 21.71 | 5.59 |
| A2 | 30 | 10 | 346.96 | 396.34 | 360.44 | 1.5 | 25.25 | 6.99 |
| A3 | 30 | 10 | 346.52 | 403.99 | 361.04 | 2.0 | 27.20 | 8.36 |
| A4 | 30 | 10 | 347.58 | 385.83 | 358.16 | 2.5 | 19.82 | 5.39 |
| A5 | 30 | 10 | 344.77 | 403.45 | 359.41 | 3.0 | 27.42 | 8.57 |
| A6 | 30 | 10 | 346.19 | 387.13 | 356.55 | 3.5 | 19.41 | 5.95 |
| A7 | 30 | 10 | 342.09 | 390.82 | 354.09 | 4.0 | 22.48 | 7.15 |
| A8 | 30 | 10 | 340.84 | 394.92 | 353.06 | 4.5 | 22.89 | 8.15 |
| A9 | 30 | 10 | 341.88 | 382.89 | 352.37 | 5.0 | 15.32 | 5.94 |
| A10 | 30 | 10 | 344.19 | 383.35 | 354.63 | 5.5 | 16.56 | 5.59 |
| A11 | 30 | 10 | 343.79 | 384.96 | 353.24 | 6.0 | 17.70 | 6.17 |
| A12 | 30 | 10 | 340.60 | 380.85 | 351.11 | 6.5 | 18.02 | 5.79 |
| S/State Quartz Recovery | | | **18.43** | % | Air Holdup | | 4.42 | % |
| S/State Water Recovery | | | **5.85** | % | Conditioning Time | | 11.5 | min |

Table 86 : Flotation Response of the Jameson Cell Configuration with the -106 μm Particle Size Fraction at a Collector Dosage of 80 g/t.

| | | | | | | | | |
|---|---|---|---|---|---|---|---|---|
| Pulp Flow Rate | | | 3.5 | l/min | Water pH | | 8.26 | |
| Air Flow Rate | | | 3.0 | l/min | Pulp pH | | 7.72 | |
| Measured Froth Depth | | | 20 | mm | Adjusted pH | | 7.00 | |
| Decrease in Pulp Level | | | 109 | mm | Fill-up Time | | 6.50 | min |
| Sample No | Sample Interval (s) | Sample Time (s) | Sample Bottle Mass (g) | Froth+ Bottle Mass (g) | Quartz+ Bottle Mass (g) | Flotation Time (min) | Quartz Rec (%) | Water Rec (%) |
| 1 | 60 | 10 | 343.65 | 490.50 | 400.72 | 1.0 | 97.83 | 15.99 |
| 2 | 30 | 10 | 346.06 | 496.45 | 404.25 | 1.5 | 99.75 | 16.43 |
| 3 | 30 | 10 | 347.22 | 491.19 | 401.40 | 2.0 | 92.88 | 16.00 |
| 4 | 30 | 10 | 348.21 | 488.22 | 401.59 | 2.5 | 91.51 | 15.43 |
| 5 | 30 | 10 | 345.14 | 497.47 | 399.81 | 3.0 | 93.72 | 17.40 |
| 6 | 30 | 10 | 344.88 | 186.58 | 396.10 | 3.5 | 87.81 | 16.12 |
| 7 | 30 | 10 | 346.86 | 501.90 | 397.77 | 4.0 | 87.27 | 18.55 |
| 8 | 30 | 10 | 348.66 | 474.66 | 390.40 | 4.5 | 71.55 | 15.01 |
| 9 | 30 | 10 | 345.70 | 464.84 | 385.83 | 5.0 | 68.79 | 14.08 |
| 10 | 30 | 10 | 346.55 | | | 5.5 | | |
| 11 | 30 | 10 | 345.28 | | | 6.0 | | |
| 12 | 30 | 10 | 344.42 | | | 6.5 | | |
| Steady State Quartz Recovery | | | **68.79** | % | Air Holdup | | 5.52 | % |
| Steady State Water Recovery | | | **14.08** | % | Conditioning Time | | 11.5 | min |

Table 87 : Flotation Response of the Jameson Cell Configuration with the -106 μm Particle Size Fraction at a Collector Dosage of 200 g/t.

| | | | | | | | | |
|---|---|---|---|---|---|---|---|---|
| Pulp Flow Rate | | | 3.5 | l/min | Water pH | | 8.25 | |
| Air Flow Rate | | | 3.0 | l/min | Pulp pH | | 7.50 | |
| Measured Froth Depth | | | 15 | mm | Adjusted pH | | 7.00 | |
| Decrease in Pulp Level | | | 126 | mm | Fill-up Time | | 6.50 | min |
| Sample No | Sample Interval (s) | Sample Time (s) | Sample Bottle Mass (g) | Froth+ Bottle Mass (g) | Quartz+ Bottle Mass (g) | Flotation Time (min) | Quartz Rec (%) | Water Rec (%) |
| 1 | 60 | 7 | 347.94 | 530.06 | 408.75 | 1.0 | 148.92 | 30.78 |
| 2 | 30 | 7 | 346.96 | 532.36 | 404.33 | 1.5 | 140.50 | 32.58 |
| 3 | 30 | 7 | 346.52 | 517.53 | 399.32 | 2.0 | 129.31 | 30.08 |
| 4 | 30 | 7 | 347.58 | 490.81 | 389.17 | 2.5 | 101.85 | 25.87 |
| 5 | 30 | 7 | 344.77 | 489.66 | 385.61 | 3.0 | 100.02 | 26.48 |
| 6 | 30 | 7 | 346.19 | 485.34 | 386.23 | 3.5 | 98.06 | 25.22 |
| 7 | 30 | 7 | 342.09 | 473.39 | 381.49 | 4.0 | 96.49 | 23.39 |
| 8 | 30 | 7 | 340.84 | 471.78 | 379.65 | 4.5 | 95.04 | 23.45 |
| 9 | 30 | 7 | 341.88 | 486.26 | 375.42 | 5.0 | 82.14 | 28.21 |
| 10 | 30 | 7 | 344.19 | 455.19 | 377.19 | 5.5 | 80.82 | 19.85 |
| 11 | 30 | 7 | 343.79 | 459.12 | 378.81 | 6.0 | 85.76 | 20.44 |
| 12 | 30 | 7 | 340.60 | 442.16 | 366.11 | 6.5 | 62.33 | 19.35 |
| Steady State Quartz Recovery | | | **95.53** | % | Air Holdup | | 6.34 | % |
| Steady State Water Recovery | | | **24.02** | % | Conditioning Time | | 11.5 | min |

Table 88 : Flotation Response of the Jameson Cell Configuration with the +106 -150 μm Particle Size Fraction with No Collector Added to the Pulp.

| | | | | | | | | |
|---|---|---|---|---|---|---|---|---|
| Pulp Flow Rate | | | 3.0 | l/min | Water pH | | 8.86 | |
| Air Flow Rate | | | 3.5 | l/min | Pulp pH | | 8.46 | |
| Measured Froth Depth | | | 20 | mm | Adjusted pH | | 7.00 | |
| Decrease in Pulp Level | | | 88 | mm | Fill-up Time | | 9.00 | min |
| Sample No | Sample Interval (s) | Sample Time (s) | Sample Bottle Mass (g) | Froth+ Bottle Mass (g) | Quartz+ Bottle Mass (g) | Flotation Time (min) | Quartz Rec (%) | Water Rec (%) |
| A1 | 60 | 10 | 347.94 | 347.94 | 347.94 | 1.0 | 0.00 | 0.00 |
| A2 | 30 | 10 | 346.96 | 346.96 | 346.96 | 1.5 | 0.00 | 0.00 |
| A3 | 30 | 10 | 346.52 | 346.52 | 346.52 | 2.0 | 0.00 | 0.00 |
| A4 | 30 | 10 | 347.58 | 347.58 | 347.58 | 2.5 | 0.00 | 0.00 |
| A5 | 30 | 10 | 344.77 | 344.77 | 344.77 | 3.0 | 0.00 | 0.00 |
| A6 | 30 | 10 | 346.19 | 346.19 | 346.19 | 3.5 | 0.00 | 0.00 |
| A7 | 30 | 10 | 342.09 | 342.09 | 342.09 | 4.0 | 0.00 | 0.00 |
| A8 | 30 | 10 | 340.84 | 340.84 | 340.84 | 4.5 | 0.00 | 0.00 |
| A9 | 30 | 10 | 344.14 | 344.14 | 344.14 | 5.0 | 0.00 | 0.00 |
| A10 | 30 | 10 | 344.19 | 344.19 | 344.19 | 5.5 | 0.00 | 0.00 |
| A11 | 30 | 10 | 343.79 | 343.79 | 343.79 | 6.0 | 0.00 | 0.00 |
| A12 | 30 | 10 | 341.49 | 341.49 | 341.49 | 6.5 | 0.00 | 0.00 |
| Steady State Quartz Recovery | | | **0.00** | % | Air Holdup | | 4.42 | % |
| Steady State Water Recovery | | | **0.00** | % | Conditioning Time | | 14.0 | min |

Table 89 : Flotation Response of the Jameson Cell Configuration with the +106 -150 μm Particle Size Fraction at a Collector Dosage of 25 g/t.

| | | | | | | | | |
|---|---|---|---|---|---|---|---|---|
| Pulp Flow Rate | | | 3.5 | l/min | Water pH | | 9.08 | |
| Air Flow Rate | | | 3.0 | l/min | Pulp pH | | 7.87 | |
| Measured Froth Depth | | | 20 | mm | Adjusted pH | | 7.00 | |
| Decrease in Pulp Level | | | 98 | mm | Fill-up Time | | 7.50 | min |
| Sample No | Sample Interval (s) | Sample Time (s) | Sample Bottle Mass (g) | Froth+ Bottle Mass (g) | Quartz+ Bottle Mass (g) | Flotation Time (min) | Quartz Rec (%) | Water Rec (%) |
| 1 | 60 | 10 | 343.69 | 349.77 | 347.44 | 1.0 | 6.41 | 0.41 |
| 2 | 30 | 10 | 347.88 | 349.75 | 348.81 | 1.5 | 1.59 | 0.17 |
| 3 | 30 | 10 | 347.25 | 350.50 | 348.81 | 2.0 | 2.67 | 0.30 |
| 4 | 30 | 10 | 348.24 | 351.85 | 350.21 | 2.5 | 3.37 | 0.29 |
| 5 | 30 | 10 | 345.18 | 346.47 | 345.72 | 3.0 | 0.92 | 0.13 |
| 6 | 30 | 10 | 344.70 | 348.20 | 346.55 | 3.5 | 3.16 | 0.29 |
| 7 | 30 | 10 | 346.88 | 347.67 | 347.15 | 4.0 | 0.46 | 0.09 |
| 8 | 30 | 10 | 348.72 | 353.01 | 351.11 | 4.5 | 4.09 | 0.34 |
| 9 | 30 | 10 | 345.71 | 345.87 | 345.72 | 5.0 | 0.02 | 0.03 |
| 10 | 30 | 10 | 346.57 | | | 5.5 | | |
| 11 | 30 | 10 | 345.31 | | | 6.0 | | |
| 12 | 30 | 10 | 344.44 | | | 6.5 | | |
| S/State Quartz Recovery | | | **2.00** | % | Air Holdup | | 4.97 | % |
| S/State Water Recovery | | | **0.20** | % | Conditioning Time | | 12.5 | min |

Table 90 : Flotation Response of the Jameson Cell Configuration with the +106 -150 μm Particle Size Fraction at a Collector Dosage of 80 g/t.

| | | | | | | | | |
|---|---|---|---|---|---|---|---|---|
| Pulp Flow Rate | | | 3.5 | l/min | Water pH | | 9.12 | |
| Air Flow Rate | | | 3.0 | l/min | Pulp pH | | 7.97 | |
| Measured Froth Depth | | | 22 | mm | Adjusted pH | | 7.00 | |
| Decrease in Pulp Level | | | 104 | mm | Fill-up Time | | 9.00 | min |
| Sample No | Sample Interval (s) | Sample Time (s) | Sample Bottle Mass (g) | Froth+ Bottle Mass (g) | Quartz+ Bottle Mass (g) | Flotation Time (min) | Quartz Rec (%) | Water Rec (%) |
| 1 | 60 | 10 | 343.69 | 392.94 | 368.35 | 1.0 | 42.15 | 4.37 |
| 2 | 30 | 10 | 347.88 | 414.62 | 377.75 | 1.5 | 51.06 | 6.55 |
| 3 | 30 | 10 | 347.25 | 397.84 | 371.69 | 2.0 | 41.78 | 4.65 |
| 4 | 30 | 10 | 348.24 | 398.55 | 372.59 | 2.5 | 41.62 | 4.61 |
| 5 | 30 | 10 | 345.18 | 391.38 | 367.46 | 3.0 | 38.09 | 4.25 |
| 6 | 30 | 10 | 344.70 | 390.67 | 367.26 | 3.5 | 38.56 | 4.16 |
| 7 | 30 | 10 | 346.88 | 389.78 | 367.27 | 4.0 | 34.85 | 4.00 |
| 8 | 30 | 10 | 348.72 | 395.49 | 371.46 | 4.5 | 38.87 | 4.27 |
| 9 | 30 | 10 | 345.71 | 389.78 | 367.21 | 5.0 | 36.75 | 4.01 |
| 10 | 30 | 10 | 346.57 | 393.36 | 369.38 | 5.5 | 38.99 | 4.26 |
| 11 | 30 | 10 | 345.31 | 392.06 | 367.90 | 6.0 | 38.62 | 4.29 |
| 12 | 30 | 10 | 344.44 | 391.90 | 367.57 | 6.5 | 39.54 | 4.32 |
| Steady State Quartz Recovery | | | **38.77** | % | Air Holdup | | 5.52 | % |
| Steady State Water Recovery | | | **4.28** | % | Conditioning Time | | 14.0 | min |

Table 91 : Flotation Response of the Jameson Cell Configuration with the +106 -150 μm Particle Size Fraction at a Collector Dosage of 200 g/t.

| | | | | | |
|---|---|---|---|---|---|
| Pulp Flow Rate | 3.5 | l/min | Water pH | 9.12 | |
| Air Flow Rate | 3.0 | l/min | Pulp pH | 7.90 | |
| Measured Froth Depth | 29 | mm | Adjusted pH | 7.00 | |
| Decrease in Pulp Level | 115 | mm | Fill-up Time | 11.5 | min |

| Sample No | Sample Interval (s) | Sample Time (s) | Sample Bottle Mass (g) | Froth+ Bottle Mass (g) | Quartz+ Bottle Mass (g) | Flotation Time (min) | Quartz Rec (%) | Water Rec (%) |
|---|---|---|---|---|---|---|---|---|
| 1 | 60 | 10 | 343.69 | 484.43 | 402.03 | 1.0 | 99.53 | 14.61 |
| 2 | 30 | 10 | 347.88 | 471.86 | 400.73 | 1.5 | 90.16 | 12.61 |
| 3 | 30 | 10 | 347.25 | 482.20 | 399.61 | 2.0 | 89.33 | 14.64 |
| 4 | 30 | 10 | 348.24 | 471.59 | 401.41 | 2.5 | 90.71 | 12.44 |
| 5 | 30 | 10 | 345.18 | 481.88 | 401.15 | 3.0 | 95.48 | 13.31 |
| 6 | 30 | 10 | 344.70 | 470.75 | 398.11 | 3.5 | 91.12 | 12.88 |
| 7 | 30 | 10 | 346.88 | 479.79 | 401.90 | 4.0 | 93.86 | 13.81 |
| 8 | 30 | 10 | 348.72 | 793.22 | 410.13 | 4.5 | 104.77 | 14.73 |
| 9 | 30 | 10 | 345.71 | 490.86 | 406.87 | 5.0 | 104.34 | 14.89 |
| 10 | 30 | 10 | 346.57 | 489.34 | 411.82 | 5.5 | 111.32 | 15.34 |
| 11 | 30 | 10 | 345.31 | 504.18 | 412.55 | 6.0 | 114.71 | 16.25 |
| 12 | 30 | 10 | 344.44 | 394.01 | 365.68 | 6.5 | 36.24 | 5.02 |

| | | | | | |
|---|---|---|---|---|---|
| Steady State Quartz Recovery | **90.07** | % | Air Holdup | 5.83 | % |
| Steady State Water Recovery | **13.23** | % | Conditioning Time | 16.5 | min |

Table 92 : Flotation Response of the Jameson Cell Configuration with the +150 -300 μm Particle Size Fraction with No Collector Added to the Pulp.

| | | | | | |
|---|---|---|---|---|---|
| Pulp Flow Rate | 3.6 | l/min | Water pH | 8.42 | |
| Air Flow Rate | 3.0 | l/min | Pulp pH | 8.44 | |
| Measured Froth Depth | 20 | mm | Adjusted pH | 7.00 | |
| Decrease in Pulp Level | 88 | mm | Fill-up Time | 7.00 | min |

| Sample No | Sample Interval (s) | Sample Time (s) | Sample Bottle Mass (g) | Froth+ Bottle Mass (g) | Quartz+ Bottle Mass (g) | Flotation Time (min) | Quartz Rec (%) | Water Rec (%) |
|---|---|---|---|---|---|---|---|---|
| 1 | 60 | 10 | 347.94 | 347.94 | 347.94 | 1.0 | 0.00 | 0.00 |
| 2 | 30 | 10 | 346.96 | 346.96 | 346.96 | 1.5 | 0.00 | 0.00 |
| 3 | 30 | 10 | 346.52 | 346.52 | 346.52 | 2.0 | 0.00 | 0.00 |
| 4 | 30 | 10 | 347.58 | 347.58 | 347.58 | 2.5 | 0.00 | 0.00 |
| 5 | 30 | 10 | 344.77 | 344.77 | 344.77 | 3.0 | 0.00 | 0.00 |
| 6 | 30 | 10 | 346.19 | 346.19 | 346.19 | 3.5 | 0.00 | 0.00 |
| 7 | 30 | 10 | 342.09 | 342.09 | 342.09 | 4.0 | 0.00 | 0.00 |
| 8 | 30 | 10 | 340.84 | 340.84 | 340.84 | 4.5 | 0.00 | 0.00 |
| 9 | 30 | 10 | 344.14 | 344.14 | 344.14 | 5.0 | 0.00 | 0.00 |
| 10 | 30 | 10 | 344.19 | 344.19 | 344.19 | 5.5 | 0.00 | 0.00 |
| 11 | 30 | 10 | 343.79 | 343.79 | 343.79 | 6.0 | 0.00 | 0.00 |
| 12 | 30 | 10 | 341.49 | 341.49 | 341.49 | 6.5 | 0.00 | 0.00 |

| | | | | | |
|---|---|---|---|---|---|
| Steady State Quartz Recovery | **0.00** | % | Air Holdup | 4.42 | % |
| Steady State Water Recovery | **0.00** | % | Conditioning Time | 12.0 | min |

Table 93 : Flotation Response of the Jameson Cell Configuration with the +150 -300 μm Particle Size Fraction at a Collector Dosage of 25 g/t.

| | | | | | | | | |
|---|---|---|---|---|---|---|---|---|
| Pulp Flow Rate | | | 3.5 | l/min | Water pH | | 8.13 | |
| Air Flow Rate | | | 3.0 | l/min | Pulp pH | | 8.22 | |
| Measured Froth Depth | | | 20 | mm | Adjusted pH | | 7.00 | |
| Decrease in Pulp Level | | | 120 | mm | Fill-up Time | | 6.00 | min |
| Sample No | Sample Interval (s) | Sample Time (s) | Sample Bottle Mass (g) | Froth+ Bottle Mass (g) | Quartz+ Bottle Mass (g) | Flotation Time (min) | Quartz Rec (%) | Water Rec (%) |
| 1 | 60 | 10 | 347.94 | 364.69 | 349.89 | 1.0 | 3.34 | 2.64 |
| 2 | 30 | 10 | 346.96 | 365.22 | 348.31 | 1.5 | 2.31 | 3.01 |
| 3 | 30 | 10 | 346.52 | 360.92 | 347.42 | 2.0 | 1.54 | 0.41 |
| 4 | 30 | 10 | 347.58 | 364.93 | 348.42 | 2.5 | 1.44 | 2.94 |
| 5 | 30 | 10 | 344.77 | 362.58 | 345.44 | 3.0 | 1.15 | 3.05 |
| 6 | 30 | 10 | 346.19 | 365.52 | 346.77 | 3.5 | 0.99 | 3.34 |
| 7 | 30 | 10 | 342.09 | 362.47 | 342.71 | 4.0 | 1.06 | 3.52 |
| 8 | 30 | 10 | 340.84 | 359.37 | 341.36 | 4.5 | 0.89 | 3.21 |
| 9 | 30 | 10 | 341.88 | 368.55 | 342.57 | 5.0 | 1.18 | 4.63 |
| 10 | 30 | 10 | 344.19 | 362.45 | 344.74 | 5.5 | 0.94 | 3.16 |
| 11 | 30 | 10 | 343.79 | 358.92 | 344.23 | 6.0 | 0.75 | 2.62 |
| 12 | 30 | 10 | 340.60 | | | 6.5 | | |
| S/State Quartz Recovery | | | **0.97** | % | Air Holdup | | 6.08 | % |
| S/State Water Recovery | | | **3.41** | % | Conditioning Time | | 11.0 | min |

Table 94 : Flotation Response of the Jameson Cell Configuration with the +150 -300 μm Particle Size Fraction at a Collector Dosage of 80 g/t.

| | | | | | | | | |
|---|---|---|---|---|---|---|---|---|
| Pulp Flow Rate | | | 3.5 | l/min | Water pH | | 8.13 | |
| Air Flow Rate | | | 3.0 | l/min | Pulp pH | | 8.14 | |
| Measured Froth Depth | | | 25 | mm | Adjusted pH | | 7.00 | |
| Decrease in Pulp Level | | | 143 | mm | Fill-up Time | | 6.50 | min |
| Sample No | Sample Interval (s) | Sample Time (s) | Sample Bottle Mass (g) | Froth+ Bottle Mass (g) | Quartz+ Bottle Mass (g) | Flotation Time (min) | Quartz Rec (%) | Water Rec (%) |
| 1 | 60 | 10 | 343.65 | 472.00 | 392.09 | 1.0 | 83.04 | 12.24 |
| 2 | 30 | 10 | 346.06 | 460.03 | 393.50 | 1.5 | 81.33 | 11.58 |
| 3 | 30 | 10 | 347.22 | 443.14 | 387.27 | 2.0 | 68.66 | 9.95 |
| 4 | 30 | 10 | 348.21 | 449.05 | 387.56 | 2.5 | 67.46 | 10.95 |
| 5 | 30 | 10 | 345.14 | 428.74 | 379.17 | 3.0 | 58.34 | 8.83 |
| 6 | 30 | 10 | 344.68 | 451.96 | 380.06 | 3.5 | 60.65 | 12.81 |
| 7 | 30 | 10 | 346.88 | 420.50 | .76.41 | 4.0 | 50.62 | 7.85 |
| 8 | 30 | 10 | 348.66 | 435.65 | 379.74 | 4.5 | 53.28 | 9.96 |
| 9 | 30 | 10 | 345.70 | 440.24 | 377.77 | 5.0 | 54.98 | 11.13 |
| 10 | 30 | 10 | 346.55 | 437.45 | 376.43 | 5.5 | 51.22 | 10.87 |
| 11 | 30 | 10 | 345.28 | 427.05 | 372.18 | 6.0 | 46.11 | 9.78 |
| 12 | 30 | 10 | 344.42 | 431.91 | 370.74 | 6.5 | 45.12 | 10.90 |
| Steady State Quartz Recovery | | | **51.24** | % | Air Holdup | | 7.22 | % |
| Steady State Water Recovery | | | **9.92** | % | Conditioning Time | | 11.5 | min |

Table 95 : Flotation Response of the Jameson Cell Configuration with the +150 -300 μm Particle Size Fraction at a Collector Dosage of 200 g/t.

| | | | | | | | |
|---|---|---|---|---|---|---|---|
| Pulp Flow Rate | 3.6 | l/min | Water pH | 8.42 | | | |
| Air Flow Rate | 3.0 | l/min | Pulp pH | 8.31 | | | |
| Measured Froth Depth | 20 | mm | Adjusted pH | 7.00 | | | |
| Decrease in Pulp Level | 219 | mm | Fill-up Time | 6.50 | min | | |

| Sample No | Sample Interval (s) | Sample Time (s) | Sample Bottle Mass (g) | Froth+ Bottle Mass (g) | Quartz+ Bottle Mass (g) | Flotation Time (min) | Quartz Rec (%) | Water Rec (%) |
|---|---|---|---|---|---|---|---|---|
| 1 | 60 | 10 | 347.94 | 473.21 | 387.24 | 1.0 | 72.46 | 12.66 |
| 2 | 30 | 10 | 346.96 | 450.22 | 390.12 | 1.5 | 71.93 | 10.41 |
| 3 | 30 | 10 | 346.52 | 470.60 | 389.74 | 2.0 | 72.03 | 14.01 |
| 4 | 30 | 10 | 347.58 | 463.24 | 379.21 | 2.5 | 71.45 | 13.23 |
| 5 | 30 | 10 | 344.77 | | | 3.0 | | |
| 6 | 30 | 10 | 346.19 | 475.36 | 391.73 | 3.5 | 72.57 | 14.56 |
| 7 | 30 | 10 | 342.09 | 466.31 | 387.27 | 4.0 | 68.63 | 12.96 |
| 8 | 30 | 10 | 340.84 | 470.02 | 390.99 | 4.5 | 70.25 | 12.96 |
| 9 | 30 | 10 | 341.88 | | | 5.0 | | |
| 10 | 30 | 10 | 344.19 | | | 5.5 | | |
| 11 | 30 | 10 | 343.79 | | | 6.0 | | |
| 12 | 30 | 10 | 340.60 | | | 6.5 | | |

| | | | | | |
|---|---|---|---|---|---|
| Steady State Quartz Recovery | **71.98** | % | Air Holdup | 11.05 | % |
| Steady State Water Recovery | **12.21** | % | Conditioning Time | 11.5 | min |

Table 96 : Flotation Response of the Jameson Cell Configuration with the +300 μm Particle Size Fraction with No Collector Added to the Pulp.

| | | | | | | | |
|---|---|---|---|---|---|---|---|
| Pulp Flow Rate | 3.6 | l/min | Water pH | 8.25 | | | |
| Air Flow Rate | 3.0 | l/min | Pulp pH | 7.96 | | | |
| Measured Froth Depth | 20 | mm | Adjusted pH | 7.00 | | | |
| Decrease in Pulp Level | 77 | mm | Fill-up Time | 7.00 | min | | |

| Sample No | Sample Interval (s) | Sample Time (s) | Sample Bottle Mass (g) | Froth+ Bottle Mass (g) | Quartz+ Bottle Mass (g) | Flotation Time (min) | Quartz Rec (%) | Water Rec (%) |
|---|---|---|---|---|---|---|---|---|
| 1 | 60 | 10 | 347.94 | 347.94 | 347.94 | 1.0 | 0.00 | 0.00 |
| 2 | 30 | 10 | 346.96 | 346.96 | 346.96 | 1.5 | 0.00 | 0.00 |
| 3 | 30 | 10 | 346.52 | 346.52 | 346.52 | 2.0 | 0.00 | 0.00 |
| 4 | 30 | 10 | 347.58 | 347.58 | 347.58 | 2.5 | 0.00 | 0.00 |
| 5 | 30 | 10 | 344.77 | 344.77 | 344.77 | 3.0 | 0.00 | 0.00 |
| 6 | 30 | 10 | 346.19 | 346.19 | 346.19 | 3.5 | 0.00 | 0.00 |
| 7 | 30 | 10 | 342.09 | 342.09 | 342.09 | 4.0 | 0.00 | 0.00 |
| 8 | 30 | 10 | 340.84 | 340.84 | 340.84 | 4.5 | 0.00 | 0.00 |
| 9 | 30 | 10 | 344.14 | 344.14 | 344.14 | 5.0 | 0.00 | 0.00 |
| 10 | 30 | 10 | 344.19 | 344.19 | 344.19 | 5.5 | 0.00 | 0.00 |
| 11 | 30 | 10 | 343.79 | 343.79 | 343.79 | 6.0 | 0.00 | 0.00 |
| 12 | 30 | 10 | 341.49 | 341.49 | 341.49 | 6.5 | 0.00 | 0.00 |

| | | | | | |
|---|---|---|---|---|---|
| Steady State Quartz Recovery | **0.00** | % | Air Holdup | 3.87 | % |
| Steady State Water Recovery | **0.00** | % | Conditioning Time | 12.0 | min |

Table 97 : Flotation Response of the Jameson Cell Configuration with the +300 μm Particle Size Fraction at a Collector Dosage of 25 g/t.

| | | | | | | | | |
|---|---|---|---|---|---|---|---|---|
| Pulp Flow Rate | | | 3.7 | l/min | Water pH | | 8.80 | |
| Air Flow Rate | | | 3.0 | l/min | Pulp pH | | 8.45 | |
| Measured Froth Depth | | | 20 | mm | Adjusted pH | | 7.00 | |
| Decrease in Pulp Level | | | 88 | mm | Fill-up Time | | 7.50 | min |
| Sample No | Sample Interval (s) | Sample Time (s) | Sample Bottle Mass (g) | Froth + Bottle Mass (g) | Quartz + Bottle Mass (g) | Flotation Time (min) | Quartz Rec (%) | Water Rec (%) |
| 1 | 60 | 10 | 343.69 | 364.42 | 354.20 | 1.0 | 17.00 | 1.72 |
| 2 | 30 | 10 | 347.88 | 355.60 | 350.09 | 1.5 | 3.57 | 0.93 |
| 3 | 30 | 10 | 347.25 | 373.66 | 359.62 | 2.0 | 20.01 | 2.36 |
| 4 | 30 | 10 | 348.24 | 353.50 | 350.26 | 2.5 | 3.27 | 0.54 |
| 5 | 30 | 10 | 345.18 | 357.33 | 351.37 | 3.0 | 10.01 | 1.00 |
| 6 | 30 | 10 | 344.70 | 349.52 | 346.81 | 3.5 | 3.41 | 0.46 |
| 7 | 30 | 10 | 346.88 | 357.85 | 352.88 | 4.0 | 9.70 | 0.84 |
| 8 | 30 | 10 | 348.72 | 358.24 | 353.05 | 4.5 | 7.00 | 0.87 |
| 9 | 30 | 10 | 345.71 | 358.89 | 353.17 | 5.0 | 12.06 | 0.96 |
| 10 | 30 | 10 | 346.57 | 350.27 | 348.05 | 5.5 | 2.39 | 0.37 |
| 11 | 30 | 10 | 345.31 | 349.76 | 347.28 | 6.0 | 3.19 | 0.42 |
| 12 | 30 | 10 | 344.44 | 347.63 | 345.77 | 6.5 | 2.15 | 0.31 |
| S/State Quartz Recovery | | | **8.44** | % | Air Holdup | | 4.42 | % |
| S/State Water Recovery | | | **0.83** | % | Conditioning Time | | 12.5 | min |

Table 98 : Flotation Response of the Jameson Cell Configuration with the +300 μm Particle Size Fraction at a Collector Dosage of 80 g/t.

| | | | | | | | | |
|---|---|---|---|---|---|---|---|---|
| Pulp Flow Rate | | | 3.5 | l/min | Water pH | | 9.11 | |
| Air Flow Rate | | | 3.0 | l/min | Pulp pH | | 8.67 | |
| Measured Froth Depth | | | 27 | mm | Adjusted pH | | 7.00 | |
| Decrease in Pulp Level | | | 121 | mm | Fill-up Time | | 6.50 | min |
| Sample No | Sample Interval (s) | Sample Time (s) | Sample Bottle Mass (g) | Froth + Bottle Mass (g) | Quartz + Bottle Mass (g) | Flotation Time (min) | Quartz Rec (%) | Water Rec (%) |
| 1 | 60 | 10 | 343.69 | 487.21 | 427.52 | 1.0 | 143.71 | 10.63 |
| 2 | 30 | 10 | 347.88 | 537.81 | 447.20 | 1.5 | 170.26 | 16.14 |
| 3 | 30 | 10 | 347.25 | 515.56 | 434.18 | 2.0 | 149.02 | 14.50 |
| 4 | 30 | 10 | 348.24 | 487.34 | 415.84 | 2.5 | 115.89 | 12.74 |
| 5 | 30 | 10 | 345.18 | 499.96 | 416.81 | 3.0 | 122.79 | 14.81 |
| 6 | 30 | 10 | 344.70 | 484.92 | 409.68 | 3.5 | 111.39 | 13.40 |
| 7 | 30 | 10 | 346.88 | 502.05 | 417.77 | 4.0 | 121.53 | 15.01 |
| 8 | 30 | 10 | 348.72 | 478.82 | 407.98 | 4.5 | 101.59 | 12.62 |
| 9 | 30 | 10 | 345.71 | 493.29 | 383.37 | 5.0 | 64.56 | 19.58 |
| 10 | 30 | 10 | 346.57 | 454.11 | 381.55 | 5.5 | 59.96 | 12.93 |
| 11 | 30 | 10 | 345.31 | 462.59 | 387.34 | 6.0 | 72.05 | 13.41 |
| 12 | 30 | 10 | 344.44 | 416.40 | 367.89 | 6.5 | 40.20 | 8.64 |
| Steady State Quartz Recovery | | | **65.52** | % | Air Holdup | | 6.10 | % |
| Steady State Water Recovery | | | **15.31** | % | Conditioning Time | | 11.5 | min |

Table 99 : Flotation Response of the Jameson Cell Configuration with the +300 μm Particle Size Fraction at a Collector Dosage of 200 g/t.

| | | | | | | | | |
|---|---|---|---|---|---|---|---|---|
| Pulp Flow Rate | | | 3.7 | l/min | Water pH | | 8.97 | |
| Air Flow Rate | | | 3.0 | l/min | Pulp pH | | 8.35 | |
| Measured Froth Depth | | | 21 | mm | Adjusted pH | | 7.00 | |
| Decrease in Pulp Level | | | 241 | mm | Fill-up Time | | 7.00 | min |
| Sample No | Sample Interval (s) | Sample Time (s) | Sample Bottle Mass (g) | Froth+ Bottle Mass (g) | Quartz+ Bottle Mass (g) | Flotation Time (min) | Quartz Rec (%) | Water Rec (%) |
| 1 | 60 | 10 | 345.18 | 494.58 | 412.69 | 1.0 | 109.18 | 13.76 |
| 2 | 30 | 10 | 346.97 | 484.12 | 409.35 | 1.5 | 100.88 | 12.57 |
| 3 | 30 | 10 | 346.53 | 493.96 | 409.25 | 2.0 | 101.43 | 14.24 |
| 4 | 30 | 10 | 347.59 | 506.35 | 411.21 | 2.5 | 102.89 | 15.99 |
| 5 | 30 | 10 | 344.78 | 486.16 | 401.89 | 3.0 | 92.36 | 14.16 |
| 6 | 30 | 10 | 346.20 | 490.94 | 401.27 | 3.5 | 89.06 | 15.07 |
| 7 | 30 | 10 | 342.09 | 480.59 | 394.70 | 4.0 | 85.08 | 14.44 |
| 8 | 30 | 10 | 340.84 | 483.84 | 389.64 | 4.5 | 78.92 | 15.83 |
| 9 | 30 | 10 | 344.15 | 470.67 | 385.26 | 5.0 | 66.49 | 14.35 |
| 10 | 30 | 10 | 344.20 | 486.56 | 387.87 | 5.5 | 70.63 | 16.59 |
| 11 | 30 | 10 | 343.81 | 490.00 | 386.25 | 6.0 | 68.64 | 17.44 |
| 12 | 30 | 10 | 345.62 | 481.35 | 382.26 | 6.5 | 59.26 | 16.65 |
| Steady State Quartz Recovery | | | **66.25** | % | Air Holdup | | 12.16 | % |
| Steady State Water Recovery | | | **16.26** | % | Conditioning Time | | 12.0 | min |

Table 100 : Flotation Response of the Jameson Cell Configuration with the +300 μm Particle Size Fraction at a Collector Dosage of 200 g/t (40 g/t Dispersant Added).

| | | | | | | | | |
|---|---|---|---|---|---|---|---|---|
| Pulp Flow Rate | | | 3.6 | l/min | Water pH | | 8.60 | |
| Air Flow Rate | | | 3.0 | l/min | Pulp pH | | 8.42 | |
| Measured Froth Depth | | | 20 | mm | Adjusted pH | | 7.00 | |
| Decrease in Pulp Level | | | 241 | mm | Fill-up Time | | 8.00 | min |
| Sample No | Sample Interval (s) | Sample Time (s) | Sample Bottle Mass (g) | Froth+ Bottle Mass (g) | Quartz+ Bottle Mass (g) | Flotation Time (min) | Quartz Rec (%) | Water Rec (%) |
| 1 | 60 | 10 | 347.94 | 436.78 | 369.06 | 1.0 | 35.41 | 11.80 |
| 2 | 30 | 10 | 346.96 | 428.79 | 368.47 | 1.5 | 36.06 | 10.51 |
| 3 | 30 | 10 | 346.52 | 411.13 | 367.47 | 2.0 | 35.12 | 7.61 |
| 4 | 30 | 10 | 347.58 | 442.77 | 373.63 | 2.5 | 43.67 | 12.05 |
| 5 | 30 | 10 | 344.77 | 447.79 | 371.04 | 3.0 | 44.04 | 13.37 |
| 6 | 30 | 10 | 346.19 | 458.49 | 379.68 | 3.5 | 56.14 | 13.73 |
| 7 | 30 | 10 | 342.09 | 467.43 | 384.79 | 4.0 | 71.58 | 14.40 |
| 8 | 30 | 10 | 340.84 | 462.20 | 382.93 | 4.5 | 70.56 | 13.81 |
| 9 | 30 | 10 | 341.88 | 465.98 | 380.73 | 5.0 | 61.34 | 14.85 |
| 10 | 30 | 10 | 344.19 | 468.42 | 384.85 | 5.5 | 38.16 | 14.56 |
| 11 | 30 | 10 | 343.79 | 468.60 | 385.77 | 6.0 | 70.38 | 14.43 |
| 12 | 30 | 10 | 340.60 | | | 6.5 | | |
| Steady State Quartz Recovery | | | **68.41** | % | Air Holdup | | 12.15 | % |
| Steady State Water Recovery | | | **14.41** | % | Conditioning Time | | 13.0 | min |

Table 101 : Flotation Response of the Laboratory Batch Cell with the -106 μm Particle Size Fraction with No Collector Added to the Pulp.

| Air Flow Rate | 3 | l/min | Water pH | 8.29 |
|---|---|---|---|---|
| Measured Froth Depth | 10 | mm | Adjusted pH | 7.00 |

| Sampl No | Pan Mass (g) | Froth + Pan Mass (g) | Quartz + Pan Mass (g) | Bottle Mass (g) | Wash Water Mass 1 (g) | Wash Water Mass 2 (g) | Flot Time (min) | Cum Quartz Rec (%) | Cum Water Rec (%) |
|---|---|---|---|---|---|---|---|---|---|
| 1 | 370.91 | 370.91 | 370.91 | 343.65 | 535.32 | 535.32 | 0.5 | 0.00 | 0.00 |
| 2 | 377.60 | 377.60 | 377.60 | 346.06 | 520.29 | 520.29 | 1.0 | 0.00 | 0.00 |
| 3 | 357.63 | 357.63 | 357.63 | 347.22 | 479.18 | 479.18 | 1.5 | 0.00 | 0.00 |
| 4 | 383.89 | 383.89 | 383.89 | 348.21 | 534.04 | 534.04 | 2.0 | 0.00 | 0.00 |
| 5 | 363.86 | 363.86 | 363.86 | 345.14 | 529.75 | 529.75 | 2.5 | 0.00 | 0.00 |
| 6 | 364.39 | 364.39 | 364.39 | 344.68 | 512.18 | 512.18 | 3.0 | 0.00 | 0.00 |
| 7 | 363.18 | 363.18 | 363.18 | 346.88 | 573.67 | 573.67 | 3.5 | 0.00 | 0.00 |
| 8 | 359.60 | 359.60 | 359.60 | 348.66 | 513.28 | 513.28 | 4.0 | 0.00 | 0.00 |
| 9 | 371.74 | 371.74 | 371.74 | 345.70 | 558.06 | 558.06 | 4.5 | 0.00 | 0.00 |

| Cumulative Quartz Recovery | **0.00** | % | Conditioning | 5.0 | min |
|---|---|---|---|---|---|
| Cumulative Water Recovery | **0.00** | % | Time | | |

Table 102 : Flotation Response of the Laboratory Batch Cell with the -106 μm Particle Size Fraction at a Collector Dosage of 25 g/t.

| Air Flow Rate | 3 | l/min | Water pH | 8.29 |
|---|---|---|---|---|
| Measured Froth Depth | 10 | mm | Adjusted pH | 7.00 |

| Sampl No | Pan Mass (g) | Froth + Pan Mass (g) | Quartz + Pan Mass (g) | Bottle Mass (g) | Wash Water Mass 1 (g) | Wash Water Mass 2 (g) | Flot Time (min) | Cum Quartz Rec (%) | Cum Water Rec (%) |
|---|---|---|---|---|---|---|---|---|---|
| 1 | 370.91 | 446.08 | 360.89 | 343.65 | 535.32 | 516.51 | 0.5 | 5.75 | 1.36 |
| 2 | 377.60 | 439.52 | 359.60 | 346.06 | 520.29 | 495.90 | 1.0 | 10.26 | 2.19 |
| 3 | 357.63 | 393.43 | 354.01 | 347.22 | 479.18 | 460.95 | 1.5 | 12.52 | 2.56 |
| 4 | 383.89 | 414.01 | 352.86 | 348.21 | 534.04 | 515.41 | 2.0 | 14.07 | 2.80 |
| 5 | 363.86 | 392.01 | 348.58 | 345.14 | 529.75 | 509.64 | 2.5 | 15.22 | 2.96 |
| 6 | 364.39 | 394.93 | 347.39 | 344.68 | 512.18 | 487.94 | 3.0 | 16.06 | 3.09 |
| 7 | 363.18 | 379.64 | 348.44 | 346.88 | 573.67 | 562.12 | 3.5 | 16.58 | 3.20 |
| 8 | 359.60 | 388.23 | 350.16 | 348.66 | 513.28 | 488.39 | 4.0 | 17.08 | 3.28 |
| 9 | 371.74 | 371.74 | 345.70 | 345.70 | 558.06 | 558.06 | 4.5 | 17.08 | 3.28 |

| Cumulative Quartz Recovery | **17.08** | % | Conditioning | 6.0 | min |
|---|---|---|---|---|---|
| Cumulative Water Recovery | **3.28** | % | Time | | |

Table 103 : Flotation Response of the Laboratory Batch Cell with the -106 μm Particle Size Fraction at a Collector Dosage of 50 g/t.

| Air Flow Rate | 3 | l/min | Water pH | 8.29 |
|---|---|---|---|---|
| Measured Froth Depth | 10 | mm | Adjusted pH | 7.00 |

| Sampl No | Pan Mass (g) | Froth + Pan Mass (g) | Quartz + Pan Mass (g) | Bottle Mass (g) | Wash Water Mass 1 (g) | Wash Water Mass 2 (g) | Flot Time (min) | Cum Quartz Rec (%) | Cum Water Rec (%) |
|---|---|---|---|---|---|---|---|---|---|
| 1 | 370.91 | 507.22 | 423.15 | 343.65 | 534.18 | 516.51 | 0.5 | 17.41 | 2.30 |
| 2 | 377.60 | 481.02 | 405.11 | 346.06 | 519.56 | 495.90 | 1.0 | 26.58 | 4.11 |
| 3 | 357.63 | 417.76 | 376.15 | 347.22 | 479.18 | 460.95 | 1.5 | 32.76 | 4.92 |
| 4 | 383.89 | 426.91 | 396.44 | 348.21 | 534.04 | 515.41 | 2.0 | 36.94 | 5.33 |
| 5 | 363.86 | 398.22 | 373.78 | 345.14 | 529.75 | 509.64 | 2.5 | 40.25 | 5.46 |
| 6 | 364.39 | 391.47 | 367.81 | 344.68 | 512.18 | 487.94 | 3.0 | 41.39 | 5.51 |
| 7 | 363.18 | 381.62 | 366.89 | 346.88 | 573.67 | 562.12 | 3.5 | 42.62 | 5.57 |
| 8 | 359.60 | 389.05 | 363.01 | 348.66 | 513.28 | 488.39 | 4.0 | 43.76 | 5.61 |
| 9 | 371.74 | 372.89 | 371.74 | 345.70 | 558.06 | 558.06 | 4.5 | 43.76 | 5.65 |

| Cumulative Quartz Recovery | **43.76** | % | Conditioning Time | 5.0 | min |
|---|---|---|---|---|---|
| Cumulative Water Recovery | **5.65** | % | | | |

Table 104 : Flotation Response of the Laboratory Batch Cell with the -106 μm Particle Size Fraction at a Collector Dosage of 80 g/t.

| Air Flow Rate | 3 | l/min | Water pH | 8.29 |
|---|---|---|---|---|
| Measured Froth Depth | 20 | mm | Adjusted pH | 7.00 |

| Sampl No | Pan Mass (g) | Froth + Pan Mass (g) | Quartz + Pan Mass (g) | Bottle Mass (g) | Wash Water Mass 1 (g) | Wash Water Mass 2 (g) | Flot Time (min) | Cum Quartz Rec (%) | Cum Water Rec (%) |
|---|---|---|---|---|---|---|---|---|---|
| 1 | 370.91 | 560.26 | 429.65 | 347.94 | 535.63 | 515.74 | 0.5 | 27.24 | 3.04 |
| 2 | 377.60 | 559.91 | 427.48 | 346.96 | 495.90 | 478.02 | 1.0 | 54.08 | 5.95 |
| 3 | 357.63 | 438.59 | 376.61 | 346.52 | 460.95 | 443.55 | 1.5 | 64.11 | 7.11 |
| 4 | 383.89 | 433.78 | 361.22 | 347.58 | 515.41 | 494.93 | 2.0 | 68.65 | 7.65 |
| 5 | 363.86 | 399.14 | 351.26 | 344.77 | 509.64 | 487.57 | 2.5 | 70.82 | 7.88 |
| 6 | 364.39 | 391.80 | 348.67 | 346.19 | 487.94 | 464.65 | 3.0 | 71.64 | 7.94 |
| 7 | 363.18 | 385.07 | 344.98 | 342.09 | 562.12 | 453.05 | 3.5 | 72.61 | 7.96 |
| 8 | 359.60 | 384.50 | 342.31 | 340.84 | 488.39 | 466.29 | 4.0 | 73.10 | 7.99 |
| 9 | 371.74 | 371.74 | 341.88 | 341.88 | 558.06 | 558.06 | 4.5 | 73.10 | 7.99 |

| Cumulative Quartz Recovery | **73.10** | % | Conditioning Time | 5.0 | min |
|---|---|---|---|---|---|
| Cumulative Water Recovery | **7.99** | % | | | |

Table 105 : Flotation Response of the Laboratory Batch Cell with the -106 μm Particle Size Fraction at a Collector Dosage of 160 g/t.

| Air Flow Rate | 3 | l/min | Water pH | 8.29 |
|---|---|---|---|---|
| Measured Froth Depth | 10 | mm | Adjusted pH | 7.00 |

| Sampl No | Pan Mass (g) | Froth + Pan Mass (g) | Quartz + Pan Mass (g) | Bottle Mass (g) | Wash Water Mass 1 (g) | Wash Water Mass 2 (g) | Flot Time (min) | Cum Quartz Rec (%) | Cum Water Rec (%) |
|---|---|---|---|---|---|---|---|---|---|
| 1 | 370.91 | 392.39 | 512.86 | 343.65 | 535.63 | 515.74 | 0.5 | 47.32 | 5.53 |
| 2 | 377.60 | 598.75 | 431.04 | 346.06 | 495.90 | 478.02 | 1.0 | 65.13 | 10.72 |
| 3 | 357.63 | 435.18 | 381.12 | 347.22 | 460.95 | 443.55 | 1.5 | 72.96 | 11.99 |
| 4 | 383.89 | 431.99 | 399.10 | 348.21 | 515.41 | 494.93 | 2.0 | 78.03 | 12.42 |
| 5 | 363.86 | 397.82 | 369.98 | 345.14 | 509.64 | 487.57 | 2.5 | 80.07 | 12.62 |
| 6 | 364.39 | 393.84 | 368.53 | 344.68 | 487.94 | 464.65 | 3.0 | 81.45 | 12.69 |
| 7 | 363.18 | 390.66 | 370.44 | 346.88 | 562.12 | 543.05 | 3.5 | 83.87 | 12.73 |
| 8 | 359.60 | 385.66 | 362.33 | 348.66 | 488.39 | 466.29 | 4.0 | 84.78 | 12.75 |
| 9 | 371.74 | 374.67 | 374.38 | 345.70 | 558.06 | 558.06 | 4.5 | 85.66 | 12.76 |

| Cumulative Quartz Recovery | **85.66** | % | Conditioning Time | 5.0 | min |
|---|---|---|---|---|---|
| Cumulative Water Recovery | **12.76** | % | | | |

Table 106 : Flotation Response of the Laboratory Batch Cell with the -106 μm Particle Size Fraction at a Collector Dosage of 200 g/t.

| Air Flow Rate | 3 | l/min | Water pH | 8.29 |
|---|---|---|---|---|
| Measured Froth Depth | 28 | mm | Adjusted pH | 7.00 |

| Sampl No | Pan Mass (g) | Froth + Pan Mass (g) | Quartz + Pan Mass (g) | Bottle Mass (g) | Wash Water Mass 1 (g) | Wash Water Mass 2 (g) | Flot Time (min) | Cum Quartz Rec (%) | Cum Water Rec (%) |
|---|---|---|---|---|---|---|---|---|---|
| 1 | 370.91 | 769.36 | 524.31 | 343.65 | 450.92 | 436.09 | 0.5 | 51.13 | 7.97 |
| 2 | 377.60 | 698.06 | 472.78 | 346.06 | 478.02 | 458.66 | 1.0 | 82.86 | 15.11 |
| 3 | 357.63 | 458.49 | 377.62 | 347.22 | 443.55 | 421.87 | 1.5 | 89.52 | 17.16 |
| 4 | 383.89 | 414.43 | 386.89 | 348.21 | 494.93 | 474.65 | 2.0 | 90.52 | 17.41 |
| 5 | 363.86 | 390.48 | 364.74 | 345.14 | 487.57 | 461.86 | 2.5 | 90.82 | 17.41 |
| 6 | 364.39 | 383.32 | 365.01 | 344.68 | 464.65 | 446.60 | 3.0 | 91.02 | 17.42 |
| 7 | 363.18 | 379.41 | 363.70 | 346.88 | 543.05 | 527.05 | 3.5 | 91.20 | 17.42 |
| 8 | 359.60 | 380.88 | 359.76 | 348.66 | 466.29 | 443.25 | 4.0 | 91.25 | 17.34 |
| 9 | 371.74 | 371.74 | 371.74 | 345.70 | 558.06 | 558.06 | 4.5 | 91.25 | 17.34 |

| Cumulative Quartz Recovery | **91.25** | % | Conditioning Time | 5.0 | min |
|---|---|---|---|---|---|
| Cumulative Water Recovery | **17.34** | % | | | |

Table 107 : Flotation Response of the Laboratory Batch Cell with the +106 -150 μm Particle Size Fraction with No Collector Added to the Pulp.

| Air Flow Rate | 3 | l/min | Water pH | 8.75 |
|---|---|---|---|---|
| Measured Froth Depth | 20 | mm | Adjusted pH | 7.00 |

| Sampl No | Pan Mass (g) | Froth+ Pan Mass (g) | Quartz +Pan Mass (g) | Bottle Mass (g) | Wash Water Mass 1 (g) | Wash Water Mass 2 (g) | Flot Time (min) | Cum Quartz Rec (%) | Cum Water Rec (%) |
|---|---|---|---|---|---|---|---|---|---|
| 1 | 370.98 | 370.98 | 370.98 | 343.65 | 386.60 | 386.60 | 0.5 | 0.00 | 0.00 |
| 2 | 377.67 | 377.67 | 377.67 | 346.06 | 275.15 | 275.15 | 1.0 | 0.00 | 0.00 |
| 3 | 357.63 | 357.63 | 357.63 | 347.22 | 265.84 | 265.84 | 1.5 | 0.00 | 0.00 |
| 4 | 383.86 | 383.86 | 383.86 | 348.21 | 234.64 | 234.64 | 2.0 | 0.00 | 0.00 |
| 5 | 363.86 | 363.86 | 363.86 | 345.14 | 308.34 | 308.34 | 2.5 | 0.00 | 0.00 |
| 6 | 364.39 | 364.39 | 364.39 | 344.68 | 362.25 | 362.25 | 3.0 | 0.00 | 0.00 |
| 7 | 363.18 | 363.18 | 363.18 | 346.88 | 386.63 | 386.63 | 3.5 | 0.00 | 0.00 |
| 8 | 359.60 | 359.60 | 359.60 | 348.66 | 364.92 | 364.92 | 4.0 | 0.00 | 0.00 |
| 9 | 371.74 | 371.74 | 371.74 | 345.70 | 517.49 | 517.49 | 4.5 | 0.00 | 0.00 |

| Cumulative Quartz Recovery | **0.00** | % | Conditioning | 5.0 | min |
|---|---|---|---|---|---|
| Cumulative Water Recovery | **0.00** | % | Time | | |

Table 108 : Flotation Response of the Laboratory Batch Cell with the +106 -150 μm Particle Size Fraction at a Collector Dosage of 25 g/t.

| Air Flow Rate | 3 | l/min | Water pH | 8.75 |
|---|---|---|---|---|
| Measured Froth Depth | 20 | mm | Adjusted pH | 7.00 |

| Sampl No | Pan Mass (g) | Froth+ Pan Mass (g) | Quartz +Pan Mass (g) | Bottle Mass (g) | Wash Water Mass 1 (g) | Wash Water Mass 2 (g) | Flot Time (min) | Cum Quartz Rec (%) | Cum Water Rec (%) |
|---|---|---|---|---|---|---|---|---|---|
| 1 | 370.98 | 370.98 | 370.98 | 343.65 | 537.79 | 537.79 | 0.5 | 0.00 | 0.00 |
| 2 | 377.67 | 377.67 | 377.67 | 346.06 | 548.34 | 548.34 | 1.0 | 0.00 | 0.00 |
| 3 | 357.63 | 357.63 | 357.63 | 347.22 | 530.14 | 530.14 | 1.5 | 0.00 | 0.00 |
| 4 | 383.91 | 383.91 | 383.91 | 348.21 | 529.85 | 529.85 | 2.0 | 0.00 | 0.00 |
| 5 | 363.86 | 363.86 | 363.86 | 345.14 | 541.85 | 541.85 | 2.5 | 0.00 | 0.00 |
| 6 | 364.39 | 364.39 | 364.39 | 344.68 | 538.74 | 538.74 | 3.0 | 0.00 | 0.00 |
| 7 | 363.18 | 363.18 | 363.18 | 346.88 | 533.69 | 533.69 | 3.5 | 0.00 | 0.00 |
| 8 | 359.60 | 359.60 | 359.60 | 348.66 | 545.13 | 545.13 | 4.0 | 0.00 | 0.00 |
| 9 | 371.74 | 371.74 | 371.74 | 345.70 | 517.49 | 517.49 | 4.5 | 0.00 | 0.00 |

| Cumulative Quartz Recovery | **0.00** | % | Conditioning | 5.0 | min |
|---|---|---|---|---|---|
| Cumulative Water Recovery | **0.00** | % | Time | | |

Table 109 : Flotation Response of the Laboratory Batch Cell with the +106 -150 μm Particle Size Fraction at a Collector Dosage of 50 g/t.

| Air Flow Rate | 3 | l/min | Water pH | 8.88 |
|---|---|---|---|---|
| Measured Froth Depth | 12 | mm | Adjusted pH | 7.00 |

| Sampl No | Pan Mass (g) | Froth+ Pan Mass (g) | Quartz +Pan Mass (g) | Bottle Mass (g) | Wash Water Mass 1 (g) | Wash Water Mass 2 (g) | Flot Time (min) | Cum Quartz Rec (%) | Cum Water Rec (%) |
|---|---|---|---|---|---|---|---|---|---|
| 1 | 370.98 | 429.26 | 388.83 | 343.65 | 425.21 | 399.15 | 0.5 | 5.95 | 0.50 |
| 2 | 377.67 | 420.97 | 388.15 | 346.06 | 443.84 | 421.59 | 1.0 | 9.44 | 0.86 |
| 3 | 357.63 | 390.70 | 362.31 | 347.22 | 438.43 | 418.17 | 1.5 | 11.00 | 1.15 |
| 4 | 383.86 | 411.49 | 386.24 | 348.21 | 443.90 | 424.61 | 2.0 | 11.78 | 1.35 |
| 5 | 363.86 | 392.40 | 364.91 | 345.14 | 435.24 | 413.89 | 2.5 | 12.13 | 1.56 |
| 6 | 364.39 | 387.72 | 364.70 | 344.68 | 470.83 | 452.92 | 3.0 | 12.23 | 1.74 |
| 7 | 363.18 | 385.16 | 363.29 | 346.88 | 447.32 | 428.93 | 3.5 | 12.27 | 1.86 |
| 8 | 359.60 | 374.36 | 359.63 | 348.66 | 459.50 | 446.94 | 4.0 | 12.28 | 1.94 |
| 9 | 371.74 | 371.74 | 371.74 | 345.70 | 417.49 | 417.49 | 4.5 | 12.28 | 1.94 |

| Cumulative Quartz Recovery | **12.28** | % | Conditioning Time | 5.0 | min |
|---|---|---|---|---|---|
| Cumulative Water Recovery | **1.94** | % | | | |

Table 110 : Flotation Response of the Laboratory Batch Cell with the +106 -150 μm Particle Size Fraction at a Collector Dosage of 80 g/t.

| Air Flow Rate | 3 | l/min | Water pH | 8.75 |
|---|---|---|---|---|
| Measured Froth Depth | 13 | mm | Adjusted pH | 7.00 |

| Sampl No | Pan Mass (g) | Froth+ Pan Mass (g) | Quartz +Pan Mass (g) | Bottle Mass (g) | Wash Water Mass 1 (g) | Wash Water Mass 2 (g) | Flot Time (min) | Cum Quartz Rec (%) | Cum Water Rec (%) |
|---|---|---|---|---|---|---|---|---|---|
| 1 | 370.98 | 533.42 | 449.52 | 343.65 | 537.79 | 501.59 | 0.5 | 26.18 | 1.65 |
| 2 | 377.67 | 502.75 | 433.26 | 346.06 | 548.34 | 519.68 | 1.0 | 44.71 | 3.07 |
| 3 | 357.63 | 415.57 | 376.00 | 347.22 | 530.14 | 506.66 | 1.5 | 50.83 | 3.62 |
| 4 | 383.86 | 424.66 | 392.31 | 348.21 | 529.85 | 505.77 | 2.0 | 53.63 | 3.91 |
| 5 | 363.86 | 407.61 | 369.45 | 345.14 | 541.85 | 510.12 | 2.5 | 55.50 | 4.13 |
| 6 | 364.39 | 393.40 | 367.08 | 344.68 | 538.74 | 518.43 | 3.0 | 56.39 | 4.34 |
| 7 | 363.18 | 393.03 | 365.29 | 346.88 | 533.69 | 512.30 | 3.5 | 57.10 | 4.56 |
| 8 | 359.60 | 391.30 | 360.44 | 348.66 | 545.13 | 519.37 | 4.0 | 57.38 | 4.74 |
| 9 | 371.74 | 371.74 | 371.74 | 345.70 | 517.49 | 517.49 | 4.5 | 57.38 | 4.74 |

| Cumulative Quartz Recovery | **57.38** | % | Conditioning Time | 5.0 | min |
|---|---|---|---|---|---|
| Cumulative Water Recovery | **4.74** | % | | | |

Table 111 : Flotation Response of the Laboratory Batch Cell with the +106 -150 μm Particle Size Fraction at a Collector Dosage of 160 g/t.

| Air Flow Rate | 3 | l/min | Water pH | 8.80 |
|---|---|---|---|---|
| Measured Froth Depth | 11 | mm | Adjusted pH | 7.00 |

| Sampl No | Pan Mass (g) | Froth+ Pan Mass (g) | Quartz +Pan Mass (g) | Bottle Mass (g) | Wash Water Mass 1 (g) | Wash Water Mass 2 (g) | Flot Time (min) | Cum Quartz Rec (%) | Cum Water Rec (%) |
|---|---|---|---|---|---|---|---|---|---|
| 1 | 370.98 | 665.60 | 518.00 | 343.65 | 399.12 | 375.05 | 0.5 | 49.01 | 4.28 |
| 2 | 377.67 | 576.14 | 456.40 | 346.06 | 421.55 | 397.70 | 1.0 | 75.25 | 7.60 |
| 3 | 357.63 | 445.70 | 376.25 | 347.22 | 418.05 | 396.10 | 1.5 | 81.46 | 9.25 |
| 4 | 383.86 | 447.68 | 393.78 | 348.21 | 424.53 | 402.43 | 2.0 | 84.75 | 10.35 |
| 5 | 363.86 | 419.76 | 368.59 | 345.14 | 413.70 | 387.86 | 2.5 | 86.32 | 11.23 |
| 6 | 364.39 | 417.35 | 367.66 | 344.68 | 452.74 | 433.15 | 3.0 | 87.41 | 12.27 |
| 7 | 363.18 | 414.85 | 364.80 | 346.88 | 428.86 | 406.38 | 3.5 | 87.95 | 13.22 |
| 8 | 359.60 | 393.68 | 360.05 | 348.66 | 446.84 | 433.28 | 4.0 | 88.10 | 13.92 |
| 9 | 371.74 | 371.74 | 371.74 | 345.70 | 517.46 | 517.46 | 4.5 | 88.10 | 13.92 |

| Cumulative Quartz Recovery | **88.10** | % | Conditioning Time | 5.0 | min |
|---|---|---|---|---|---|
| Cumulative Water Recovery | **13.92** | % | | | |

Table 112 : Flotation Response of the Laboratory Batch Cell with the +106 -150 μm Particle Size Fraction at a Collector Dosage of 200 g/t.

| Air Flow Rate | 3 | l/min | Water pH | 8.67 |
|---|---|---|---|---|
| Measured Froth Depth | 15 | mm | Adjusted pH | 7.00 |

| Sampl No | Pan Mass (g) | Froth+ Pan Mass (g) | Quartz +Pan Mass (g) | Bottle Mass (g) | Wash Water Mass 1 (g) | Wash Water Mass 2 (g) | Flot Time (min) | Cum Quartz Rec (%) | Cum Water Rec (%) |
|---|---|---|---|---|---|---|---|---|---|
| 1 | 370.98 | 749.99 | 495.18 | 343.65 | 501.48 | 477.48 | 0.5 | 50.51 | 7.05 |
| 2 | 377.67 | 651.40 | 425.73 | 346.06 | 519.62 | 494.61 | 1.0 | 77.07 | 12.90 |
| 3 | 357.63 | 497.45 | 377.73 | 347.22 | 506.55 | 485.36 | 1.5 | 87.24 | 15.96 |
| 4 | 383.86 | 445.09 | 353.91 | 348.21 | 505.73 | 488.31 | 2.0 | 89.14 | 17.28 |
| 5 | 363.86 | 412.23 | 347.44 | 345.14 | 509.97 | 484.28 | 2.5 | 89.90 | 17.98 |
| 6 | 364.39 | 394.52 | 346.08 | 344.68 | 518.24 | 502.44 | 3.0 | 90.37 | 18.43 |
| 7 | 363.18 | 400.36 | 348.11 | 346.88 | 512.21 | 484.97 | 3.5 | 90.78 | 18.73 |
| 8 | 359.60 | 390.65 | 349.78 | 348.66 | 519.15 | 502.44 | 4.0 | 91.15 | 19.19 |
| 9 | 371.74 | 371.74 | 371.74 | 345.70 | 517.47 | 517.47 | 4.5 | 91.15 | 19.19 |

| Cumulative Quartz Recovery | **91.15** | % | Conditioning Time | 6.0 | min |
|---|---|---|---|---|---|
| Cumulative Water Recovery | **19.19** | % | | | |

Table 113 : Flotation Response of the Laboratory Batch Cell with the +150 -300 μm Particle Size Fraction with No Collector Added to the Pulp.

| Air Flow Rate | 3 | l/min | Water pH | 8.73 |
|---|---|---|---|---|
| Measured Froth Depth | 20 | mm | Adjusted pH | 7.00 |

| Sampl No | Pan Mass (g) | Froth+ Pan Mass (g) | Quartz +Pan Mass (g) | Bottle Mass (g) | Wash Water Mass 1 (g) | Wash Water Mass 2 (g) | Flot Time (min) | Cum Quartz Rec (%) | Cum Water Rec (%) |
|---|---|---|---|---|---|---|---|---|---|
| 1 | 370.98 | 370.98 | 370.98 | 343.65 | 463.87 | 463.87 | 0.5 | 0.00 | 0.00 |
| 2 | 377.67 | 377.67 | 377.67 | 346.06 | 348.28 | 348.28 | 1.0 | 0.00 | 0.00 |
| 3 | 357.63 | 357.63 | 357.63 | 347.22 | 332.48 | 332.48 | 1.5 | 0.00 | 0.00 |
| 4 | 383.86 | 383.86 | 383.86 | 348.21 | 300.71 | 300.71 | 2.0 | 0.00 | 0.00 |
| 5 | 363.86 | 363.86 | 363.86 | 345.14 | 384.59 | 384.59 | 2.5 | 0.00 | 0.00 |
| 6 | 364.39 | 364.39 | 364.39 | 344.68 | 412.00 | 412.00 | 3.0 | 0.00 | 0.00 |
| 7 | 363.18 | 363.18 | 363.18 | 346.88 | 448.47 | 448.47 | 3.5 | 0.00 | 0.00 |
| 8 | 359.60 | 359.60 | 359.60 | 348.66 | 403.44 | 403.44 | 4.0 | 0.00 | 0.00 |
| 9 | 371.74 | 371.74 | 371.74 | 345.70 | 517.51 | 517.51 | 4.5 | 0.00 | 0.00 |

| Cumulative Quartz Recovery | **0.00** | % | Conditioning | 5.0 | min |
|---|---|---|---|---|---|
| Cumulative Water Recovery | **0.00** | % | Time | | |

Table 114 : Flotation Response of the Laboratory Batch Cell with the +150 -300 μm Particle Size Fraction at a Collector Dosage of 25 g/t.

| Air Flow Rate | 3 | l/min | Water pH | 8.88 |
|---|---|---|---|---|
| Measured Froth Depth | 20 | mm | Adjusted pH | 7.00 |

| Sampl No | Pan Mass (g) | Froth+ Pan Mass (g) | Quartz +Pan Mass (g) | Bottle Mass (g) | Wash Water Mass 1 (g) | Wash Water Mass 2 (g) | Flot Time (min) | Cum Quartz Rec (%) | Cum Water Rec (%) |
|---|---|---|---|---|---|---|---|---|---|
| 1 | 370.98 | 370.98 | 370.98 | 343.65 | 451.83 | 451.83 | 0.5 | 0.00 | 0.00 |
| 2 | 377.67 | 377.67 | 377.67 | 346.06 | 472.01 | 472.01 | 1.0 | 0.00 | 0.00 |
| 3 | 357.63 | 357.63 | 357.63 | 347.22 | 460.77 | 460.77 | 1.5 | 0.00 | 0.00 |
| 4 | 383.86 | 383.86 | 383.86 | 348.21 | 465.14 | 465.14 | 2.0 | 0.00 | 0.00 |
| 5 | 363.86 | 363.86 | 363.86 | 345.14 | 459.02 | 459.02 | 2.5 | 0.00 | 0.00 |
| 6 | 364.39 | 364.39 | 364.39 | 344.68 | 487.64 | 487.64 | 3.0 | 0.00 | 0.00 |
| 7 | 363.18 | 363.18 | 363.18 | 346.88 | 468.54 | 468.54 | 3.5 | 0.00 | 0.00 |
| 8 | 359.60 | 359.60 | 359.60 | 348.66 | 479.23 | 479.23 | 4.0 | 0.00 | 0.00 |
| 9 | 371.74 | 371.74 | 371.74 | 345.70 | 517.49 | 517.49 | 4.5 | 0.00 | 0.00 |

| Cumulative Quartz Recovery | **0.00** | % | Conditioning | 5.0 | min |
|---|---|---|---|---|---|
| Cumulative Water Recovery | **0.00** | % | Time | | |

Table 115 : Flotation Response of the Laboratory Batch Cell with the +150 -300 μm Particle Size Fraction at a Collector Dosage of 50 g/t.

| Air Flow Rate | 3 | l/min | Water pH | 8.73 |
|---|---|---|---|---|
| Measured Froth Depth | 13 | mm | Adjusted pH | 7.00 |

| Sampl No | Pan Mass (g) | Froth+ Pan Mass (g) | Quartz +Pan Mass (g) | Bottle Mass (g) | Wash Water Mass 1 (g) | Wash Water Mass 2 (g) | Flot Time (min) | Cum Quartz Rec (%) | Cum Water Rec (%) |
|---|---|---|---|---|---|---|---|---|---|
| 1 | 370.98 | 424.18 | 354.75 | 343.65 | 463.87 | 438.50 | 0.5 | 3.70 | 0.58 |
| 2 | 377.67 | 419.99 | 351.76 | 346.06 | 348.28 | 328.32 | 1.0 | 5.60 | 1.03 |
| 3 | 357.63 | 388.63 | 349.03 | 347.22 | 332.48 | 315.83 | 1.5 | 6.20 | 1.08 |
| 4 | 383.86 | 412.50 | 349.01 | 348.21 | 330.71 | 281.36 | 2.0 | 6.47 | 1.11 |
| 5 | 363.86 | 392.53 | 345.45 | 345.14 | 384.59 | 362.80 | 2.5 | 6.57 | 1.17 |
| 6 | 364.39 | 384.78 | 344.82 | 344.68 | 412.00 | 397.85 | 3.0 | 6.62 | 1.28 |
| 7 | 363.18 | 387.52 | 347.00 | 346.88 | 448.47 | 428.16 | 3.5 | 6.66 | 1.35 |
| 8 | 359.60 | 374.08 | 348.71 | 348.66 | 403.44 | 389.48 | 4.0 | 6.68 | 1.43 |
| 9 | 371.74 | 371.74 | 371.74 | 345.70 | 517.49 | 517.49 | 4.5 | 6.68 | 1.43 |

| Cumulative Quartz Recovery | **6.68** | % | Conditioning | 6.0 | min |
|---|---|---|---|---|---|
| Cumulative Water Recovery | **1.43** | % | Time | | |

Table 116 : Flotation Response of the Laboratory Batch Cell with the +150 -300 μm Particle Size Fraction at a Collector Dosage of 80 g/t.

| Air Flow Rate | 3 | l/min | Water pH | 8.88 |
|---|---|---|---|---|
| Measured Froth Depth | 15 | mm | Adjusted pH | 7.00 |

| Sampl No | Pan Mass (g) | Froth+ Pan Mass (g) | Quartz +Pan Mass (g) | Bottle Mass (g) | Wash Water Mass 1 (g) | Wash Water Mass 2 (g) | Flot Time (min) | Cum Quartz Rec (%) | Cum Water Rec (%) |
|---|---|---|---|---|---|---|---|---|---|
| 1 | 370.98 | 492.56 | 397.56 | 343.65 | 451.83 | 425.21 | 0.5 | 18.00 | 1.42 |
| 2 | 377.67 | 468.34 | 378.92 | 346.06 | 472.01 | 443.84 | 1.0 | 28.95 | 2.45 |
| 3 | 357.63 | 408.71 | 358.17 | 347.22 | 460.77 | 438.43 | 1.5 | 32.60 | 3.06 |
| 4 | 383.86 | 423.28 | 352.99 | 348.21 | 465.14 | 443.90 | 2.0 | 34.20 | 3.52 |
| 5 | 363.86 | 398.96 | 347.23 | 345.14 | 459.02 | 435.24 | 2.5 | 34.89 | 3.84 |
| 6 | 364.39 | 389.90 | 345.50 | 344.68 | 487.64 | 470.83 | 3.0 | 35.17 | 4.12 |
| 7 | 363.18 | 390.33 | 347.31 | 346.88 | 468.54 | 447.32 | 3.5 | 35.31 | 4.31 |
| 8 | 359.60 | 382.93 | 349.04 | 348.66 | 479.23 | 459.50 | 4.0 | 35.44 | 4.42 |
| 9 | 371.74 | 371.74 | 371.74 | 345.70 | 517.49 | 517.49 | 4.5 | 35.44 | 4.42 |

| Cumulative Quartz Recovery | **35.44** | % | Conditioning | 6.0 | min |
|---|---|---|---|---|---|
| Cumulative Water Recovery | **4.42** | % | Time | | |

Table 117 : Flotation Response of the Laboratory Batch Cell with the +150 -300 μm Particle Size Fraction at a Collector Dosage of 160 g/t.

| Air Flow Rate | 3 | l/min | Water pH | 8.73 |
|---|---|---|---|---|
| Measured Froth Depth | 18 | mm | Adjusted pH | 7.00 |

| Sampl No | Pan Mass (g) | Froth+ Pan Mass (g) | Quartz +Pan Mass (g) | Bottle Mass (g) | Wash Water Mass 1 (g) | Wash Water Mass 2 (g) | Flot Time (min) | Cum Quartz Rec (%) | Cum Water Rec (%) |
|---|---|---|---|---|---|---|---|---|---|
| 1 | 370.98 | 669.75 | 560.50 | 343.65 | 438.50 | 409.20 | 0.5 | 63.17 | 2.77 |
| 2 | 377.67 | 581.56 | 434.13 | 346.06 | 328.32 | 298.71 | 1.0 | 81.99 | 6.85 |
| 3 | 357.63 | 446.14 | 369.70 | 347.22 | 315.83 | 290.55 | 1.5 | 86.02 | 8.62 |
| 4 | 383.86 | 446.33 | 389.46 | 348.21 | 281.36 | 257.70 | 2.0 | 87.87 | 9.77 |
| 5 | 363.86 | 425.88 | 366.46 | 345.14 | 362.80 | 332.76 | 2.5 | 88.73 | 10.79 |
| 6 | 364.39 | 409.47 | 365.89 | 344.68 | 397.85 | 379.62 | 3.0 | 89.23 | 11.67 |
| 7 | 363.18 | 407.08 | 363.75 | 346.88 | 428.16 | 407.32 | 3.5 | 89.42 | 12.45 |
| 8 | 359.60 | 398.49 | 359.83 | 348.66 | 389.48 | 372.81 | 4.0 | 89.50 | 13.21 |
| 9 | 371.74 | 371.74 | 371.74 | 345.70 | 517.51 | 517.51 | 4.5 | 89.50 | 13.21 |

| Cumulative Quartz Recovery | **89.50** | % | Conditioning Time | 5.0 | min |
|---|---|---|---|---|---|
| Cumulative Water Recovery | **13.21** | % | | | |

Table 118 : Flotation Response of the Laboratory Batch Cell with the +150 -300 μm Particle Size Fraction at a Collector Dosage of 200 g/t.

| Air Flow Rate | 3 | l/min | Water pH | 8.75 |
|---|---|---|---|---|
| Measured Froth Depth | 10 | mm | Adjusted pH | 7.00 |

| Sampl No | Pan Mass (g) | Froth+ Pan Mass (g) | Quartz +Pan Mass (g) | Bottle Mass (g) | Wash Water Mass 1 (g) | Wash Water Mass 2 (g) | Flot Time (min) | Cum Quartz Rec (%) | Cum Water Rec (%) |
|---|---|---|---|---|---|---|---|---|---|
| 1 | 370.98 | 751.50 | 523.47 | 343.65 | 409.13 | 386.60 | 0.5 | 59.94 | 6.17 |
| 2 | 377.67 | 596.94 | 419.30 | 346.06 | 298.69 | 275.15 | 1.0 | 84.35 | 10.42 |
| 3 | 357.63 | 461.21 | 366.28 | 347.22 | 290.46 | 265.84 | 1.5 | 90.71 | 12.49 |
| 4 | 383.86 | 462.10 | 355.22 | 348.21 | 257.67 | 234.64 | 2.0 | 93.04 | 14.16 |
| 5 | 363.86 | 426.92 | 347.97 | 345.14 | 332.66 | 308.34 | 2.5 | 93.99 | 15.40 |
| 6 | 364.39 | 400.12 | 345.45 | 344.68 | 379.43 | 362.25 | 3.0 | 94.24 | 16.02 |
| 7 | 363.18 | 397.90 | 347.28 | 346.88 | 407.29 | 386.63 | 3.5 | 94.38 | 16.49 |
| 8 | 359.60 | 376.49 | 348.01 | 348.66 | 372.73 | 364.92 | 4.0 | 94.42 | 16.83 |
| 9 | 371.74 | 371.74 | 371.74 | 345.70 | 517.49 | 517.49 | 4.5 | 94.42 | 16.83 |

| Cumulative Quartz Recovery | **94.42** | % | Conditioning Time | 6.0 | min |
|---|---|---|---|---|---|
| Cumulative Water Recovery | **4.42** | % | | | |

Table 119 : Flotation Response of the Laboratory Batch Cell with the +300 μm Particle Size Fraction with No Collector Added to the Pulp.

| Air Flow Rate | 3 | l/min | Water pH | 8.60 |
|---|---|---|---|---|
| Measured Froth Depth | 15 | mm | Adjusted pH | 7.00 |

| Sampl No | Pan Mass (g) | Froth+ Pan Mass (g) | Quartz +Pan Mass (g) | Bottle Mass (g) | Wash Water Mass 1 (g) | Wash Water Mass 2 (g) | Flot Time (min) | Cum Quartz Rec (%) | Cum Water Rec (%) |
|---|---|---|---|---|---|---|---|---|---|
| 1 | 370.98 | 370.98 | 370.98 | 343.65 | 522.84 | 522.84 | 0.5 | 0.00 | 0.00 |
| 2 | 377.67 | 377.67 | 377.67 | 346.06 | 382.10 | 382.10 | 1.0 | 0.00 | 0.00 |
| 3 | 357.63 | 357.63 | 357.63 | 347.22 | 381.47 | 381.47 | 1.5 | 0.00 | 0.00 |
| 4 | 383.86 | 383.86 | 383.86 | 348.21 | 349.57 | 349.57 | 2.0 | 0.00 | 0.00 |
| 5 | 363.86 | 363.86 | 363.86 | 345.14 | 446.34 | 446.34 | 2.5 | 0.00 | 0.00 |
| 6 | 364.39 | 364.39 | 364.39 | 344.68 | 449.62 | 449.62 | 3.0 | 0.00 | 0.00 |
| 7 | 363.18 | 363.18 | 363.18 | 346.88 | 495.15 | 495.15 | 3.5 | 0.00 | 0.00 |
| 8 | 359.60 | 359.60 | 359.60 | 348.66 | 431.31 | 431.31 | 4.0 | 0.00 | 0.00 |
| 9 | 371.74 | 371.74 | 371.74 | 345.70 | 533.43 | 533.43 | 4.5 | 0.00 | 0.00 |

| Cumulative Quartz Recovery | **0.00** | % | Conditioning Time | 5.0 | min |
|---|---|---|---|---|---|
| Cumulative Water Recovery | **0.00** | % | | | |

Table 120 : Flotation Response of the Laboratory Batch Cell with the +300 μm Particle Size Fraction at a Collector Dosage of 25 g/t.

| Air Flow Rate | 3 | l/min | Water pH | 8.67 |
|---|---|---|---|---|
| Measured Froth Depth | 20 | mm | Adjusted pH | 7.00 |

| Sampl No | Pan Mass (g) | Froth+ Pan Mass (g) | Quartz +Pan Mass (g) | Bottle Mass (g) | Wash Water Mass 1 (g) | Wash Water Mass 2 (g) | Flot Time (min) | Cum Quartz Rec (%) | Cum Water Rec (%) |
|---|---|---|---|---|---|---|---|---|---|
| 1 | 370.98 | 370.98 | 370.98 | 343.65 | 477.44 | 477.44 | 0.5 | 0.00 | 0.00 |
| 2 | 377.67 | 377.67 | 377.67 | 346.06 | 494.60 | 494.60 | 1.0 | 0.00 | 0.00 |
| 3 | 357.63 | 357.63 | 357.63 | 347.22 | 485.33 | 485.33 | 1.5 | 0.00 | 0.00 |
| 4 | 383.86 | 383.86 | 383.86 | 348.21 | 488.30 | 488.30 | 2.0 | 0.00 | 0.00 |
| 5 | 363.86 | 363.86 | 363.86 | 345.14 | 484.19 | 484.19 | 2.5 | 0.00 | 0.00 |
| 6 | 364.39 | 364.39 | 364.39 | 344.68 | 502.37 | 502.37 | 3.0 | 0.00 | 0.00 |
| 7 | 363.18 | 363.18 | 363.18 | 346.88 | 489.95 | 489.95 | 3.5 | 0.00 | 0.00 |
| 8 | 359.60 | 359.60 | 359.60 | 348.66 | 502.38 | 502.38 | 4.0 | 0.00 | 0.00 |
| 9 | 371.74 | 371.74 | 371.74 | 345.70 | 517.48 | 517.48 | 4.5 | 0.00 | 0.00 |

| Cumulative Quartz Recovery | **0.00** | % | Conditioning Time | 5.0 | min |
|---|---|---|---|---|---|
| Cumulative Water Recovery | **0.00** | % | | | |

Table 121 : Flotation Response of the Laboratory Batch Cell with the +300 μm Particle Size Fraction at a Collector Dosage of 50 g/t.

| Air Flow Rate | 3 | l/min | Water pH | 8.60 |
|---|---|---|---|---|
| Measured Froth Depth | 12 | mm | Adjusted pH | 7.00 |

| Sampl No | Pan Mass (g) | Froth + Pan Mass (g) | Quartz +Pan Mass (g) | Bottle Mass (g) | Wash Water Mass 1 (g) | Wash Water Mass 2 (g) | Flot Time (min) | Cum Quartz Rec (%) | Cum Water Rec (%) |
|---|---|---|---|---|---|---|---|---|---|
| 1 | 370.98 | 501.34 | 406.57 | 343.65 | 522.84 | 4489.3 | 0.5 | 20.97 | 1.18 |
| 2 | 377.67 | 456.39 | 369.30 | 346.06 | 382.10 | 354.13 | 1.0 | 28.72 | 2.13 |
| 3 | 357.63 | 396.27 | 351.12 | 347.22 | 381.47 | 358.36 | 1.5 | 30.02 | 2.53 |
| 4 | 383.86 | 417.24 | 349.56 | 348.21 | 349.57 | 323.15 | 2.0 | 30.47 | 2.73 |
| 5 | 363.86 | 393.19 | 346.26 | 345.14 | 446.34 | 420.79 | 2.5 | 30.84 | 2.82 |
| 6 | 364.39 | 385.11 | 345.16 | 344.68 | 449.62 | 431.19 | 3.0 | 31.00 | 2.88 |
| 7 | 363.18 | 386.23 | 347.24 | 346.88 | 495.15 | 472.90 | 3.5 | 31.12 | 2.90 |
| 8 | 359.60 | 376.35 | 348.87 | 348.66 | 431.31 | 413.98 | 4.0 | 31.19 | 2.91 |
| 9 | 371.74 | 371.74 | 371.74 | 345.70 | 533.43 | 533.43 | 4.5 | 31.19 | 2.91 |

| Cumulative Quartz Recovery | **31.19** | % | Conditioning Time | 6.0 | min |
|---|---|---|---|---|---|
| Cumulative Water Recovery | **2.91** | % | | | |

Table 122 : Flotation Response of the Laboratory Batch Cell with the +300 μm Particle Size Fraction at a Collector Dosage of 80 g/t.

| Air Flow Rate | 3 | l/min | Water pH | 8.67 |
|---|---|---|---|---|
| Measured Froth Depth | 14 | mm | Adjusted pH | 7.00 |

| Sampl No | Pan Mass (g) | Froth + Pan Mass (g) | Quartz +Pan Mass (g) | Bottle Mass (g) | Wash Water Mass 1 (g) | Wash Water Mass 2 (g) | Flot Time (min) | Cum Quartz Rec (%) | Cum Water Rec (%) |
|---|---|---|---|---|---|---|---|---|---|
| 1 | 370.98 | 621.80 | 496.09 | 343.65 | 477.44 | 451.92 | 0.5 | 41.70 | 3.47 |
| 2 | 377.67 | 536.21 | 435.22 | 346.06 | 494.60 | 472.08 | 1.0 | 60.89 | 6.19 |
| 3 | 357.63 | 417.15 | 365.19 | 347.22 | 485.33 | 460.98 | 1.5 | 63.41 | 7.15 |
| 4 | 383.86 | 423.76 | 386.68 | 348.21 | 488.30 | 465.25 | 2.0 | 64.33 | 7.63 |
| 5 | 363.86 | 396.97 | 365.28 | 345.14 | 484.19 | 459.18 | 2.5 | 64.80 | 7.86 |
| 6 | 364.39 | 383.95 | 356.32 | 344.68 | 502.37 | 487.78 | 3.0 | 65.11 | 8.00 |
| 7 | 363.18 | 387.18 | 363.98 | 346.88 | 489.95 | 468.62 | 3.5 | 65.38 | 8.07 |
| 8 | 359.60 | 383.94 | 360.49 | 348.66 | 502.38 | 479.43 | 4.0 | 65.68 | 8.08 |
| 9 | 371.74 | 371.74 | 371.74 | 345.70 | 517.48 | 517.48 | 4.5 | 65.68 | 8.08 |

| Cumulative Quartz Recovery | **65.68** | % | Conditioning Time | 5.0 | min |
|---|---|---|---|---|---|
| Cumulative Water Recovery | **8.08** | % | | | |

Table 123 : Flotation Response of the Laboratory Batch Cell with the +300 μm Particle Size Fraction at a Collector Dosage of 160 g/t.

| Air Flow Rate | 3 | l/min | Water pH | 8.73 |
|---|---|---|---|---|
| Measured Froth Depth | 10 | mm | Adjusted pH | 7.00 |

| Sampl No | Pan Mass (g) | Froth+ Pan Mass (g) | Quartz +Pan Mass (g) | Bottle Mass (g) | Wash Water Mass 1 (g) | Wash Water Mass 2 (g) | Flot Time (min) | Cum Quartz Rec (%) | Cum Water Rec (%) |
|---|---|---|---|---|---|---|---|---|---|
| 1 | 370.98 | 736.10 | 486.09 | 343.65 | 489.17 | 463.99 | 0.5 | 47.48 | 6.84 |
| 2 | 377.67 | 674.70 | 419.71 | 346.06 | 345.08 | 348.31 | 1.0 | 72.03 | 14.69 |
| 3 | 357.63 | 566.45 | 380.16 | 347.22 | 358.13 | 332.52 | 1.5 | 83.01 | 19.89 |
| 4 | 383.86 | 451.66 | 255.42 | 348.21 | 323.04 | 300.76 | 2.0 | 85.41 | 20.22 |
| 5 | 363.86 | 416.22 | 346.85 | 345.14 | 420.63 | 348.63 | 2.5 | 85.98 | 20.48 |
| 6 | 364.39 | 393.86 | 345.64 | 344.68 | 431.00 | 412.07 | 3.0 | 86.30 | 20.81 |
| 7 | 363.18 | 393.66 | 347.53 | 346.88 | 472.88 | 448.47 | 3.5 | 86.52 | 21.00 |
| 8 | 359.60 | 376.31 | 349.09 | 348.66 | 413.85 | 403.46 | 4.0 | 86.66 | 21.20 |
| 9 | 371.74 | 392.17 | 345.96 | 345.70 | 533.42 | 517.57 | 4.5 | 86.75 | 21.35 |

| Cumulative Quartz Recovery | **86.75** | % | Conditioning Time | 6.0 | min |
|---|---|---|---|---|---|
| Cumulative Water Recovery | **21.35** | % | | | |

Table 124 : Flotation Response of the Laboratory Batch Cell with the +300 μm Particle Size Fraction at a Collector Dosage of 200 g/t.

| Air Flow Rate | 3 | l/min | Water pH | 8.75 |
|---|---|---|---|---|
| Measured Froth Depth | 15 | mm | Adjusted pH | 7.00 |

| Sampl No | Pan Mass (g) | Froth+ Pan Mass (g) | Quartz +Pan Mass (g) | Bottle Mass (g) | Wash Water Mass 1 (g) | Wash Water Mass 2 (g) | Flot Time (min) | Cum Quartz Rec (%) | Cum Water Rec (%) |
|---|---|---|---|---|---|---|---|---|---|
| 1 | 370.98 | 704.20 | 464.81 | 343.65 | 386.60 | 364.96 | 0.5 | 40.39 | 6.60 |
| 2 | 377.67 | 752.70 | 438.11 | 346.06 | 275.15 | 264.05 | 1.0 | 71.07 | 16.01 |
| 3 | 357.63 | 607.50 | 377.52 | 347.22 | 265.88 | 248.04 | 1.5 | 81.17 | 23.00 |
| 4 | 383.86 | 490.62 | 359.78 | 348.21 | 234.64 | 210.23 | 2.0 | 85.03 | 25.45 |
| 5 | 363.86 | 416.22 | 347.94 | 345.14 | 308.34 | 283.22 | 2.5 | 85.96 | 26.30 |
| 6 | 364.39 | 402.10 | 345.75 | 344.68 | 362.25 | 342.05 | 3.0 | 86.32 | 26.87 |
| 7 | 363.18 | 406.94 | 347.32 | 346.88 | 386.63 | 355.72 | 3.5 | 86.46 | 27.30 |
| 8 | 359.60 | 385.48 | 348.92 | 348.66 | 364.92 | 350.40 | 4.0 | 86.55 | 27.68 |
| 9 | 371.74 | 371.74 | 371.74 | 345.70 | 517.49 | 517.49 | 4.5 | 86.55 | 27.68 |

| Cumulative Quartz Recovery | **86.55** | % | Conditioning Time | 6.0 | min |
|---|---|---|---|---|---|
| Cumulative Water Recovery | **27.68** | % | | | |

Table 125 : Flotation Response of the Laboratory Batch Cell with the +106 -150 μm Particle Size Fraction at a Collector Dosage of 80 g/t (Agitation Speed = 800 rpm).

| Air Flow Rate | 3 | l/min | Water pH | 8.35 |
|---|---|---|---|---|
| Measured Froth Depth | 15 | mm | Adjusted pH | 7.00 |

| Sampl No | Pan Mass (g) | Froth+ Pan Mass (g) | Quartz +Pan Mass (g) | Bottle Mass (g) | Wash Water Mass 1 (g) | Wash Water Mass 2 (g) | Flot Time (min) | Cum Quartz Rec (%) | Cum Water Rec (%) |
|---|---|---|---|---|---|---|---|---|---|
| 1 | 370.98 | 553.63 | 437.01 | 347.94 | 486.38 | 461.96 | 0.5 | 29.69 | 2.40 |
| 2 | 377.67 | 562.14 | 415.45 | 346.96 | 482.49 | 460.60 | 1.0 | 52.52 | 5.66 |
| 3 | 357.63 | 457.59 | 365.55 | 346.52 | 503.10 | 480.24 | 1.5 | 58.86 | 7.67 |
| 4 | 383.86 | 452.36 | 357.42 | 347.58 | 478.58 | 458.92 | 2.0 | 62.14 | 9.02 |
| 5 | 363.86 | 422.03 | 350.31 | 344.77 | 501.68 | 476.21 | 2.5 | 63.99 | 9.96 |
| 6 | 364.39 | 399.82 | 347.69 | 346.19 | 501.31 | 483.11 | 3.0 | 64.49 | 10.50 |
| 7 | 363.18 | 396.33 | 342.90 | 342.09 | 499.27 | 480.34 | 3.5 | 64.76 | 10.97 |
| 8 | 359.60 | 380.03 | 341.37 | 340.84 | 511.42 | 500.73 | 4.0 | 64.94 | 11.29 |
| 9 | 371.74 | 393.83 | 344.54 | 344.14 | 526.62 | 509.78 | 4.5 | 65.07 | 11.45 |

| Cumulative Quartz Recovery | **65.07** | % | Conditioning Time | 6.0 | min |
|---|---|---|---|---|---|
| Cumulative Water Recovery | **4.85** | % | | | |

Table 126 : Flotation Response of the Laboratory Batch Cell with the +106 -150 μm Particle Size Fraction at a Collector Dosage of 80 g/t (Agitation Speed = 1000 rpm).

| Air Flow Rate | 3 | l/min | Water pH | 8.35 |
|---|---|---|---|---|
| Measured Froth Depth | 13 | mm | Adjusted pH | 7.00 |

| Sampl No | Pan Mass (g) | Froth+ Pan Mass (g) | Quartz +Pan Mass (g) | Bottle Mass (g) | Wash Water Mass 1 (g) | Wash Water Mass 2 (g) | Flot Time (min) | Cum Quartz Rec (%) | Cum Water Rec (%) |
|---|---|---|---|---|---|---|---|---|---|
| 1 | 370.98 | 544.42 | 417.03 | 343.65 | 461.96 | 436.96 | 0.5 | 24.46 | 2.60 |
| 2 | 377.67 | 499.90 | 401.92 | 346.06 | 460.60 | 440.42 | 1.0 | 43.08 | 4.20 |
| 3 | 357.63 | 418.44 | 365.79 | 347.22 | 480.24 | 455.61 | 1.5 | 49.27 | 4.81 |
| 4 | 383.86 | 413.16 | 354.37 | 348.21 | 458.92 | 441.40 | 2.0 | 51.32 | 5.00 |
| 5 | 363.86 | 391.83 | 347.81 | 345.14 | 476.21 | 454.29 | 2.5 | 52.21 | 5.12 |
| 6 | 364.39 | 381.80 | 346.55 | 344.68 | 483.11 | 468.44 | 3.0 | 52.84 | 5.15 |
| 7 | 363.18 | 383.73 | 348.13 | 346.88 | 480.34 | 462.19 | 3.5 | 53.25 | 5.19 |
| 8 | 359.60 | 374.07 | 349.68 | 348.66 | 500.73 | 487.86 | 4.0 | 53.59 | 5.21 |
| 9 | 371.74 | 371.74 | 371.74 | 345.70 | 509.78 | 509.78 | 4.5 | 53.59 | 5.21 |

| Cumulative Quartz Recovery | **53.59** | % | Conditioning Time | 6.0 | min |
|---|---|---|---|---|---|
| Cumulative Water Recovery | **5.21** | % | | | |

Table 127 : Flotation Response of the Laboratory Batch Cell with the +106 -150 μm Particle Size Fraction at a Collector Dosage of 80 g/t (Agitation Speed = 1400 rpm).

| Air Flow Rate | 3 | l/min | Water pH | 8.35 |
|---|---|---|---|---|
| Measured Froth Depth | 15 | mm | Adjusted pH | 7.00 |

| Sampl No | Pan Mass (g) | Froth+ Pan Mass (g) | Quartz +Pan Mass (g) | Bottle Mass (g) | Wash Water Mass 1 (g) | Wash Water Mass 2 (g) | Flot Time (min) | Cum Quartz Rec (%) | Cum Water Rec (%) |
|---|---|---|---|---|---|---|---|---|---|
| 1 | 370.98 | 498.08 | 423.23 | 343.65 | 436.96 | 416.99 | 0.5 | 17.42 | 1.90 |
| 2 | 377.67 | 515.06 | 432.72 | 346.06 | 440.42 | 414.93 | 1.0 | 35.77 | 3.87 |
| 3 | 357.63 | 436.70 | 379.74 | 347.22 | 455.61 | 425.79 | 1.5 | 43.14 | 4.81 |
| 4 | 383.86 | 524.13 | 392.65 | 348.21 | 441.40 | 419.93 | 2.0 | 46.05 | 5.19 |
| 5 | 363.86 | 397.63 | 368.99 | 345.14 | 454.29 | 430.14 | 2.5 | 47.76 | 5.35 |
| 6 | 364.39 | 388.42 | 367.89 | 344.68 | 468.44 | 450.33 | 3.0 | 48.93 | 5.43 |
| 7 | 363.18 | 390.59 | 366.85 | 346.88 | 462.19 | 439.42 | 3.5 | 50.15 | 5.46 |
| 8 | 359.60 | 372.94 | 359.88 | 348.66 | 487.86 | 475.47 | 4.0 | 50.24 | 5.49 |
| 9 | 371.74 | 371.74 | 371.74 | 345.70 | 509.78 | 509.78 | 4.5 | 50.24 | 5.49 |

| Cumulative Quartz Recovery | **50.24** | % | Conditioning Time | 5.0 | min |
|---|---|---|---|---|---|
| Cumulative Water Recovery | **5.49** | % | | | |

Table 128 : Flotation Response of the Laboratory Batch Cell with the +106 -150 μm Particle Size Fraction at a Collector Dosage of 80 g/t (Agitation Speed = 1570 rpm).

| Air Flow Rate | 3 | l/min | Water pH | 8.35 |
|---|---|---|---|---|
| Measured Froth Depth | 14 | mm | Adjusted pH | 7.00 |

| Sampl No | Pan Mass (g) | Froth+ Pan Mass (g) | Quartz +Pan Mass (g) | Bottle Mass (g) | Wash Water Mass 1 (g) | Wash Water Mass 2 (g) | Flot Time (min) | Cum Quartz Rec (%) | Cum Water Rec (%) |
|---|---|---|---|---|---|---|---|---|---|
| 1 | 370.98 | 480.38 | 384.79 | 343.65 | 514.80 | 486.38 | 0.5 | 13.71 | 1.38 |
| 2 | 377.67 | 494.44 | 386.61 | 346.06 | 520.32 | 482.49 | 1.0 | 27.23 | 2.71 |
| 3 | 357.63 | 424.46 | 364.14 | 347.22 | 531.07 | 503.10 | 1.5 | 32.87 | 3.47 |
| 4 | 383.86 | 425.15 | 354.84 | 348.21 | 506.26 | 478.58 | 2.0 | 35.08 | 3.71 |
| 5 | 363.86 | 419.19 | 350.54 | 345.14 | 545.55 | 501.68 | 2.5 | 36.88 | 3.92 |
| 6 | 364.39 | 392.10 | 346.72 | 344.68 | 522.94 | 501.31 | 3.0 | 37.56 | 4.06 |
| 7 | 363.18 | 394.40 | 349.43 | 346.88 | 524.16 | 499.27 | 3.5 | 38.41 | 4.19 |
| 8 | 359.60 | 321.69 | 350.36 | 348.66 | 531.26 | 571.42 | 4.0 | 38.98 | 4.21 |
| 9 | 371.74 | 371.74 | 371.74 | 345.70 | 526.62 | 526.62 | 4.5 | 38.98 | 4.21 |

| Cumulative Quartz Recovery | **38.98** | % | Conditioning Time | 6.0 | min |
|---|---|---|---|---|---|
| Cumulative Water Recovery | **4.21** | % | | | |